1969

Dynamic response of circular plates to transient and harmonic transverse loads including the effect of transverse shear and rotary inertia

Perakatte Joseph George

Department: Mechanical and Aerospace Engineering

DYNAMIC RESPONSE OF CIRCULAR PLATES TO TRANSIENT AND HARMONIC TRANSVERSE LOADS INCLUDING THE EFFECT OF TRANSVERSE SHEAR AND ROTARY INERTIA

by

PERAKATTE JOSEPH GEORGE, 1931-

A DISSERTATION

Presented to the Faculty of the Graduate School of the

UNIVERSITY OF MISSOURI - ROLLA

In Partial Fulfillment of the Requirements for the Degree

DOCTOR OF PHILOSOPHY

in

MECHANICAL ENGINEERING

1969

I. F. Lehnhoff
Advisor

Lloyd M. Cunningham

T. R. Faucett

Robert L. Davis

H. J. Sauer

S J Pagano

ABSTRACT

Using an improved theory of plate vibration suggested by R. D. Mindlin which takes into account the effects of transverse shear and rotary inertia, free and forced transverse vibrations of uniform circular plates are studied and the results compared with those obtained using the classical theory of plate vibration.

The governing equations are developed in polar coordinates using the equations of elasticity. Frequency equations for axisymmetric and antisymmetric vibrations are derived for solid circular plates under different boundary conditions and for an annular plate rigidly mounted on a shaft.

The response of plates to different types of rapidly applied axisymmetric steady loads and pulse loads is investigated in detail using an improved normal-mode solution suggested by D. Williams.

Frequency equations for plates loaded with arbitrary impedance at the center are derived by three different methods. Two methods make use of conventional mode summation techniques and result in series forms of the frequency equation. The third method results in a closed-form frequency equation which makes it very convenient for use in many applications. A number of typical applications of the closed-form frequency equation are also considered.

The driving-point impedance and transmissibility of free and constrained circular plates driven by harmonically oscillating forces at the center are studied by extending the principles used in the derivation of the closed-form frequency equation. The effect of attaching dynamic vibration absorbers at the center of the plate and their tuning are also investigated. Internal material damping is treated in general, but no numerical results are presented for damped systems.

Several examples are given detailed consideration. Numerical results are given in nondimensional quantities and are presented in a series of graphs and tables.

ACKNOWLEDGEMENTS

The author wishes to express his sincere thanks and appreciation to Dr. T. F. Lehnhoff, his advisor, for his encouragement, direction and assistance throughout the course of this investigation, to Dr. R. L. Davis for his careful and thorough review of this dissertation, and to Dr. T. R. Faucett, Dr. H. J. Sauer and Prof. S. J. Pagano for their help during the author's graduate program.

Sincere gratitude is due the Government of India and the United Nations Educational, Scientific and Cultural Organization for the financial support of the author's graduate studies.

The author is also thankful to Mrs. Johnnye Allen for typing this dissertation.

TABLE OF CONTENTS

TABLE OF CONTENTS

(continued)

TABLE OF CONTENTS

(continued)

TABLE OF CONTENTS
(continued)

LIST OF FIGURES

LIST OF FIGURES
(continued)

LIST OF FIGURES

(Continued)

LIST OF FIGURES
(continued)

LIST OF FIGURES
(continued)

LIST OF FIGURES
(continued)

LIST OF FIGURES
(continued)

LIST OF FIGURES
(continued)

LIST OF FIGURES
(continued)

LIST OF TABLES

LIST OF TABLES
(continued)

LIST OF TABLES
(continued)

LIST OF SYMBOLS

r, θ, z	Cylindrical coordinates
$\sigma_r, \sigma_\theta, \sigma_z$; $\tau_r, \tau_{rz}, \tau_{\theta z}$	Stress components in cylindrical coordinates
$\varepsilon_r, \varepsilon_\theta, \varepsilon_z$; $\gamma_{rz}, \gamma_{r\theta}, \gamma_{\theta z}$	Strain components in cylindrical coordinates
u_r, u_θ, u_z	Displacements in the coordinate directions
Q_r, Q_θ; $M_r, M_\theta, M_{r\theta}$	Plate-stress components defined by equations (4.1)
$\Gamma_r, \Gamma_\theta, \Gamma_z$; $\Gamma_{rz}, \Gamma_{r\theta}, \Gamma_{\theta z}$	Plate-strain components defined by equations (6.8)
ψ_r, ψ_θ, w	Plate-displacement components defined by equations (4.7)
ν	Poisson's ratio
E	Young's modulus of elasticity
$E_{\omega,\theta}$	Young's modulus which depends on ω and θ
G	Shear modulus of elasticity
$G_{\omega,\theta}$	Shear modulus which depends on ω and θ
D	Flexural rigidity of plate defined in equation (4.13)
h	Thickness of plate
a	Outside radius of plate
b	Inner radius of plate
c	Radius of loaded portion of plate
p	Load intensity
p_g	Gas pressure
t	Time
t_0	Initial time
t_1	Final time

LIST OF SYMBOLS
(continued)

ρ	Mass density
k	Spring stiffness
C_c	Dashpot strength
θ	Temperature; polar coordinate
λ	Lame constant
$\bar{T}$	Total kinetic energy of plate
$\bar{V}$	Total potential energy of plate
$\bar{W}$	Strain energy per unit area of plate
W_s	Strain energy density function
k^2	Shear coefficient defined in equations (4.11)
q	Generalized coordinate defined in equations (7.18)
$\bar{q}$	Amplitude of q
A, B, C, F; A, B, C, with subscripts	Constants
J_m, Y_m	Bessel functions of order m and of the first and second kinds respectively
I_m, K_m	Modified Bessel functions of order m and of the first and second kinds respectively
R, W, T, P, Ω, β, γ	Dimensionless quantities defined on page 31 (R also denotes coefficient of rotary inertia)
$\bar{\Omega}$	Dimensionless frequency of the first thickness-shear mode of an infinite plate

LIST OF SYMBOLS
(continued)

T_1	Time of rise of pulse load
α	Parameter defined by equation (7.5)
K^2	Shear coefficient defined by equation (7.5)
P_0	Dimensionless total load
τ	Dummy time variable
ϕ, w_3	Displacement potentials defined by equations (5.1)
w_1, w_2	Displacement components defined by equations (5.10)
W_1, W_2	Dimensionless displacement components
W_3	Dimensionless displacement potential
η	Function defined by equation (4.17)
μ	Decay constant (dimensional and nondimensional)
N_1, N_2, N_3	Quantities defined by equations (8.41)
M_1, M_2, M_3	Quantities defined by equations (8.44)
δ_0, δ_3	Quantities defined in equations (5.4)
δ_1, δ_2	Quantities defined in equation (5.9)
σ_1, σ_2	Quantities defined in equation (5.16)
δ	Quantity defined in equation (10.2)
m	Mass attached to plate
m_p	Mass of plate
Λ	Mass ratio defined by equation (9.11)
M, K	Dimensionless mass and spring stiffness defined on page 92
M_p	Dimensionless plate mass
x_1, x_2, x_3	Coordinates, displacements
L	Wavelength

LIST OF SYMBOLS

(continued)

c_f	Velocity of flexural waves
c_s	Velocity of shear waves
c_1	Velocity of dilational waves
$a_1, a_2, a_3 \ldots$ $b_1, b_2, b_3 \ldots$	Fourier coefficients defined in equation (8.47)
ω_r	Angular velocity of rotating disk
M_a	Absorber mass
K_a	Absorber spring stiffness
Ω_a	Natural frequency of absorber
M_d	Dimensionless mass per unit area of plate
Z	Total impedance
Z_m	Impedance of mass M
Z_k	Impedance of spring K
Z_c	Impedance of dashpot C_c
Z_0	Driving-point impedance of plate
Z_{m0}	Driving-point impedance of mass-loaded plate
Z_n	Normalized impedance
Z_a	Absorber impedance
Z_{ch}	Characteristic impedance
Z_{k0}	Driving-point impedance of spring-loaded plate

LIST OF SYMBOLS
(continued)

Z_{a0}	Driving-point impedance of plate to which absorber is attached
Z_{mn}	Normalized driving-point impedance of mass-loaded plate
F_0	Applied force
F_1	Transmitted force
F_z	Force due to motion of impedance
F_p	Force due to motion of plate; force in the link joining mass and plate
V	Velocity
V_0	Velocity of the center of plate
T_0	Transmissibility across plate
T_m	Transmissibility across mass-loaded plate
T_a	Transmissibility across absorber-mounted plate
T_{am}	Transmissibility across mass-loaded and absorber-mounted plate
T_k	Transmissibility across spring-loaded plate
T_{km}	Transmissibility across mass and spring-loaded plate
δ_e	Loss factor associated with linear deformation and defined by equation (F.4)
s, g, D_e	Quantities defined by equations (F.7)
e	Base of natural logarithm
i	$\sqrt{-1}$ when used as a complex quantity
$i = 1,2,3 \ldots$ $j = 1,2,3 \ldots$ $n = 1,2,3 \ldots$	Running index; number of modes
m	Number of diametral nodes

LIST OF SYMBOLS

(continued)

∇^2	$\frac{\partial^2}{\partial r^2} + \frac{1}{r}\frac{\partial}{\partial r} + \frac{1}{r^2}\frac{\partial^2}{\partial \theta^2}$
$-$ ($\bar{F}$)	Bar over letter denotes amplitude
* (x^*)	Asterisk denotes complex quantity
$\cdot$ ($\dot{W}$)	Dot over letter denotes differentiation with respect to time
~ ($\tilde{V}$)	Tilde over letter denotes sinusoidally varying quantity
' (J')	Prime denotes differentiation with respect to spatial coordinate
[ ]	Square matrix
{ }	Column matrix
$\Vert\ \Vert$	Determinant
$\vert\ \vert$	Absolute value
$U(R)$, $U(T)$, $U(R-\gamma)$	Unit step functions defined by, for example $U(R-\gamma) = 0, \quad -\infty < R < \gamma$ $U(R-\gamma) = 1, \quad \gamma \le R < \infty$
$\delta(R)$, $\delta(R-\gamma)$	Dirac delta functions defined by, for example, $\delta(R-\gamma) = 0, \quad R \neq \gamma$ $\int_{-\infty}^{\infty} \delta(R-\gamma)dR = 1$ $\int_{-\infty}^{\infty} \delta(R-\gamma)F(R)dR = F(\gamma)$
$\Vert\ \Vert_{(\delta)}$, $[\ ]_{(\delta)}$	δ denotes argument of function

I. INTRODUCTION

A. Importance of the Problem

In the design of structures and equipment utilizing plate components, a major problem is concerned with the determination of deformation and stresses in plates when subjected to rapidly applied, time-dependent transverse surface loads as well as time-dependent boundary conditions. Such problems arise especially in the aircraft industry since aircraft structures and mounted equipment must withstand blasts, landing impacts and a variety of other transient loads.

A complex structure of plates and framing does not seem to be amenable to detailed mathematical analysis. However, some insight into the problem may be obtained by considering a model system, suitably idealized to permit correct mathematical analysis. Toward this end, the vibratory response of a uniform circular plate to axisymmetric loading is studied in detail in this investigation.

In some acoustical devices, circular disks are required to resonate at certain frequencies at particular modes. For example, the clamped plate is used in electromagnetic telephone receivers, carbon microphones and subaqueous condenser microphones. Such applications require accurate computation of the first few natural frequencies of the disk. Since many such devices are required to function satisfactorily over a wide range of temperatures and since for most materials Poisson's ratio varies with temperature, the study of the effect of Poisson's ratio on frequencies of transverse vibration is also of practical significance.

For the past few years there has been a growing interest in the field of noise control. Quieting of noisy equipment necessitates the consideration of both vibration and sound [1]*. In many instances, the noise radiating part may be a plate component, or a plate on which a machine is mounted [2]. Accurate determination of flexural vibration frequencies and impedance of the system are essential in analyzing the noise problem and devising means to reduce or to eliminate the noise.

In many applications, the frequencies of nonaxisymmetrical vibrations are of interest. For example, in cases like turbine disks, vibrations with one or more diametral nodes are of concern because failures of such disks are generally attributed to resonance with one of these frequencies [3]. Correct determination of such frequencies are therefore helpful in the design and operation of turbines.

In the case of equipment mounted on a component plate, the determination of the forces which act on the equipment as a result of excitation to the structure, is of great practical importance. In other cases, the forces that are transmitted to the structure as a result of unbalance in the moving parts of the equipment may be of interest. In both cases, the determination of the transmissibility across the plate for the common types of loading and boundary conditions is essential for the design of the structure and the equipment mounting. The design of dynamic vibration absorbers for isolating one or more dangerous frequencies is also important in many applications.

B. Available Theories and Methods

In all the cases mentioned above, the scope and usefulness of the classical Poisson-Kirchoff plate equation are limited because, even for a thin plate, it predicts the actual behavior only for the first few

Numbers in brackets refer to the bibliography.

modes [4]. It is observed that for higher flexural modes the influence of coupling between flexure and thickness-shear modes, and that between flexure and thickness-twist modes, becomes increasingly important. R. D. Mindlin [4] has recently published a refined plate theory, a two dimensional analog of Rayleigh-Timoshenko beam equation, which takes into account the above coupling effects by including shear deformation and rotary inertia effects in the equations of motion. The improved theory is found to yield satisfactory results for thick plates and for higher modes [4].

The conventional normal-mode solution [5,6] for the response of a structure to transient loads is not suitable for time-dependent boundary conditions. An improved normal-mode solution suggested by D. Williams [7] is readily applicable to time-dependent boundary conditions. In the Williams method, the dynamic solution is represented as an eigenfunction expansion about the so-called static solution [8]. It is particularly suitable where the response function is discontinuous because the discontinuity can be contained in the static portion of the solution, and the series is only required to produce a continuous remainder. The static part of the solution can be easily obtained by direct integration of the homogeneous plate equation. Moreover, the Williams-type series is found to converge more rapidly than the conventional type modal series [8,9]. These so-called static solutions differ from the Reissner-Goodier solutions for plates only in the value of a constant for which Reissner uses 5/6, whereas Mindlin uses $\pi^2/12$ or a value which depends on the Poisson's ratio.

The conventional methods for determining the frequencies of vibration of constrained structures employ mode-summation techniques and usually result in series-type frequency equations [6]. These equations require as many natural frequencies of the unconstrained structure as there are terms in the series and give only the same number of constrained frequencies. The accuracy of the calculated frequencies depends on the number of terms included in the series. Moreover, computations with series solutions are time consuming and laborious.

C. Methods Developed in this Investigation

Using Mindlin's improved theory of plates, two series type frequency equations and one closed-form frequency equation are developed in this investigation for a circular plate loaded with an arbitrary load impedance at the center. The closed-form frequency equation can be solved to yield an infinite number of frequencies of the constrained plate without using the frequencies of the unconstrained plate as is required in series type equations. Also, the closed-form equation is less time consuming and easier to program on a digital computer.

From the extensive literature in the field of sound and vibration isolation, very little information is available on methods to determine the impedance and transmissibility of free and constrained plates which are driven by time-varying forces. It is found that the method used for deriving the closed-form frequency equation for constrained plates can be extended to obtain closed-form expressions for impedance and transmissibility of circular plates which are constrained at the center and driven by time-varying forces at the center. Expressions for transmissibility of plates loaded at the center and to which dynamic vibration absorbers are attached at the center are also derived in closed-form in this investigation.

Nondimensional quantities are used throughout this work in order to make derivations and computations easier and the results more general for applications.

II. REVIEW OF LITERATURE

The problem of free transverse vibration of circular elastic plates has attracted the interest of investigators for well over a century. Poisson [10] analyzed radially symmetric, free transverse vibrations, and Kirchoff [11] considered nonaxisymmetric vibrations. More recent investigations of plate vibration include the integral-transform approach of Sneddon [12] who treats axisymmetric vibrations; the separable product solutions of Flynn [13] who analyzes plates with impulsive pressure loading, and Wah [14] who considers vibration of circular plates with large initial tension or compression; the harmonic analysis approach of Eringen [15] who treats damped plates under stochastic loading; the Laplace-transform method of Mase [16] who investigates the dynamic response of viscoelastic plates; the Ritz-Galerkin method of Bauer [17] who analyzes nonlinear response of elastic plates to pulse excitations; and the singularity solution concept of Reismann [18] who treats a clamped plate with a harmonically oscillating transverse load. Kantham [19] determined the frequencies and normal modes of an elastically built-in plate; Reid [20] considered the free vibration of an initially deformed circular plate following its sudden release; and Weiner [21] investigated the response of a thin elastic plate to axisymmetric, time-varying transverse loading. The response of a circular plate of large radius to sharp transient loading was investigated by Medick [22] both analytically and experimentally.

Transverse vibrations of clamped and free circular plates of uniform thickness carrying concentrated masses at the center are investigated by Roberson [23,24] using Laplace transform methods. Tyutekin [25] has presented a solution to the flexural vibrations of a circular disk loaded at the center with an arbitrary load impedance. Vibrations of rectangular plates are investigated by Das [26] who derived a series form solution for the frequencies of plates loaded with concentrated masses, springs and dashpots and by Stokey [27], who employed Lagrange's equation and a series solution for the frequency of a plate carrying any number of finite masses.

Other important investigators of plate vibrations include Kirk [28], Stanisic [29], Greene [30], Lange [31], Skudrzyk [32], Flinn [33], Hencky [34], Heckel [35,36], Chou [37] and Chree [38].

All the investigations mentioned above are based on the classical Poisson-Kirchoff plate equation. An improved theory of plate vibrations which takes into account the effect of transverse shear and rotary inertia was published by Mindlin [4] in 1951. Applications of his theory to disk vibrations [39,40], to crystal plate vibrations [41,42] and to wave propagation [43] were subsequently published by him. A detailed discussion on the boundary conditions applicable to Mindlin's theory is given by Callahan [44]. Kalnins [45,46] has successfully applied Mindlin's theory to vibration of a spherical shell. Sharma [47] has made use of Mindlin's equations to study the effect of Poisson's ratio on frequency of vibration. More recent contributions using Mindlin's theory include the forced motion solution of Reismann [8] who uses a Williams-type normal-mode solution to determine the response of a plate to a rapidly applied transverse load, and the fundamental solution [48] of Kalnins [49] who utilizes Green's functions to determine the response of a plate to a harmonically oscillating load situated at an arbitrary point on the plate.

Vibration of plates including the effect of transverse shear deformation and rotary inertia is investigated also by Reissner [50] who gives a solution expressed in terms of Bessel functions for axisymmetric vibration of circular plates of uniform thickness and by Huang [51], who discusses the application of variational methods for the formulation of plate vibration problems. Closed-form solutions for the static response of plates of variable thickness are given by Conway [52,53].

Since most vibration problems in plates, beams and other continuous structures use identical solution techniques, it will be worthwhile to examine some useful developments in beam vibrations and related topics. Williams [7] has developed an improved normal mode solution for forced vibration problems which can be applied to time-dependent boundary conditions. The Williams method was discussed favourably by Ramberg [54] in the analysis of transient vibration of an airplane wing. Recently Leonard [9] employed the Williams method to transient response of beams and Sheng [55] extended it to vibration of shell structures. Transient response problems are also investigated by Isakon [56], Dohrenwend [57] and Plass [58]. Vibrations of constrained beams are studied in detail by Dana Young [59] and by Lee [60].

Practically no literature was found during the course of this investigation on impedance and transmissibility of force-driven plates. For rods and beams, a major contribution to this field is due to Snowdon [61-67] who treats beams with internal damping using both Bernoulli-Euler and Rayleigh-Timoshenko theories. He has also given a detailed study on internal material damping [68-70]. A good treatment of sound radiation, material damping and plate vibrators is given by Skudrzyk [71].

Properties of Bessel functions and integrals of products of Bessel functions which are very useful in this investigation are treated elaborately by Watson [72] and by McLachlan [73].

III. OBJECTIVES OF INVESTIGATION

A number of desirable areas of investigation in circular plate vibration in the fields of general design, acoustics and vibration isolation are mentioned in the first chapter. The limitations of conventional theories and methods, new theories and methods which are recently introduced, and methods developed in this investigation are also discussed. It is also found from the survey of literature that only a very limited amount of work has been done in many of the areas of practical interest mentioned earlier. The objective of this work is to investigate several of the above problems in detail using improved theories and methods and to provide as much information and data as is possible that will be of use in the proper design of plate components in their respective fields of application.

The basic equations of transverse vibrations of plates will be derived in polar coordinates using Mindlin's improved theory. The homogeneous solution of the equation of motion will be used to determine axisymmetric and antisymmetric natural frequencies of plates under different boundary conditions. The effect of Poisson's ratio on natural frequencies will also be studied.

Using a Williams-type normal-mode solution, the displacement and acceleration response of circular plates to different types of rapidly applied steady loads and pulse loads will be investigated in detail. The effect of load distribution, pulse shape and duration of pulse on response and on the convergence of the modal series will also be considered.

A closed-form frequency equation will be derived for transverse vibration of circular plates loaded at the center with an arbitrary impedance and this will be used to determine the frequencies for a number of specific forms of the impedance. It is also proposed to derive closed-form expressions for the impedance and transmissibility of plates loaded at the center and driven at the center by time-varying forces and to use these expressions to obtain impedance and transmissibility curves for the most common types of loading. The design of dynamic vibration absorbers and their tuning to provide isolation for a particular excitation frequency will also be considered in detail. The effect of material damping on impedance and transmissibility will be treated in general, but detailed application will be limited to the classical theory.

Wherever desirable, the results of the improved theory will be compared with those obtained using the classical theory. The main objective of this comparison will be to assess the applicability and limitations of the classical theory in the fields of free, transient and steady state vibrations.

IV. DEVELOPMENT OF THE THEORY

Differential equations for flexural vibration of circular plates, allowing for the effect of transverse shear and rotary inertia, can be developed in a very straightforward manner suggested by Mindlin [4]. Mindlin described the derivation in rectangular coordinates. In polar coordinates the procedure is similar and will be given here.

A. Basic Equations

The plate-stress components are (see Lehnhoff [74], p. 7)

$$\begin{aligned} M_r &= \int z\, \sigma_r \, dz \\ M_\theta &= \int z\, \sigma_\theta \, dz \\ M_{r\theta} &= \int z\, \tau_{r\theta} \, dz = M_{\theta r} \\ Q_r &= \int \tau_{rz} \, dz \\ Q_\theta &= \int \tau_{\theta z} \, dz \end{aligned} \tag{4.1}$$

Neglecting body forces, the stress equations of motion in cylindrical coordinates are [75]

$$\begin{aligned} \frac{\partial \sigma_r}{\partial r} + \frac{1}{r}\frac{\partial \tau_{r\theta}}{\partial \theta} + \frac{\partial \tau_{rz}}{\partial z} + \frac{\sigma_r - \sigma_\theta}{r} &= \rho \frac{\partial^2 u_r}{\partial t^2} \\ \frac{\partial \tau_{r\theta}}{\partial r} + \frac{1}{r}\frac{\partial \sigma_\theta}{\partial \theta} + \frac{\partial \tau_{\theta z}}{\partial z} + \frac{2\tau_{r\theta}}{r} &= \rho \frac{\partial^2 u_\theta}{\partial t^2} \\ \frac{\partial \tau_{rz}}{\partial r} + \frac{1}{r}\frac{\partial \tau_{\theta z}}{\partial \theta} + \frac{\partial \sigma_z}{\partial z} + \frac{\tau_{rz}}{r} &= \rho \frac{\partial^2 u_z}{\partial t^2} \end{aligned} \tag{4.2}$$

The stress-strain relations are (see Boresi [76], p. 114)

$$\begin{aligned} \sigma_r &= \lambda(\varepsilon_r + \varepsilon_\theta + \varepsilon_z) + 2G\varepsilon_r \\ \sigma_\theta &= \lambda(\varepsilon_r + \varepsilon_\theta + \varepsilon_z) + 2G\varepsilon_\theta \\ \sigma_z &= \lambda(\varepsilon_r + \varepsilon_\theta + \varepsilon_z) + 2G\varepsilon_z \\ \tau_{r\theta} &= G\gamma_{r\theta} \\ \tau_{rz} &= G\gamma_{rz} \\ \tau_{\theta z} &= G\gamma_{\theta z} \end{aligned} \tag{4.3}$$

The strain-displacement relations in polar coordinates are (see Boresi [76], p. 248)

$$\begin{aligned}
\varepsilon_r &= \frac{\partial u_r}{\partial r}, \quad \varepsilon_\theta = \frac{\partial u_\theta}{r\partial\theta} + \frac{u_r}{r}, \quad \varepsilon_z = \frac{\partial w}{\partial z} \\
\gamma_{\theta z} &= \frac{\partial w}{r\partial\theta} + \frac{\partial u_\theta}{\partial z} \\
\gamma_{rz} &= \frac{\partial w}{\partial r} + \frac{\partial u_r}{\partial z} \\
\gamma_{r\theta} &= \frac{\partial u_r}{r\partial\theta} + \frac{\partial u_\theta}{\partial r} - \frac{u_\theta}{r}
\end{aligned} \tag{4.4}$$

The relations between elastic constants are [76]

$$G = \frac{E}{2(1+\nu)}, \quad \lambda = \frac{\nu E}{(1+\nu)(1-2\nu)} \tag{4.5}$$

B. Derivation of Mindlin's Improved Theory

The plate is referred to a r, θ, z coordinate system (see figure 1). The faces of the plate are the planes $z = \pm \frac{h}{2}$ and its cylindrical surfaces are defined by plane curves or polygons parallel to the r-θ plane. The faces of the plate are assumed to be free of tangential traction, but under normal pressures p_1 and p_2. Thus, we have

$$\begin{aligned}
\tau_{rz}\Big]_{z=\pm\frac{h}{2}} &= \tau_{\theta z}\Big]_{z=\pm\frac{h}{2}} = 0 \\
\sigma_z\Big]_{z=+\frac{h}{2}} &= -p_1(r,\theta,t) \\
\sigma_z\Big]_{z=-\frac{h}{2}} &= -p_2(r,\theta,t)
\end{aligned} \tag{4.6}$$

Let $p = p_2 - p_1$

Normal pressures are retained on both faces in order that one of them may, if desired, be made proportional to the transverse displacement to simulate the effect of an elastic foundation [4].

It is assumed that u_r and u_θ are proportional to z and u_z is independent of z (see reference 4, p. 32 and appendix A). Thus, we have

$$u_r = z\psi_r(r,\theta,t)$$
$$u_\theta = z\psi_\theta(r,\theta,t) \qquad (4.7)$$
$$u_z = w(r,\theta,t)$$

ψ_r, ψ_θ, and w are called plate-displacement components.

1. Plate-Stress-Displacement Relations

In the three-dimensional theory of elasticity there are six components of stress which are expressed in terms of six components of strain through Hooke's law. In the present theory there are only five "plate-stress components" [see equation (4.1)] and these will be expressed in terms of the same number of strain components. The latter will be expressed in terms of three "plate-displacement components".

From equations (4.3), solving the equation containing σ_z for ε_z gives

$$\varepsilon_z = \frac{\sigma_z - \lambda(\varepsilon_r+\varepsilon_\theta)}{(2G+\lambda)} \qquad (4.8)$$

Substituting this value of ε_z in the first of equations (4.3) one obtains

$$\sigma_r = \frac{(4G^2+4G\lambda)}{(2G+\lambda)}\varepsilon_r + \frac{2G\lambda}{(2G+\lambda)}\varepsilon_\theta + \frac{\lambda}{(2G+\lambda)}\sigma_z \qquad (4.9)$$

Using equations (4.5), equation (4.9) yields

$$\sigma_r = \frac{E}{1-\nu^2}\varepsilon_r + \frac{\nu E}{1-\nu^2}\varepsilon_\theta + \frac{\nu}{1-\nu}\sigma_z \qquad (4.10a)$$

A similar procedure on the other equations of (4.3) gives

$$\sigma_\theta = \frac{E}{1-\nu^2}\varepsilon_\theta + \frac{\nu E}{1-\nu^2}\varepsilon_r + \frac{\nu}{1-\nu}\sigma_z$$

$$\tau_{r\theta} = \frac{E}{2(1+\nu)}\gamma_{r\theta}\ ,\ \tau_{rz} = G\gamma_{rz}\ ,\ \tau_{\theta z} = G\gamma_{\theta z} \qquad (4.10b)$$

Equations (4.10) are now integrated over the plate thickness to convert them into plate-stress components in accordance with equations (4.1). The results are then altered in two respects: (a) the integrals containing σ_z are dropped; (b) the coefficients of the integrals containing γ_{rz} and $\gamma_{\theta z}$ are replaced by constants whose magnitudes are to be determined later (see reference 4, p. 32 and appendix A).

This process yields

$$
\begin{aligned}
M_r &= \frac{E}{1-\nu^2}\int \varepsilon_r z\,dz + \frac{\nu E}{1-\nu^2}\int \varepsilon_\theta z\,dz \\
M_\theta &= \frac{E}{1-\nu^2}\int \varepsilon_\theta z\,dz + \frac{\nu E}{1-\nu^2}\int \varepsilon_r z\,dz \\
M_{r\theta} &= \frac{E}{2(1+\nu)}\int \gamma_{r\theta} z\,dz \qquad (4.11) \\
Q_r &= k^2 G\int \gamma_{rz}\,dz \\
Q_\theta &= k^2 G\int \gamma_{\theta z}\,dz
\end{aligned}
$$

Substituting equations (4.4) into equations (4.11) and using equations (4.7) one obtains

$$
\begin{aligned}
M_r &= \frac{E}{1-\nu^2}\int \frac{\partial\psi_r}{\partial r} z^2 dz + \frac{\nu E}{1-\nu^2}\int \left(\frac{\partial\psi_\theta}{r\partial\theta} + \frac{\psi_r}{r}\right) z^2 dz \\
M_\theta &= \frac{\nu E}{1-\nu^2}\int \frac{\partial\psi_r}{\partial r} z^2 dz + \frac{E}{1-\nu^2}\int \left(\frac{\partial\psi_\theta}{r\partial\theta} + \frac{\psi_r}{r}\right) z^2 dz \\
M_{r\theta} &= \frac{E}{2(1+\nu)}\int \left(\frac{1}{r}\frac{\partial\psi_r}{\partial\theta} + \frac{\partial\psi_\theta}{\partial r} - \frac{1}{r}\psi_\theta\right) z^2 dz \qquad (4.12) \\
Q_r &= k^2 G\int \left[\frac{\partial w}{\partial r} + \frac{\partial(z\psi_r)}{\partial z}\right] dz \\
Q_\theta &= k^2 G\int \left[\frac{\partial w}{r\partial\theta} + \frac{\partial(z\psi_\theta)}{\partial z}\right] dz
\end{aligned}
$$

Carrying out the integrations from $-\frac{h}{2}$ to $+\frac{h}{2}$, equations (4.12) yields

$$
\begin{aligned}
M_r &= D\left[\frac{\partial\psi_r}{\partial r} + \frac{\nu}{r}\left(\psi_r + \frac{\partial\psi_\theta}{\partial\theta}\right)\right] \\
M_\theta &= D\left[\nu\frac{\partial\psi_r}{\partial r} + \frac{1}{r}\left(\psi_r + \frac{\partial\psi_\theta}{\partial\theta}\right)\right] \\
M_{r\theta} &= \frac{D}{2}(1-\nu)\left[\frac{1}{r}\left(\frac{\partial\psi_r}{\partial\theta} - \psi_\theta\right) + \frac{\partial\psi_\theta}{\partial r}\right] \qquad (4.13) \\
Q_r &= k^2 Gh\left(\psi_r + \frac{\partial w}{\partial r}\right) \\
Q_\theta &= k^2 Gh\left(\psi_\theta + \frac{1}{r}\frac{\partial w}{\partial\theta}\right)
\end{aligned}
$$

where $D = \dfrac{Eh^3}{12(1-\nu^2)}$ is the flexural rigidity of the plate.

k^2 is a constant which depends on the z-dependence of the shear stress through the thickness of the plate (see appendices A and B).

Equations (4.13) would have been obtained if it had been assumed that $\sigma_z = 0$ at the start. However, the procedure adopted reveals that only a linearly weighted, average effect of σ_z is neglected, rather than σ_z itself (see reference 4, p. 32).

2. Plate-Stress Equations of Motion

The first two of equations (4.2) are multiplied by z and integrated over the plate thickness. This gives

$$\int \frac{\partial \sigma_r}{\partial r} zdz + \frac{1}{r} \int \frac{\partial \tau_{r\theta}}{\partial \theta} zdz + \int \frac{\partial \tau_{rz}}{\partial z} zdz + \int \frac{(\sigma_r - \sigma_\theta)}{r} zdz = \int \rho \frac{\partial^2 u_r}{\partial t^2} zdz$$

$$\int \frac{\partial \tau_{r\theta}}{\partial \theta} zdz + \frac{1}{r} \int \frac{\partial \sigma_\theta}{\partial \theta} zdz + \int \frac{\partial \tau_{\theta z}}{\partial z} zdz + \int \frac{2\tau_{r\theta}}{r} zdz = \int \rho \frac{\partial^2 u_\theta}{\partial t^2} zdz$$

The third of equations (4.2) is integrated over the plate thickness to give

$$\int \frac{\partial \tau_{zr}}{\partial r} dz + \frac{1}{r} \int \frac{\partial \tau_{z\theta}}{\partial \theta} dz + \int \frac{\partial \sigma_z}{\partial z} dz + \int \frac{\tau_{rz}}{r} dz = \int \rho \frac{\partial^2 u_z}{\partial t^2} dz$$

Using equations (4.1), (4.6) and (4.7), these become

$$\begin{aligned}
&\frac{\partial M_r}{\partial r} + \frac{1}{r} \frac{\partial M_{r\theta}}{\partial \theta} + \frac{M_r - M_\theta}{r} - Q_r = \frac{\rho h^3}{12} \frac{\partial^2 \psi_r}{\partial t^2} \\
&\frac{\partial M_{r\theta}}{\partial r} + \frac{1}{r} \frac{\partial M_\theta}{\partial \theta} + \frac{2M_{r\theta}}{r} - Q_\theta = \frac{\rho h^3}{12} \frac{\partial^2 \psi_\theta}{\partial t^2} \\
&\frac{\partial Q_r}{\partial r} + \frac{1}{r} \frac{\partial Q_\theta}{\partial \theta} + \frac{Q_r}{r} + p = \rho h \frac{\partial^2 w}{\partial t^2}
\end{aligned} \tag{4.14}$$

The right hand sides of the first two of equations (4.14) represent the effect of rotary inertia.

3. Plate-Displacement Equations of Motion

The plate-stress equations of motion, equations (4.14), may be expressed in terms of plate displacements ψ_r, ψ_θ, and w by using equations (4.13). The result is

$$\frac{D}{2}\left[(1-\nu)\nabla^2\psi_r + (1+\nu)\frac{\partial\eta}{\partial r}\right] - \frac{D}{2}(1-\nu)\left(\frac{\psi_r}{r^2} + \frac{2}{r^2}\frac{\partial\psi_\theta}{\partial\theta}\right)$$
$$- k^2Gh\left(\psi_r + \frac{\partial w}{\partial r}\right) = \frac{\rho h^3}{12}\frac{\partial^2\psi_r}{\partial t^2}$$

$$\frac{D}{2}\left[(1-\nu)\nabla^2\psi_\theta + (1+\nu)\frac{\partial\eta}{r\partial\theta}\right] - \frac{D}{2}(1-\nu)\left(\frac{\psi_\theta}{r^2} - \frac{2}{r^2}\frac{\partial\psi_r}{\partial r}\right)$$
$$- k^2Gh\left(\psi_\theta + \frac{\partial w}{r\partial\theta}\right) = \frac{\rho h^3}{12}\frac{\partial^2\psi_\theta}{\partial t^2} \qquad (4.15)$$

$$k^2Gh\left(\nabla^2 w + \eta\right) + p = \rho h\frac{\partial^2 w}{\partial t^2}$$

where

$$\nabla^2 = \left(\frac{\partial^2}{\partial r^2} + \frac{1}{r}\frac{\partial}{\partial r} + \frac{1}{r^2}\frac{\partial^2}{\partial\theta^2}\right) \qquad (4.16)$$

$$\eta = \left(\frac{\partial\psi_r}{\partial r} + \frac{1}{r}\frac{\partial\psi_\theta}{\partial\theta} + \frac{\psi_r}{r}\right) \qquad (4.17)$$

Equations (4.13) and equations (4.14) or (4.15) form a set of eight coupled linear partial differential equations governing the forces, moments and displacements of plates.

It may be noted that at various stages of the development there is a very close similarity between Mindlin's theory and Reissner's theory [77-81] of flexural equilibrium of plates. Of special interest is the fact that, as in Reissner's theory, three boundary conditions are to be satisfied rather than the two of the classical theory. Also, the constant k^2 which depends on the z-dependence of the shear stress through the thickness of the plate is taken as $\pi^2/12$ in Mindlin's theory, a value very close to Reissner's 5/6.

V. HOMOGENEOUS SOLUTION

The subsequent investigation of forced motion of plates will require a study of free vibrations with homogeneous boundary conditions. Moreover, in many applications the frequencies and mode shapes of free vibration are important. For this reason we consider solutions of the homogeneous differential equations which are obtained by setting p = 0 in equations (4.15).

A. Uncoupling the Equations of Motion

In the absence of applied loads the equations (4.15) can be uncoupled by making the substitution

$$\begin{aligned} \psi_r &= \frac{\partial \phi}{\partial r} + \frac{\partial w_3}{r\partial \theta} \\ \psi_\theta &= \frac{\partial \phi}{r\partial \theta} - \frac{\partial w_3}{\partial r} \end{aligned} \tag{5.1}$$

Setting p = 0 in equations (4.15) and assuming separable solutions of the form

$$\begin{aligned} w(r,\theta,t) &= w(r,\theta)\ e^{i\omega t} \\ \psi_r(r,\theta,t) &= \psi_r(r,\theta)\ e^{i\omega t} \\ \psi_\theta(r,\theta,t) &= \psi_\theta(r,\theta)\ e^{i\omega t} \end{aligned} \tag{5.2}$$

one obtains by using equations (5.1) and manipulating the result

$$\begin{aligned} &\frac{\partial}{\partial r}\,[\nabla^2\phi + (R\delta_o^{\,4} - S^{-1})\phi - S^{-1}w] + \frac{1-\nu}{2}\,\frac{\partial}{r\partial\theta}\,(\nabla^2+\delta_3^{\,2})w_3 = 0 \\ &\frac{\partial}{r\partial\theta}\,[\nabla^2\phi + (R\delta_o^{\,4} - S^{-1})\phi - S^{-1}w] - \frac{1-\nu}{2}\,\frac{\partial}{\partial r}\,(\nabla^2+\delta_3^{\,2})w_3 = 0 \\ &\nabla^2(\phi+w) + S\delta_o^{\,4}w = 0 \end{aligned} \tag{5.3}$$

where

$$\begin{aligned} R &= \frac{h^2}{12}\ \text{(coefficient of rotary inertia)} \\ S &= \frac{D}{k^2Gh}\ \text{(coefficient of transverse shear)} \end{aligned} \tag{5.4}$$

$$\delta_o^{\ 4} = \frac{\rho\omega^2 h}{D}$$

$$\delta_3^{\ 2} = \frac{2}{1-\nu}\,(R\delta_o^{\ 4} - S^{-1})$$

Differentiating the first of equations (5.3) with respect to r and the second with respect to θ, one obtains

$$\frac{\partial^2}{\partial r^2}\,[\nabla^2\phi + (R\delta_o^{\ 4} - S^{-1})\phi - S^{-1}w] + \frac{1-\nu}{2}\,\frac{\partial^2}{r\partial\theta\partial r}\,(\nabla^2 + \delta_3^{\ 2})w_3$$
$$- \frac{1-\nu}{2}\,\frac{1}{r^2}\,\frac{\partial}{\partial\theta}\,(\nabla^2 + \delta_3^{\ 2})w_3 = 0$$

$$\frac{\partial^2}{r^2\partial\theta^2}\,[\nabla^2\phi + (R\delta_o^{\ 4} - S^{-1})\phi - S^{-1}w] - \frac{1-\nu}{2}\,\frac{\partial^2}{r\partial\theta\partial r}\,(\nabla^2 + \delta_3^{\ 2})w_3 = 0$$

Dividing the first of equations (5.3) by r, one gets

$$\frac{1}{r}\,\frac{\partial}{\partial r}\,[\nabla^2\phi + (R\delta_o^{\ 4} - S^{-1})\phi - S^{-1}w] + \frac{1-\nu}{2}\,\frac{1}{r^2}\,\frac{\partial}{\partial\theta}\,(\nabla^2 + \delta_3^{\ 2})w_3 = 0$$

Adding the above three equations gives

$$\nabla^2[\nabla^2\phi + (R\delta_o^{\ 4} - S^{-1})\phi - S^{-1}w] = 0 \qquad (5.5)$$

Differentiating the first of equations (5.3) with respect to θ and the second with respect to r yields

$$\frac{\partial^2}{r\partial\theta\partial r}\,[\nabla^2\phi + (R\delta_o^{\ 4} - S^{-1})\phi - S^{-1}w] + \frac{1-\nu}{2}\,\frac{\partial^2}{r^2\partial\theta^2}\,(\nabla^2 + \delta_3^{\ 2})w_3 = 0$$

$$\frac{\partial^2}{r\partial\theta\partial r}\,[\nabla^2\phi + (R\delta_o^{\ 4} - S^{-1})\phi - S^{-1}w] - \frac{1}{r^2}\,\frac{\partial}{\partial\theta}\,[\nabla^2\phi + (R\delta_o^{\ 4} - S^{-1})\phi - S^{-1}w]$$
$$- \frac{1-\nu}{2}\,\frac{\partial^2}{\partial r^2}\,(\nabla^2 + \delta_3^{\ 2})\,w_3 = 0$$

Dividing the second of equations (5.3) by r, one obtains

$$\frac{\partial}{r^2\partial\theta}\,[\nabla^2\phi + (R\delta_o^{\ 4} - S^{-1})\phi - S^{-1}w] - \frac{1-\nu}{2}\,\frac{\partial}{r\partial r}\,(\nabla^2 + \delta_3^{\ 2})w_3 = 0$$

Subtracting the last two from the first of the above three equations, we obtain

$$\nabla^2(\nabla^2 + \delta_3^{\ 2})w_3 = 0 \qquad (5.6)$$

Eliminating ϕ from equations (5.5) with the aid of the third of equations (5.3), we get

$$\nabla^4 w + [(R + S)\delta_o^4]\nabla^2 w + (R\delta_o^4 - 1)\delta_o^4 w = 0 \tag{5.7}$$

Equation (5.7) is the uncoupled equation in w. This can be written as

$$(\nabla^2 + \delta_1^2)(\nabla^2 + \delta_2^2)w = 0 \tag{5.8}$$

where

$$\begin{Bmatrix} \delta_1^2 \\ \delta_2^2 \end{Bmatrix} = \frac{\delta_o^4}{2} \left\{ (R+S) \pm \sqrt{(R-S)^2 + 4\delta_o^{-4}} \right\} \tag{5.9}$$

Equation (5.8) can be solved in the form

$$w = w_1 + w_2$$

$$(\nabla^2 + \delta_1^2)w_1 = 0, \quad (\nabla^2 + \delta_2^2)w_2 = 0 \tag{5.10}$$

Let $\phi = (\sigma - 1)\, w$, where σ is a constant. (5.11)

Substituting ϕ in equation (5.5) and in the third of equations (5.3) yields

$$\begin{aligned} &\nabla^2[\nabla^2(\sigma - 1)w + (R\delta_o^4 - S^{-1})(\sigma - 1)w - S^{-1}w] = 0 \\ &\nabla^2 w + \nabla^2\ (\sigma - 1)w + S\delta_o^4 w = 0 \end{aligned} \tag{5.12}$$

From equations (5.12) one obtains

$$\begin{aligned} &\nabla^2[\nabla^2 w + (R\delta_o^4 - S^{-1} - \left\{S(\sigma - 1)\right\}^{-1})w] = 0 \\ &\nabla^2 w + S\delta_o^4\sigma^{-1}w = 0 \end{aligned} \tag{5.13}$$

Equations (5.13) reduce to

$$(\nabla^2 + \delta^2)w = 0 \tag{5.14}$$

if $$\delta^2 = S\delta_o^4\sigma^{-1} = R\delta_o^4 - S^{-1} - \left\{S(\sigma - 1)\right\}^{-1} \tag{5.15}$$

Solving equations (5.15) for σ, one obtains

$$\begin{Bmatrix} \sigma_1 \\ \sigma_1 \end{Bmatrix} = \begin{Bmatrix} \delta_2^{\ 2} \\ \delta_1^{\ 2} \end{Bmatrix} (R\delta_o^{\ 4} - S^{-1})^{-1} \tag{5.16}$$

Now in view of equations (5.11) and (5.14), the square-bracketed terms in equations (5.3) vanish, so that the equation governing w_3 reduces to

$$(\nabla^2 + \delta_3^{\ 2})w_3 = 0 \tag{5.17}$$

To sum up, we may write

$$\begin{aligned} w &= w_1 + w_2 \\ \psi_r &= (\sigma_1 - 1)\frac{\partial w_1}{\partial r} + (\sigma_2 - 1)\frac{\partial w_2}{\partial r} + \frac{\partial w_3}{r\partial\theta} \\ \psi_\theta &= (\sigma_1 - 1)\frac{\partial w_1}{r\partial\theta} + (\sigma_2 - 1)\frac{\partial w_2}{r\partial\theta} - \frac{\partial w_3}{\partial r} \end{aligned} \tag{5.18}$$

and

$$\begin{aligned} (\nabla^2 + \delta_1^{\ 2})w_1 &= 0 \\ (\nabla^2 + \delta_2^{\ 2})w_2 &= 0 \\ (\nabla^2 + \delta_3^{\ 2})w_3 &= 0 \end{aligned} \tag{5.19}$$

It should be noted that w_1 and w_2 are components of displacement perpendicular to the middle plane of the plate, and w_3 is a potential function which gives rise to the twist about the normal to the plane of the plate.

It may also be observed that, if $R = S = 0$, w_3 and σ vanish and $\delta^2 = \pm\delta_o^{\ 2}$. The present equations will then reduce to those of the classical theory where the effects of transverse shear and rotary inertia are ignored.

B. Solution of the Uncoupled Equations

We can obtain a general solution to equations (5.19) without reference to boundary conditions, and to render this solution unique we must specify and satisfy the boundary conditions of the problem. Assuming a separable solution of the form [5]

$$w_1(r,\theta) = R(r)\ \Theta(\theta) \tag{5.20}$$

the first of equations (5.19) yields

$$\left(\frac{d^2R}{dr^2} + \frac{1}{r}\frac{dR}{dr}\right)\Theta + \frac{R}{r^2}\frac{d^2\Theta}{d\theta^2} + \delta_1{}^2 R\Theta = 0$$

This can be separated into two equations

$$-\frac{1}{\Theta}\frac{d^2\Theta}{d\theta^2} = \frac{r^2}{R}\left(\frac{d^2R}{dr^2} + \frac{1}{r}\frac{dR}{dr}\right) + \delta_1{}^2 r^2 = m^2$$

or

$$\frac{d^2\Theta}{d\theta^2} + m^2\Theta = 0 \tag{5.21}$$

$$\frac{d^2R}{dr^2} + \frac{1}{r}\frac{dR}{dr} + (\delta_1{}^2 - \frac{m^2}{r^2})R = 0 \tag{5.22}$$

where the constant m^2 has been chosen to obtain a harmonic equation in θ. Also, because the solution of equation (5.21) must be continuous, implying that the solution for $\theta = \theta_0$ must be identical to the solution for $\theta = \theta_0 + 2\pi i$ $(i = 1,2,3,\ldots)$ for any value of θ_0, m must be an integer.

Equation (5.21) has the solution

$$\Theta_m = C_{1m} \sin m\theta + C_{2m} \cos m\theta, \qquad m = 0,1,2,\ldots \tag{5.23}$$

Equation (5.22) has the solution

$$R_m = C_{3m}J_m(\delta_1 r) + C_{4m}Y_m(\delta_1 r), \qquad m = 0,1,2,\ldots \tag{5.24}$$

where $J_m(\delta_1 r)$ and $Y_m(\delta_1 r)$ are Bessel functions of order m and of the first and second kinds respectively.

Hence the solution for the first of equations (5.19) can be written as

$$\begin{aligned} w_{1mn}(r,\theta) = {} & [A_{1m}J_m(\delta_1 r) + A_{3m}Y_m(\delta_1 r)] \sin m\theta \\ & + [A_{2m}J_m(\delta_1 r) + A_{4m}Y_m(\delta_1 r)] \cos m\theta, \quad m = 0,1,2.. \end{aligned} \tag{5.25}$$

In a similar manner, the solution for the second of equations (5.19) is obtained as

$$w_{2mn}(r,\theta) = [B_{1m}J_m(\delta_2 r) + B_{3m}Y_m(\delta_2 r)]\sin m\theta$$
$$+ [B_{2m}J_m(\delta_2 r) + B_{4m}Y_m(\delta_2 r)]\cos m\theta,$$
$$m = 0,1,2,... \tag{5.26}$$

The solution of equation (5.8) is the sum of solutions (5.25) and (5.26). Hence, we have

$$w_{mn}(r,\theta) = [A_{1m}J_m(\delta_1 r) + A_{3m}Y_m(\delta_1 r) + B_{1m}J_m(\delta_2 r) + B_{3m}Y_m(\delta_2 r)]\sin m\theta$$
$$+ [A_{2m}J_m(\delta_1 r) + A_{4m}Y_m(\delta_1 r) + B_{2m}J_m(\delta_2 r) + B_{4m}Y_m(\delta_2 r)]\cos m\theta,$$
$$m = 0,1,2,... \tag{5.27}$$

The third of equations (5.19) yields

$$w_{3mn}(r,\theta) = [C_{1m}J_m(\delta_3 r) + C_{3m}Y_m(\delta_3 r)]\sin m\theta$$
$$+ [C_{2m}J_m(\delta_3 r) + C_{4m}Y_m(\delta_3 r)]\cos m\theta,$$
$$m = 0,1,2,... \tag{5.28}$$

Having obtained solutions for w_1, w_2 and w_3, ψ_r and ψ_θ are determined by equations (5.18).

For a plate without holes, the solution must be finite at every interior point. This condition eliminates Bessel functions of the second kind from equations (5.27) and (5.28). Hence for a solid plate without holes, the appropriate solutions for w and w_3 are [5,39]

$$\begin{aligned} w_{mn}(r,\theta) &= [A_{1m}J_m(\delta_1 r) + A_{2m}J_m(\delta_2 r)]\cos m\theta \\ w_{3mn}(r,\theta) &= A_{3m}J_m(\delta_3 r)\sin m\theta \end{aligned} \tag{5.29}$$

The subscript n represents the mode number and the subscript m represents the number of diametral nodes. For m = 0, there are no diametral nodes and n - 1 circular nodes. For this case, equation (5.29) specializes to

$$w_{0n}(r,\theta) = A_{10}J_0(\delta_1 r) + A_{20}J_0(\delta_2 r)$$
$$w_{30n}(r,\theta) = 0 \tag{5.30}$$

Equations (5.30) thus represent the solutions of equations (5.19) for the case of axisymmetric vibration of a solid circular plate.

It should be noted that for each frequency ω_{mn} there are two modes, except when m=0, for which we obtain only one mode [5]. Therefore, for $m \neq 0$, the natural modes are degenerate. Since we are interested only in the frequency equations for vibrations with diametral nodes, the form of solution given by equations (5.29) is used for a solid circular plate in view of equations (5.18).

VI. FORMULATION OF BOUNDARY CONDITIONS

The differential equations together with the associated boundary conditions constitute the boundary value problem. The geometry of a system is not always able to provide the necessary number of boundary conditions. Whenever a strain-energy function exists, it is possible to form an expression for the total energy of the system as the sum of kinetic and potential energies. For two-dimensional systems the expression for total energy at time t consists of a line integral and a surface integral, the former representing the work done by external forces along the boundary and the latter representing the work done over the surface. Appropriate initial and boundary conditions which are necessary to ensure a unique solution can be obtained from the expression for total energy. This method will be followed here to establish the necessary initial and boundary conditions for the improved theory of plate vibrations.

A. Energy Functions

The kinetic energy per unit volume according to the general linear theory of elasticity is

$$\frac{\rho}{2}\left[\left(\frac{\partial u_r}{\partial t}\right)^2 + \left(\frac{\partial u_\theta}{\partial t}\right)^2 + \left(\frac{\partial u_z}{\partial t}\right)^2\right]$$

By using equations (4.7) and integrating over the thickness, the kinetic energy per unit area of the plate becomes

$$\frac{\rho h^3}{24}\left[\left(\frac{\partial \psi_r}{\partial t}\right)^2 + \left(\frac{\partial \psi_\theta}{\partial t}\right)^2\right] + \frac{\rho h}{2}\left(\frac{\partial w}{\partial t}\right)^2 \qquad (6.1)$$

The total kinetic energy of the plate at time t is given by

$$\bar{T} = \iint \left\{\frac{\rho h^3}{24}\left[\left(\frac{\partial \psi_r}{\partial t}\right)^2 + \left(\frac{\partial \psi_\theta}{\partial t}\right)^2\right] + \rho h \left(\frac{\partial w}{\partial t}\right)^2\right\} r d\theta dr \qquad (6.2)$$

The strain-energy function W_s in the three-dimensional theory of elasticity is given by

$$2W_s = \sigma_r \varepsilon_r + \sigma_\theta \varepsilon_\theta + \sigma_z \varepsilon_z + \tau_{r\theta}\gamma_{r\theta} + \tau_{rz}\gamma_{rz} + \tau_{\theta z}\gamma_{\theta z} \tag{6.3}$$

Using equations (4.4) and integrating over the plate thickness, the strain energy per unit area of plate becomes

$$\begin{aligned} 2\bar{W} = {} & M_r(\frac{\partial\psi_r}{\partial r}) + M_\theta(\frac{\partial\psi_\theta}{r\partial\theta} + \frac{\psi_r}{r}) + M_{r\theta}(\frac{\partial\psi_r}{r\partial\theta} + \frac{\partial\psi_\theta}{\partial r} - \frac{\psi_\theta}{r}) \\ & + Q_r(\psi_r + \frac{\partial w}{\partial r}) + Q_\theta(\psi_\theta + \frac{\partial w}{r\partial\theta}) \end{aligned} \tag{6.4}$$

The potential energy in the plate at time t is given by

$$\bar{V} = \iint \bar{W} r d\theta dr \tag{6.5}$$

B. Total Energy and External Work

The total energy at time t is the sum of $\bar{T}$ and $\bar{V}$, which may be written as

$$\begin{aligned} \bar{T} + \bar{V} = {} & \int_{t_0}^{t_1} dt \iint \frac{\partial}{\partial t} \left\{ \frac{\rho h^3}{24} \left[(\frac{\partial\psi_r}{\partial t})^2 + (\frac{\partial\psi_\theta}{\partial t})^2 \right] + \rho h (\frac{\partial w}{\partial t})^2 \right\} r d\theta dr \\ & + \int_{t_0}^{t_1} dt \iint \frac{\partial}{\partial t} \bar{W} r d\theta dr + \bar{T}_0 + \bar{V}_0 \end{aligned} \tag{6.6}$$

where $\bar{T}_0$ and $\bar{V}_0$ are the values of $\bar{T}$ and $\bar{V}$ at an initial time t_0.

Performing the operation $\frac{\partial}{\partial t}$, the first integrand becomes

$$\frac{\rho h^3}{12} [\frac{\partial\psi_r}{\partial t} \frac{\partial^2\psi_r}{\partial t^2} + \frac{\partial\psi_\theta}{\partial t} \frac{\partial^2\psi_\theta}{\partial t^2}] + \rho h \frac{\partial w}{\partial t} \frac{\partial^2 w}{\partial t^2} \tag{6.7}$$

Defining plate-strain components

$$\Gamma_r,\ \Gamma_\theta,\ \Gamma_{r\theta} = \frac{12}{h^3}\int_{-\frac{h}{2}}^{\frac{h}{2}} (\varepsilon_r,\ \varepsilon_\theta,\ \varepsilon_z) z dz$$

$$\Gamma_{rz},\ \Gamma_{\theta z} = \frac{1}{h}\int_{-\frac{h}{2}}^{\frac{h}{2}} (\gamma_{rz},\ \gamma_{\theta z}) dz \qquad (6.8)$$

and using equations (4.4), equations (4.13) yield after manipulation

$$\begin{aligned} M_r &= D(\Gamma_r + \nu\Gamma_\theta) \\ M_\theta &= D(\nu\Gamma_r + \Gamma_\theta) \\ M_{r\theta} &= \frac{D}{2}(1-\nu)\Gamma_{r\theta} \\ Q_r &= k^2 G h \Gamma_{rz} \\ Q_\theta &= k^2 G h \Gamma_{\theta z} \end{aligned} \qquad (6.9)$$

In view of equations (6.9), equation (6.4) can be written as

$$2\bar{W} = D(\Gamma_r + \nu\Gamma_\theta)\ \Gamma_r + D(\nu\Gamma_r + \Gamma_\theta)\ \Gamma_\theta + \frac{D}{2}(1-\nu)\ \Gamma_{r\theta}^{\ 2} + k^2 G h(\Gamma_{rz}^{\ 2} + \Gamma_{\theta z}^{\ 2})$$

Rearranging this, one obtains

$$4\bar{W} = D(1+\nu)(\Gamma_r + \Gamma_\theta)^2 + D(1-\nu)[(\Gamma_r - \Gamma_\theta)^2 + \Gamma_{r\theta}^{\ 2}] + 2k^2 G h(\Gamma_{rz}^{\ 2} + \Gamma_{\theta z}^{\ 2}) \qquad (6.10)$$

The second integrand in equation (6.6) now becomes

$$\frac{\partial\bar{W}}{\partial t} = \frac{\partial\bar{W}}{\partial\Gamma_r}\frac{\partial\Gamma_r}{\partial t} + \frac{\partial\bar{W}}{\partial\Gamma_\theta}\frac{\partial\Gamma_\theta}{\partial t} + \frac{\partial\bar{W}}{\partial\Gamma_{r\theta}}\frac{\partial\Gamma_{r\theta}}{\partial t} + \frac{\partial\bar{W}}{\partial\Gamma_{rz}}\frac{\partial\Gamma_{rz}}{\partial t} + \frac{\partial\bar{W}}{\partial\Gamma_{\theta z}}\frac{\partial\Gamma_{\theta z}}{\partial t} \qquad (6.11)$$

From equations (6.10), using equations (6.9), we get

$$\begin{aligned} \frac{\partial\bar{W}}{\partial\Gamma_r} &= M_r \\ \frac{\partial\bar{W}}{\partial\Gamma_\theta} &= M_\theta \\ \frac{\partial\bar{W}}{\partial\Gamma_{r\theta}} &= M_{r\theta} \qquad (6.12) \\ \frac{\partial\bar{W}}{\partial\Gamma_{rz}} &= Q_r \end{aligned}$$

$$\frac{\partial \bar{W}}{\partial \Gamma_{\theta z}} = Q_\theta$$

In view of equations (4.4) and (4.7), equations (6.8) yield

$$\begin{aligned}
\Gamma_r &= \frac{\partial \psi_r}{\partial r} \\
\Gamma_\theta &= \frac{\partial \psi_\theta}{r\partial \theta} + \frac{\psi_r}{r} \\
\Gamma_{r\theta} &= \frac{\partial \psi_r}{r\partial \theta} + \frac{\partial \psi_\theta}{\partial r} - \frac{\psi_\theta}{r} \\
\Gamma_{rz} &= \frac{\partial w}{\partial r} + \psi_r \\
\Gamma_{\theta z} &= \frac{\partial w}{r\partial \theta} + \psi_\theta
\end{aligned} \tag{6.13}$$

Substituting equations (6.12) and (6.13), one obtains from equation (6.10)

$$\begin{aligned}
\frac{\partial \bar{W}}{\partial t} = &\left(M_r \frac{\partial}{\partial r} + M_{r\theta} \frac{\partial}{r\partial \theta} + \frac{M_\theta}{r} + Q_r\right) \frac{\partial \psi_r}{\partial t} \\
&+ \left(M_\theta \frac{\partial}{r\partial \theta} + M_{r\theta} \frac{\partial}{\partial r} - \frac{M_{r\theta}}{r} + Q_\theta\right) \frac{\partial \psi_\theta}{\partial t} \\
&+ \left(Q_r \frac{\partial}{\partial r} + Q_\theta \frac{\partial}{r\partial \theta}\right) \frac{\partial w}{\partial t}
\end{aligned} \tag{6.14}$$

In the surface integral of $\frac{\partial \bar{W}}{\partial t}$, equation (6.6), the terms containing space derivatives may be integrated by parts to obtain

$$\begin{aligned}
\iint \frac{\partial \bar{W}}{\partial t}\, r d\theta dr = &\oint \left(M_r \frac{\partial \psi_r}{\partial t} + M_{r\theta} \frac{\partial \psi_\theta}{\partial t} + Q_r \frac{\partial w}{\partial t}\right) dS \\
&- \iint \frac{\partial \psi_r}{\partial t} \left(\frac{\partial M_r}{\partial r} + \frac{\partial M_{r\theta}}{r\partial \theta} + \frac{M_r}{r}\right) r d\theta dr \\
&- \iint \frac{\partial \psi_\theta}{\partial t} \left(\frac{\partial M_{r\theta}}{\partial r} + \frac{\partial M_\theta}{r\partial \theta} + \frac{M_{r\theta}}{r}\right) r d\theta dr \\
&- \iint \frac{\partial w}{\partial t} \left(\frac{\partial Q_r}{\partial r} + \frac{\partial Q_\theta}{r\partial \theta} + \frac{Q_r}{r}\right) r d\theta dr \\
&+ \iint \frac{\partial \psi_r}{\partial t} \left(\frac{M_\theta}{r} + Q_r\right) r d\theta dr
\end{aligned} \tag{6.15}$$

$$+ \iint \frac{\partial \psi_\theta}{\partial t} \left(- \frac{M_{r\theta}}{r} + Q_\theta \right) r d\theta dr$$

where $dS = rd\theta$

Combining equations (6.7) and (6.15), equation (6.6) becomes

$$\begin{aligned} \bar{T} + \bar{V} = & \int_{t_0}^{t_1} dt \oint \left(M_r \frac{\partial \psi_r}{\partial t} + M_{r\theta} \frac{\partial \psi_\theta}{\partial t} + Q_r \frac{\partial w}{\partial t}\right) dS \\ & + \int_{t_0}^{t_1} dt \iint \left[\frac{\partial \psi_r}{\partial t} \left(\frac{\rho h^3}{12} \frac{\partial^2 \psi_r}{\partial t^2} - \frac{\partial M_r}{\partial r} - \frac{\partial M_{r\theta}}{r \partial \theta} - \frac{M_r - M_\theta}{r} + Q_r \right) \right. \\ & + \frac{\partial \psi_\theta}{\partial t} \left(\frac{\rho h^3}{12} \frac{\partial^2 \psi_\theta}{\partial t^2} - \frac{\partial M_{r\theta}}{\partial r} - \frac{\partial M_\theta}{r \partial \theta} - \frac{2M_{r\theta}}{r} + Q_\theta \right) \\ & \left. + \frac{\partial w}{\partial t} \left(\rho h \frac{\partial^2 w}{\partial t^2} - \frac{\partial Q_r}{\partial r} - \frac{\partial Q_\theta}{r \partial \theta} - \frac{Q_r}{r} \right) \right] r d\theta dr + \bar{T}_0 + \bar{V}_0 \end{aligned} \tag{6.16}$$

If the equations (4.14) of motion are satisfied this reduces to

$$\begin{aligned} \bar{T} + \bar{V} = & \int_{t_0}^{t_1} dt \oint \left(M_r \frac{\partial \psi_r}{\partial t} + M_{r\theta} \frac{\partial \psi_\theta}{\partial t} + Q_r \frac{\partial w}{\partial t}\right) dS \\ & + \int_{t_0}^{t_1} dt \iint p \frac{\partial w}{\partial t} r d\theta dr + \bar{T}_0 + \bar{V}_0 \end{aligned} \tag{6.17}$$

Equations (6.17) shows that the total energy in the plate at time t is equal to the sum of the energy at time t_0 and the work done by the external forces along the edge and over the surface of the plate during the time interval $t_1 - t_0$.

C. Initial and Boundary Conditions

From equation (6.17) the appropriate initial and boundary conditions for the system of differential equations of the improved theory of plate vibration can be deduced. These are: (1) Any combination which contains one member of each of the three pairs of terms in the parentheses under the line integral in equation (6.17) must be specified along the edges of the plate. (2) Either p or w and the initial values of ψ_r, ψ_θ and w and their time derivatives must be specified on the surface of the plate.

It is the specification of the above quantities that makes the solution of the differential equations of the system unique. For homogeneous boundary conditions, equation (6.17) shows that one member of each of the pairs of terms $M_r \frac{\partial \psi_r}{\partial t}$, $M_{r\theta} \frac{\partial \psi_\theta}{\partial t}$ and $Q_r \frac{\partial w}{\partial t}$ must vanish at the boundary.

A discussion of boundary conditions for classical and Mindlin's theories of plate vibration is given in appendix C. A variational formulation of the plate vibration problem is presented in appendix D.

VII. FORCED MOTION SOLUTION

Using an improved normal-mode solution suggested by Williams, a formal solution is presented here for the response of a circular plate under axisymmetric, but otherwise arbitrarily distributed, time-dependent transverse loads and a set of very general stationary or time-dependent boundary conditions.

A. Williams-Type Normal-Mode Solution

In the conventional normal-mode solution for the response of plates to transient loads, the response is expanded in terms of a series of normal modes of the plate. The coefficients of the expansion (the generalized coordinates) are determined from the governing differential equations and the associated boundary and initial conditions. Williams type modal solutions [7] differ from ordinary normal-mode solutions by virtue of the isolation of that part of the response which may be obtained in closed-form by a process of direct integration - the so-called "static" part of the response. Only the remaining "dynamic" part of the response is expanded in series form.

The advantage of the Williams method over the conventional modal solution is its ability to obtain, for many loading conditions, a more accurate result with the same number of terms in the series [8,9]. In the ordinary normal-mode solution, the generalized coordinates are determined from the equation

$$\ddot{q}_i + \Omega_i^2 q_i = \int P(R,T) W_i(R) R dR \tag{7.1}$$

In the Williams method, the corresponding equation is given by equations (7.22) and (7.24). The presence of Ω_i^2 in the denominators of the two terms in equation (7.24) manifests the more rapid convergence of the Williams type solution as compared with that of the ordinary modal analysis.

The Williams method is particularly advantageous where the response function is discontinuous. The discontinuity is contained exactly in the separated static part of the response and the series is only required to produce a continuous remainder.

In the Williams method, the isolated part of the response is called static because significant parts of inertia forces are ignored in its determination. In general, however, the static solution of a particular problem is time-dependent by virtue of the time-dependence of the applied load, and of the nonhomogeneous time-dependent boundary conditions, if such are imposed. In the case of plates with a fixed point of reference, such as clamped or supported plates, all inertia forces are ignored in the determination of the static part of the solution. For plates with rigid-body freedoms, however, the inertia forces due to the rigid body motion must be taken into account.

It may be noted that the Williams method is directly applicable to the solution of problems with nonhomogeneous boundary conditions. Such problems require the separation of the solution into two parts, one satisfying the time-dependent boundary conditions, and the other capable of being expanded in terms of time-dependent functions such as the natural modes of the plate. In the Williams method, this separation is already made and time-dependent boundary displacements or forces are simply introduced into the boundary conditions for the static solution or into the equations for rigid-body displacements [44].

B. Basic Equations in Nondimensional Form

For the case of axisymmetric motions, the plate-displacement equations of motion (4.15) reduce to

$$\frac{D}{2}[(1-\nu)\nabla^2\psi_r + (1+\nu)\frac{\partial\eta}{\partial r}] - \frac{D}{2}(1-\nu)\frac{\psi_r}{r^2} - k^2Gh(\psi_r + \frac{\partial w}{\partial r}) = \frac{\rho h^3}{12}\frac{\partial^2\psi_r}{\partial t^2}$$

$$k^2Gh(\nabla^2 w + \eta) + p = \rho h\frac{\partial^2 w}{\partial t^2} \tag{7.2}$$

In the expanded form these become

$$\frac{Eh^3}{12(1-\nu^2)}(\frac{\partial^2\psi_r}{\partial r^2} + \frac{1}{r}\frac{\partial\psi_r}{\partial r} - \frac{\psi_r}{r^2}) - \frac{k^2Eh}{2(1+\nu)}(\psi_r + \frac{\partial w}{\partial r}) = \frac{\rho h^3}{12}\frac{\partial^2\psi_r}{\partial t^2}$$

$$\frac{k^2Eh}{2(1+\nu)}(\frac{\partial^2 w}{\partial r^2} + \frac{1}{r}\frac{\partial w}{\partial r} + \frac{\partial\psi_r}{\partial r} + \frac{\psi_r}{r}) + p(r,t) = \rho h\frac{\partial^2 w}{\partial t^2} \tag{7.3}$$

The following dimensionless quantities are now introduced for ease of computation and more generality of the results

Dimensional Quantity	To convert to dimensionless form divide by	Dimensionless Quantity
r	a	R
w	a	W
ψ_r, ψ_θ	-	ψ_r, ψ_θ
t	$a\sqrt{\frac{(1-\nu^2)}{E}}$	T
M_r, M_θ, $M_{r\theta}$	$\frac{Eh^3}{12a(1-\nu^2)}$	M_r, M_θ, $M_{r\theta}$
Q_r, Q_θ	$\frac{Eh}{(1-\nu^2)}$	Q_r, Q_θ
p	$\frac{Eh}{a(1-\nu^2)}$	P
ω	$\frac{1}{a}\sqrt{\frac{E}{\rho(1-\nu^2)}}$	Ω
b	a	β
c	a	γ

Using the above conversion factors in equations (7.3) and manipulating the results, one obtains

$$\frac{\partial}{\partial R}\left[\frac{1}{R}\frac{\partial}{\partial R}(R\psi_r)\right] - \frac{K^2}{\alpha^2}\left(\psi_r + \frac{\partial W}{\partial R}\right) = \frac{\partial^2\psi_r}{\partial T^2}$$

$$\frac{K^2}{R}\frac{\partial}{\partial R}\left[R\left(\psi_r + \frac{\partial W}{\partial R}\right)\right] + P(R,T) = \frac{\partial^2 W}{\partial T^2} \tag{7.4}$$

where

$$K^2 = \frac{k^2(1-\nu)}{2}$$

$$\alpha^2 = \frac{h^2}{12a^2} \tag{7.5}$$

The plate-stress displacement equations (4.13) for the case of axial symmetry reduce to the following nondimensional equations:

$$M_r = \frac{\partial\psi_r}{\partial R} + \frac{\nu}{R}\psi_r$$

$$M_\theta = \nu\frac{\partial\psi_r}{\partial R} + \frac{\psi_r}{R} \tag{7.6}$$

$$Q_r = K^2\left(\psi_r + \frac{\partial W}{\partial R}\right)$$

Equations (7.4) and (7.6) are the nondimensional equations of the improved theory of plate vibration.

C. Formulation of the Dynamic Response Problem

Within the framework of the theory characterized by equations (7.4) and (7.6), a properly posed dynamic response problem may be defined by specifying the following:

1. Time-dependent load, $P = P(R,T)$
2. Boundary conditions; for an annular plate these are

$$\begin{aligned} &\text{either } W(\beta,T) \text{ or } Q_r(\beta,T) = f_1(T)\\ &\text{either } \psi_r(\beta,T) \text{ or } M_r(\beta,T) = f_2(T)\\ &\text{either } W(1,T) \text{ or } Q_r(1,T) = f_3(T)\\ &\text{either } \psi_r(1,T) \text{ or } M_r(1,T) = f_4(T)\end{aligned} \tag{7.7}$$

3. Initial conditions:

$$
\begin{aligned}
W(R,0) &= W_0(R) \\
\dot{W}(R,0) &= \dot{W}_0(R) \\
\psi_r(R,0) &= \psi_{r0}(R) \\
\dot{\psi}_r(R,0) &= \dot{\psi}_{r0}(R)
\end{aligned}
\tag{7.8}
$$

It is required to find the displacement components W and ψ_r in the area bounded by the circular boundary curves.

D. Orthogonality Relations of the Eigenfunctions

Consider the solution of the homogeneous differential equations which are obtained by setting P = 0 in equations (7.4) subject to the boundary conditions that at R = β and R = 1, one member of each of the products WQ_r and $\psi_r M_r$ vanishes.

Assume a separable solution of the form

$$
\begin{aligned}
W(R,T) &= W_i(R)\ e^{i\Omega_i T} \\
\psi_r(R,T) &= \psi_{ri}(R)\ e^{i\Omega_i T}
\end{aligned}
\tag{7.9}
$$

Substituting this in equations (7.4) and (7.6), one gets

$$
\begin{aligned}
\frac{\partial}{\partial R}\left[\frac{1}{R}\frac{\partial}{\partial R}(R\psi_{ri})\right] - \frac{K^2}{\alpha^2}\left(\psi_{ri} + \frac{\partial W_i}{\partial R}\right) + \Omega_i^{\,2}\psi_{ri} &= 0 \\
\frac{K^2}{R}\frac{\partial}{\partial R}\left[R\left(\psi_{ri} + \frac{\partial W_i}{\partial R}\right)\right] + \Omega_i^{\,2} W_i &= 0
\end{aligned}
\tag{7.10}
$$

$$
\begin{aligned}
M_{ri} &= \frac{\partial \psi_{ri}}{\partial R} + \frac{\nu}{R}\psi_{ri} \\
M_{\theta i} &= \nu\frac{\partial \psi_{ri}}{\partial R} + \frac{1}{R}\psi_{ri} \\
Q_{ri} &= K^2\left(\psi_{ri} + \frac{\partial W_i}{\partial R}\right)
\end{aligned}
\tag{7.11}
$$

In view of equations (7.11), equations (7.10) become

$$\Omega_i^{\,2} W_i = -\frac{1}{R}\frac{\partial}{\partial R}(RQ_{ri})$$
$$\Omega_i^{\,2}\psi_{ri} = -\frac{\partial}{\partial R}\left[\frac{1}{R}\frac{\partial}{\partial R}(R\psi_{ri})\right] + \frac{Q_{ri}}{\alpha^2} \tag{7.12}$$

Multiply the first of equations (7.12) by W_j and the second by $\alpha^2\psi_j$ and integrate the products over the surface of the plate. This process yields (the subscript r on ψ is deleted for convenience)

$$\int_\beta^1 \Omega_i^{\,2} W_i W_j R dR = -\int_\beta^1 \frac{\partial}{\partial R}(RQ_{ri})W_j dR$$
$$\alpha^2 \int_\beta^1 \Omega_i^{\,2}\psi_i\psi_j R dR = -\int_\beta^1 R\frac{\partial}{\partial R}\left[\frac{1}{R}\frac{\partial}{\partial R}(R\psi_i)\right]\alpha^2\psi_j dR$$
$$+\int_\beta^1 Q_{ri}\psi_j R dR$$

After integration by parts the above equations become

$$\Omega_i^{\,2}\int_\beta^1 W_i W_j R dR = -\left[RQ_{ri}W_j\right]_\beta^1 + \int_\beta^1 RQ_{ri}\frac{\partial W_j}{\partial R} dR$$
$$\alpha^2\Omega_i^{\,2}\int_\beta^1 \psi_i\psi_j R dR = -\left[\frac{\alpha^2}{R}\frac{\partial}{\partial R}(R\psi_i)(R\psi_j)\right]_\beta^1$$
$$+\int_\beta^1 \frac{\alpha^2}{R}\frac{\partial}{\partial R}(R\psi_i)\frac{\partial}{\partial R}(R\psi_j)dR + \int_\beta^1 Q_{ri}\psi_j R dR \tag{7.13}$$

For another mode j, a similar set of equations are obtained by interchanging the subscripts i and j in the above equations. The result is

$$\Omega_j^{\,2}\int_\beta^1 W_j W_i R dR = -\left[RQ_{rj}W_i\right]_\beta^1 + \int_\beta^1 RQ_{rj}\frac{\partial W_i}{\partial R} dR$$
$$\alpha^2\Omega_j^{\,2}\int_\beta^1 \psi_j\psi_i R dR = -\left[\frac{\alpha^2}{R}\frac{\partial}{\partial R}(R\psi_j)(R\psi_i)\right]_\beta^1$$
$$+\int_\beta^1 \frac{\alpha^2}{R}\frac{\partial}{\partial R}(R\psi_j)\frac{\partial}{\partial R}(R\psi_i)dR + \int_\beta^1 Q_{rj}\psi_i R dR \tag{7.14}$$

Adding the two equations of each set and subtracting the resulting second relationship from the first relationship we obtain

$$(\Omega_i^2 - \Omega_j^2) \int_\beta^1 (W_iW_j + \alpha^2\psi_i\psi_j)RdR = [R(Q_{rj}W_i - Q_{ri}W_j)]_\beta^1$$
$$+ \alpha^2[R(\frac{\partial\psi_j}{R}\psi_i - \frac{\partial\psi_i}{\partial R}\psi_j)]_\beta^1 \tag{7.15}$$
$$+ \int_\beta^1 [Q_{ri}(\frac{\partial W_j}{\partial R} + \psi_j) - Q_{rj}(\frac{\partial W_i}{\partial R} + \psi_i)]RdR$$

Now in view of equations (7.11) and the condition that at $R = \beta$ and $R = 1$, one member of each of the products WQ_r and ψM_r vanishes, the right hand side of equation (7.15) vanishes. Hence, one obtains

$$(\Omega_i^2 - \Omega_j^2) \int_\beta^1 (W_iW_j + \alpha^2\psi_i\psi_j)RdR = 0$$

Thus the pertinent orthogonality relation for the principal modes of free vibration is

$$\int_\beta^1 (W_iW_j + \alpha^2\psi_i\psi_j)RdR = 0, \quad i \neq j \tag{7.16}$$

By selecting a normalization condition, unique expressions for the mode shapes are obtained. The following mode normalization condition is used for the subsequent solution of the forced motion problem [8].

$$\int_\beta^1 (W_i^2 + \alpha^2\psi_i^2)RdR = 1 \tag{7.17}$$

E. Response to Transverse Load, $P = P(R,T)$

Assume the response in the form

$$\begin{aligned} W(R,T) &= W_s(R,T) + \sum_{i=1}^{\infty} W_i(R)q_i(T) \\ \psi(R,T) &= \psi_s(R,T) + \sum_{i=1}^{\infty} \psi_i(R)q_i(T) \end{aligned} \tag{7.18}$$

where

q_i is the generalized coordinate

$W_s(R,T)$ and $\psi_s(R,T)$ are the static solutions obtained by solving equations (7.4) with inertial terms equal to zero:

$$\frac{\partial}{\partial R}\left[\frac{1}{R}\frac{\partial}{\partial R}(R\psi_s)\right] - \frac{K^2}{\alpha^2}\left(\psi_s + \frac{\partial W_s}{\partial R}\right) = 0$$

$$\frac{K^2}{R}\frac{\partial}{\partial R}\left[R\left(\psi_s + \frac{\partial W_s}{\partial R}\right)\right] + P(R,T) = 0 \qquad (7.19)$$

Since the static solutions must satisfy the boundary conditions (7.7), the boundary conditions for the eigenfunctions reduce to

$$\begin{aligned}
&\text{either } W_i(\beta) = 0 \quad \text{or} \quad Q_{ri}(\beta) = 0\\
&\text{either } \psi_i(\beta) = 0 \quad \text{or} \quad M_{ri}(\beta) = 0\\
&\text{either } W_i(1) = 0 \quad \text{or} \quad Q_{ri}(1) = 0\\
&\text{either } \psi_i(1) = 0 \quad \text{or} \quad M_{ri}(1) = 0
\end{aligned} \qquad (7.20)$$

Substituting equations (7.18) into equations (7.4), one obtains

$$\frac{\partial}{\partial R}\left[\frac{1}{R}\frac{\partial}{\partial R}(R\psi_s)\right] - \frac{K^2}{\alpha^2}\left(\psi_s + \frac{\partial W_s}{\partial R}\right) + \frac{\partial}{\partial R}\left[\frac{1}{R}\frac{\partial}{\partial R}(R\Sigma\psi_i q_i)\right]$$
$$- \frac{K^2}{\alpha^2}\left(\frac{\partial \Sigma W_i q_i}{\partial R} + \Sigma\psi_i q_i\right) = \frac{\partial^2\psi_s}{\partial T^2} + \frac{\partial^2\Sigma\psi_i q_i}{\partial T^2}$$

$$\frac{K^2}{R}\frac{\partial}{\partial R}\left[R\left(\psi_s + \frac{\partial W_s}{\partial R}\right)\right] + P(R,T)$$
$$+ \frac{K^2}{R}\frac{\partial}{\partial R}\left[R\left(\frac{\partial \Sigma W_i q_i}{\partial R} + \Sigma\psi_i q_i\right)\right] = \frac{\partial^2 W_s}{\partial T^2} + \frac{\partial^2\Sigma W_i q_i}{\partial T^2}$$

Using equations (7.10) and (7.19), the above equations reduce to

$$\sum_{i=1}^{\infty} \psi_i(\ddot{q}_i + \Omega_i^2 q_i) = - \ddot{W}_s$$

$$\sum_{i=1}^{\infty} W_i(\ddot{q}_i + \Omega_i^2 q_i) = - \ddot{\psi}_s \qquad (7.21)$$

Multiplying the first of equation (7.21) by $\alpha^2\psi_j$ and the second by W_j, adding the result and integrating over the surface of the plate, one obtains

$$\int_\beta^1 \sum_{i=1}^{\infty} (\ddot{q}_i + \Omega_i^2 q_i)(W_i W_j + \alpha^2\psi_i\psi_j)RdR = - \int_\beta^1 (\ddot{W}_s W_j + \alpha^2\ddot{\psi}_s\psi_j)RdR$$

By applying the orthogonality relation (7.16) and the normalization condition (7.17), the above equation reduces to

$$\ddot{q}_i + \Omega_i^{\,2} q_i = - \int_\beta^1 (\ddot{W}_s W_i + \alpha^2 \ddot{\psi}_s \psi_i) R dR = - \ddot{P}_i(T) \tag{7.22}$$

where

$$P_i(T) = \int_\beta^1 (W_s W_i + \alpha^2 \psi_s \psi_i) R dR \tag{7.23}$$

Substituting for W_i and ψ_i from equations (7.12), integrating by parts and using equations (7.11) and (7.19), we obtain

$$\int W_s W_i R dR = - \frac{1}{\Omega_i^{\,2}} \int W_s \frac{\partial}{\partial R} (R Q_{ri}) dR$$

$$= - \frac{R}{\Omega_i^{\,2}} W_s Q_{ri} \Big]_\beta^1 + \frac{1}{\Omega_i^{\,2}} \int R Q_{ri} \frac{\partial W_s}{\partial R} dR$$

$$\int \alpha^2 \psi_s \psi_i R dR = - \int \frac{\alpha^2}{\Omega_i^{\,2}} \psi_s \frac{\partial}{\partial R} \left[\frac{1}{R} \frac{\partial}{\partial R} (R\psi_i)\right] RdR$$

$$+ \int \frac{\psi_s}{\Omega_i^{\,2}} Q_{ri} RdR$$

$$= - \frac{\alpha^2}{\Omega_i^{\,2}} \left[R\psi_s \frac{\partial \psi_i}{\partial R} - R\psi_i \frac{\partial \psi_s}{\partial R}\right]_\beta^1$$

$$+ \int R\psi_i \frac{\partial}{\partial R} \left[\frac{1}{R} \frac{\partial}{\partial R} (R\psi_s)\right] dR + \int \frac{\psi_s}{\Omega_i^{\,2}} Q_{ri} RdR$$

$$= \frac{\alpha^2 R}{\Omega_i^{\,2}} \left[M_{rs} \psi_i - M_{ri} \psi_s\right]_\beta^1$$

$$- \frac{1}{\Omega_i^{\,2}} \int R Q_{rs} \psi_i dR - \frac{1}{\Omega_i^{\,2}} \int R Q_{ri} \psi_s dR$$

Therefore, we have

$$P_i(T) = \frac{\alpha^2 R}{\Omega_i^{\,2}} \left[M_{rs} \psi_i - M_{ri} \psi_s - \frac{W_s Q_{ri}}{\alpha^2}\right]_\beta^1$$

$$+ \frac{1}{\Omega_i^{\,2}} \int (\psi_s Q_{ri} - \psi_i Q_{rs} + Q_{ri} \frac{\partial W_s}{\partial R}) RdR$$

$$= \frac{\alpha^2 R}{\Omega_i^2} [M_{rs}\psi_i - M_{ri}\psi_s - \frac{W_s Q_{ri}}{\alpha^2}]_\beta^1$$

$$+ \frac{1}{\Omega_i^2} RQ_{rs}W_i \Big]_\beta^1 - \frac{1}{\Omega_i^2} \int W_i \frac{\partial}{\partial R} (RQ_{rs})dR$$

The above equation can be written as

$$P_i(T) = \frac{R}{\Omega_i^2} [\alpha^2(M_{rs}\psi_i - M_{ri}\psi_s) + Q_{rs}W_i - Q_{ri}W_s]_\beta^1$$
$$+ \frac{1}{\Omega_i^2} \int_\beta^1 P(R,T)\ W_i RdR \tag{7.24}$$

where

$$M_{rs} = \frac{\partial\psi_s}{\partial R} + \frac{\nu}{R}\psi_s$$
$$Q_{rs} = K^2\ (\psi_s + \frac{\partial W_s}{\partial R}) \tag{7.25}$$

The form of $P_i(T)$ as given by equation (7.24) is particularly useful for solving problems with time-dependent boundary conditions.

Initial Conditions for equation (7.22):

In view of equations (7.8) and (7.18)

$$W_0(R) = W_s(R,0) + \sum_{i=1}^{\infty} W_i(R)q_i(0)$$
$$\psi_0(R) = \psi_s(R,0) + \sum_{i=1}^{\infty} \psi_i(R)q_i(0) \tag{7.26}$$

Multiplying the first of equations (7.26)by W_j and the second by $\alpha^2\psi_j$, adding the products so obtained and integrating over the surface of the plate, we obtain

$$\int[W_0(R)W_j + \alpha^2\psi_0(R)\psi_j]RdR = \int[W_s(R,0)W_j + \alpha^2\psi_s(R,0)\psi_j]RdR$$

$$+ \int[W_j\Sigma W_i(R)q_i(0) + \alpha^2\psi_j\Sigma\psi_i(R)q_i(0)]RdR$$

Applying equations (7.16), (7.17) and (7.23), the above equation yields

$$q_i(0) = \int_\beta^1 (W_0 W_i + \alpha^2 \psi_0 \psi_i) R dR - P_i(0) \tag{7.27}$$

A similar process yields

$$\dot{q}_i(0) = \int_\beta^1 (\dot{W}_0 W_i + \alpha^2 \dot{\psi}_0 \psi_i) R dR - \dot{P}_i(0) \tag{7.28}$$

The solution of equation (7.22) is [6]

$$\begin{aligned} q_i(T) &= q_i(0)\cos\Omega_i T + \frac{\dot{q}_i(0)}{\Omega_i}\sin\Omega_i T \\ &- \frac{1}{\Omega_i}\int_0^T \ddot{P}_i(\tau)\sin\Omega_i(T-\tau)d\tau \end{aligned} \tag{7.29}$$

Equations (7.27), (7.28) and (7.29), together with the solutions of equations (7.1Q) and (7.19), constitute the solution of the forced motion problem.

VIII. APPLICATIONS OF THE SOLUTIONS

Using the homogeneous solution developed in Chapter V, the natural frequencies and corresponding mode shapes of solid circular plates with clamped, simply supported and free edges are determined. Axisymmetric and one diametral node free vibrations of an annular plate rigidly mounted on a shaft are also investigated.

Using the forced motion solution developed in Chapter VII, the response of a clamped plate and a simply supported plate to a rapidly applied transverse load is investigated under three different load distributions; namely, load distributed uniformly over a circular area, load distributed uniformly over a circle, and load concentrated at the center of the plate. The center deflections and bending moments at critical sections are determined in each case as a function of time and compared with the results obtained by using the classical theory. The behaviour of a plate with an elastically built-in edge is intermediate between that of the two limiting cases of simply supported edges and clamped edges and is not considered here as a separate case.

To illustrate the generality of the forced motion solution, the response of a circular disk rigidly mounted on a shaft with a time-dependent load at the outer edge is also considered in detail.

The frequency equations, the eigenfunctions, the static solutions, and the dynamic solutions for the different cases mentioned above will now be given.

A. Homogeneous Solution in Nondimensional Form

Equations (5.18) and (5.19) can be written in nondimensional form as follows:

$$W = W_1 + W_2$$

$$\psi_r = (\sigma_1 - 1)\frac{\partial W_1}{\partial R} + (\sigma_2 - 1)\frac{\partial W_2}{\partial R} + \frac{\partial W_3}{R\partial\theta} \tag{8.1}$$

$$\psi_\theta = (\sigma_1 - 1)\frac{\partial W_1}{R\partial\theta} + (\sigma_2 - 1)\frac{\partial W_2}{R\partial\theta} - \frac{\partial W_3}{\partial R}$$

and

$$(\nabla^2 + \delta_1^{\,2})\, W_1 = 0$$

$$(\nabla^2 + \delta_2^{\,2})\, W_2 = 0 \tag{8.2}$$

$$(\nabla^2 + \delta_3^{\,3})\, W_3 = 0$$

where

$$\left\{\begin{matrix} \delta_1^{\,2} \\ \delta_2^{\,2} \end{matrix}\right\} = \frac{\Omega^2}{2}\left[\; 1 + \frac{1}{K^2} \pm \sqrt{\left(1 - \frac{1}{K^2}\right)^2 + \frac{4}{\Omega^2\alpha^2}}\;\right]$$

$$\delta_3^{\,2} = \frac{2}{1-\nu}\left(\Omega^2 - \frac{K^2}{\alpha^2}\right) \tag{8.3}$$

$$\left\{\begin{matrix} \sigma_1 \\ \sigma_2 \end{matrix}\right\} = \left\{\begin{matrix} \delta_2^{\,2} \\ \delta_1^{\,2} \end{matrix}\right\}\left(\Omega^2 - \frac{K^2}{\alpha^2}\right)^{-1}$$

It is observed from equations (8.3) that $\delta_1^{\,2} > 0$ for all values of $\Omega > 0$ while $\delta_2^{\,2} \gtrless 0$ according as $\Omega \gtrless \bar{\Omega}$, where $\bar{\Omega} = \frac{K}{\alpha}$ is the frequency of the first thickness-shear mode of an infinite plate [see equation (B.17)]. The same condition holds for $\delta_3^{\,2}$ also, so that $\delta_3^{\,2} \gtrless 0$ according as $\Omega \gtrless \frac{K}{\alpha}$. Hence δ_2 and δ_3 will be real or imaginary according as $\Omega \gtrless \frac{K}{\alpha}$. The solutions of equations (8.2) will depend on whether δ_2 and δ_3 are real or imaginary.

For $\Omega > \frac{K}{\alpha}$, the appropriate solutions of equations (8.2) are

$$W_{1mn} = [A_{1m}J_m(\delta_1 R) + B_{1m}Y_m(\delta_1 R)] \text{ Cos } m\theta$$

$$W_{2mn} = [A_{2m}J_m(\delta_2 R) + B_{2m}Y_m(\delta_2 R)] \text{ Cos } m\theta \tag{8.4}$$

$$W_{3mn} = [A_{3m}\, J_m(\delta_3 R) + B_{3m}Y_m(\delta_3 R)] \text{ Sin } m\theta$$

For $0 < \Omega < \frac{K}{\alpha}$, the solutions are

$$W_{1mn} = [A_{1m}J_m(\delta_1 R) + B_{1m}Y_m(\delta_1 R)] \text{ Cos } m\theta$$

$$W_{2mn} = [A_{2m}I_m(\bar{\delta}_2 R) + B_{2m}K_m(\bar{\delta}_2 R)] \text{ Cos } m\theta \tag{8.5}$$

$$W_{3mn} = [A_{3m}I_m(\bar{\delta}_3 R) + B_{3m}K_m(\bar{\delta}_3 R)] \text{ Sin } m\theta$$

where I_m and K_m are the modified Bessel Functions of the first and second kinds respectively and of order m and

$$\bar{\delta}_2 = \left|\delta_2\right| \text{ , when } \delta_2 \text{ is imaginary}$$
$$\bar{\delta}_3 = \left|\delta_3\right| \text{ , when } \delta_3 \text{ is imaginary} \tag{8.6}$$

B. Frequency Equations and Mode Shapes

1. Clamped Plate

a. Axisymmetric Vibration

The appropriate boundary conditions for a clamped plate are

$$W(1,T) = 0$$
$$\psi_r(1,T) = 0 \tag{8.7}$$

Hence the boundary conditions for the eigenfunctions are (the subscripts i which denote mode numbers are omitted for convenience)

$$W(1) = 0$$
$$\psi_r(1) = 0 \tag{8.8}$$

The solutions of equations (8.2) for axisymmetric vibrations are, for $\Omega > \frac{K}{\alpha}$

$$W(R) = A_1 J_0(\delta_1 R) + A_2 J_0(\delta_2 R)$$

$$\psi_r(R) = A_1(1-\sigma_1)\delta_1 J_1(\delta_1 R) + A_2(1-\sigma_2)\delta_2 J_1(\delta_2 R) \tag{8.9}$$

and for $0 < \Omega < \frac{K}{\alpha}$

$$\begin{aligned} W(R) &= A_1 J_0(\delta_1 R) + A_2 I_0(\bar{\delta}_2 R) \\ \psi_r(R) &= A_1(1-\sigma_1)\delta_1 J_1(\delta_1 R) - A_2(1-\sigma_2)\bar{\delta}_2 I_1(\bar{\delta}_2 R) \end{aligned} \tag{8.10}$$

Applying the boundary conditions (8.8) on equations (8.9) and (8.10), the frequency determinants are obtained as given below:

For $\Omega > \frac{K}{\alpha}$

$$\begin{bmatrix} J_0(\delta_1) & J_0(\delta_2) \\ (1-\sigma_1)\delta_1 J_1(\delta_1) & (1-\sigma_2)\delta_2 J_1(\delta_2) \end{bmatrix} \begin{Bmatrix} A_1 \\ A_2 \end{Bmatrix} = 0 \tag{8.11}$$

For $0 < \Omega < \frac{K}{\alpha}$

$$\begin{bmatrix} J_0(\delta_1) & I_0(\bar{\delta}_2) \\ (1-\sigma_1)\delta_1 J_1(\delta_1) & -(1-\sigma_2)\bar{\delta}_2 I_1(\bar{\delta}_2) \end{bmatrix} \begin{Bmatrix} A_1 \\ A_2 \end{Bmatrix} = 0 \tag{8.12}$$

The determinant of the coefficient matrix is the frequency determinant. The frequency determinant equated to zero gives the frequency equation which can be solved for the frequencies Ω_i, $i = 1,2,3,\ldots..$

Unique solutions for A_1 and A_2:

From the first of equations (8.11) one obtains, for $\Omega > \frac{K}{\alpha}$

$$A_2 = -\frac{J_0(\delta_1)}{J_0(\delta_2)} A_1 \tag{8.13}$$

In view of equations (7.17), equations (8.9) and (8.13) yield

$$\begin{aligned} \int_0^1 (W^2+\alpha^2\psi_r^{\,2})\, RdR &= 1 \\ &= A_1^{\,2} \int_0^1 \Big[J_0^{\,2}(\delta_1 R) + \frac{J_0^{\,2}(\delta_1)}{J_0^{\,2}(\delta_2)} J_0^{\,2}(\delta_2 R) \\ &\quad - 2\frac{J_0(\delta_1)}{J_0(\delta_2)} J_0(\delta_1 R) J_0(\delta_2 R) \end{aligned}$$

$$+ \alpha^2\delta_1{}^2(1-\sigma_1)^2J_1{}^2(\delta_1R) + \alpha^2 \frac{J_0{}^2(\delta_1)}{J_0{}^2(\delta_2)} \delta_2{}^2(1-\sigma_2)^2J_1{}^2(\delta_2R)$$

$$- 2\alpha^2 \frac{J_0(\delta_1)}{J_0(\delta_2)} \delta_1\delta_2(1-\sigma_1)(1-\sigma_2)J_1(\delta_1R)J_1(\delta_2R)]\ RdR$$

On integration and rearrangement, the above equation yields

$$A_1 = \frac{\sqrt{2}}{J_0(\delta_1)\sqrt{\begin{aligned} &2 + \frac{J_1{}^2(\delta_1)}{J_0{}^2(\delta_1)} + \frac{J_1{}^2(\delta_2)}{J_0{}^2(\delta_2)} + \alpha^2\delta_1{}^2(1-\sigma_1)^2\left[\frac{J_1{}^2(\delta_1)}{J_0{}^2(\delta_1)} - \frac{J_2(\delta_1)}{J_0(\delta_1)}\right] \\ &+ \alpha^2\delta_2{}^2(1-\sigma_2)^2\left[\frac{J_1{}^2(\delta_2)}{J_0{}^2(\delta_2)} - \frac{J_2(\delta_2)}{J_0(\delta_2)}\right] \\ &+ \frac{4}{\delta_1{}^2-\delta_2{}^2}\left[\delta_2 \frac{J_1(\delta_2)}{J_0(\delta_2)} - \delta_1 \frac{J_1(\delta_1)}{J_0(\delta_1)}\right] \\ &+ \frac{4}{\delta_1{}^2-\delta_2{}^2}\alpha^2\delta_1\delta_2(1-\sigma_1)(1-\sigma_2)\left[\delta_1 \frac{J_1(\delta_2)}{J_0(\delta_2)} - \delta_2 \frac{J_1(\delta_1)}{J_0(\delta_1)}\right]\end{aligned}}} \tag{8.14}$$

Following a similar procedure, by using equations (8.10) and (7.17), one obtains for $0 < \Omega < \frac{K}{\alpha}$

$$A_2 = -\frac{J_0(\delta_1)}{I_0(\bar{\delta}_2)} A_1 \tag{8.15}$$

and

$$A_1 = \frac{\sqrt{2}}{J_0(\delta_1)\sqrt{\begin{aligned} &2 + \frac{J_1{}^2(\delta_1)}{J_0{}^2(\delta_1)} - \frac{I_1{}^2(\bar{\delta}_2)}{I_0{}^2(\bar{\delta}_2)} + \alpha^2\delta_1{}^2(1-\sigma_1)^2\left[\frac{J_1{}^2(\delta_1)}{J_0{}^2(\delta_1)} - \frac{J_2(\delta_1)}{J_0(\delta_1)}\right] \\ &+ \alpha^2\bar{\delta}_2{}^2(1-\sigma_2)^2\left[\frac{I_1{}^2(\bar{\delta}_2)}{I_0{}^2(\bar{\delta}_2)} - \frac{I_2(\bar{\delta}_2)}{I_0(\bar{\delta}_2)}\right] \\ &- \frac{4}{\delta_1{}^2+\bar{\delta}_2{}^2}\left[\bar{\delta}_2 \frac{I_1(\bar{\delta}_2)}{I_0(\bar{\delta}_2)} + \delta_1 \frac{J_1(\delta_1)}{J_0(\delta_1)}\right] \\ &+ \frac{4}{\delta_1{}^2+\bar{\delta}_2{}^2}\alpha^2\delta_1\bar{\delta}_2(1-\sigma_1)(1-\sigma_2)\left[\bar{\delta}_2 \frac{J_1(\delta_1)}{J_0(\delta_1)} - \delta_1 \frac{I_1(\bar{\delta}_2)}{I_0(\bar{\delta}_2)}\right]\end{aligned}}} \tag{8.16}$$

A_1 and A_2 uniquely determine the mode shapes given by equations (8.9) and (8.10). The positive square roots have been chosen in equations (8.14) and (8.15) since only the squares and products of A_1 and A_2 will appear in the forced motion problem to be considered later in this chapter.

b. Vibration with One Diametral Node

This case is considered to illustrate the coupling between thickness-twist and flexural modes of vibration. The appropriate boundary conditions for this case are

$$\begin{aligned} W(1,T) &= 0 \\ \psi_r(1,T) &= 0 \\ \psi_\theta(1,T) &= 0 \end{aligned} \tag{8.17}$$

Hence the boundary conditions for the eigenfunctions are

$$\begin{aligned} W(1) &= 0 \\ \psi_r(1) &= 0 \\ \psi_\theta(1) &= 0 \end{aligned} \tag{8.18}$$

In view of the modes of motion of interest, the appropriate solutions of equations (8.2) are, for $\Omega > \frac{K}{\alpha}$

$$\begin{aligned} W_1 &= A_1 J_1(\delta_1 R) \cos\theta \\ W_2 &= A_2 J_1(\delta_2 R) \cos\theta \\ W_3 &= A_3 J_1(\delta_3 R) \sin\theta \end{aligned} \tag{8.19}$$

Substituting these in equations (8.1), one obtains

$$\psi_r = A_1(\sigma_1-1)[\delta_1 J_0(\delta_1 R) - \frac{1}{R} J_1(\delta_1 R)] \cos\theta$$
$$+ A_2(\sigma_2-1)[\delta_2 J_0(\delta_2 R) - \frac{1}{R} J_1(\delta_2 R)] \cos\theta$$
$$+ A_3 \frac{1}{R} J_1(\delta_3 R) \cos\theta \tag{8.20}$$

$$\psi_\theta = - A_1(\sigma_1-1) \frac{1}{R} J_1(\delta_1 R) \sin\theta - A_2(\sigma_2-1) \frac{1}{R} J_1(\delta_2 R) \sin\theta$$
$$- A_3[\delta_3 J_0(\delta_3 R) - \frac{1}{R} J_1(\delta_3 R)] \sin\theta$$

On applying the boundary conditions (8.18), equations (8.19) and (8.20) yield

$$\begin{bmatrix} J_1(\delta_1) & J_1(\delta_2) & 0 \\ (\sigma_1-1)[\delta_1 J_0(\delta_1) - J_1(\delta_1)] & (\sigma_2-1)[\delta_2 J_0(\delta_2) - J_1(\delta_2)] & J_1(\delta_3) \\ (\sigma_1-1)\ J_1(\delta_1) & (\sigma_2-1)\ J_1(\delta_2) & [\delta_3 J_0(\delta_3) - J_1(\delta_3)] \end{bmatrix} \begin{Bmatrix} A_1 \\ A_2 \\ A_3 \end{Bmatrix} = 0 \tag{8.21}$$

For $0 < \Omega < \frac{K}{\alpha}$, a similar process yields

$$\begin{bmatrix} J_1(\delta_1) & I_1(\bar{\delta}_2) & 0 \\ (\sigma_1-1)[\delta_1 J_0(\delta_1) - J_1(\delta_1)] & (\sigma_2-1)[\bar{\delta}_2 I_0(\bar{\delta}_2) - I_1(\bar{\delta}_2)] & I_1(\bar{\delta}_3) \\ (\sigma_1-1) J_1(\delta_1) & (\sigma_2-1) I_1(\bar{\delta}_2) & [\bar{\delta}_3 I_0(\bar{\delta}_3) - I_1(\bar{\delta}_3)] \end{bmatrix} \begin{Bmatrix} A_1 \\ A_2 \\ A_3 \end{Bmatrix} = 0 \tag{8.22}$$

A necessary and sufficient condition for the existence of a non-trivial solution for the mode coefficients A_1, A_2 and A_3 is provided by the vanishing of the determinant of the coefficient matrix in (8.21) and (8.22). This results in a transcendental equation which can be solved for the frequencies via digital computer.

2. Simply Supported Plate: Axisymmetric Vibration

The appropriate boundary conditions for the mode shapes are

$$W(1) = 0$$
$$M_r(1) = 0 \tag{8.23}$$

where M_r, the modal bending moment, is

$$M_r = \frac{\partial \psi_r}{\partial R} + \frac{\nu}{R}\,\psi_r$$

For $\Omega > \frac{K}{\alpha}$, we obtain

$$\begin{aligned} M_r = {} & A_1(1-\sigma_1)\left[\delta_1^{\,2} J_0(\delta_1 R) + \frac{(\nu-1)}{R}\,\delta_1 J_1(\delta_1 R)\right] \\ & + A_2(1-\sigma_2)\left[\delta_2^{\,2} J_0(\delta_2 R) + \frac{(\nu-1)}{R}\,\delta_2 J_1(\delta_2 R)\right] \end{aligned} \tag{8.24}$$

Applying the boundary conditions (8.23) to equations (8.9) and (8.24), one obtains, for $\Omega > \frac{K}{\alpha}$

$$\begin{bmatrix} J_0(\delta_1) & J_0(\delta_2) \\ (1-\sigma_1)[\delta_1^{\,2} J_0(\delta_1) + (\nu-1)\delta_1 J_1(\delta_1)] & (1-\sigma_2)[\delta_2^{\,2} J_0(\delta_2) + (\nu-1)\delta_2 J_1(\delta_2)] \end{bmatrix} \begin{Bmatrix} A_1 \\ A_2 \end{Bmatrix} = 0 \tag{8.25}$$

For $0 < \Omega < \frac{K}{\alpha}$, the corresponding equations are

$$\begin{aligned} M_r = {} & A_1(1-\sigma_1)\left[\delta_1^{\,2} J_0(\delta_1 R) + \frac{(\nu-1)}{R}\,\delta_1 J_1(\delta_1 R)\right] \\ & - A_2(1-\sigma_2)\left[\bar{\delta}_2^{\,2} I_0(\bar{\delta}_2 R) + \frac{(\nu-1)}{R}\,\bar{\delta}_2 I_1(\bar{\delta}_2 R)\right] \end{aligned} \tag{8.26}$$

and

$$\begin{bmatrix} J_0(\delta_1) & I_0(\bar{\delta}_2) \\ (1-\sigma_1)[\delta_1^{\,2}J_0(\delta_1) + (\nu-1)\delta_1 J_1(\delta_1)] & -(1-\sigma_2)[\bar{\delta}_2^{\,2}I_0(\bar{\delta}_2) + (\nu-1)\bar{\delta}_2 I_1(\bar{\delta}_2)] \end{bmatrix}$$

$$\begin{Bmatrix} A_1 \\ A_2 \end{Bmatrix} = 0 \qquad (8.27)$$

The frequency equation is obtained by equating the determinant of the coefficient matrix to zero. It can be easily verified that the form of the unique solutions for A_1 and A_2 for a simply supported plate is the same as that of the solutions for a clamped plate. Hence A_1 and A_2 are given by equations (8.13-8.16) with eigenvalues for a simply supported plate.

3. Free Plate: Axisymmetric Vibration

For the mode shapes of axisymmetric vibration, the boundary conditions are

$$\begin{aligned} M_r(1) &= 0 \\ Q_r(1) &= 0 \end{aligned} \qquad (8.28)$$

where Q_r, the modal shearing force, is

$$Q_r = K^2(\psi_r + \frac{\partial W}{\partial R}) \qquad (8.29)$$

For $\Omega > \frac{K}{\alpha}$, we have

$$Q_r = -K^2[A_1\sigma_1\delta_1 J_1(\delta_1 R) + A_2\sigma_2\delta_2 J_1(\delta_2 R)] \qquad (8.30)$$

On applying the boundary conditions (8.28), equations (8.24) and (8.30) yield

$$\begin{bmatrix} (1-\sigma_1)[\delta_1{}^2 J_0(\delta_1) + (\nu-1)\delta_1 J_1(\delta_1)] & (1-\sigma_2)[\delta_2{}^2 J_0(\delta_2) + (\nu-1)\delta_2 J_1(\delta_2)] \\ -\sigma_1\delta_1 J_1(\delta_1) & -\sigma_2\delta_2 J_1(\delta_2) \end{bmatrix} \begin{Bmatrix} A_1 \\ A_2 \end{Bmatrix} = 0 \qquad (8.31)$$

For $0 < \Omega < \frac{K}{\alpha}$, one has

$$Q_r = K^2[-A_1\sigma_1\delta_1 J_1(\delta_1 R) + A_2\sigma_2\bar{\delta}_2 I_1(\bar{\delta}_2 R) \qquad (8.32)$$

and

$$\begin{bmatrix} (1-\sigma_1)[\delta_1{}^2 J_0(\delta_1) + (\nu-1)\delta_1 J_1(\delta_1)] & -(1-\sigma_2)[\bar{\delta}_2{}^2 I_0(\bar{\delta}_2) + (\nu-1)\bar{\delta}_2 I_1(\bar{\delta}_2)] \\ -\sigma_1\delta_1 J_1(\delta_1) & \sigma_2\bar{\delta}_2 I_1(\bar{\delta}_2) \end{bmatrix} \begin{Bmatrix} A_1 \\ A_2 \end{Bmatrix} = 0 \qquad (8.33)$$

The frequency equation is obtained by setting the determinant of the coefficient matrix to zero.

4. Circular Disk Rigidly Mounted on a Shaft

a. Axisymmetric Vibration

For this case, the boundary conditions for the eigenfunctions are

$$\begin{aligned} W(\beta) &= 0 \\ \psi_r(\beta) &= 0 \\ M_r(1) &= 0 \\ Q_r(1) &= 0 \end{aligned} \qquad (8.34)$$

The appropriate solutions of equations (8.2) are, for $\Omega > \frac{K}{\alpha}$

$$W(R) = A_1 J_0(\delta_1 R) + A_2 J_0(\delta_2 R) + B_1 Y_0(\delta_1 R) + B_2 Y_0(\delta_2 R)$$

$$\psi_r(R) = A_1 \delta_1 (1-\sigma_1) J_1(\delta_1 R) + A_2 \delta_2 (1-\sigma_2) J_1(\delta_2 R) \qquad (8.35)$$

$$+ B_1 \delta_1 (1-\sigma_1) Y_1(\delta_1 R) + B_2 \delta_2 (1-\sigma_2) Y_1(\delta_2 R)$$

For $0 < \Omega < \frac{K}{\alpha}$, the solutions are

$$W(R) = A_1 J_0(\delta_1 R) + A_2 I_0(\bar{\delta}_2 R) + B_1 Y_0(\delta_1 R) + B_2 K_0(\bar{\delta}_2 R)$$

$$\psi_r(R) = A_1 (1-\sigma_1) \delta_1 J_1(\delta_1 R) - A_2 (1-\sigma_2) \bar{\delta}_2 I_1(\bar{\delta}_2 R) \qquad (8.36)$$

$$+ B_1 (1-\sigma_1) \delta_1 Y_1(\delta_1 R) + B_2 (1-\sigma_2) \bar{\delta}_2 K_1(\bar{\delta}_2 R)$$

On applying the boundary conditions (8.34), equations (8.35) yield, for $\Omega > \frac{K}{\alpha}$

$$[A_{ij}] \begin{Bmatrix} A_1 \\ A_2 \\ B_1 \\ B_2 \end{Bmatrix} = 0 \qquad (8.37)$$

where

$$A_{11} = J_0(\delta_1 \beta)$$

$$A_{12} = J_0(\delta_2 \beta)$$

$$A_{13} = Y_0(\delta_1 \beta)$$

$$A_{14} = Y_0(\delta_2 \beta)$$

$$A_{21} = \delta_1 (1-\sigma_1) J_1(\delta_1 \beta)$$

$$A_{22} = \delta_2 (1-\sigma_2) J_1(\delta_2 \beta)$$

$$A_{23} = \delta_1(1-\sigma_1)Y_1(\delta_1\beta)$$

$$A_{24} = \delta_2(1-\sigma_2)Y_2(\delta_2\beta)$$

$$A_{31} = (1-\sigma_1)[\delta_1^2 J_0(\delta_1) + (\nu-1)\delta_1 J_1(\delta_1)]$$

$$A_{32} = (1-\sigma_2)[\delta_2^2 J_0(\delta_2) + (\nu-1)\delta_2 J_1(\delta_2)]$$

$$A_{33} = (1-\sigma_1)[\delta_1^2 Y_0(\delta_1) + (\nu-1)\delta_1 Y_1(\delta_1)]$$

$$A_{34} = (1-\sigma_2)[\delta_2^2 Y_0(\delta_2) + (\nu-1)\delta_2 Y_1(\delta_2)]$$

$$A_{41} = \delta_1\sigma_1 J_1(\delta_1)$$

$$A_{42} = \delta_2\sigma_2 J_1(\delta_2)$$

$$A_{43} = \delta_1\sigma_1 Y_1(\delta_1)$$

$$A_{44} = \delta_2\sigma_2 Y_1(\delta_2)$$

For $0 < \Omega < \frac{K}{\alpha}$, equations (8.36) yield

$$[B_{ij}]\begin{Bmatrix} A_1 \\ A_2 \\ B_1 \\ B_2 \end{Bmatrix} = 0 \qquad (8.38)$$

where

$$B_{11} = J_0(\delta_1\beta)$$

$$B_{12} = I_0(\bar{\delta}_2\beta)$$

$$B_{13} = Y_0(\delta_1\beta)$$

$$B_{14} = K_0(\bar{\delta}_2\beta)$$

$$B_{21} = \delta_1(1-\sigma_1)J_1(\delta_1\beta)$$

$$B_{22} = -\bar{\delta}_2(1-\sigma_2)I_1(\bar{\delta}_2\beta)$$

$$B_{23} = \delta_1(1-\sigma_1)Y_1(\delta_1\beta)$$

$$B_{24} = \bar{\delta}_2(1-\sigma_2)K_1(\bar{\delta}_2\beta)$$

$$B_{31} = (1-\sigma_1)[\delta_1{}^2 J_0(\delta_1) + (\nu-1)\delta_1 J_1(\delta_1)]$$

$$B_{32} = -(1-\sigma_2)[\bar{\delta}_2{}^2 I_0(\bar{\delta}_2) + (\nu-1)\bar{\delta}_2 I_1(\bar{\delta}_2)]$$

$$B_{33} = (1-\sigma_1)[\delta_1{}^2 Y_0(\delta_1) + (\nu-1)\delta_1 Y_1(\delta_1)]$$

$$B_{34} = -(1-\sigma_2)[\bar{\delta}_2{}^2 K_0(\bar{\delta}_2) - (\nu-1)\bar{\delta}_2 K_1(\bar{\delta}_2)]$$

$$B_{41} = \delta_1\sigma_1 J_1(\delta_1)$$

$$B_{42} = -\bar{\delta}_2\sigma_2 I_1(\delta_2)$$

$$B_{43} = \delta_1\sigma_1 Y_1(\delta_1)$$

$$B_{44} = \bar{\delta}_2\sigma_2 K_1(\bar{\delta}_2)$$

The determinants of the coefficient matrices $[A_{ij}]$ and $[B_{ij}]$ equated to zero give the frequency equations.

Unique Solutions for A_1, A_2, B_1 and B_2:

Solving for A_2, B_1 and B_2 in terms of A_1 from the first, second and fourth of equations (8.37), one obtains, for $\Omega > \frac{K}{\alpha}$

$$A_2 = \frac{\begin{Vmatrix} -J_0(\delta_1\beta) & Y_0(\delta_1\beta) & Y_0(\delta_2\beta) \\ -\delta_1(1-\sigma_1)J_1(\delta_1\beta) & \delta_1(1-\sigma_1)Y_1(\delta_1\beta) & \delta_2(1-\sigma_2)Y_1(\delta_2\beta) \\ -\delta_1\sigma_1 J_1(\delta_1) & \delta_1\sigma_1 Y_1(\delta_1) & \delta_2\sigma_2 Y_1(\delta_2) \end{Vmatrix}}{\mathrm{DET}} A_1$$

$$B_1 = \frac{\begin{Vmatrix} J_0(\delta_2\beta) & -J_0(\delta_1\beta) & Y_0(\delta_2\beta) \\ \delta_2(1-\sigma_2)J_1(\delta_2\beta) & -\delta_1(1-\sigma_1)J_1(\delta_1\beta) & \delta_2(1-\sigma_2)Y_1(\delta_2\beta) \\ \delta_2\sigma_2 J_1(\delta_2) & -\delta_1\sigma_1 J_1(\delta_1) & \delta_2\sigma_2 Y_1(\delta_2) \end{Vmatrix}}{\mathrm{DET}} A_1 \qquad (8.39)$$

$$B_2 = \frac{\begin{Vmatrix} J_0(\delta_2\beta) & Y_0(\delta_1\beta) & -J_0(\delta_1\beta) \\ \delta_2(1-\sigma_2)J_1(\delta_2\beta) & \delta_1(1-\sigma_1)Y_1(\delta_1\beta) & -\delta_1(1-\sigma_1)J_1(\delta_1\beta) \\ \delta_2\sigma_2J_1(\delta_2) & \delta_1\sigma_1Y_1(\delta_1) & -\delta_1\sigma_1J_1(\delta_1) \end{Vmatrix}}{DET} A_1$$

where DET is the determinant given by

$$DET = \begin{Vmatrix} J_0(\delta_2\beta) & Y_0(\delta_1\beta) & Y_0(\delta_2\beta) \\ \delta_2(1-\sigma_2)J_1(\delta_2\beta) & \delta_1(1-\sigma_1)Y_1(\delta_1\beta) & \delta_2(1-\sigma_2)Y_1(\delta_2\beta) \\ \delta_2\sigma_2J_1(\delta_2) & \delta_1\sigma_1Y_1(\delta_1) & \delta_2\sigma_2Y_1(\delta_2) \end{Vmatrix} \tag{8.40}$$

For brevity let

$$\begin{aligned} A_2 &= N_1A_1 \\ B_1 &= N_2A_1 \\ B_2 &= N_3A_1 \end{aligned} \tag{8.41}$$

For $0 < \Omega < \frac{K}{\alpha}$, the first, second and fourth of equations (8.38) yield

$$A_2 = \frac{\begin{Vmatrix} -J_0(\delta_1\beta) & Y_0(\delta_1\beta) & K_0(\bar{\delta}_2\beta) \\ -\delta_1(1-\sigma_1)J_1(\delta_1\beta) & \delta_1(1-\sigma_1)Y_1(\delta_1\beta) & \bar{\delta}_2(1-\sigma_2)K_1(\bar{\delta}_2\beta) \\ -\delta_1\sigma_1J_1(\delta_1) & \delta_1\sigma_1Y_1(\delta_1) & \bar{\delta}_2\sigma_2K_1(\bar{\delta}_2) \end{Vmatrix}}{DETT} A_1$$

$$B_1 = \frac{\begin{Vmatrix} I_0(\bar{\delta}_2\beta) & -J_0(\delta_1\beta) & K_0(\bar{\delta}_2\beta) \\ -\bar{\delta}_2(1-\sigma_2)I_1(\bar{\delta}_2\beta) & -\delta_1(1-\sigma_1)J_1(\delta_1\beta) & \bar{\delta}_2(1-\sigma_2)K_1(\bar{\delta}_2\beta) \\ -\bar{\delta}_2\sigma_2I_1(\bar{\delta}_2) & -\delta_1\sigma_1J_1(\delta_1) & \bar{\delta}_2\sigma_2K_1(\bar{\delta}_2) \end{Vmatrix}}{DETT} A_1 \tag{8.42}$$

$$B_2 = \frac{\begin{Vmatrix} I_0(\bar{\delta}_2\beta) & Y_0(\delta_1\beta) & -J_0(\delta_1\beta) \\ -\bar{\delta}_2(1-\sigma_2)I_1(\bar{\delta}_2\beta) & \delta_1(1-\sigma_1)Y_1(\delta_1\beta) & -\delta_1(1-\sigma_1)J_1(\delta_1\beta) \\ -\bar{\delta}_2\sigma_2 I_1(\bar{\delta}_2) & \delta_1\sigma_1 Y_1(\delta_1) & -\delta_1\sigma_1 J_1(\delta_1) \end{Vmatrix}}{DETT} A_1$$

where DETT is the determinant defined by

$$DETT = \begin{Vmatrix} I_0(\bar{\delta}_2\beta) & Y_0(\delta_1\beta) & K_0(\bar{\delta}_2\beta) \\ -\bar{\delta}_2(1-\sigma_2)I_1(\bar{\delta}_2\beta) & \delta_1(1-\sigma_1)Y_1(\delta_1\beta) & \bar{\delta}_2(1-\sigma_2)K_1(\bar{\delta}_2\beta) \\ -\bar{\delta}_2\sigma_2 I_1(\bar{\delta}_2) & \delta_1\sigma_1 Y_1(\delta_1) & \bar{\delta}_2\sigma_2 K_1(\bar{\delta}_2) \end{Vmatrix} \tag{8.43}$$

For brevity let

$$\begin{aligned} A_2 &= M_1 A_1 \\ B_1 &= M_2 A_1 \\ B_2 &= M_3 A_1 \end{aligned} \tag{8.44}$$

Applying the normalization condition (7.17) on the modes given by equations (8.35), one obtains after integration and necessary manipulation, for $\Omega > \frac{K}{\alpha}$

$$A_1 = \frac{1}{\sqrt{QJ}} \tag{8.45}$$

where

$$\begin{aligned} QJ = {} & \frac{1}{2}[J_1{}^2(\delta_1)+J_0{}^2(\delta_1)] - \frac{\beta^2}{2}[J_1{}^2(\delta_1\beta)+J_0{}^2(\delta_1\beta)] \\ & + \frac{N_1{}^2}{2}[J_1{}^2(\delta_2)+J_0{}^2(\delta_2)] - \frac{N_1{}^2\beta^2}{2}[J_1{}^2(\delta_2\beta)+J_0{}^2(\delta_2\beta)] \\ & + \frac{N_2{}^2}{2}[Y_1{}^2(\delta_1)+Y_0{}^2(\delta_1)] - \frac{N_2{}^2\beta^2}{2}[Y_1{}^2(\delta_1\beta)+Y_0{}^2(\delta_1\beta)] \\ & + \frac{N_3{}^2}{2}[Y_1{}^2(\delta_2)+Y_0{}^2(\delta_2)] - \frac{N_3{}^2\beta^2}{2}[Y_1{}^2(\delta_2\beta)+Y_0{}^2(\delta_2\beta)] \end{aligned}$$

$$+ \frac{2N_1}{\delta_1^{\,2}-\delta_2^{\,2}}[\delta_1 J_1(\delta_1)J_0(\delta_2)-\delta_2 J_1(\delta_2)J_0(\delta_1)]$$

$$- \frac{2N_1\beta}{\delta_1^{\,2}-\delta_2^{\,2}}[\delta_1 J_1(\delta_1\beta)J_0(\delta_2\beta)-\delta_2 J_1(\delta_2\beta)J_0(\delta_1\beta)]$$

$$+ N_2[J_0(\delta_1)Y_0(\delta_1)+J_1(\delta_1)Y_1(\delta_1)-N_2\beta^2[J_0(\delta_1\beta)Y_0(\delta_1\beta)+J_1(\delta_1\beta)Y_1(\delta_1\beta)]$$

$$+ \frac{2N_3}{\delta_1^{\,2}-\delta_2^{\,2}}[\delta_1 Y_0(\delta_2)J_1(\delta_1)-\delta_2 J_0(\delta_1)Y_1(\delta_2)]$$

$$- \frac{2N_3\beta}{\delta_1^{\,2}-\delta_2^{\,2}}[\delta_1 Y_0(\delta_2\beta)J_1(\delta_1\beta)-\delta_2 J_0(\delta_1\beta)Y_1(\delta_2\beta)]$$

$$- \frac{2N_1N_2}{\delta_1^{\,2}-\delta_2^{\,2}}[\delta_2 Y_0(\delta_1)J_1(\delta_2)-\delta_1 J_0(\delta_2)Y_1(\delta_1)]$$

$$+ \frac{2N_1N_2\beta}{\delta_1^{\,2}-\delta_2^{\,2}}[\delta_2 Y_0(\delta_1\beta)J_1(\delta_2\beta)-\delta_1 J_0(\delta_2\beta)Y_1(\delta_1\beta)]$$

$$+ N_1N_3[J_0(\delta_2)Y_0(\delta_2)+J_1(\delta_2)Y_1(\delta_2)]$$

$$- N_1N_3\beta^2[J_0(\delta_2\beta)Y_0(\delta_2\beta)+J_1(\delta_2\beta)Y_1(\delta_2\beta)]$$

$$+ \frac{2N_2N_3}{\delta_1^{\,2}-\delta_2^{\,2}}[\delta_1 Y_0(\delta_2)Y_1(\delta_1)-\delta_2 Y_0(\delta_1)Y_1(\delta_2)]$$

$$- \frac{2N_2N_3\beta}{\delta_1^{\,2}-\delta_2^{\,2}}[\delta_1 Y_0(\delta_2\beta)Y_1(\delta_1\beta)-\delta_2 Y_0(\delta_1\beta)Y_1(\delta_2\beta)]$$

$$+ \alpha^2\delta_1^{\,2}(1-\sigma_1)^2\{\tfrac{1}{2}[J_1^{\,2}(\delta_1)-J_0(\delta_1)J_2(\delta_1)]$$

$$- \frac{\beta^2}{2}[J_1^{\,2}(\delta_1\beta)-J_0(\delta_1\beta)J_2(\delta_1\beta)] + \frac{N_2^{\,2}}{2}[Y_1^{\,2}(\delta_1)-Y_0(\delta_1)Y_2(\delta_1)]$$

$$- \frac{N_2^{\,2}\beta^2}{2}[Y_1^{\,2}(\delta_1\beta)-Y_0(\delta_1\beta)Y_2(\delta_1\beta)]$$

$$+ \frac{N_2}{2}[2J_1(\delta_1)Y_1(\delta_1)-J_0(\delta_1)Y_2(\delta_1)-J_2(\delta_1)Y_0(\delta_1)]$$

$$- \frac{N_2\beta^2}{2}[2J_1(\delta_1\beta)Y_1(\delta_1\beta)-J_0(\delta_1\beta)Y_2(\delta_1\beta)-J_2(\delta_1\beta)Y_0(\delta_1\beta)]\}$$

$$+ \alpha^2\delta_2{}^2(1-\sigma_2)^2\{\frac{N_1{}^2}{2}[J_1{}^2(\delta_2)-J_0(\delta_2)J_2(\delta_2)$$

$$- \frac{N_1{}^2\beta^2}{2}[J_1{}^2(\delta_2\beta)-J_0(\delta_2\beta)J_2(\delta_2\beta)] + \frac{N_3{}^2}{2}[Y_1{}^2(\delta_2)-Y_0(\delta_2)Y_2(\delta_2)$$

$$- \frac{N_3{}^2\beta^2}{2}[Y_1{}^2(\delta_2\beta)-Y_0(\delta_2\beta)Y_2(\delta_2\beta)]$$

$$+ \frac{N_1N_3}{2}[2J_1(\delta_2)Y_1(\delta_2)-J_0(\delta_2)Y_2(\delta_2)-J_2(\delta_2)Y_0(\delta_2)]$$

$$- \frac{N_1N_3\beta^2}{2}[2J_1(\delta_2\beta)Y_1(\delta_2\beta)-J_0(\delta_2\beta)Y_2(\delta_2\beta)-J_2(\delta_2\beta)Y_0(\delta_2\beta)]\}$$

$$+ 2\alpha^2\delta_1\delta_2(1-\sigma_1)(1-\sigma_2)\{\frac{N_1}{\delta_1{}^2-\delta_2{}^2}[\delta_2J_0(\delta_2)J_1(\delta_1)-\delta_1J_0(\delta_1)J_1(\delta_2)]$$

$$- \frac{N_1\beta}{\delta_1{}^2-\delta_2{}^2}[\delta_2J_0(\delta_2\ )J_1(\delta_1\beta)-\delta_1J_0(\delta_1\beta)J_1(\delta_2\beta)]$$

$$+ \frac{N_3}{\delta_1{}^2-\delta_2{}^2}[\delta_1Y_1(\delta_2)J_2(\delta_1)-\delta_2J_1(\delta_1)Y_2(\delta_2)]$$

$$- \frac{N_3\beta}{\delta_1{}^2-\delta_2{}^2}[\delta_1Y_1(\delta_2\beta)J_2(\delta_1\beta)-\delta_2J_1(\delta_1\beta)Y_2(\delta_2\beta)]$$

$$- \frac{N_1N_2}{\delta_1{}^2-\delta_2{}^2}[\delta_2Y_1(\delta_1)J_2(\delta_2)-\delta_1J_1(\delta_2)Y_2(\delta_1)]$$

$$+ \frac{N_1N_2\beta}{\delta_1{}^2-\delta_2{}^2}[\delta_2Y_1(\delta_1\beta)J_2(\delta_2\beta)-\delta_1Y_2(\delta_1\beta)J_1(\delta_2\beta)]$$

$$+ \frac{N_2N_3}{\delta_1{}^2-\delta_2{}^2}[\delta_2Y_0(\delta_2)Y_1(\delta_1)-\delta_1Y_0(\delta_1)Y_1(\delta_2)]$$

$$- \frac{N_2N_3\beta}{\delta_1^2-\delta_2^2}[\delta_2 Y_0(\delta_2\beta)Y_1(\delta_1\beta)-\delta_1 Y_0(\delta_1\beta)Y_1(\delta_2\beta)]\}$$

For $0 < \Omega < \frac{K}{\alpha}$, by a similar process, equations (8.36) yield

$$A_1 = \frac{1}{\sqrt{QI}} \tag{8.46}$$

where

$$QI = \frac{1}{2}[J_1^2(\delta_1)+J_0^2(\delta_1)] - \frac{\beta^2}{2}[J_1^2(\delta_1\beta)+J_0^2)(\delta_1\beta)]$$

$$- \frac{M_1^2}{2}[I_1^2(\bar{\delta}_2)-I_0^2(\bar{\delta}_2)] + \frac{M_1^2\beta^2}{2}[I_1^2(\bar{\delta}_2\beta)-I_0^2(\bar{\delta}_2\beta)]$$

$$+ \frac{M_2^2}{2}[Y_1^2(\delta_1)+Y_0^2(\delta_1)] - \frac{M_2^2\beta^2}{2}[Y_1^2(\delta_1\beta)+Y_0^2(\delta_1\beta)]$$

$$- \frac{M_3^2}{2}[K_1^2(\bar{\delta}_2)-K_0^2(\bar{\delta}_2)] + \frac{M_3^2\beta^2}{2}[K_1^2(\bar{\delta}_2\beta)-K_0^2(\bar{\delta}_2\beta)]$$

$$+ \frac{2M_1}{\delta_1^2+\bar{\delta}_2^2}[\bar{\delta}_2 J_0(\delta_1)I_1(\bar{\delta}_2)+\delta_1 I_0(\bar{\delta}_2)J_1(\delta_1)]$$

$$- \frac{2M_1\beta}{\delta_1^2+\bar{\delta}_2^2}[\bar{\delta}_2 J_0(\delta_1\beta)I_1(\bar{\delta}_2\beta)+\delta_1 I_0(\bar{\delta}_2\beta)J_1(\delta_1\beta)]$$

$$+ M_2[J_0(\delta_1)Y_0(\delta_1)+J_1(\delta_1)Y_1(\delta_1)] - N_2\beta^2[J_0(\delta_1\beta)Y_0(\delta_1\beta)+J_1(\delta_1\beta)Y_1(\delta_1\beta)]$$

$$+ \frac{2M_3}{\delta_1^2+\bar{\delta}_2^2}[\delta_1 K_0(\bar{\delta}_2)J_1(\delta_1)-\bar{\delta}_2 J_0(\delta_1)K_1(\bar{\delta}_2)]$$

$$- \frac{2M_3\beta}{\delta_1^2+\bar{\delta}_2^2}[\delta_1 K_0(\bar{\delta}_2\beta)J_1(\delta_1\beta)-\bar{\delta}_2 J_0(\delta_1\beta)K_1(\bar{\delta}_2\beta)]$$

$$+ \frac{2M_1M_2}{\delta_1^2+\bar{\delta}_2^2}[\delta_2 Y_0(\delta_1)I_1(\bar{\delta}_2)+\delta_1 I_0(\bar{\delta}_2)Y_1(\delta_1)]$$

$$- \frac{2M_1M_2\beta}{\delta_1^2+\bar{\delta}_2^2}[\delta_2 Y_0(\delta_1\beta)I_1(\bar{\delta}_2\beta)+\delta_1 I_0(\bar{\delta}_2\beta)Y_1(\delta_1\beta)]$$

$$+ M_1M_3[K_1(\bar{\delta}_2)I_1(\bar{\delta}_2)+K_0(\bar{\delta}_2)I_0(\bar{\delta}_2)]$$

$$- M_1M_3\beta^2[K_1(\bar{\delta}_2\beta)I_1(\bar{\delta}_2\beta)+K_0(\bar{\delta}_2\beta)I_0(\bar{\delta}_2\beta)]$$

$$+ \frac{2M_2M_3}{\delta_1{}^2+\bar{\delta}_2{}^2}[\delta_1K_0(\bar{\delta}_2)Y_1(\delta_1)-\bar{\delta}_2Y_0(\delta_1)K_1(\bar{\delta}_2)]$$

$$- \frac{2M_2M_3\beta}{\delta_1{}^2+\bar{\delta}_2{}^2}[\delta_1K_0(\bar{\delta}_2\beta)Y_1(\delta_1\beta)-\bar{\delta}_2Y_0(\delta_1\beta)K_1(\bar{\delta}_2\beta)]$$

$$+ \delta_1{}^2\alpha^2(1-\sigma_1)^2\{\frac{1}{2}[J_1{}^2(\delta_1)-J_0(\delta_1)J_2(\delta_1)]$$

$$- \frac{\beta^2}{2}[J_1{}^2(\delta_1\beta)-J_0(\delta_1\beta)J_2(\delta_1\beta)]$$

$$+ \frac{M_2{}^2}{2}[Y_1{}^2(\delta_1)-Y_0(\delta_1)Y_2(\delta_1)] - \frac{M_2{}^2\beta^2}{2}[Y_1{}^2(\delta_1\beta)-Y_0(\delta_1\beta)Y_2(\delta_1\beta)]$$

$$+ \frac{M_2}{2}[2J_1(\delta_1)Y_1(\delta_1)-J_0(\delta_1)Y_2(\delta_1)-J_2(\delta_1)Y_0(\delta_1)]$$

$$- \frac{M_2\beta^2}{2}[2J_1(\delta_1\beta)Y_1(\delta_1\beta)-J_0(\delta_1\beta)Y_2(\delta_1\beta)-J_2(\delta_1\beta)Y_0(\delta_1\beta)]$$

$$+ \alpha^2\ \bar{\delta}_2{}^2(1-\sigma_2)^2\{\frac{M_1{}^2}{2}[I_1{}^2(\bar{\delta}_2)-I_0(\bar{\delta}_2)I_2(\bar{\delta}_2)]$$

$$- \frac{M_1{}^2\beta^2}{2}[I_1{}^2(\bar{\delta}_2\beta)-I_0(\bar{\delta}_2\beta)I_2(\bar{\delta}_2\beta)] + \frac{M_3{}^2}{2}[K_1{}^2(\bar{\delta}_2)-K_2(\bar{\delta}_2)K_0(\bar{\delta}_2)]$$

$$- \frac{M_3{}^2\beta^2}{2}[K_1{}^2(\bar{\delta}_2\ )-K_2(\bar{\delta}_2\beta)K_0(\bar{\delta}_2\beta)]$$

$$- M_1M_3[\frac{1}{\bar{\delta}_2}K_2(\bar{\delta}_2)I_1(\bar{\delta}_2)+K_2(\bar{\delta}_2)I_2(\bar{\delta}_2)+K_1(\bar{\delta}_2)I_1(\bar{\delta}_2)$$

$$- \frac{1}{\bar{\delta}_2}K_1(\bar{\delta}_2)I_2(\bar{\delta}_2)]$$

$$+ M_1M_3\beta^2[\frac{1}{\bar{\delta}_2\beta}K_2(\bar{\delta}_2\beta)I_1(\bar{\delta}_2\beta)+K_2(\bar{\delta}_2\beta)I_2(\bar{\delta}_2\beta)$$

$$+ K_1(\bar{\delta}_2\beta)I_1(\bar{\delta}_2\beta) - \frac{1}{\bar{\delta}_2\beta} K_1(\bar{\delta}_2\beta)I_2(\bar{\delta}_2\beta)]$$

$$+ 2\alpha^2\delta_1\bar{\delta}_2(1-\sigma_1)(1-\sigma_2)\left\{\frac{-M_1}{\delta_1{}^2+\bar{\delta}_2{}^2}[\bar{\delta}_2J_1(\delta_1)I_0(\bar{\delta}_2)-\delta_1I_1(\bar{\delta}_2)J_0(\delta_1)]\right.$$

$$+ \frac{M_1\beta}{\delta_1{}^2+\bar{\delta}_2{}^2}[\bar{\delta}_2J_1(\delta_1\beta)I_0(\bar{\delta}_2\beta)-\delta_1I_1(\bar{\delta}_2\beta)J_0(\delta_1\beta)]$$

$$+ \frac{M_3}{\delta_1{}^2+\bar{\delta}_2{}^2}[\delta_1K_1(\bar{\delta}_2)J_2(\delta_1)-\bar{\delta}_2K_2(\bar{\delta}_2)J_1(\delta_1)]$$

$$- \frac{M_3\beta}{\delta_1{}^2+\bar{\delta}_2{}^2}[\delta_1K_1(\bar{\delta}_2\beta)J_2(\delta_1\beta)-\bar{\delta}_2K_2(\bar{\delta}_2\beta)J_1(\delta_1\beta)]$$

$$- \frac{M_1M_2}{\delta_1{}^2+\bar{\delta}_2{}^2}[\bar{\delta}_2Y_1(\delta_1)I_0(\bar{\delta}_2)-\delta_1I_1(\bar{\delta}_2)Y_0(\delta_1)]$$

$$+ \frac{M_1M_2\beta}{\delta_1{}^2+\bar{\delta}_2{}^2}[\bar{\delta}_2Y_1(\delta_1\beta)I_0(\bar{\delta}_2\beta)-\delta_1I_1(\bar{\delta}_2\beta)Y_0(\delta_1\beta)]$$

$$+ \frac{M_2M_3}{\delta_1{}^2+\bar{\delta}_2{}^2}[\delta_1K_1(\bar{\delta}_2)Y_2(\delta_1)-\bar{\delta}_2K_2(\bar{\delta}_2)Y_1(\delta_1)]$$

$$\left.- \frac{M_2M_3\beta}{\delta_1{}^2+\bar{\delta}_2{}^2}[\delta_1K_1(\bar{\delta}_2\beta)Y_2(\delta_1\beta)-\bar{\delta}_2K_2(\bar{\delta}_2\beta)Y_1(\delta_1\beta)]\right\}$$

The mode shapes W and ψ_r are uniquely determined by knowing the values of A_1, A_2, B_1 and B_2 as given by the equations (8.39 - 8.46).

b. Vibration with One Diametral Node

It is now fairly well established that fractures which occur in turbine disks, and which cannot be attributed to defects in the material of the disks or to excessive centrifugal forces, are caused by flexural vibrations of these disks [3]. There are various causes which may produce these flexural vibrations, but the most important is that due to non-uniform gas pressure. An irregularity in the nozzles may cause non-uniform pressure. Assuming that the turbine disk is rotating with constant angular velocity ω_r in the field of such a pressure, then for a certain point on the rim of the disk, the pressure may vary with the angle of rotation of the disk, and this may be represented by a periodic function

$$p_g = a_o + a_1 \sin \omega_r t + a_2 \sin 2\,\omega_r t + a_3 \sin 3\,\omega_r t + \text{---}$$
$$+ b_1 \cos \omega_r t + b_2 \cos 2\,\omega_r t + b_3 \cos 3\,\omega_r t + \text{----} \quad (8.47)$$

Taking only one term in the series, such as $a_1 \sin \omega_r t$, large lateral vibration of the disk occurs when the frequency $\omega_r/2\pi$ of the force coincides with one of the natural frequencies of the disk. Experiments [3] have shown that the axisymmetric type of vibration seldom occurs in turbine disks and no disk failure can be attributed to this type of vibration. Failure is mainly attributed to lateral vibrations with one or more diametral nodes. The frequency equation for vibration with one diametral node will be derived now and the same procedure can be used for obtaining the frequency equations for vibrations with more diametral nodes.

For a disk rigidly mounted on a shaft, the boundary conditions for the mode shapes are

$$\begin{aligned} W(\beta) &= 0 \\ \psi_r(\beta) &= 0 \\ \psi_\theta(\beta) &= 0 \\ M_r(1) &= 0 \\ M_{r\theta}(1) &= 0 \\ Q_r(1) &= 0 \end{aligned} \qquad (8.48)$$

The solutions of equations (8.2) for one diametral node vibration are, for $\Omega > \frac{K}{\alpha}$

$$W = [A_1 J_1(\delta_1 R) + A_2 J_1(\delta_2 R) + B_1 Y_1(\delta_1 R) + B_2 Y_1(\delta_2 R)] \cos\theta$$
$$W_3 = [A_3 J_1(\delta_3 R) + B_3 Y_1(\delta_3 R)] \sin\theta \tag{8.49}$$

for $0 < \Omega < \frac{K}{\alpha}$

$$W = [A_1 J_1(\delta_1 R) + A_2 I_1(\bar{\delta}_2 R) + B_1 Y_1(\delta_1 R) + B_2 K_1(\bar{\delta}_2 R)] \cos\theta$$
$$W_3 = [A_3 I_1(\bar{\delta}_3 R) + B_3 K_1(\bar{\delta}_3 R)] \sin\theta \tag{8.50}$$

The modal bending moments and shearing force are given by

$$M_r = (\frac{\partial\psi_r}{\partial R} + \frac{\nu}{R}\psi_r + \frac{\nu}{R}\frac{\partial\psi_\theta}{\partial\theta})$$

$$\tilde{M}_{r\theta} = \frac{1-\nu}{2}[\frac{1}{R}(\frac{\partial\psi_r}{\partial\theta} - \psi_\theta) + \frac{\partial\psi_\theta}{\partial R})] \tag{8.51}$$

$$Q_r = K^2 (\psi_r + \frac{\partial W}{\partial R})$$

In view of equations (8.1) and (8.51), equations (8.49) yield, for $\Omega > \frac{K}{\alpha}$

$$\begin{aligned}\psi_r = \{&A_1(\sigma_1-1)[\delta_1 J_0(\delta_1 R) - \tfrac{1}{R}J_1(\delta_1 R)]\\ &+ A_2(\sigma_2-1)[\delta_2 J_0(\delta_2 R) - \tfrac{1}{R}J_1(\delta_2 R)] + A_3\tfrac{1}{R}J_1(\delta_3 R)\\ &+ B_1(\sigma_1-1)[\delta_1 Y_0(\delta_1 R) - \tfrac{1}{R}Y_1(\delta_1 R)]\\ &+ B_2(\delta_2-1)[\delta_2 Y_0(\delta_2 R) - \tfrac{1}{R}Y_1(\delta_2 R)] + B_3\tfrac{1}{R}Y_1(\delta_3 R)\}\cos\theta\end{aligned} \tag{8.52}$$

$$\begin{aligned}\psi_\theta = -\{&A_1(\sigma_1-1)\tfrac{1}{R}J_1(\delta_1 R) + A_2(\sigma_2-1)\tfrac{1}{R}J_1(\delta_2 R)\\ &+ A_3[\delta_3 J_0(\delta_3 R) - \tfrac{1}{R}J_1(\delta_3 R)]\\ &+ B_1(\sigma_1-1)\tfrac{1}{R}Y_1(\delta_1 R) + B_2(\sigma_2-1)\tfrac{1}{R}Y_1(\delta_2 R)\end{aligned} \tag{8.53}$$

$$+ B_3[\delta_3 Y_0(\delta_3 R) - \frac{1}{R}Y_1(\delta_3 R)]\} \sin\theta$$

$$M_r = \{A_1(\sigma_1-1)[\frac{(\nu-1)}{R}\delta_1 J_0(\delta_1 R)+(\frac{2}{R^2} - \frac{2\nu}{R^2} - \delta_1{}^2)J_1(\delta_1 R)]$$

$$+ A_2(\sigma_2-1)[\frac{(\nu-1)}{R}\delta_2 J_0(\delta_2 R)+(\frac{2}{R^2} - \frac{2\nu}{R^2} - \delta_2{}^2)J_1(\delta_2 R)]$$

$$+ A_3[\frac{(1-\nu)}{R}\delta_3 J_0(\delta_3 R)+ \frac{(2\nu-2)}{R^2}J_1(\delta_3 R)] \tag{8.54}$$

$$+ B_1(\sigma_1-1)[\frac{(\nu-1)}{R}\delta_1 Y_0(\delta_1 R)+(\frac{2}{R^2} - \frac{2\nu}{R^2} - \delta_1{}^2)Y_1(\delta_1 R)]$$

$$+ B_2(\sigma_2-1)[\frac{(\nu-1)}{R}\delta_2 Y_0(\delta_2 R)+(\frac{2}{R^2} - \frac{2\nu}{R^2} - \delta_2{}^2)Y_1(\delta_2 R)]$$

$$+ B_3[\frac{(1-\nu)}{R}\delta_3 Y_0(\delta_3 R)+ \frac{(2\nu-2)}{R^2}Y_1(\delta_3 R)]\} \cos\theta$$

$$M_{r\theta} = \frac{1-\nu}{2}\{A_1(\sigma_1-1)[\frac{-4}{R^2}J_1(\delta_1 R)- \frac{2\delta_1}{R}J_0(\delta_1 R)]$$

$$+ A_2(\sigma_2-1)[\frac{4}{R^2}J_1(\delta_1 R)- \frac{2\delta_2}{R}J_0(\delta_1 R)]$$

$$+ A_3[\delta_3{}^2 J_1(\delta_3 R)- \frac{4}{R^2}J_1(\delta_3 R)+ \frac{2\delta_3}{R}J_0(\delta_3 R)]$$

$$+ B_1(\sigma_1-1)[\frac{4}{R^2}Y_1(\delta_1 R)- \frac{2\delta_1}{R}Y_0(\delta_1 R)] \tag{8.55}$$

$$+ B_2(\sigma_2-1)[\frac{4}{R^2}Y_1(\delta_2 R)- \frac{2\delta_2}{R}Y_0(\delta_2 R)]$$

$$+ B_3[\delta_3{}^2 Y_1(\delta_3 R)- \frac{4}{R^2}Y_1(\delta_3 R)+ \frac{2\delta_3}{R}Y_0(\delta_3 R)]\} \sin\theta$$

$$Q_r = K^2 \quad \{A_1\sigma_1[\delta_1 J_0(\delta_1 R)- \frac{1}{R}J_1(\delta_1 R)]$$

$$+ A_2\sigma_2[\delta_2 J_0(\delta_2 R)- \frac{1}{R}J_1(\delta_2 R)]$$

$$+ A_3 \frac{1}{R}J_1(\delta_3 R)$$

$$+ B_1\sigma_1[\delta_1 Y_0(\delta_1 R)- \frac{1}{R}Y_1(\delta_1 R)] \qquad (8.56$$

$$+ B_2\sigma_2[\delta_2 Y_0(\delta_2 R)- \frac{1}{R}Y_1(\delta_2 R)]$$

$$+ B_3 \frac{1}{R} Y_1(\delta_3 R)\} \cos\theta$$

Applying the boundary conditions (8.48) to the above equations, one obtains, for $\Omega > \frac{K}{\alpha}$

$$[C_{ij}]\begin{Bmatrix} A_1 \\ A_2 \\ A_3 \\ B_1 \\ B_2 \\ B_3 \end{Bmatrix} = 0 \tag{8.57}$$

where

$$C_{11} = J_1(\delta_1\beta)$$

$$C_{12} = J_1(\delta_2\beta)$$

$$C_{13} = 0$$

$$C_{14} = Y_1(\delta_1\beta)$$

$$C_{15} = Y_1(\delta_2\beta)$$

$$C_{16} = 0$$

$$C_{21} = (\sigma_1 - 1)[\delta_1 J_0(\delta_1\beta) - \frac{1}{\beta} J_1(\delta_1\beta)]$$

$$C_{22} = (\sigma_2 - 1)[\delta_2 J_0(\delta_2\beta) - \frac{1}{\beta} J_1(\delta_2\beta)]$$

$$C_{23} = \frac{1}{\beta} J_1(\delta_3\beta)$$

$$C_{24} = (\sigma_1 - 1)[\delta_1 Y_0(\delta_1\beta) - \frac{1}{\beta} Y_1(\delta_1\beta)]$$

$$C_{25} = (\sigma_2 - 1)[\delta_2 Y_0(\delta_2\beta) - \frac{1}{\beta} Y_1(\delta_2\beta)]$$

$$C_{26} = \frac{1}{\beta} Y_1(\delta_3\beta)$$

$$C_{31} = (\sigma_1-1)\frac{1}{\beta}J_1(\delta_1\beta)$$

$$C_{32} = (\sigma_2-1)\frac{1}{\beta}J_1(\delta_2\beta)$$

$$C_{33} = [\delta_3 J_0(\delta_3\beta) - \frac{1}{\beta}J_1(\delta_3\beta)]$$

$$C_{34} = (\sigma_1-1)\frac{1}{\beta}Y_1(\delta_1\beta)$$

$$C_{35} = (\sigma_2-1)\frac{1}{\beta}Y_1(\delta_2\beta)$$

$$C_{36} = [\delta_3 Y_0(\delta_3\beta) - \frac{1}{\beta}Y_1(\delta_3\beta)]$$

$$C_{41} = (\sigma_1-1)[(\nu-1)\delta_1 J_0(\delta_1)+(2-2\nu-\delta_1{}^2)J_1(\delta_1)]$$

$$C_{42} = (\sigma_2-1)[(\nu-1)\delta_2 J_0(\delta_2)+(2-2\nu-\delta_2{}^2)J_1(\delta_2)]$$

$$C_{43} = [(1-\nu)\delta_3 J_0(\delta_3)+(2\nu-2)J_1(\delta_3)]$$

$$C_{44} = (\sigma_1-1)[(\nu-1)\delta_1 Y_0(\delta_1)+(2-2\nu-\delta_1{}^2)Y_1(\delta_1)]$$

$$C_{45} = (\sigma_2-1)[(\nu-1)\delta_2 Y_0(\delta_2)+(2-2\nu-\delta_2{}^2)Y_1(\delta_2)]$$

$$C_{46} = [(1-\nu)\delta_3 Y_0(\delta_3)+(2\nu-2)Y_1(\delta_3)]$$

$$C_{51} = (\sigma_1-1)[4J_1(\delta_1)-2\delta_1 J_0(\delta_1)]$$

$$C_{52} = (\sigma_2-1)[4J_1(\delta_2)-2\delta_2 J_0(\delta_2)]$$

$$C_{53} = [\delta_3{}^2 J_1(\delta_3)-4J_1(\delta_3)+2\delta_3 J_0(\delta_3)]$$

$$C_{54} = (\sigma_1-1)[4Y_1(\delta_1)-2\delta_1 Y_0(\delta_1)]$$

$$C_{55} = (\sigma_2-1)[4Y_1(\delta_2)-2\delta_2 Y_0(\delta_2)]$$

$$C_{56} = [\delta_3{}^2 Y_1(\delta_3)-4Y_1(\delta_3)+2\delta_3 Y_0(\delta_3)]$$

$$C_{61} = \sigma_1[\delta_1 J_0(\delta_1)-J_1(\delta_1)]$$

$$C_{62} = \sigma_2[\delta_2 J_0(\delta_2)-J_1(\delta_2)]$$

$$C_{63} = J_1(\delta_3)$$

$$C_{64} = \sigma_1[\delta_1 Y_0(\delta_1)-Y_1(\delta_1)]$$

$$C_{65} = \sigma_2[\delta_2 Y_0(\delta_2) - Y_1(\delta_2)]$$

$$C_{66} = Y_1(\delta_3)$$

For $0 < \Omega < \frac{K}{\alpha}$, a similar process yields

$$[D_{ij}] \begin{Bmatrix} A_1 \\ A_2 \\ A_3 \\ B_1 \\ B_2 \\ B_3 \end{Bmatrix} = 0 \tag{8.58}$$

where

$$D_{11} = J_1(\delta_1\beta)$$

$$D_{12} = I_1(\bar{\delta}_2\beta)$$

$$D_{13} = 0$$

$$D_{14} = Y_1(\delta_1\beta)$$

$$D_{15} = K_1(\bar{\delta}_2\beta)$$

$$D_{16} = 0$$

$$D_{21} = (\sigma_1 - 1)[\delta_1 J_0(\delta_1\beta) - \frac{1}{\beta}J_1(\delta_1\beta)]$$

$$D_{22} = (\sigma_2 - 1)[\bar{\delta}_2 I_0(\bar{\delta}_2\beta) - \frac{1}{\beta}I_1(\bar{\delta}_2\beta)]$$

$$D_{23} = \frac{1}{\beta}I_1(\bar{\delta}_3\beta)$$

$$D_{24} = (\sigma_1 - 1)[\delta_1 Y_0(\delta_1\beta) - \frac{1}{\beta}Y_1(\delta_1\beta)]$$

$$D_{25} = -(\sigma_2 - 1)[\bar{\delta}_2 K_0(\bar{\delta}_2\beta) + \frac{1}{\beta}K_1(\bar{\delta}_2\beta)]$$

$$D_{26} = \frac{1}{\beta}K_1(\bar{\delta}_3\beta)$$

$$D_{31} = (\sigma_1-1)\frac{1}{\beta}J_1(\delta_2\beta)$$

$$D_{32} = (\sigma_2-1)\frac{1}{\beta}I_1(\bar{\delta}_2\beta)$$

$$D_{33} = [\bar{\delta}_3 I_0(\bar{\delta}_3\beta) - \frac{1}{\beta}I_1(\bar{\delta}_3\beta)]$$

$$D_{34} = (\sigma_1-1)\frac{1}{\beta}Y_1(\delta_1\beta)$$

$$D_{35} = (\sigma_2-1)\frac{1}{\beta}K_1(\bar{\delta}_2\beta)$$

$$D_{36} = -[\bar{\delta}_3 K_0(\bar{\delta}_3\beta) + \frac{1}{\beta}K_1(\bar{\delta}_3\beta)]$$

$$D_{41} = (\sigma_1-1)[(\nu-1)\delta_1 J_0(\delta_1)+(2-2\nu-\delta_1{}^2)J_1(\delta_1)]$$

$$D_{42} = (\delta_2-1)[(\nu-1)\bar{\delta}_2 I_0(\bar{\delta}_2)+(2-2\nu+\bar{\delta}_2{}^2)I_1(\bar{\delta}_2)]$$

$$D_{43} = [(1-\nu)\bar{\delta}_3 I_0(\bar{\delta}_3)+(2\nu-2)I_1(\bar{\delta}_3)]$$

$$D_{44} = (\sigma_1-1)[(\nu-1)\delta_1 Y_0(\delta_1)+(2-2\nu-\delta_1{}^2)Y_1(\delta_1)]$$

$$D_{45} = (\sigma_2-1)[(1-\nu)\bar{\delta}_2 K_0(\bar{\delta}_2)+(2-2\nu+\bar{\delta}_2{}^2)K_1(\bar{\delta}_2)]$$

$$D_{46} = [(\nu-1)\bar{\delta}_3 K_0(\bar{\delta}_3)+(2\nu-2)K_1(\bar{\delta}_3)]$$

$$D_{51} = (\sigma_1-1)[4J_1(\delta_1)-2\delta_1 J_0(\delta_1)]$$

$$D_{52} = (\sigma_2-1)[4I_1(\bar{\delta}_2)-2\bar{\delta}_2 I_0(\bar{\delta}_2)]$$

$$D_{53} = [-\bar{\delta}_3{}^2 I_1(\bar{\delta}_3)-4I_1(\bar{\delta}_3)+2\bar{\delta}_3 I_0(\bar{\delta}_3)]$$

$$D_{54} = (\sigma_1-1)[4Y_1(\delta_1)-2\delta_1 Y_0(\delta_1)]$$

$$D_{55} = (\sigma_2-1)[4K_1(\bar{\delta}_2)+2\bar{\delta}_2 K_0(\bar{\delta}_2)]$$

$$D_{56} = [-\bar{\delta}_3{}^2 K_1(\bar{\delta}_3)-4K_1(\bar{\delta}_3)-2\bar{\delta}_3 K_0(\bar{\delta}_3)]$$

$$D_{61} = \sigma_1[\delta_1 J_0(\delta_1)-J_1(\delta_1)]$$

$$D_{62} = \sigma_2[\bar{\delta}_2 I_0(\bar{\delta}_2)-I_1(\bar{\delta}_2)]$$

$$D_{63} = I_1(\bar{\delta}_3)$$

$$D_{64} = \sigma_1[\delta_1 Y_0(\delta_1)-Y_1(\delta_1)]$$

$$D_{65} = -\sigma_2[\bar{\delta}_2 K_0(\bar{\delta}_2) + K_1(\bar{\delta}_2)]$$

$$D_{66} = K_1(\bar{\delta}_3)$$

The determinants of the coefficient matrices $[C_{ij}]$ and $[D_{ij}]$ equated to zero give the frequency equations.

C. Forced Motion under a Step Function Load (see figure 21a)

Case 1. Clamped Plate with Load Uniformly Distributed over a Circular Area (see figure 2)

The loading for this case is given by

$$P(R,T) = -P[U(R)-U(R-\gamma)]\ U(T) \tag{8.59}$$

where

P is the load intensity

$U(R)$, $U(R-\gamma)$ and $U(T)$ are Unit Step Functions (see list of symbols)

Static Solution:

The governing equations are equations (7.19) with load intensity of equation (8.59). Thus we have

$$\begin{aligned} &\frac{\partial}{\partial R}\left[\frac{1}{R}\frac{\partial}{\partial R}(R\psi_s)\right] - \frac{K^2}{\alpha^2}\left(\psi_s + \frac{\partial W_s}{\partial R}\right) = 0 \\ &\frac{K^2}{R}\frac{\partial}{\partial R}\left[R\left(\psi_s + \frac{\partial W_s}{\partial R}\right)\right] = P[U(R)-U(R-\gamma)]\ U(T) \end{aligned} \tag{8.60}$$

The boundary conditions are

$$\begin{aligned} W_s(1,T) &= 0 \\ \psi_s(1,T) &= 0 \end{aligned} \tag{8.61}$$

Eliminating W_s from equations (8.60), one obtains, for $T > 0$

$$\frac{\alpha^2}{R}\frac{\partial}{\partial R}\{R\frac{\partial}{\partial R}[\frac{1}{R}\frac{\partial}{\partial R}(R\psi_s)]\} = PU(R) - PU(R-\gamma) \tag{8.62}$$

Successive integration of the above yields

$$\alpha^2\psi_s = \frac{P}{16}R^3U(R) + [\frac{P}{16}\frac{\gamma^4}{R} - \frac{PR^3}{16} + \frac{P}{4}\gamma^2 R\log R$$

$$- \frac{P}{4}\gamma^2 R\log\gamma]\ U(R-\gamma) \tag{8.63}$$

$$+ C_1[\frac{R}{2}\log R - \frac{R}{4}] + C_2\frac{R}{2} + \frac{C_3}{R}$$

Since W_s and ψ_s must be finite at $R = 0$, one has

$$C_1 = C_3 = 0$$

Applying the boundary conditions, equation (8.63) yields

$$C_2 = \frac{P}{2}\gamma^2\log\gamma - \frac{P}{8}\gamma^4 \tag{8.64}$$

From the first of equations (8.60) one gets

$$\alpha^2\frac{\partial}{\partial R}[\frac{1}{R}\frac{\partial}{\partial R}(R\psi_s)] = K^2(\psi_s + \frac{\partial W_s}{\partial R}) \tag{8.65}$$

In view of equations (8.63) and (8.64), one obtains from the above equation

$$\alpha^2\frac{\partial W_s}{\partial R} = (\frac{\alpha^2}{K^2}\frac{P}{2}R - \frac{P}{16}R^3)U(R) + (\frac{\alpha^2}{K^2}\frac{P}{2}\frac{\gamma^2}{R} - \frac{\alpha^2}{K^2}\frac{P}{2}R$$

$$+ \frac{P}{16}R^3 - \frac{P}{16}\frac{\gamma^4}{R} + \frac{P}{4}\gamma^2 R\log\gamma - \frac{P}{4}\gamma^2 R\log R)$$

$$U(R-\gamma) - \frac{P}{4}R\gamma^2\log\gamma + \frac{P}{16}R\gamma^4$$

Integrating the above equation, we obtain

$$\alpha^2 W_s = (\frac{\alpha^2}{K^2}\frac{P}{4}R^2 - \frac{P}{64}R^4)U(R) + \frac{\alpha^2}{K^2}(\frac{P}{4}\gamma^2 - \frac{P}{4}R^2$$

$$+ \frac{P}{2}\gamma^2 \log R - \frac{P}{2}\gamma^2 \log\gamma)U(R-\gamma)$$

$$+ (\frac{P}{64}R^4 - \frac{P}{64}\gamma^4 + \frac{P}{16}\gamma^4 \log\gamma - \frac{P}{16}\gamma^4 \log R \tag{8.66}$$

$$- \frac{P}{8}\gamma^2 R^2 \log R + \frac{P}{8}\gamma^2 R^2 \log\gamma + \frac{P}{16}\gamma^2 R^2 - \frac{P}{16}\gamma^4)$$

$$U(R-\gamma) + \frac{P}{32}\gamma^4 R^2 - \frac{P}{8}\gamma^2 R^2 \log\gamma + C_4$$

Applying the boundary condition $W_s(1) = 0$, the above equation yields

$$C_4 = \frac{\alpha^2}{K^2}(\frac{P}{2}\gamma^2 \log\gamma - \frac{P}{4}\gamma^2) + \frac{3}{64}P\gamma^4$$

$$- \frac{P}{16}\gamma^4 \log\gamma - \frac{P}{16}\gamma^2 \tag{8.67}$$

Hence the required static solutions are, for $0 < R < \gamma$

$$\frac{\psi_s}{P_0} = \frac{1}{\pi\alpha^2}(\frac{R^3}{16\gamma^2} + \frac{R\log\gamma}{4} - \frac{R}{16}\gamma^2)$$

$$\frac{W_s}{P_0} = \frac{1}{\pi K^2}(\frac{R^2}{4\gamma^2} + \frac{\log\gamma}{2} - \frac{1}{4}) \tag{8.68}$$

$$+ \frac{1}{\pi\alpha^2}(- \frac{R^4}{62\gamma^2} - \frac{R^2}{8}\log\gamma + \frac{R^2}{32}\gamma^2 + \frac{3}{64}\gamma^2 - \frac{\gamma^2}{16}\log\gamma - \frac{1}{16})$$

For $R > \gamma$

$$\frac{\psi_s}{P_0} = \frac{1}{\pi\alpha^2}(\frac{\gamma^2}{16R} + \frac{R}{4}\log R - \frac{R}{16}\gamma^2)$$

$$\frac{W_s}{P_0} = \frac{\log R}{2\pi K^2} + \frac{1}{\pi\alpha^2}(- \frac{\gamma^2}{16}\log R - \frac{R^2}{8}\log R + \frac{R^2}{16} \tag{8.69}$$

$$+ \frac{R^2}{32}\gamma^2 - \frac{\gamma^2}{32} - \frac{1}{16})$$

where the total load, P_0, is

$$P_0 = \pi\gamma^2 P \tag{8.70}$$

Now in view of equations (7.25), equations (8.68) and (8.69) yield, for $0 < R < \gamma$

$$\begin{aligned} \frac{M_{rs}}{P_0} &= \frac{1}{\pi\alpha^2}\left(\frac{3+\nu}{16\gamma^2} R^2 + \frac{1+\nu}{4}\log\gamma - \frac{(1+\nu)}{16}\gamma^2\right) \\ \frac{Q_{rs}}{P_0} &= \frac{R}{2\pi\gamma^2} \end{aligned} \tag{8.71}$$

For $R > \gamma$, we obtain

$$\begin{aligned} \frac{M_{rs}}{P_0} &= \frac{1}{\pi\alpha^2}\left(\frac{\nu-1}{16}\frac{\gamma^2}{R^2} + \frac{(1+\nu)}{4}\log R - \left(\frac{1+\nu}{16}\right)\gamma^2 + \frac{1}{4}\right) \\ \frac{Q_{rs}}{P_0} &= \frac{1}{2\pi R} \end{aligned} \tag{8.72}$$

Dynamic Solution:

Initial conditions are assumed as

$$\begin{aligned} W(R,0) &= \dot{W}(R,0) = 0 \\ \psi(R,0) &= \dot{\psi}(R,0) = 0 \end{aligned} \tag{8.73}$$

In view of equations (8.59), (8.61), (8.70) and (8.8), equation (7.24) yields

$$P_i(T) = -\frac{P_0\, U(T)}{\pi\gamma^2\Omega_i^2}\int_0^\gamma W_i(R) R dR \tag{8.74}$$

Consequently, one obtains

$$P_i(0) = -\frac{P_0}{\pi\gamma^2\Omega_i^2}\int_0^\gamma W_i(R) R dR \tag{8.75}$$

$$\dot{P}_i(0) = \ddot{P}_i(0) = 0 \tag{8.76}$$

Using equations (8.73) and (8.76), we obtain from equations (7.27) and (7.28)

$$\begin{aligned} q_i(0) &= -P_i(0) = \frac{P_0}{\pi\gamma^2\Omega_i^2} \int_0^\gamma W_i(R)RdR \\ \dot{q}_i(0) &= -\dot{P}_i(0) = 0 \end{aligned} \tag{8.77}$$

Substituting equations (8.74) and (8.77) into equation (7.29) one gets

$$q_i(T) = \frac{P_0}{\pi\gamma^2\Omega_i^2} \int_0^\gamma W_i(R)RdR\cos\Omega_i T \tag{8.78}$$

In view of equations (8.9) and (8.10), equation (8.78) yields on integration, for $0 < \Omega < \frac{K}{\alpha}$

$$\frac{q_i(T)}{P_0} = \left[A_1 \frac{J_1(\delta_1\gamma)}{\delta_1} + A_2 \frac{I_1(\bar{\delta}_2\gamma)}{\bar{\delta}_2} \right] \frac{\cos\Omega_i T}{\pi\gamma\Omega_i^2} \tag{8.79}$$

and for $\Omega > \frac{K}{\alpha}$

$$\frac{q_i(T)}{P_0} = \left[A_1 \frac{J_1(\delta_1\gamma)}{\delta_1} + A_2 \frac{J_1(\delta_2\gamma)}{\delta_2} \right] \frac{\cos\Omega_i T}{\pi\gamma\Omega_i^2} \tag{8.80}$$

where A_1 and A_2 are given by equations (8.13-8.16).

The complete solution to the forced motion problem is now given by

$$\begin{aligned} W(R,T) &= W_s(R,T) + \sum_{i=1}^{\infty} W_i(R)q_i(T) \\ \psi(R,T) &= \psi_s(R,T) + \sum_{i=1}^{\infty} \psi_i(R)q_i(T) \\ M_r(R,T) &= M_{rs}(R,T) + \sum_{i=1}^{\infty} M_{ri}(R)q_i(T) \\ Q_r(R,T) &= Q_{rs}(R,T) + \sum_{i=1}^{\infty} Q_{ri}(R)q_i(T) \end{aligned} \tag{8.81}$$

The values of W_i, ψ_{ri}, M_{ri} and Q_{ri} are given by equations (8.9), (8.24) and (8.30) for $\Omega > \frac{K}{\alpha}$, and by equations (8.10), (8.26) and (8.32) for $0 < \Omega < \frac{K}{\alpha}$.

Case 2. Clamped Plate with Load Uniformly Distributed over a Circle (see figure 3)

The loading for this case is given by

$$P(R,T) = -P\delta(R-\gamma)U(T) \tag{8.82}$$

where $\delta(R-\gamma)$ is a Dirac Delta Function (see list of symbols) and P is the load per unit arc length.

The boundary conditions are the same as those for case 1. Initial conditions are also assumed to be the same as those of case 1.

Static Solution:

The governing equations are

$$\begin{aligned} &\frac{\partial}{\partial R}\left[\frac{1}{R}\frac{\partial}{\partial R}(R\psi_s)\right] - \frac{K^2}{\alpha^2}\left(\psi_s + \frac{\partial W_s}{\partial R}\right) = 0 \\ &\frac{K^2}{R}\frac{\partial}{\partial R}\left[R\left(\psi_s + \frac{\partial W_s}{\partial R}\right)\right] = P\delta(R-\gamma)U(T) \end{aligned} \tag{8.83}$$

Eliminating W_s, equation (8.83) yields, for T > 0

$$\frac{\alpha^2}{R}\frac{\partial}{\partial R}\left\{R\frac{\partial}{\partial R}\left[\frac{1}{R}\frac{\partial}{\partial R}(R\psi_s)\right]\right\} = P\delta(R-\gamma) \tag{8.84}$$

Integrating equation (8.84) successively, we get

$$\begin{aligned} \alpha^2\psi_s = &\left(\frac{P}{2}R\gamma\log R - \frac{P}{4}R\gamma + \frac{P}{4}\frac{\gamma^3}{R} - \frac{P}{2}R\gamma\log\gamma\right)U(R-\gamma) \\ &+ C_1\left(\frac{R}{2}\log R - \frac{R}{4}\right) + C_2\frac{R}{2} + \frac{C_3}{R} \end{aligned} \tag{8.85}$$

Since W_s and ψ_s must be finite at R = 0, we have

$$C_1 = C_3 = 0$$

Applying the boundary condition $\psi_s(1) = 0$, yields

$$C_2 = \frac{P}{2}\gamma - \frac{P}{2}\gamma^3 + P\gamma\log\gamma \tag{8.86}$$

From the first of equations (8.83), one obtains

$$K^2\left(\psi_s + \frac{\partial W_s}{\partial R}\right) = \alpha^2\frac{\partial}{\partial R}\left[\frac{1}{R}\frac{\partial}{\partial R}(R\psi_s)\right]$$

In view of equations (8.85) and (8.86), the above yields

$$\alpha^2 \frac{\partial W_s}{\partial R} = \left(\frac{\alpha^2}{K^2}\frac{P\gamma}{R} - \frac{P}{2} R\gamma\log R + \frac{P}{2} R\gamma\log\gamma + \frac{P}{4} R\gamma - \frac{P}{4}\frac{\gamma^3}{R}\right)U(R-\gamma)$$
$$- \frac{P}{2} R\gamma\log\gamma - \frac{P}{4} R\gamma + \frac{P}{4} R\gamma^3$$

Integrating the above, we get

$$\alpha^2 W_s = \Big[\frac{\alpha^2}{K^2} (P\gamma\log R - P\gamma\log\gamma) - \frac{P}{4} R^2\gamma\log R$$
$$+ \frac{P}{4} R^2\gamma\log\gamma + \frac{P}{4} R^2\gamma - \frac{P}{4}\gamma^3 + \frac{P}{4}\gamma^3\log\gamma - \frac{P}{4}\gamma^3\log R\Big] U(R-\gamma) \tag{8.87}$$
$$- \frac{P}{4} R^2\gamma\log\gamma - \frac{P}{8} R^2\gamma + \frac{P}{8} R^2\gamma^3 + C_4$$

Applying the boundary condition $W_s(1) = 0$, the above yields

$$C_4 = \frac{\alpha^2}{K^2} P\gamma\log\gamma - \frac{P}{4}\gamma^3\log\gamma + \frac{P}{8}\gamma^3 - \frac{P}{8}\gamma \tag{8.88}$$

Using equation (7.25), equations (8.85-8.88) yield, for $0 < R < \gamma$

$$\frac{\psi_s}{P_0} = \frac{1}{\pi\alpha^2}\left(\frac{R}{4}\log\gamma - \frac{R}{8}\gamma^2 + \frac{R}{8}\right)$$

$$\frac{W_s}{P_0} = \frac{1}{K^2}\frac{\log\gamma}{2} + \frac{1}{\pi\alpha^2}\Big(- \frac{\gamma^2}{8}\log\gamma - \frac{R^2}{8}\log\gamma + \frac{R^2}{16}\gamma^2 \tag{8.89}$$
$$- \frac{R^2}{16} + \frac{\gamma^2}{16} - \frac{1}{16}\Big)$$

$$\frac{M_{rs}}{P_0} = \frac{1}{4\pi\alpha^2}\left[(1+\nu)\log\gamma + \frac{(1+\nu)}{2} - \frac{(1+\nu)}{2}\gamma^2\right]$$

$$\frac{Q_{rs}}{P_0} = 0$$

where the total load, P_0, is

$$P_0 = 2\pi\gamma P$$

For $R > \gamma$, one has

$$\frac{\psi_s}{P_0} = \frac{1}{\pi\alpha^2} \left(\frac{R}{4} \log R + \frac{\gamma^2}{8R} - \frac{R}{8} \gamma^2\right)$$

$$\frac{W_s}{P_0} = \frac{1}{\pi K^2} \frac{\log R}{2} + \frac{1}{\pi\alpha^2} \left[- \frac{R^2}{8} \log R - \frac{\gamma^2}{8} \log R + \frac{R^2}{16} \gamma^2 + \frac{R^2}{16} - \frac{\gamma^2}{16} - \frac{1}{16}\right] \tag{8.90}$$

$$\frac{M_{rs}}{P_0} = \frac{1}{4\pi\alpha^2} \left[(1+\nu) \log R + \frac{(\nu-1)}{2R^2} \gamma^2 - \frac{(1+\nu)}{2} \gamma^2 + 1\right]$$

$$\frac{Q_{rs}}{P_0} = \frac{1}{2\pi R}$$

Dynamic Solution:

In view of equations (8.61), (8.70), (8.82) and (8.8), equation (7.24) yields

$$P_i(T) = - \frac{P_0}{2\pi\gamma\Omega_i^2} \int_0^1 W_i(R) R\delta(R-\gamma) dR$$

This becomes on integration

$$P_i(T) = - \frac{P_0 W_i(\gamma)}{2\pi\Omega_i^2} \tag{8.91}$$

By a process similar to that used in case 1, one obtains

$$q_i(0) = \frac{P_0 W_i(\gamma)}{2\pi\Omega_i^2} \tag{8.92}$$

$$\dot{q}_i(0) = 0,$$

for $0 < \Omega < \frac{K}{\alpha}$

$$\frac{q_i(T)}{P_0} = [A_1 J_0(\delta_1\gamma)+A_2 I_0(\bar{\delta}_2\gamma)] \frac{\cos\Omega_i T}{2\pi\Omega_i^2} \tag{8.93}$$

and for $\Omega > \frac{K}{\alpha}$

$$\frac{q_i(T)}{P_0} = [A_1 J_0(\delta_1\gamma)+A_2 J_0(\delta_2\gamma)] \frac{\cos\Omega_i T}{2\pi\Omega_i^2} \tag{8.94}$$

The complete solution to the forced motion problem is now given by equations (8.81). It may be noted that the values of W_i, ψ_{ri}, M_{ri} and Q_{ri} are the same as for case 1, since they relate to homogeneous solution.

Case 3. Clamped Plate with Concentrated Load at the Center (see figure 4)

In this case the load can be expressed as

$$P(R,T) = -\frac{P_0}{2\pi R}\,\delta(R)U(T) \tag{8.95}$$

where

$\delta(R)$ is a Dirac Delta Function.

The boundary conditions and the initial conditions are the same as those for case 1.

Static Solution:

The static solutions for this case are the limiting cases of the solutions for case 1 or case 2 as γ tends to zero. Hence the required solutions can be written as

$$\frac{\psi_s}{P_0} = \frac{R\log R}{4\pi\alpha^2}$$

$$\frac{W_s}{P_0} = \frac{1}{8\pi\alpha^2}\left[\frac{1}{2}(R^2-1) + \left(\frac{4\alpha^2}{K^2} - R^2\right)\log R\right]$$

$$\frac{M_{rs}}{P_0} = \frac{1}{4\pi\alpha^2}[1+(1+\nu)\log R] \tag{8.96}$$

$$\frac{Q_{rs}}{P_0} = \frac{1}{2\pi R}$$

It should be noted that the static solutions W_s, M_{rs} and Q_{rs} become infinite at R = 0 and this is consistent with the remarks given by Kalnins [49]. For the classical theory the static solutions are finite at R = 0.

Dynamic Solution:

In view of equations (8.8) and (8.61), equation (7.24) becomes

$$P_i(T) = -\frac{P_0}{2\pi\Omega_i^2}\int_0^1 W_i(R)\,\delta(R)\,dR \tag{8.97}$$

This yields on integration

$$P_i(T) = -\frac{P_0 W_i(0)}{2\pi\Omega_i^2} \tag{8.98}$$

Now, following the same procedure as used in case 1, one obtains

$$q_i(0) = \frac{P_0 W_i(0)}{2\pi\Omega_i^2} \tag{8.99}$$

$$\dot{q}_i(0) = 0$$

and

$$\frac{q_i(T)}{P_0} = \frac{(A_1+A_2)\cos\Omega_i T}{2\pi\Omega_i^2} \tag{8.100}$$

It should be noted here that the values of A_1 and A_2 are different depending on whether $\Omega > \frac{K}{\alpha}$ or $\Omega < \frac{K}{\alpha}$.

Case 4. Simply Supported Plate with Load Uniformly Distributed over a Circular Area (see figure 6)

For this case the load is given by equation (8.59). For the static solution the boundary conditions are

$$W_s(1,T) = 0$$
$$M_{rs}(1,T) = 0 \qquad (8.101)$$

where M_{rs}, the static bending moment, is

$$M_{rs} = \left(\frac{\partial \psi_s}{\partial R} + \frac{\nu}{R}\psi_s\right)$$

Since $C_1 = C_3 = 0$ for a solid plate, from equation (8.63) we obtain

$$\alpha^2 M_{rs} = \frac{(3+\nu)}{16} PR^2 U(R) + \left[-\frac{(3+\nu)}{16} PR^2 - \frac{(1-\nu)}{16}\frac{P\gamma^4}{R^2} + \frac{(1+\nu)}{4} P\gamma^2 \log R + \frac{P}{4}\gamma^2 - \frac{(1+\nu)}{4} P\gamma^2 \log\gamma \right] U(R-\gamma) + \frac{(1+\nu)}{2} C_4 \qquad (8.102)$$

Applying the boundary conditions on equations (8.66) and (8.102) yields

$$C_2 = \frac{1-\nu}{1+\nu}\frac{P}{8}\gamma^4 + \frac{P}{2}\gamma^2\log\gamma - \frac{P\gamma^2}{2(1+\nu)} \qquad (8.103)$$

$$C_4 = \frac{\alpha^2}{K^2}\left[\frac{P}{2}\gamma^2\log\gamma - \frac{P}{4}\gamma^2\right] - \frac{P}{16}\gamma^4\log\gamma - \frac{P}{16}\gamma^2 + \left[\frac{1-\nu}{32(1+\nu)} + \frac{5}{64}\right] P\gamma^4 - \frac{P\gamma^2}{8(1+\nu)} \qquad (8.104)$$

From equations (7.25), (8.63), (8.66) and (8.102), the static solutions can be written as follows:

For $0 < R < \gamma$

$$\frac{\psi_s}{P_0} = \frac{1}{4\pi\alpha^2}\left[\frac{R^3}{4\gamma^2} + \frac{1-\nu}{1+\nu}\frac{R\gamma^2}{4} + R\log\gamma - \frac{R}{(1+\nu)}\right]$$

$$\frac{W_s}{P_0} = \frac{1}{\pi K^2}\left[\frac{R^2}{4\gamma^2} + \frac{\log\gamma}{2} - \frac{1}{4}\right] + \frac{1}{\pi\alpha^2}\left[-\frac{R^4}{64\gamma^2} - \frac{R^2}{8}\log\gamma\right.$$

$$+ \frac{R^2}{8(1+\nu)} - \frac{1}{16} - \frac{\gamma^2}{16} \log\gamma - \frac{1}{8(1+\nu)} - \frac{1-\nu}{1+\nu} \frac{R^2\gamma^2}{32} \tag{8.105}$$

$$+ \frac{(1-\nu)\gamma^2}{32(1+\nu)} + \frac{5\gamma^2}{64}]$$

$$\frac{M_{rs}}{P_0} = \frac{1}{\pi\alpha^2} [\frac{(3+\nu)}{16\gamma^2} R^2 + \frac{(1-\nu)}{16} \gamma^2 + \frac{(1+\nu)}{4} \log\gamma - \frac{1}{4}]$$

$$\frac{Q_{rs}}{P_0} = \frac{R}{2\pi\gamma^2}$$

For $R > \gamma$

$$\frac{\psi_s}{P_0} = \frac{1}{4\pi\alpha^2} [\frac{\gamma^2}{4R} + R\log R + \frac{1-\nu}{1+\nu} \frac{R}{4} \gamma^2 - \frac{R}{(1+\nu)}]$$

$$\frac{W_s}{P_0} = \frac{1}{\pi K^2} \frac{\log R}{2} + \frac{1}{\pi\alpha^2} [- \frac{R^2}{8} \log R - \frac{2}{16} \log R$$

$$+ \frac{R^2-1}{16} + \frac{R^2-1}{8(1+\nu)} - \frac{(1-\nu)\gamma^2(R^2-1)}{32(1+\nu)}] \tag{8.106}$$

$$\frac{M_{rs}}{P_0} = \frac{1}{\pi\alpha^2} [\frac{(\nu-1)}{16R^2} \gamma^2 + \frac{(1+\nu)}{4} \log R + \frac{(1-\nu)}{16} \gamma^2]$$

$$\frac{Q_{rs}}{P_0} = \frac{1}{2\pi R}$$

The solutions for $q_i(T)$ are given by equations (8.79) and (8.80) with eigenvalues for a simply supported plate.

Case 5. Simply Supported Plate with Load Uniformly Distributed over a Circle (see figure 7)

The loading for this case is given by equation (8.82). For the static solution, the boundary conditions are the same as those for case 4.

Using equations (8.85) and (8.87), and the boundary conditions (8.101), one obtains for this case

$$\alpha^2 M_{rs} = \Big[\frac{1+\nu}{2} P\gamma\log R - \frac{(1+\nu)}{2} P\gamma\log\gamma + \frac{1-\nu}{4} P\gamma - \frac{1-\nu}{4}\frac{P\gamma^3}{R^2}\Big] U(R-\gamma) + \frac{1+\nu}{2} C_2 \tag{8.107}$$

$$C_2 = P\gamma\log\gamma - \frac{1-\nu}{1+\nu}\frac{P}{2}\gamma + \frac{1-\nu}{1+\nu}\frac{P}{2}\gamma^3 \tag{8.108}$$

$$C_4 = \frac{\alpha^2}{K^2} P\gamma\log\gamma - \frac{P}{4}\gamma^3\log\gamma - \frac{P}{4}\gamma + \frac{P}{4}\gamma^3 + \frac{1-\nu}{1+\nu}\frac{P}{8}\gamma^3 - \frac{1-\nu}{1+\nu}\frac{P}{8}\gamma \tag{8.109}$$

For $0 < R < \gamma$, we obtain by using the above equations

$$\frac{\psi_s}{P_0} = \frac{1}{4\pi\alpha^2}[R\log\gamma - \frac{1-\nu}{1+\nu}\frac{R}{2} + \frac{1-\nu}{1+\nu}\frac{R}{2}\gamma^2]$$

$$\frac{W_s}{P_0} = \frac{1}{\pi K^2}\frac{\log\gamma}{2} + \frac{1}{\pi^2\alpha^2}[-\frac{(R^2+\gamma^2)}{8}\log\gamma + \frac{\gamma^2-1}{8} + \frac{1-\nu}{1+\nu}\frac{(\gamma^2-1)}{16} - \frac{1-\nu}{1+\nu}\frac{(\gamma^2-1)}{16}R^2] \tag{8.110}$$

$$\frac{M_{rs}}{P_0} = \frac{1}{4\pi\alpha^2}[(1+\nu)\log\gamma - \frac{(1-\nu)}{2} + \frac{(1-\nu)}{2}\gamma^2]$$

$$\frac{Q_{rs}}{P_0} = 0$$

For $R > \gamma$, one has

$$\frac{\psi_s}{P_0} = \frac{1}{\pi\alpha^2}[\frac{R}{4}\log R - \frac{R}{8} + \frac{\gamma^2}{8R} + \frac{1-\nu}{1+\nu}(\frac{R\gamma^2}{8} - \frac{R}{8})]$$

$$\frac{W_s}{P_0} = \frac{1}{\pi K^2}\frac{\log R}{2} + \frac{1}{\pi\alpha^2}\left[-\frac{(R^2+\gamma^2)}{8}\log R + \frac{R^2-1}{8}\right.$$

$$\left.+\frac{1-\nu}{1+\nu}\frac{R^2}{16}(1-\gamma^2) + \frac{1-\nu}{1+\nu}\left(\frac{\gamma^2}{16} - \frac{1}{16}\right)\right] \qquad (8.111)$$

$$\frac{M_{rs}}{P_0} = \frac{1}{4\pi\alpha^2}\left[(1+\nu)\log R + \frac{(1-\nu)}{2} + \frac{(1-\nu)}{2}\gamma^2 + \frac{(\nu-1)}{2R^2}\gamma^2\right]$$

$$\frac{Q_{rs}}{P_0} = \frac{1}{2\pi R}$$

Solutions for $q_i(T)$ are given by equations (8.93) and (8.94) with eigenvalues for a simply supported plate.

Case 6. Simply Supported Plate with Concentrated Load at the Center (see figure 5)

The loading for this case is given by equation (8.95). Boundary conditions for the static solution are the same as those for case 4.

The static solutions for this case are the limiting cases of the solutions for case 4 or case 5 as γ tends to zero. Taking these limits, one obtains

$$\frac{\psi_s}{P_0} = \frac{1}{4\pi\alpha^2}\left[R\log R - \frac{R}{1+\nu}\right]$$

$$\frac{W_s}{P_0} = \frac{1}{\pi K^2}\frac{\log R}{2} + \frac{1}{\pi\alpha^2}\left[-\frac{R^2}{8}\log R + \frac{R^2-1}{16} + \frac{R^2-1}{8(1+\nu)}\right]$$

(8.112)

$$\frac{M_{rs}}{P_0} = \frac{(1+\nu)}{4\pi\alpha^2}\log R$$

$$\frac{Q_s}{P_0} = \frac{1}{2\pi R}$$

For this case, the value of $q_i(T)$ is given by equation (8.100) with eigenvalues for a simply supported plate.

Case 7. Disk Mounted on a Shaft with Uniform Load at the Outer Edge (see figure 8)

The loading for this case can be expressed as

$$P(R,T) = \frac{P_0}{2\pi}\,\delta(R-1)U(T) \tag{8.113}$$

Static Solution:

We seek a solution of equations (7.19) with $P(R,T) = 0$, and boundary conditions

$$\begin{aligned} W_s(\beta,T) &= 0 \\ \psi_s(\beta,T) &= 0 \\ M_{rs}(1,T) &= 0 \\ Q_{rs}(1,T) &= \frac{P_0}{2\pi}\,U(T) \end{aligned} \tag{8.114}$$

From equations (7.19) one obtains

$$\begin{aligned} \frac{\alpha^2}{R}\frac{\partial}{\partial R}\quad R\,\frac{\partial}{\partial R}\Big[\frac{1}{R}\,\frac{\partial}{\partial R}(R\psi_s)\Big] &= 0 \\ \frac{K^2}{\alpha^2}\Big(\psi_s + \frac{\partial W_s}{\partial R}\Big) &= \frac{\partial}{\partial R}\Big[\frac{1}{R}\,\frac{\partial}{\partial R}(R\psi_s)\Big] \end{aligned} \tag{8.115}$$

The above equations yield on successive integration

$$\begin{aligned} \alpha^2\psi_s &= C_1\Big(\frac{R}{2}\log R - \frac{R}{4}\Big) + C_2\,\frac{R}{2} + \frac{C_3}{R} \\ \alpha^2 W_s &= C_1\Big(\frac{\alpha^2}{K^2}\log R + \frac{R^2}{4} - \frac{R^2}{4}\log R\Big) - C_2\,\frac{R^2}{4} - C_3\log R + C_4 \end{aligned} \tag{8.116}$$

From equations (7.25) and (8.116), we get

$$\begin{aligned} \alpha^2 M_{rs} &= \Big[\frac{(1+\nu)}{2}\log R\Big]\,C_1 + \frac{(1-\nu)}{4}\,C_1 + \frac{(1+\nu)}{2}\,C_2 + \frac{(\nu-1)}{R^2}\,C_3 \\ \alpha^2 Q_{rs} &= \frac{\alpha^2}{R}\,C_1 \end{aligned} \tag{8.117}$$

Applying the boundary conditions to equations (8.116) and (8.117), one obtains

$$C_1 = \frac{P_0}{2\pi}$$

$$C_2 = \frac{\nu-1}{\nu+1}\frac{P_0}{4\pi} + \frac{2(1-\nu)}{1+\nu}C_3$$

$$C_3 = \frac{\beta^2 P_0}{(1+\nu+\beta^2-\beta^2\nu)4\pi}[1+(1+\nu)\log\beta] \tag{8.118}$$

$$C_4 = C_2\frac{\beta^2}{4} + C_3 \log\beta - C_1 \left[\frac{\alpha^2}{K^2}\log\beta + \frac{\beta^2}{4} - \frac{\beta^2}{4}\log\beta\right]$$

Hence, W_s, ψ_s, M_{rs} and Q_{rs} are completely determined.

Dynamic Solution:

In view of the boundary conditions and since $P(R,T) = 0$, equation (7.24) reduces to

$$P_i(T) = \frac{R}{\Omega_i^2}[\alpha^2(M_{rs}\psi_i - \psi_s M_{ri}) + Q_{rs}W_i - W_s Q_{ri}]_\beta^1$$

$$P_i(T) = \frac{Q_{rs}W_i(1)}{\Omega_i^2} = \frac{P_0 W_i(1)}{2\pi\Omega_i^2}U(T)$$

$$P_i(0) = \frac{P_0 W_i(1)}{2\pi\Omega_i^2}$$

$$\dot{P}_i(0) = 0 \tag{8.119}$$

$$q_i(0) = -P_i(0) = -\frac{P_0 W_i(1)}{2\pi\Omega_i^2}$$

$$\dot{q}_i(0) = 0$$

Hence, from equation (7.29), we obtain, for $T > 0$

$$\frac{q_i(T)}{P_0} = -\frac{W_i(1)}{2\pi\Omega_i^{\,2}} \cos \Omega_i T \tag{8.120}$$

where, for $\Omega > \frac{K}{\alpha}$ (the subscript i is omitted for convenience)

$$W(1) = A_1 J_0(\delta_1)+A_2 J_0(\delta_2)+B_1 Y_0(\delta_1)+B_2 Y_0(\delta_2) \tag{8.121}$$

and for $0 < \Omega < \frac{K}{\alpha}$

$$W(1) = A_1 J_0(\delta_1)+A_2 I_0(\bar{\delta}_2)+B_1 Y_0(\delta_1)+B_2 K_0(\bar{\delta}_2) \tag{8.122}$$

The modal bending moments are, for $\Omega > \frac{K}{\alpha}$

$$\begin{aligned} M_r(R) = {} & A_1(1-\sigma_1)[\delta_1^{\,2} J_0(\delta_1 R)+(\nu-1)\delta_1 J_1(\delta_1 R)] \\ & + A_2(1-\sigma_2)[\delta_2^{\,2} Y_0(\delta_2 R)+(\nu-1)\delta_2 J_1(\delta_2 R)] \\ & + B_1(1-\sigma_1)[\delta_1^{\,2} Y_0(\delta_1 R)+(\nu-1)\delta_1 Y_1(\delta_1 R)] \\ & + B_2(1-\sigma_2)[\delta_2^{\,2} Y_0(\delta_2 R)+(\nu-1)\delta_2 Y_1(\delta_2 R)] \end{aligned} \tag{8.123}$$

and for $0 < \Omega < \frac{K}{\alpha}$

$$\begin{aligned} M_r(R) = {} & A_1(1-\sigma_1)[\delta_1^{\,2} J_0(\delta_1 R)+(\nu-1)\delta_1 J_1(\delta_1 R)] \\ & - A_2(1-\sigma_2)[\bar{\delta}_2^{\,2} I_0(\bar{\delta}_2 R)+(\nu-1)\bar{\delta}_2 I_1(\bar{\delta}_2 R)] \\ & + B_1(1-\sigma_1)[\delta_1^{\,2} Y_0(\delta_1 R)+(\nu-1)\delta_1 Y_1(\delta_1 R)] \\ & + B_2(1-\sigma_2)[-\bar{\delta}_2^{\,2} K_0(\bar{\delta}_2 R)+(\nu-1)\bar{\delta}_2 K_1(\bar{\delta}_2 R)] \end{aligned} \tag{8.124}$$

The complete solution to the forced motion problem is now given by equations (8.81).

It may be noted that if, instead of a step function load, we consider a square pulse load of duration one unit of time, the appropriate solutions for $q_i(T)$ become, for $0 < T \leq 1$

$$\frac{q_i(T)}{P_0} = -\frac{W_i(1)}{2\pi\Omega_i^2}\cos\,\Omega_i T \tag{8.125a}$$

and for T > 1

$$\frac{q_i(T)}{P_0} = -\frac{W_i(1)}{2\pi\Omega_i^2}[\cos\,\Omega_i T-\cos\,\Omega_i(T-1)] \tag{8.125b}$$

D. Response of a Circular Plate to a Ramp-Platform Load (see figure 21b)

The loading for this case can be stated as

$$\begin{aligned} P(R,T) &= -P\frac{T}{T_1}, \quad 0 < T \leq T_1 \\ P(R,T) &= -P, \quad T > T_1 \end{aligned} \tag{8.126}$$

where T_1 is the rise time of the load.

The load is assumed to be uniformly distributed over a circular area of radius γ. The boundary conditions and initial conditions are the same as those for case 1 or case 4.

Hence, for this case, equation (7.24) yields

$$P_i(T) = -\frac{PT}{\Omega_i^2 T_1}\int_0^\gamma W_i(R)RdR \tag{8.127}$$

From the above equation we get

$$\begin{aligned} P_i(0) &= 0 \\ \dot{P}_i(0) &= -\frac{P}{\Omega_i^2 T_1}\int_0^\gamma W_i(R)RdR \\ \ddot{P}_i(0) &= 0 \end{aligned} \tag{8.128}$$

Also, in view of the initial conditions

$$q_i(0) = 0$$

$$\dot{q}_i(0) = -\dot{P}_i(0) = \frac{P}{\Omega_i^{\,2} T_1} \int_0^{\gamma} W_i(R) R dR \tag{8.129}$$

Now equation (7.29) yields

$$q_i(T) = \frac{P}{\Omega_i^{\,3} T_1} [\int_0^{\gamma} W_i(R) R dR] \sin\Omega_i T \tag{8.130}$$

Substituting the expressions for the modal displacements from equations (8.9) and (8.10) and integrating, one obtains from equation (8.130), for $0 < T < T_1$

$$\frac{q_i(T)}{P_0} = [A_1 \frac{J_1(\delta_1\gamma)}{\delta_1} + A_2 \frac{J_1(\delta_2\gamma)}{\delta_2}] \frac{\sin \Omega_i T}{T_1 \pi\gamma\Omega_i^{\,3}} , \quad \Omega > \frac{K}{\alpha}$$

(8.131)

$$\frac{q_i(T)}{P_0} = [A_1 \frac{J_1(\delta_1\gamma)}{\delta_1} + A_2 \frac{I_1(\bar{\delta}_2\gamma)}{\bar{\delta}_2}] \frac{\sin \Omega_i T}{T_1 \pi\gamma\Omega_i^{\,3}} , \quad 0 < \Omega < \frac{K}{\alpha}$$

For $T > T_1$, using a superposition as shown in figure 21a, we get

$$\frac{q_i(T)}{P_0} = \frac{1}{T_1 \pi\gamma\Omega_i^{\,3}} [A_1 \frac{J_1(\delta_1\gamma)}{\delta_1} + A_2 \frac{J_1(\delta_2\gamma)}{\delta_2}]$$

$$[\sin \Omega_i T - \sin \Omega_i (T-T_1)] , \quad \Omega > \frac{K}{\alpha}$$

(8.132)

$$\frac{q_i(T)}{P_0} = \frac{1}{T_1 \pi\gamma\Omega_i^{\,3}} [A_1 \frac{J_1(\delta_1\gamma)}{\delta_1} + A_2 \frac{I_1(\bar{\delta}_2\gamma)}{\bar{\delta}_2}]$$

$$[\sin \Omega_i T - \sin \Omega_i (T-T_1)] , \quad 0 < \Omega < \frac{K}{\alpha}$$

The acceleration response of the plate can be expressed in the form

$$\ddot{W}(R,T) = \ddot{W}_s(R,T) + \sum_{i=1}^{\infty} W_i(R)\, \ddot{q}_i(T) \tag{8.133}$$

where $\ddot{W}_s$ and $\ddot{q}_i$ can be obtained directly by differenting the expressions for the static response and the q_i twice with respect to time.

E. Response of a Circular Plate to Pulse Loads

The question of which theory (classical or Mindlin's) should be used to determine the response of a plate to transient loads is intimately related to the convergence of the resulting modal series. This is because the secondary effects of transverse shear and rotary inertia become increasingly important for higher modes of vibration. Thus if it is found that, for a given plate subjected to a certain load, modes which are strongly affected by transverse shear and rotary inertia contribute a large share of the response, it is unlikely that the classical theory will yield correct results. If, on the other hand, the higher modes contribute only a small share of the total response, the classical theory may give correct results.

Convergence of the modal series depends on many factors like the duration of the applied load, the shape of the load pulse, the manner in which the load is distributed and the area or the length over which the load is distributed. Reducing the duration of the pulse or area over which the load is distributed may even produce divergence in certain transient response problems [9].

The response of a circular plate to blast, triangular, square and half-sine pulses will be given now. In each case the load is assumed to be uniformly distributed over a concentric circular area of the plate.

1. Blast Pulse: (see figure 21c)

The time history for this load can be stated as

$$P(R,T) = -\ (P - \frac{T}{T_1} P) \ , \quad 0 < T \leq T_1$$
$$P(R,T) = 0 \tag{8.134}$$

where T_1 is the duration of the pulse.

For brevity let

$$[A_1 \frac{J_1(\delta_1\gamma)}{\delta_1} + A_2 \frac{J_1(\delta_2\gamma)}{\delta_2}] = WJ$$
$$[A_1 \frac{J_1(\delta_1\gamma)}{\delta_1} + A_2 \frac{I_1(\bar{\delta}_2\gamma)}{\bar{\delta}_2}] = WI \tag{8.135}$$

By using a superposition of step function and ramp-platform loads as shown in figure 21c and using equations (8.79), (8.80), (8.131) and (8.132), we obtain for $0 < T \leq T_1$

$$\frac{q_i(T)}{P_0} = \frac{WJ}{\pi\gamma\Omega_i^2}[\cos \Omega_i T - \frac{\sin \Omega_i T}{\Omega_i T_1}] \ , \quad \Omega > \frac{K}{\alpha}$$
$$\frac{q_i(T)}{P_0} = \frac{WI}{\pi\gamma\Omega_i^2}[\cos \Omega_i T - \frac{\sin \Omega_i T}{\Omega_i T_1}] \ , \quad 0 < \Omega < \frac{K}{\alpha} \tag{8.136}$$

For $T > T_1$, we have

$$\frac{q_i(T)}{P_0} = \frac{WJ}{\pi\gamma\Omega_i^2}[\cos \Omega_i T - \frac{\sin \Omega_i T}{\Omega_i T_1} + \frac{\sin \Omega_i (T-T_1)}{\Omega_i T_1}] \ , \quad \Omega > \frac{K}{\alpha}$$
$$\frac{q_i(T)}{P_0} = \frac{WI}{\pi\gamma\Omega_i^2}[\cos \Omega_i T - \frac{\sin \Omega_i T}{\Omega_i T_1} + \frac{\sin \Omega_i (T-T_1)}{\Omega_i T_1}] \ , \quad 0 < \Omega < \frac{K}{\alpha} \tag{8.137}$$

2. Triangular Pulse: (see figure 21d)

The time history of this load is given by

$$P(R,T) = - P \frac{T}{T_1} , \quad 0 < T \le T_1$$

$$P(R,T) = - [P - \frac{P(T-T_1)}{T_1}] , \quad T_1 \le T \le 2T_1 \tag{8.138}$$

$$P(R,T) = 0 , \quad T > 2T_1$$

where T_1 is the rise time of the pulse.

In view of equations (8.131) and (8.132) and using a superposition of two ramp-platform loads as shown in figure 21d, one obtains for $0 < T \le T_1$

$$\frac{q_i(T)}{P_0} = \frac{WJ}{\pi\gamma\Omega_i^{\ 3}T_1} \sin \Omega_i T , \quad \Omega > \frac{K}{\alpha}$$

(8.139)

$$\frac{q_i(T)}{P_0} = \frac{WI}{\pi\gamma\Omega_i^{\ 3}T_1} \sin \Omega_i T , \quad 0 < \Omega < \frac{K}{\alpha}$$

For $T_1 \le T \le 2T_1$

$$\frac{q_i(T)}{P_0} = \frac{WJ}{\pi\gamma\Omega_i^{\ 3}T_1}[\sin \Omega_i T - 2\sin \Omega_i (T-T_1)] , \quad \Omega > \frac{K}{\alpha}$$

(8.140)

$$\frac{q_i(T)}{P_0} = \frac{WI}{\pi\gamma\Omega_i^{\ 3}T_1}[\sin \Omega_i T - 2\sin \Omega_i T(T-T_1)] , \quad 0 < \Omega < \frac{K}{\alpha}$$

For $T > 2T_1$

$$\frac{q_i(T)}{P_0} = \frac{WJ}{\pi\gamma\Omega_i^{\ 3}T_1}[\sin \Omega_i T - 2\sin \Omega_i (T-T_1) + \sin \Omega_i (T-2T_1)] , \quad \Omega > \frac{K}{\alpha}$$

$$\frac{q_i(T)}{P_0} = \frac{WI}{\pi\gamma\Omega_i^{\,3} T_1}[\sin\,\Omega_i T - 2\sin\,\Omega_i(T-T_1) + \sin\,\Omega_i(T-2T_1)]\ ,$$

$$0 < \Omega < \frac{K}{\alpha} \qquad (8.141)$$

3. Square Pulse: (see figure 21e)

The loading for this case is represented by

$$P(R,T) = -P, \quad 0 < T \leq T_1$$
$$P(R,T) = 0, \quad T > T_1 \qquad (8.142)$$

where T_1 is the duration of the load.

Superposition of two step-function loads as shown in figure 21e yields, for $0 < T \leq T_1$

$$\frac{q_i(T)}{P_0} = \frac{WJ}{\pi\gamma\Omega_i^{\,2}} \cos\,\Omega_i T, \quad \Omega > \frac{K}{\alpha}$$
$$\frac{q_i(T)}{P_0} = \frac{WI}{\pi\gamma\Omega_i^{\,2}} \cos\,\Omega_i T, \quad 0 < \Omega < \frac{K}{\alpha} \qquad (8.143)$$

For $T > T_1$

$$\frac{q_i(T)}{P_0} = \frac{WJ}{\pi\gamma\Omega_i^{\,2}}[\cos\,\Omega_i T - \cos\,\Omega_i(T-T_1)]\ , \quad \Omega > \frac{K}{\alpha}$$
$$\frac{q_i(T)}{P_0} = \frac{WI}{\pi\gamma\Omega_i^{\,2}}[\cos\,\Omega_i T - \cos\,\Omega_i(T-T_1)]\ , \quad 0 < \Omega < \frac{K}{\alpha} \qquad (8.144)$$

4. Half-Sine Pulse: (see figure 21f)

The load history for this case is given by

$$P(R,T) = -P\sin\left(\frac{\pi}{2}\frac{T}{T_1}\right), \quad 0 < T \le 2T_1$$
$$P(R,T) = 0, \quad T > 2T_1 \tag{8.145}$$

where T_1 is the rise time of the pulse.

The boundary conditions and initial conditions are the same as those for case 1 or case 4. In view of equations (7.24) and (7.29), and the initial conditions, we obtain for this case

$$P_i(T) = \frac{-P\sin\left(\frac{\pi}{2}\frac{T}{T_1}\right)}{\Omega_i^2}\int_0^\gamma W_i(R)RdR$$

$$P_i(0) = 0$$

$$\dot{P}_i(0) = \frac{P\pi}{2\Omega_i^2 T_1}\int_0^\gamma W_i(R)RdR$$

$$\ddot{P}_i(T) = \frac{P\pi^2}{4\Omega_i^2 T_1^2}\sin\left(\frac{\pi}{2}\frac{T}{T_1}\right)\int_0^\gamma W_i(R)RdR \tag{8.146}$$

$$q_i(0) = 0$$

$$\dot{q}_i(0) = \frac{P\pi}{2\Omega_i^2 T_1}\int_0^\gamma W_i(R)RdR$$

Therefore,

$$\int_0^T \ddot{P}_i(\tau)\sin\Omega_i(T-\tau)d\tau = \frac{P\pi^2}{4\Omega_i^2 T_1^2}\int_0^\gamma W_i(R)RdR\int_0^T \sin\left(\frac{\pi\tau}{2T_1}\right)\sin\Omega_i(T-\tau)d\tau \tag{8.147}$$

$$\int_0^T \sin\left(\frac{\pi}{2}\frac{\tau}{T_1}\right)\sin\Omega_i(T-\tau)d\tau = \frac{\Omega_i\sin\left(\frac{\pi}{2}\frac{T}{T_1}\right) - \frac{\pi}{2T_1}\sin\Omega_i T}{\Omega_i^2 - \left(\frac{\pi}{2T_1}\right)^2} \tag{8.148}$$

Using equations (8.146 - 8.148), equation (7.29) yields

$$q_i(T) = \frac{P\pi}{2\Omega_i^{\,3}T_1}\left\{\sin\Omega_i T - \frac{\pi}{2T_1}\left[\frac{\Omega_i\ \sin(\frac{\pi T}{2T_1}) - \frac{\pi}{2T_1}\sin\Omega_i T}{\Omega_i^{\,2} - (\frac{\pi}{2T_1})^2}\right]\right\}\int_0^{\gamma} W_i(R)RdR \tag{8.149}$$

Using the superposition shown in figure 22d, one obtains, for $0 < T \leq 2T_1$ and $\Omega > \frac{K}{\alpha}$

$$\frac{q_i(T)}{P_0} = \frac{WJ}{\gamma\Omega_i^{\,3}}\left\{\frac{\sin\Omega_i T}{2T_1} - \frac{\pi}{4T_1^{\,2}}\left[\frac{\Omega_i\sin(\frac{\pi T}{2T_1}) - \frac{\pi}{2T_1}\sin\Omega_i T}{\Omega_i^{\,2} - (\frac{\pi}{2T_1})^2}\right]\right\} \tag{8.150}$$

For $T > 2T_1$ and $\Omega > \frac{K}{\alpha}$

$$\frac{q_i(T)}{P_0} = \frac{WJ}{\gamma\Omega_i^{\,3}}\left\{\frac{\sin\Omega_i T + \sin\Omega_i(T-2T_1)}{2T_1} - \frac{\pi}{4T_1^{\,2}}\right.$$

$$\left.\left[\frac{\Omega_i\sin(\frac{\pi T}{2T_1}) - \frac{\pi}{2T_1}\sin\Omega_i T + \Omega_i\sin\frac{\pi}{2T_1}(T-2T_1) - \frac{\pi}{2T_1}\sin\Omega_i(T-2T_1)}{\Omega_i^{\,2} - (\frac{\pi}{2T_1})^2}\right]\right\} \tag{8.151}$$

For $0 < \Omega < \frac{K}{\alpha}$, WJ is replaced by WI in equations (8.150) and (8.151).

The static solutions for the pulse loads are obtained by using the appropriate time histories for the load P(R,T) in the solutions obtained for the step function load. The complete solution to forced motion under pulse loads is given by equations (8.81).

IX. FREE VIBRATION OF CONSTRAINED CIRCULAR PLATES

A. Frequency Equation in Matrix Form

A solution will be presented here for the natural frequencies and mode shapes of circular plates, to which masses or springs or both are attached at the center, using conventional normal mode techniques.

Consistent with the nondimensional quantities defined in chapter VII, the following nondimensional quantities are now defined for use in this chapter.

Dimensional quantity	To convert to dimensionless form divide by	Dimensionless quantity
m	$\frac{m_p}{\pi}$	M
k	$\frac{Eh}{(1-\nu^2)}$	K
C_c	$\frac{m_p}{\pi a}\sqrt{\frac{E}{\rho(1-\nu^2)}}$	C_c
μ	$\frac{1}{a}\sqrt{\frac{E}{\rho(1-\nu^2)}}$	μ

Case 1. Circular Plate with a Concentrated Mass Attached at the Center (see figure 9)

Assume a solution for equation (7.4) in the form

$$W(R,T) = \sum_{i=1}^{\infty} W_i(R)q_i(T)$$
$$\psi(R,T) = \sum_{i=1}^{\infty} \psi_i(R)q_i(T) \qquad (9.1)$$

Substituting equations (9.1) in equations (7.4), one obtains with the aid of equations (7.10)

$$\sum_{i=1}^{\infty} \psi_i(\ddot{q}_i + \Omega_i{}^2 q_i) = 0$$
$$\sum_{i=1}^{\infty} W_i(\ddot{q}_i + \Omega_i{}^2 q_i) = P(R,T) \tag{9.2}$$

Multiplying the first of equations (9.2) by $\alpha^2\psi_j$ and the second by W_j, adding and integrating over the surface of the plate, we obtain

$$\int_0^1 \sum_{i=1}^{\infty} (W_iW_j + \alpha^2\psi_i\psi_j)(\ddot{q}_i + \Omega_i{}^2 q_i)RdR$$
$$= \int_0^1 P(R,T)W_j(R)RdR$$

Using the orthogonality condition given by equation (7.17), the above equation yields

$$\ddot{q}_i + \Omega_i{}^2 q_i = \int_0^1 P(R,T)W_i(R)RdR \tag{9.3}$$

For a concentrated force P_0 at the center of the plate, this becomes

$$\ddot{q}_i + \Omega_i{}^2 q_i = \int_0^1 \frac{P_0\delta(R)}{2\pi R} W_i(R)RdR$$
$$\ddot{q}_i + \Omega_i{}^2 q_i = \frac{P_0W_i(0)}{2\pi} \tag{9.4}$$

This equation forms the starting point for the analysis of constrained plates. For a mass M attached to the center of the plate.

$$P_0 = -M\ddot{W}(0,T) = -M \sum_{j=1}^{\infty} W_j(0)\ddot{q}_j(T) \tag{9.5}$$

The normal modes of the constrained structure are also harmonic and so it can be written that

$$q_j = \bar{q}_j e^{i\Omega T} \tag{9.6}$$

Substituting this in equation (9.5), one obtains

$$P_0 = M\Omega^2 \sum_{j=1}^{\infty} W_j(0)\bar{q}_j \tag{9.7}$$

Substituting equation (9.7) in equation (9.4), yields

$$\ddot{q}_i + \Omega_i^2 q_i = \frac{M}{2\pi} \Omega^2 W_i(0) \sum_{j=1}^{\infty} W_j(0)\bar{q}_j \tag{9.8}$$

Substituting for M, this becomes

$$\ddot{q}_i + \Omega_i^2 q_i = \frac{m}{2m_p} \Omega^2 W_i(0) \sum_{j=1}^{\infty} W_j(0)\bar{q}_j \tag{9.9}$$

With the use of equation (9.6), one obtains from the above

$$\bar{q}_i = \frac{\Lambda}{2(\Omega_i^2 - \Omega^2)} [\Omega^2 W_i(0) \sum_{j=1}^{\infty} W_j(0)\bar{q}_j] \tag{9.10}$$

where Λ, the mass ratio is defined as

$$\Lambda = \frac{m}{m_p} \tag{9.11}$$

If we use n modes, there will be n values of $\bar{q}_j$ and n equations such as the one above. The determinants formed by the coefficients of the $\bar{q}_j$ will lead to the natural frequencies of the constrained modes, and the mode shapes are found by substituting the $\bar{q}_j$ into equations (9.1).

Thus by using n modes, we obtain

$$\begin{bmatrix} WM1 & W_2(0) & W_3(0) & W_4(0) & \cdots\cdots \\ W_1(0) & WM2 & W_3(0) & W_4(0) & \cdots\cdots \\ W_1(0) & W_2(0) & WM3 & W_4(0) & \cdots\cdots \\ W_1(0) & W_2(0) & W_3(0) & WM4 & \cdots\cdots \\ \cdots & \cdots & \cdots & \cdots & \cdots \end{bmatrix} \begin{Bmatrix} \bar{q}_1 \\ \bar{q}_2 \\ \bar{q}_3 \\ \bar{q}_4 \\ \vdots \end{Bmatrix} = 0 \tag{9.12}$$

where

$$\mathrm{WM1} = W_1(0) - \frac{2\left(\frac{\Omega_1^{\,2}}{\Omega^2} - 1\right)}{\Lambda W_1(0)}$$

$$\mathrm{WM2} = W_2(0) - \frac{2\left(\frac{\Omega_2^{\,2}}{\Omega^2} - 1\right)}{\Lambda W_2(0)} \tag{9.13}$$

....
....

Case 2. Circular Plate with a Spring Attached at the Center (see figure 10)

For this case, we have

$$P(R,T) = -\frac{KW(0,T)\delta(R)}{2\pi R} \tag{9.14}$$

Substituting this in equation (9.3) and using equation (9.6), one obtains

$$\bar{q}_i = -\frac{KW_i(0)}{2\pi(\Omega_i^{\,2} - \Omega^2)} \sum_{j=1}^{\infty} W_j(0)\bar{q}_j \tag{9.15}$$

$$\begin{bmatrix} \mathrm{WK1} & W_2(0) & W_3(0) & W_4(0) & \cdots \\ W_1(0) & \mathrm{WK2} & W_3(0) & W_4(0) & \cdots \\ W_1(0) & W_2(0) & \mathrm{WK3} & W_4(0) & \cdots \\ W_1(0) & W_2(0) & W_3(0) & \mathrm{WK4} & \cdots \\ \cdots & \cdots & & \cdots & \cdots \end{bmatrix} \begin{Bmatrix} \bar{q}_1 \\ \bar{q}_2 \\ \bar{q}_3 \\ \bar{q}_4 \\ \vdots \end{Bmatrix} = 0 \tag{9.16}$$

where

$$\mathrm{WK1} = W_1(0) + \frac{2\pi}{KW_1(0)}(\Omega_1^{\,2} - \Omega^2)$$

$$\mathrm{WK2} = W_2(0) + \frac{2\pi}{KW_2(0)}(\Omega_2^{\,2} - \Omega^2) \tag{9.17}$$

....
....

For a circular plate with a mass and a spring attached at the center (see figure 12), the same procedure can be used by taking

$$P(R,T) = - M\ddot{W}(0,T) - KW(0,T) \tag{9.18}$$

with the result that the diagonal terms in the matrix equation (9.12) or (9.16) become

$$\begin{aligned} WMK1 &= W_1(0) + \frac{2(\Omega_1{}^2 - \Omega^2)}{W_1(0)} \left(\frac{\pi}{K} - \frac{1}{\Lambda\Omega^2}\right) \\ WMK2 &= W_2(0) + \frac{2\ (\Omega_2{}^2 - \Omega^2)}{W_2(0)} \left(\frac{\pi}{K} - \frac{1}{\Lambda\Omega^2}\right) \\ &\cdots\cdots\cdots\cdots\cdots\cdots \end{aligned} \tag{9.19}$$

B. Frequency Equation in Series Form

If the frequencies of a composite system consisting of plate, mass, spring and dashpot alone are required, a method developed by Young [59] for the case of a beam can be extended to apply here.

Case 1. Circular Plate with a Concentrated Mass and a Spring Attached at the Center (see figure 12)

When the system is vibrating freely there is a force F_p in the link joining the mass M and the plate which may be expressed as

$$F_p = \bar{F}_p e^{i\Omega T} \tag{9.20}$$

Let the system be cut through the link so that there are two systems, one a circular plate acted on by a force $F_p = \bar{F}_p e^{i\Omega T}$ at the center, and another a spring-supported mass acted on by an equal and opposite force as shown in figure 12.

For the first system described above, we have,

$$W_1(0,T) = \sum_{i=1}^{\infty} W_i(0) q_i(T) \tag{9.21}$$

For this case equation (9.3) becomes

$$\ddot{q}_i + \Omega_i^2 q_i = \int_0^1 \frac{\bar{F}_p e^{i\Omega T}}{2\pi} \delta(R) W_i(R) dR \tag{9.22}$$

where

$$q_i(T) = \bar{q}_i e^{i\Omega T} \tag{9.23}$$

In view of equation (9.23), equation (9.22) yields

$$\bar{q}_i = \frac{\bar{F}_p W_i(0)}{2\pi(\Omega_i^2 - \Omega^2)} \tag{9.24}$$

Hence, one obtains

$$W_1(0,T) = \sum_{i=1}^{\infty} \frac{W_i^2(0)\bar{F}_p e^{i\Omega T}}{2\pi(\Omega_i^2 - \Omega^2)} \tag{9.25}$$

For the spring-mass system the equation of motion is

$$M \frac{d^2 W_2}{dT^2} + K W_2 = - \bar{F}_p e^{i\Omega T} \tag{9.26}$$

The steady state solution of equation (9.26) is given by

$$W_2(T) = \frac{- \bar{F}_p e^{i\Omega T}}{(K - M\Omega^2)} \tag{9.27}$$

Eliminating $\bar{F}_p$ between equations (9.25) and (9.27), one obtains

$$\frac{1}{(K - M\Omega^2)} = - \sum_{i=1}^{\infty} \frac{W_i^2(0)}{2\pi(\Omega_i^2 - \Omega^2)} \tag{9.28}$$

In view of equation (9.11) this becomes

$$1 + \left[\frac{K}{\pi\Omega^2} - \Lambda\right] \frac{\Omega^2}{2} \sum_{i=1}^{\infty} \frac{W_i^2(0)}{(\Omega_i^2 - \Omega^2)} = 0 \tag{9.29}$$

Equation (9.29) can be solved for the frequencies of the constrained modes of transverse vibration of the system.

Case 2. Circular Plate with a Concentrated Mass, a Spring and a Dashpot Attached at the Center (see figure 13)

If a dashpot (linearly viscous) is included along with the spring-mass system, the system will have a motion in the form of an exponentially decaying oscillation. The force between the mass and the plate may now be taken in the form

$$\begin{aligned} F_p &= \bar{F}_p e^{(-\mu+i\Omega)T} \\ &= \bar{F}_p e^{-\mu T}\ (\cos\Omega T + i\sin\Omega T) \end{aligned} \tag{9.30}$$

For this case, equation (9.3) yields

$$\begin{aligned} \ddot{q}_i + \Omega_i^{\,2} q_i &= \int_0^1 \frac{\bar{F}_p e^{(-\mu+i\Omega)T}}{2\pi}\ \delta(R) W_i(R)\, dR \\ &= \frac{\bar{F}_p}{2\pi} e^{(-\mu+i\Omega)T}\, W_i(0) \end{aligned} \tag{9.31}$$

Assume that

$$q_i(T) = \bar{q}_i e^{(-\mu+i\Omega)T} \tag{9.32}$$

Substituting equation (9.32) into equation (9.31), one gets

$$\bar{q}_i = \frac{\bar{F}_p W_i(0)}{2\pi(\mu^2 - \Omega^2 + \Omega_i^{\,2} - 2i\mu\Omega)} \tag{9.33}$$

Hence in view of equation (9.21), we have

$$W_1(0,T) = \sum_{i=1}^{\infty} \frac{W_i^{\,2}(0)\bar{F}_p e^{(-\mu+i\Omega)T}}{2\pi(\mu^2 - \Omega^2 + \Omega_i^{\,2} - 2i\mu\Omega)} \tag{9.34}$$

For the spring-mass-dashpot system, the equation of motion is

$$M \frac{d^2W_2}{dT^2} + C_c \frac{dW_2}{dT} + KW_2 = -\bar{F}_p e^{(-\mu+i\Omega)T} \tag{9.35}$$

The steady state solution of this equation is

$$W_2(T) = \frac{-\bar{F}_p e^{(-\mu+i\Omega)T}}{M(\mu^2 - \Omega^2) + K - C_c\mu + i\Omega\ (C_c\mu - 2M\mu)} \tag{9.36}$$

Equating equations (9.34) and (9.36), one obtains

$$\frac{-1}{M(\mu^2 - \Omega^2) + K - C_c\mu + i\Omega\,(C_c - 2M\mu)} = \sum_{i=1}^{\infty} \frac{W_i^{\,2}(0)}{2\pi(\mu^2 - \Omega^2 + \Omega_i^{\,2} - 2i\mu\Omega)} \tag{9.37}$$

By equating the real and imaginary parts of equation (9.37), two expressions are obtained which determine the frequency Ω and the decay constant μ in terms of the constants of the system.

To illustrate the method of computation, only the dashpot attached to the center of the plate is considered in the following analysis. With this simplification, equation (9.37) reduces to

$$\frac{1}{C_c(\mu - i\Omega)} = \frac{1}{2\pi} \sum_{i=1}^{\infty} \frac{W_i^{\,2}(0)}{(\mu^2 - \Omega^2 + \Omega_i^{\,2} - 2i\mu\Omega)} \tag{9.38}$$

Separating the real and imaginary parts from equation (9.38) and equating the corresponding parts of each side of the equation, the following two equations are obtained:

$$\frac{1}{C_c} = \frac{1}{2\pi} \sum_{i=1}^{\infty} \frac{W_i^{\,2}(0)\mu(\Omega_i^{\,2} + \mu^2 + \Omega_i^{\,2})}{(\Omega_i^{\,2} + \mu^2 - \Omega^2)^2 + 4\mu^2\Omega^2} \tag{9.39}$$

$$0 = \sum_{i=1}^{\infty} \frac{W_i^{\,2}(0)\ (\mu^2 + \Omega^2 - \Omega_i^{\,2})}{(\mu^2 + \Omega_i^{\,2} - \Omega^2)^2 + 4\mu^2\Omega^2} \tag{9.40}$$

Equation (9.40) defines the dimensionless decay constant μ as a function of the dimensionless frequency Ω. For a given value of Ω, the corresponding value of μ is calculated from equation (9.40), and for each pair of values of μ and Ω, the corresponding value of C_c is calculated from equation (9.39). This process is repeated for various values of Ω and graphs are plotted for μ versus Ω, and C_c versus Ω.

For any given value of dashpot strength, the corresponding value of the frequency Ω and the decay constant μ can be determined from these curves.

C. Frequency Equation in Closed-Form

Recently, Tyutekin [25] has given a solution for the frequency of a thin elastic circular plate loaded at the center with an arbitrary load impedance. He used the classical theory and the results were thus restricted to thin plates. A somewhat similar approach will be followed here to derive the frequency equation in closed-form for a circular plate loaded at the center with an impedance, using the improved theory of plate vibration due to Mindlin. The results are thus applicable to thick plates also.

1. Derivation of the Frequency Equation

An arbitrary load Z (in general, complex) representing an impedance that is acting on the disk normal to its surface (figure 19) is placed at the center of the disk. Flexural waves propagated through the disk satisfy the equations (the subscript r on ψ is omitted for convenience)

$$\begin{aligned} &(\nabla^2 + \delta_1{}^2)W_1 = 0 \\ &(\nabla^2 + \delta_2{}^2)W_2 = 0 \\ &W = W_1 + W_2 \\ &\psi = (\sigma_1 - 1)\frac{\partial W_1}{\partial R} + (\sigma_2 - 1)\frac{\partial W_2}{\partial R} \end{aligned} \tag{9.41}$$

For the motion under consideration, the solutions of equations (9.41) are, for $0 < \Omega < \frac{K}{\alpha}$ (the subscript i is omitted for convenience)

$$\begin{aligned} W(R) &= AJ_0(\delta_1 R) + BY_0(\delta_1 R) + CI_0(\bar{\delta}_2 R) + FK_0(\bar{\delta}_2 R) \\ \psi(R) &= A(1 - \sigma_1)\delta_1 J_1(\delta_1 R) + B(1 - \sigma_1)\delta_1 Y_1(\delta_1 R) \\ &\quad - C(1 - \sigma_2)\bar{\delta}_2 I_1(\bar{\delta}_2 R) + F(1 - \sigma_2)\bar{\delta}_2 K_1(\bar{\delta}_2 R) \end{aligned} \tag{9.42}$$

and for $\Omega > \frac{K}{\alpha}$

$$W(R) = AJ_0(\delta_1 R) + BY_0(\delta_1 R) + CJ_0(\delta_2 R) + FY_0(\delta_2 R)$$

$$\begin{aligned}\psi(R) &= A(1-\sigma_1)\delta_1 J_1(\delta_1 R) + B(1-\sigma_1)\delta_1 Y_1(\delta_1 R) \\ &\quad + C(1-\sigma_2)\delta_2 J_1(\delta_2 R) + F(1-\sigma_2)\delta_2 Y_1(\delta_2 R)\end{aligned} \tag{9.43}$$

Were the load not present at the center, from the very beginning, the coefficients B and F would have to be assumed to zero, since the functions $Y_0(\delta_1 R)$, $Y_0(\delta_2 R)$ and $K_0(\bar{\delta}_2 R)$ become infinite as R tends to zero (see reference 73, p. 26).

$$\begin{aligned}\left\{\begin{matrix} Y_0(\delta_1 R) \\ Y_0(\delta_2 R)\end{matrix}\right\}_{R\to 0} &= \frac{2}{\pi}\log\left\{\begin{matrix}\delta_1 R \\ \delta_2 R\end{matrix}\right\} \\ K_0(\bar{\delta}_2 R) \underset{R\to 0}{=} &- \log(\bar{\delta}_2 R)\end{aligned} \tag{9.44}$$

The presence of the load impedance at the center makes it necessary to retain the functions $Y_0(\delta_1 R)$, $Y_0(\delta_2 R)$ and $K_0(\bar{\delta}_2 R)$, but the coefficients B and F must be chosen such that (see reference 49, p. 34)

$$\begin{aligned}\lim_{R\to 0} R\psi(R) &= 0 \\ \lim_{R\to 0} RW(R) &= 0\end{aligned} \tag{9.45}$$

Equations (9.45) are the conditions to be satisfied at the load point. It should be noted that the first condition is a weaker restriction than $\lim_{R\to 0} \psi(R) = 0$ which could have been assumed on physical grounds due to the symmetry of the problem.

With conditions (9.45) imposed, equations (9.42) and (9.43) yield, for $0 < \Omega < \frac{K}{\alpha}$

$$W(R) = AJ_0(\delta_1 R) + B\left[Y_0(\delta_1 R) + \frac{2}{\pi}\frac{1-\sigma_1}{1-\sigma_2} K_0(\bar{\delta}_2 R)\right] + CI_0(\bar{\delta}_2 R) \tag{9.46}$$

$$\psi(R) = A(1-\sigma_1)\delta_1 J_1(\delta_1 R) + B(1-\sigma_1)[\delta_1 Y_1(\delta_1 R) + \frac{2}{\pi}\bar{\delta}_2 K_1(\bar{\delta}_2 R)]$$
$$- C(1-\sigma_2)\bar{\delta}_2 I_1(\bar{\delta}_2 R)$$

For $\Omega > \frac{K}{\alpha}$

$$W(R) = AJ_0(\delta_1 R) + B[Y_0(\delta_1 R) - \frac{1-\sigma_1}{1-\sigma_2} Y_0(\delta_2 R)] + CJ_0(\delta_2 R)$$
$$\psi(R) = A(1-\sigma_1)\delta_1 J_1(\delta_1 R) + B(1-\sigma_1)[\delta_1 Y_1(\delta_1 R) - \delta_2 Y_1(\delta_2 R)] \quad (9.47)$$
$$+ C(1-\sigma_2)\delta_2 J_1(\delta_2 R)$$

It is clear from the above equations that according to the improved dynamic theory of plates, W is infinite at R = 0.

The load acting on the disk at its center and caused by the motion of the impedance load Z is given by

$$F_z = Z\,\frac{\partial W(0)}{\partial T} \quad (9.48)$$

Since W is infinite at the center of the plate, we shall now utilize a Williams type modal solution, in which the discontinuity at the center is taken up by the static part of the solution. Then we have a continuous eigenfunction expansion to deal with in equation (9.48).

Thus we have

$$\begin{aligned} W(R,T) &= W_s(R,T) + \sum_{i=1}^{\infty} W_i(R)q_i(T) \\ \psi(R,T) &= \psi_s(R,T) + \sum_{i=1}^{\infty} \psi_i(R)q_i(T) \end{aligned} \quad (9.49)$$

Since $W_i(R)$ must be finite at the center of the plate and in view of equations (9.44), equations (9.42) and (9.43) yield, for $0 < \Omega < \frac{K}{\alpha}$

$$W(R) = AJ_0(\delta_1 R) + B[Y_0(\delta_1 R) + \frac{2}{\pi}K_0(\bar{\delta}_2 R)] + CI_0(\bar{\delta}_2 R)$$
$$\psi(R) = A(1-\sigma_1)\delta_1 J_1(\delta_1 R) + B[(1-\sigma_1)\delta_1 Y_1(\delta_1 R) + \frac{2}{\pi}(1-\sigma_2)\bar{\delta}_2 K_1(\bar{\delta}_2 R)]$$
$$- C(1-\sigma_2)\bar{\delta}_2 I_1(\bar{\delta}_2 R) \quad (9.50)$$

and for $\Omega > \frac{K}{\alpha}$

$$W(R) = AJ_0(\delta_1 R) + B[Y_0(\delta_1 R) - Y_0(\delta_2 R)] + CJ_0(\delta_2 R)$$

$$\begin{aligned} \psi(R) &= A(1-\sigma_1)\delta_1 J_1(\delta_1 R) + B[(1-\sigma_1)\delta_1 Y_1(\delta_1 R) - (1-\sigma_2)\delta_2 Y_1(\delta_2 R)] \\ &+ C(1-\sigma_2)\delta_2 J_1(\delta_2 R) \end{aligned} \tag{9.51}$$

Denoting the time dependence of $q_i(T)$ by the factor $e^{i\Omega T}$, in view of equations (9.49-9.51), equation (9.48) yields

$$\bar{F}_z = i\Omega W(0)Z = i\Omega(A+C)Z \tag{9.52}$$

The force acting at the center of the disk due to the motion of the disk is given by (see reference 18, p. 526)

$$F_p = \lim_{R\to 0} - \left[\int_0^{2\pi} Q_r R d\theta + \int_0^1 \int_0^{2\pi} M_d \frac{\partial^2 W}{\partial T^2} R d\theta dR \right] \tag{9.53}$$

where M_d is dimensionless mass per unit area of plate.

Using equation (8.29), one obtains

$$\int_0^{2\pi} Q_r R d\theta = 2\pi R K^2 (\psi + \frac{\partial W}{\partial R}) \tag{9.54}$$

From equations (9.50) and (9.51), we obtain, for $0 < \Omega < \frac{K}{\alpha}$

$$\begin{aligned} \psi + \frac{\partial W}{\partial R} &= - A\sigma_1 \delta_1 J_1(\delta_1 R) \\ &- B[\sigma_1 \delta_1 Y_1(\delta_1 R) + \frac{2}{\pi} \sigma_2 \bar{\delta}_2 K_1(\bar{\delta}_2 R)] + C\sigma_2 \bar{\delta}_2 I_1(\bar{\delta}_2 R) \end{aligned}$$

and for $\Omega > \frac{K}{\alpha}$

$$\begin{aligned} \psi + \frac{\partial W}{\partial R} &= - A\sigma_1 \delta_1 J_1(\delta_1 R) \\ &- B[\sigma_1 \delta_1 Y_1(\delta_1 R) - \sigma_2 \delta_2 Y_1(\delta_2 R)] - C\sigma_2 \delta_2 J_1(\delta_2 R) \end{aligned}$$

From the theory of Bessel functions, we have [73]

$$\begin{Bmatrix} Y_1(\delta_1 R) \\ \\ Y_1(\delta_2 R) \end{Bmatrix} \underset{R\to 0}{=} \begin{Bmatrix} \dfrac{-2}{\pi\delta_1 R} \\ \\ \dfrac{-2}{\pi\delta_2 R} \end{Bmatrix} \tag{9.56}$$

$$K_1(\bar{\delta}_2 R) \underset{R\to 0}{=} \frac{1}{\bar{\delta}_2 R}$$

Using equations (9.55) and (9.56), equation (9.54) yields for $0 < \Omega < \frac{K}{\alpha}$

$$\lim_{R\to 0} \int_0^{2\pi} Q_r R d\theta = -2\pi R K^2 B[-\frac{2\sigma_1\delta_1}{\pi\delta_1 R} + \frac{2\sigma_2\bar{\delta}_2}{\pi\bar{\delta}_2 R}] = 4K^2(\sigma_1-\sigma_2)B$$

and for $\Omega > \frac{K}{\alpha}$ (9.57)

$$\lim_{R\to 0} \int_0^{2\pi} Q_r R d\theta = -2\pi R K^2 B[-\frac{2\sigma_1\delta_1}{\pi\delta_1 R} + \frac{2\sigma_2\delta_2}{\pi\delta_2 R}] = 4K^2(\sigma_1-\sigma_2)B$$

From the second integral in equation (9.53), we have

$$\int_0^1 \int_0^{2\pi} M_d \frac{\partial^2 W}{\partial T^2} R d\theta dR = -2\pi\Omega^2 e^{i\Omega T} \int_0^1 M_d W(R) R dR \tag{9.58}$$

Substituting for W(R) from equations (9.50) or (9.51), integrating and taking the limit as R approaches zero, equation (9.58) gives

$$\lim_{R\to 0} 2\pi\Omega^2 e^{i\Omega T} \int_0^1 M_d W(R) R dR = 0 \tag{9.59}$$

In view of equations (9.57) and (9.59), equation (9.53) yields

$$\bar{F}_p = -4K^2(\sigma_1-\sigma_2)B \tag{9.60}$$

Equating F_z and $-F_p$, one obtains

$$i\Omega(A+C)Z = 4K^2(\sigma_1-\sigma_2)B$$

Rearranging the above, we have

$$A + \frac{4K^2(\sigma_1-\sigma_2)}{-i\Omega Z} B + C = 0 \tag{9.61}$$

To solve for A, B and C, we must have two more equations in A, B and C. This is obtained by using the boundary conditions at the edge of the plate where R = 1. Without limiting the generality of the solution, we consider here only the analytically simplest case of a clamped edge.

For a clamped edge, the boundary conditions are

$$\begin{aligned} W_i(1) &= 0 \\ \psi_i(1) &= 0 \end{aligned} \tag{9.62}$$

Substituting this in equations (9.46) and (9.47) and using equation (9.61), we get the following matrix equations:

For $0 < \Omega < \frac{K}{\alpha}$

$$\begin{bmatrix} 1 & \dfrac{4K^2(\sigma_1-\sigma_2)}{-i\Omega Z} & 1 \\ J_0(\delta_1) & [Y_0(\delta_1) + \dfrac{2}{\pi}\dfrac{1-\sigma_1}{1-\sigma_2} K_0(\bar{\delta}_2)] & I_0(\bar{\delta}_2) \\ \delta_1(1-\sigma_1)J_1(\delta_1) & (1-\sigma_1)[\delta_1 Y_1(\delta_1) + \frac{2}{\pi}\bar{\delta}_2 K_1(\bar{\delta}_2)] & -\bar{\delta}_2(1-\sigma_2)I_1(\bar{\delta}_2) \end{bmatrix} \begin{Bmatrix} A \\ B \\ C \end{Bmatrix} = 0 \tag{9.63}$$

For $\Omega > \frac{K}{\alpha}$

$$\begin{bmatrix} 1 & \dfrac{4K^2(\sigma_1-\sigma_2)}{-i\Omega Z} & 1 \\ J_0(\delta_1) & [Y_0(\delta_1) - \dfrac{1-\sigma_1}{1-\sigma_2} Y_0(\delta_2)] & J_0(\delta_2) \\ \delta_1(1-\sigma_1)J_1(\delta_1) & (1-\sigma_1)[\delta_1 Y_1(\delta_1) - \delta_2 Y_1(\delta_2)] & \delta_2(1-\sigma_2)J_1(\delta_2) \end{bmatrix}$$

$$\begin{Bmatrix} A \\ \\ B \\ \\ C \end{Bmatrix} = 0 \qquad (9.64)$$

The determinants of the coefficient matrices in equations (9.63) and (9.64) equated to zero yield the frequency equations.

2. Applications of the Closed-Form Frequency Equation

Case a. Mass Attached at the Center of the Plate (see figure 9)

For this case, $Z = i\Omega M$ (9.65)

Hence, we have

$$\frac{4K^2(\sigma_1-\sigma_2)}{-\,i\Omega Z} = \frac{4K^2(\sigma_1-\sigma_2)}{\pi\Lambda\Omega^2} \qquad (9.66)$$

Case b. Spring Attached at the Center of the Plate (see figure 10)

For this case

$$Z = \frac{K}{i\Omega} \qquad (9.67)$$

and thus

$$\frac{4K^2(\sigma_1-\sigma_2)}{-\,i\Omega Z} = -\,\frac{4K^2(\sigma_1-\sigma_2)}{K} \qquad (9.68)$$

Case c. Dashpot Attached at the Center of the Plate (see figure 11)

For a dashpot,

$$Z = C_c \qquad (9.69)$$

In this case the time dependence factor in equation (9.49) can be taken as $e^{i(\Omega+i\mu)T}$, where the imaginary part μ of the frequency determines the attenuation decrement of the entire system.

Hence we have

$$\frac{4K^2(\sigma_1-\sigma_2)}{-\,i(\Omega+i\mu)Z} = \frac{4K^2(\sigma_1-\sigma_2)}{(\mu-i\Omega)C_c} \qquad (9.70)$$

Case d. Center of the Plate Fixed

For this case, $Z = \infty$

Clearly, this also is a special case of 2.a with $M = \infty$, or 2.b with $K = \infty$.

Case e. Two Circular Plates Rigidly Connected at the Centers (see figure 15)

For this case,

$$Z = \frac{\bar{F}_{pa}}{\frac{\partial W_a(0)}{\partial T}} = -\frac{4K_a^{\ 2}(\sigma_{1a}-\sigma_{2a})}{i\Omega W_a(0)} B_a \tag{9.71}$$

where the subscript a refers to the attached plate.

Using equations (9.50) or (9.51), one obtains from equation (9.71)

$$Z = -\frac{4K_a^{\ 2}(\sigma_{1a} - \sigma_{2a})}{i\Omega} \frac{B_a}{A_a + C_a} \tag{9.72}$$

Hence we have

$$\frac{4K^2(\sigma_1-\sigma_2)}{-i\Omega Z} = \frac{K^2(\sigma_1-\sigma_2)}{K_a^{\ 2}(\sigma_{1a}-\sigma_{2a})} \frac{A_a + C_a}{B_a} \tag{9.73}$$

The quantity $\frac{A_a + B_a}{C_a}$ can be determined by using the boundary conditions of the attached plate. Without limiting the generality of the solution, let us consider here the analytically simplest case of a clamped edge. For the attached plate, this assumption of a boundary condition yields, for $0 < \Omega < \frac{K}{\alpha}$ (the subscript a on δ_1, δ_2 and $\bar{\delta}_2$ is deleted for convenience)

$$W_a(1) = A_a J_0(\delta_1) + B_a[Y_0(\delta_1) + \frac{2}{\pi}\frac{1-\sigma_{1a}}{1-\sigma_{2a}} K_0(\bar{\delta}_2) + C_a I_0(\bar{\delta}_2) = 0$$

$$\psi_a(1) = A_a\delta_1(1-\sigma_{1a})J_1(\delta_1) + B_a(1-\sigma_{1a})[\delta_1 Y_1(\delta_1) + \frac{2}{\pi}\bar{\delta}_2 K_1(\bar{\delta}_2)] \tag{9.74}$$

$$- C_a\bar{\delta}_2(1-\sigma_{2a})I_1(\bar{\delta}_2) = 0$$

For $\Omega > \frac{K}{\alpha}$, we have

$$W_a(1) = A_a J_0(\delta_1) + B_a[Y_0(\delta_1) - \frac{1-\sigma_{1a}}{1-\sigma_{2a}} Y_0(\delta_2)] + C_a J_0(\delta_2) = 0$$

$$\psi_a(1) = A_a \delta_1 (1-\sigma_{1a}) J_1(\delta_1) + B_a (1-\sigma_{1a})[\delta_1 Y_1(\delta_1) - \delta_2 Y_1(\delta_2)]$$

$$+ C_a \delta_2 (1-\sigma_{2a}) J_1(\delta_2) = 0$$

Solving equations (9.74) and (9.75 yields, for $0 < \Omega < \frac{K}{\alpha}$

$$\frac{A_a + C_a}{B_a} = \frac{\| L_{ij} \| + \| M_{ij} \|}{\| N_{ij} \|} \tag{9.76}$$

and for $\Omega > \frac{K}{\alpha}$

$$\frac{A_a + C_a}{B_a} = \frac{\| P_{ij} \| + \| Q_{ij} \|}{\| R_{ij} \|} \tag{9.77}$$

where

$$\| L_{ij} \| = \begin{Vmatrix} -[Y_0(\delta_1) + \frac{2}{\pi} \frac{1-\sigma_{1a}}{1-\sigma_{2a}} K_0(\bar{\delta}_2)] & I_0(\bar{\delta}_2) \\ -(1-\sigma_{1a})[\delta_1 Y_1(\delta_1) + \frac{2}{\pi} \bar{\delta}_2 K_1(\bar{\delta}_2)] & -\bar{\delta}_2 (1-\sigma_{2a}) I_1(\bar{\delta}_2) \end{Vmatrix}$$

$$\| M_{ij} \| = \begin{Vmatrix} J_0(\delta_1) & -[Y_0(\delta_1) + \frac{2}{\pi} \frac{1-\sigma_{1a}}{1-\sigma_{2a}} K_0(\bar{\delta}_2)] \\ (1-\sigma_{1a})\delta_1 J_1(\delta_1) & -(1-\sigma_{1a})[\delta_1 Y_1(\delta_1) + \frac{2}{\pi} \bar{\delta}_2 K_1(\bar{\delta}_2)] \end{Vmatrix}$$

$$\| N_{ij} \| = \begin{Vmatrix} J_0(\delta_1) & I_0(\bar{\delta}_2) \\ (1-\sigma_{1a})\delta_1 J_1(\delta_1) & -(1-\sigma_{2a})\bar{\delta}_2 I_1(\bar{\delta}_2) \end{Vmatrix}$$

$$\| P_{ij} \| = \begin{Vmatrix} -[Y_0(\delta_1) - \frac{1-\sigma_{1a}}{1-\sigma_{2a}} Y_0(\delta_2)] & J_0(\delta_2) \\ -(1-\sigma_{1a})[\delta_1 Y_1(\delta_1) - \delta_2 Y_1(\delta_2)] & -(1-\sigma_{2a})\delta_2 J_1(\delta_2) \end{Vmatrix}$$

$$\| Q_{ij} \| = \begin{Vmatrix} J_0(\delta_1) & -[Y_0(\delta_1) - \frac{1-\sigma_{1a}}{1-\sigma_{2a}} Y_0(\delta_2)] \\ (1-\sigma_{1a})\delta_1 J_1(\delta_1) & -(1-\sigma_{1a})[\delta_1 Y_1(\delta_1) - \delta_2 Y_1(\delta_2)] \end{Vmatrix}$$

$$\| R_{ij} \| \quad \begin{Vmatrix} J_0(\delta_1) & J_0(\delta_2) \\ (1-\sigma_{1a})\delta_1 J_1(\delta_1) & (1-\sigma_{2a})\delta_2 J_1(\delta_2) \end{Vmatrix}$$

It should be noted that if the two plates have the same values of $\frac{h}{a}$ and Poisson's ratio

$$\begin{aligned} K_a^2 &= K^2 \\ \sigma_{1a} &= \sigma_1 \\ \sigma_{2a} &= \sigma_2 \end{aligned} \tag{9.78}$$

and equation (9.73) therefore simplifies to

$$\frac{4K^2(\sigma_1 - \sigma_2)}{-i\Omega Z} = \frac{A_a + C_a}{B_a} \tag{9.79}$$

X. FORCED VIBRATION OF CONSTRAINED CIRCULAR PLATES

In dealing with vibration isolation of equipment mounted on plates, the driving-point impedance and transmissibility (see appendix E) of plates which are excited to transverse vibration by sinusoidally varying forces are of great importance. The driving-point impedance and transmissibility of clamped circular plates with or without mass or spring loading at the center will be investigated here. The effect of mounting a dynamic vibration absorber at the center of the plate will also be considered.

Expressions for the driving-point impedance and the transmissibility across the plate for different cases will be derived now, using both the classical theory and the improved theory due to Mindlin.

Case A. Driving-Point Impedance of a Clamped Plate Driven at the Center (see figure 16)

Let the driving force at the center of the plate be given by

$$F_0 = \bar{F}_0 e^{i\Omega T} \tag{10.1}$$

1. Classical Theory

The classical plate vibration equation in nondimensional form is given by

$$(\nabla^4 - \delta^4)W = 0 \tag{10.2}$$

where

$$\delta^4 = \frac{\Omega^2}{\alpha^2}$$

It may be readily shown that this equation possesses a solution

$$W(R) = AJ_0(\delta R) + BY_0(\delta R) + CI_0(\delta R) + FK_0(\delta R) \tag{10.3}$$

Because of the force acting at the center of the plate, $Y_0(\ R)$ and $K_0(\delta R)$ must be retained. But to make the value of W finite at R = 0, B and F must be chosen such that when R tends to zero, $BY_0(\delta R)$ and $FK_0(\delta R)$ mutually cancel one another. With this condition imposed, in view of equations (9.44), equation (10.3) becomes

$$W(R) = AJ_0(\delta R) + B[Y_0(\delta R) + \frac{2}{\pi} K_0(\delta R)] + CI_0(\delta R) \tag{10.4}$$

The force acting at the center of the plate due to the motion of the plate must balance the force F_0 exerted at the center of the plate.

The force F_p due to the motion of the plate is given by

$$F_p = \lim_{R\to 0} - \int_0^{2\pi} Q_r R d\theta = - \lim_{R\to 0} 2\pi R Q_r \tag{10.5}$$

For the classical theory, we have

$$Q_r(R) = - \alpha^2 (\frac{\partial^3 W}{\partial R^3} + \frac{1}{R} \frac{\partial^2 W}{\partial R^2} - \frac{1}{R^2} \frac{\partial W}{\partial R}) \tag{10.6}$$

In view of equation (10.6), equation (10.5) becomes

$$\bar{F}_p = \lim_{R\to 0} 2\pi R\alpha^2\delta^3 \left[AJ_1 + B(Y_1 - \frac{2}{\pi} K_1) + CI_1 \right]_{(\delta R)} \tag{10.7}$$

Substituting for $Y_1(\delta R)$ and $K_1(\delta R)$ from equations (9.56), equation (10.7) yields

$$\bar{F}_p = - 8\alpha^2\delta^2 B$$

Equating $\bar{F}_p$ and $\bar{F}_0$, one obtains

$$B = - \frac{\bar{F}_0}{8\alpha^2\delta^2} \tag{10.9}$$

The boundary conditions for the clamped plate are

$$W(1) = \frac{\partial W(1)}{\partial R} = 0 \tag{10.10}$$

Applying these on equation (10.4), we obtain

$$\begin{aligned} AJ_0(\delta) - \frac{\bar{F}_0}{8\alpha^2\delta^2} [Y_0(\delta) + \frac{2}{\pi} K_0(\delta)] + CI_0(\delta) = 0 \\ AJ_0'(\delta) - \frac{\bar{F}_0}{8\alpha^2\delta^2} [Y_0'(\delta) + \frac{2}{\pi} K_0'(\delta)] + CI_0'(\delta) = 0 \end{aligned} \tag{10.11}$$

Solving for A and C from equations (10.11), one gets

$$A = \frac{\dfrac{\bar{F}_0}{8\alpha^2\delta^2}\begin{Vmatrix} Y_0 + \frac{2}{\pi}K_0 & I_0 \\ Y_1 + \frac{2}{\pi}K_1 & -I_1 \end{Vmatrix}_{(\delta)}}{\begin{Vmatrix} J_0 & I_0 \\ J_1 & -I_1 \end{Vmatrix}_{(\delta)}} \qquad (10.12)$$

$$C = \frac{\dfrac{\bar{F}_0}{8\alpha^2\delta^2}\begin{Vmatrix} J_0 & Y_0 + \frac{2}{\pi}K_0 \\ J_1 & Y_1 + \frac{2}{\pi}K_1 \end{Vmatrix}_{(\delta)}}{\begin{Vmatrix} J_0 & I_0 \\ J_1 & -I_1 \end{Vmatrix}_{(\delta)}}$$

Hence W(R) is completely determined. The velocity at the center of the plate is given by (note that $W(R,T) = W(R)e^{i\Omega T}$)

$$\bar{V}_0 = \lim_{R\to 0} i\Omega\,[AJ_0 + B(Y_0 + \frac{2}{\pi}K_0) + CI_0]_{(\delta R)} = i\Omega\,(A+C) \qquad (10.13)$$

Hence the driving-point impedance of the plate is

$$Z_0 = \frac{\bar{F}_0}{\bar{V}_0} = \frac{\bar{F}_0}{i\Omega\,(A+C)} \qquad (10.14)$$

Substituting for A and C from equations (10.12) yields

$$Z_0 = \frac{8\alpha^2\delta^2}{i\Omega}\left[\frac{I_0J_1 + I_1J_0}{(Y_0 + \frac{2}{\pi}K_0)(J_1 + I_1) - (Y_1 + \frac{2}{\pi}K_1)(J_0 - I_0)}\right]_{(\delta)} \qquad (10.15)$$

If Z_0 is normalized by division by the impedance of a lumped mass equal to the mass M_p of the plate, one obtains

$$Z_n = \frac{Z_0}{i\Omega M_p} = \frac{Z_0}{i\Omega\pi} = \frac{8\alpha^2\delta^2}{\pi\Omega^2}\left[\frac{I_0J_1 + I_1J_0}{(Y_1+\frac{2}{\pi}K_1)(J_0-I_0)-(Y_0+\frac{2}{\pi}K_0)(J_1+I_1)}\right]_{(\delta)} \qquad (10.16)$$

In equation (10.15) $\dfrac{8\alpha^2\delta^2}{\Omega^2}$ will turn out to be the characteristic impedance of the plate which is defined as the driving-point impedance of a similar plate of infinite size (see reference 71, p. 253). Denoting the characteristic impedance of the plate by Z_{ch}, we obtain

$$\left|\frac{Z_0}{Z_{ch}}\right| = \left|\left[\frac{I_0J_1 + I_1J_0}{(Y_1+\frac{2}{\pi}K_1)(J_0-I_0) - (Y_0+\frac{2}{\pi}K_0)(J_1+I_1)}\right]\right|_{(\delta)} \tag{10.17}$$

2. Mindlin's Theory

For the improved theory of plate vibration, the equation governing transverse displacement W is given by

$$(\nabla^2 + \delta_1{}^2)(\nabla^2 + \delta_2{}^2)W = 0 \tag{10.18}$$

As higher frequencies are not of importance in vibration isolation, only the lower frequencies for which $\delta_2{}^2$ is negative will be considered here. For this case, the required solutions are

$$\begin{aligned} W(R) &= AJ_0(\delta_1R) + BY_0(\delta_1R) + CI_0(\bar{\delta}_2R) + FK_0(\bar{\delta}_2R) \\ \psi(R) &= A(1-\sigma_1)\delta_1J_1(\delta_1R) + B(1-\sigma_1)\delta_1Y_1(\delta_1R) \\ &\quad - C(1-\sigma_2)\bar{\delta}_2I_1(\bar{\delta}_2R) + F(1-\sigma_2)\bar{\delta}_2K_1(\bar{\delta}_2R) \end{aligned} \tag{10.19}$$

Since the procedure used in section IX.C.1 is applicable here, rewriting equations (9.46) and (9.60), we have

$$\begin{aligned} W(R) &= AJ_0(\delta_1R) + B[Y_0(\delta_1R) + \frac{2}{\pi}\frac{1-\sigma_1}{1-\sigma_2}K_0(\bar{\delta}_2R)] + CI_0(\bar{\delta}_2R) \\ \psi(R) &= A(1-\sigma_1)\delta_1J_1(\delta_1R) + B(1-\sigma_1)[\delta_1Y_1(\delta_1R) + \frac{2}{\pi}\bar{\delta}_2K_1(\bar{\delta}_2R)] \\ &\quad - C(1-\sigma_2)\bar{\delta}_2I_1(\bar{\delta}_2R) \end{aligned} \tag{10.20}$$

and

$$\bar{F}_p = -4K^2(\sigma_1 - \sigma_2)B \tag{10.21}$$

Equating $\bar{F}_p$ and $\bar{F}_0$, one obtains

$$B = -\frac{\bar{F}_0}{4K^2(\sigma_1 - \sigma_2)} \tag{10.22}$$

Applying the boundary conditions $W(1) = 0$ and $\psi(1) = 0$ to equations (10.20) yields

$$A = \frac{\dfrac{\bar{F}_0}{4K^2(\sigma_1-\sigma_2)} \begin{Vmatrix} [Y_0(\delta_1)+\frac{2}{\pi}\frac{1-\sigma_1}{1-\sigma_2}K_0(\bar{\delta}_2)] & I_0(\bar{\delta}_2) \\ (1-\sigma_1)[\delta_1 Y_1(\delta_1) + \frac{2}{\pi}\bar{\delta}_2 K_1(\bar{\delta}_2)] & -\bar{\delta}_2(1-\sigma_2)I_1(\bar{\delta}_2) \end{Vmatrix}}{\begin{Vmatrix} J_0(\delta_1) & I_0(\bar{\delta}_2) \\ \delta_1(1-\sigma_1)J_1(\delta_1) & -\bar{\delta}_2(1-\sigma_2)I_1(\bar{\delta}_2) \end{Vmatrix}}$$

$$C = \frac{\dfrac{\bar{F}_0}{4K^2(\sigma_1-\sigma_2)} \begin{Vmatrix} J_0(\delta_1) & [Y_0(\delta_1)+\frac{2}{\pi}\frac{1-\sigma_1}{1-\sigma_2}K_0(\bar{\delta}_2)] \\ \delta_1(1-\sigma_1)J_1(\delta_1) & (1-\sigma_1)[\delta_1 Y_1(\delta_1) + \frac{2}{\pi}\bar{\delta}_2 K_1(\bar{\delta}_2)] \end{Vmatrix}}{\begin{Vmatrix} J_0(\delta_1) & I_0(\bar{\delta}_2) \\ \delta_1(1-\sigma_1)J_1(\delta_1) & -\bar{\delta}_2(1-\sigma_2)I_1(\bar{\delta}_2) \end{Vmatrix}} \tag{10.23}$$

The transverse motion of the plate is given by

$$W(R,T) = W(R)e^{i\Omega T} \tag{10.24}$$

Hence the velocity at the center of the plate becomes

$$V_0 = \lim_{R\to 0} \frac{\partial W(R)}{\partial T} e^{i\Omega T} = i\Omega(A+C)e^{i\Omega T} \tag{10.25}$$

Therefore, the driving-point impedance of the plate is

$$Z_0 = \frac{\bar{F}_0}{\bar{V}_0} = \frac{\bar{F}_0}{i\Omega(A+C)} \tag{10.26}$$

On normalization, the above yields

$$Z_n = \frac{Z_0}{i\Omega\pi} = \frac{\bar{F}_0}{-\pi\Omega^2(A+C)} \tag{10.27}$$

Case B. Transmissibility Across a Clamped Plate Driven at the Center

The transmissibility across the plate is given by (see figure 16)

$$T_0 = \left| \frac{F_1}{F_0} \right| \tag{10.28}$$

where

$$F_0 = \bar{F}_0 e^{i\Omega T}, \text{ the force applied at the center}$$
$$F_1 = \bar{F}_1 e^{i\Omega T}, \text{ the force transmitted}$$

F_1 is given by the relation

$$F_1 = \lim_{R\to 1} - \int_0^{2\pi} Q_r R d\theta = \lim_{R\to 1} - 2\pi R Q_r \tag{10.29}$$

1. Classical Theory

For the classical theory, using equations (10.4) and (10.6) equation (10.29) yields

$$F_1 = 2\pi\alpha^2\delta^3[AJ_1 + B(Y_1 - \tfrac{2}{\pi} K_1) + CI_1]_{(\delta)} \tag{10.30}$$

where A, B and C are determined from equations (10.9) and (10.12).

Hence the transmissibility across the plate can be written in the form

$$T_0 = \left| \frac{2\pi\alpha^2\delta^3[AJ_1 + B(Y_1 - \frac{2}{\pi} K_1) + CI_1]_{(\delta)}}{F_0} \right| \tag{10.31}$$

2. Mindlin's Theory

For the improved theory of plate vibration, in view of equations (8.29), (10.20) and (10.29), one obtains

$$\bar{F}_1 = 2\pi K^2 [A\sigma_1\delta_1 J_1(\delta_1) + B\left\{\sigma_1\delta_1 Y_1(\delta_1) + \frac{2}{\pi}\sigma_2\bar{\delta}_2 K_1(\bar{\delta}_2)\right\} - C\sigma_2\bar{\delta}_2 I_1(\bar{\delta}_2)] \tag{10.32}$$

where A, B and C are given by equations (10.22) and (10.23).

Hence the transmissibility across the plate

$$T_0 = \left| \frac{F_1}{F_0} \right|$$

is completely determined.

Case C. Driving-Point Impedance and Transmissibility of a Clamped Plate, Mass-Loaded and Driven at the Center (see figure 17)

Expressions for the driving-point impedance and transmissibility of a mass-loaded plate follow directly from knowledge of the expressions for Z_0 and T_0 that were derived earlier. Because of the continuity of motion between the load mass M and the center of the plate it is possible to state

$$Z_{m0} = Z_m + Z_0 = i\Omega M + Z_0 \tag{10.33}$$

where

Z_{m0} is the driving-point impedance of mass-loaded plate

Z_m is the impedance of the load mass and

Z_0 is the driving-point impedance of the unloaded plate.

Since $\frac{M}{M_p} = \Lambda$, the mass ratio, the normalized driving-point impedance of the mass-loaded plate can be expressed by

$$Z_{mn} = \frac{Z_{m0}}{i\Omega M_p} = \Lambda + Z_n \tag{10.34}$$

where Z_n is given by equation (10.16) for the classical theory and by equation (10.27) for the improved theory.

The driving force at the center of the plate is given by

$$F_0 = \bar{F}_0 e^{i\Omega T}$$

If the force which the mass M exerts on the plate is F_{01}, the total force F_1 transmitted to the plate support can be expressed by the relation

$$T_0 = \left| \frac{F_1}{F_{01}} \right| \tag{10.35}$$

where

$$F_{01} = \bar{F}_{01} e^{i\Omega T}$$

Also, if V_0 is the common velocity of the load mass M and the center of the plate, we have

$$Z_0 = \frac{F_{01}}{V_0} \tag{10.36}$$

where

$$V_0 = \bar{V}_0 e^{i\Omega T}$$

and

$$Z_{m0} = \frac{F_0}{V_0} = (i\Omega M + Z_0) \tag{10.37}$$

Substituting for V_0 in equation (10.37) from equation (10.36), one obtains

$$Z_{m0} = \frac{F_0}{F_{01}} Z_0 \tag{10.38}$$

In view of equation (10.35), this becomes

$$\frac{F_{01}}{F_0}\left|\frac{F_1}{F_{01}}\right| = T_0 \frac{Z_0}{Z_{m0}}$$

Hence for the transmissibility of the mass-loaded plate, we obtain

$$T_m = \left|\frac{F_1}{F_0}\right| = T_0 \left|\frac{Z_0}{i\Omega M+Z_0}\right| = T_0 \left|\frac{Z_0}{i\Omega\pi\Lambda+Z_0}\right| \tag{10.39}$$

where Z_0 is given by equation (10.15) for the classical theory and by equation (10.26) for the improved theory.

Case D. Driving-Point Impedance and Transmissibility of a Clamped Plate, Spring-Loaded and Driven at the Center (see figure 18)

The driving-point impedance for this case is given by

$$Z_{k0} = Z_k + Z_0 = \frac{K}{i\Omega} + Z_0 \tag{10.40}$$

where

Z_{k0} is the driving-point impedance of the spring-loaded plate and

Z_k is the impedance of a spring element

The normalized driving-point impedance is

$$Z_{kn} = \frac{Z_{k0}}{i\Omega M_p} = \frac{Z_{k0}}{i\Omega\pi} = Z_n - \frac{K}{\pi\Omega^2} \qquad (10.41)$$

Following a similar procedure as in case C, for the transmissibility across the spring-loaded plate, we obtain

$$T_k = T_0 \left| \frac{Z_0}{Z_0 + Z_k} \right| \qquad (10.42)$$

Case E. Transmissibility Across a Clamped Plate with Mass and Spring Loading at the Center and Driven at the Center

For this case, the transmissibility across the plate follows directly from the results of case C and case D. It is easily seen that

$$T_{km} = T_0 \left| \frac{Z_0}{Z_0 + Z_m + Z_k} \right| = \left| \frac{Z_0}{Z_0 + i\Omega M + \frac{K}{i\Omega}} \right| T_0 \qquad (10.43)$$

Case F. Transmissibility Across a Clamped Plate, Driven at the Center and to which a Dynamic Absorber is Attached at the Center (see figure 19)

The plate is driven by a harmonically oscillating force F_0 at its center. A dynamic absorber which consists of a spring-mass system is attached at the center of the plate to suppress the transmissibility at the first or any other resonant frequency of the plate.

The impedance of the absorber is given by the relation

$$Z_a = \left[\frac{1}{i\Omega M_a} + \frac{1}{\frac{K_a}{i\Omega}} \right]^{-1} \qquad (10.44)$$

where M_a and K_a represents respectively the mass and stiffness of the absorber elements.

Making the substitution

$$\Omega_a = \left(\frac{K_a}{M_a}\right)^{\frac{1}{2}} , \qquad (10.45)$$

for the natural frequency of the absorber, the above yields

$$Z_a = \frac{i\Omega M_a}{1 - \left(\frac{\Omega}{\Omega_a}\right)^2} \tag{10.46}$$

The driving-point impedance of the system is given by

$$Z_{a0} = Z_0 + Z_a \tag{10.47}$$

Hence the transmissibility across the plate becomes

$$T_a = T_0 \left| \frac{Z_0}{Z_0 + Z_a} \right| = T_0 \left| \frac{Z_0}{Z_0 + \frac{i\Omega M_a}{1-\left(\frac{\Omega}{\Omega_a}\right)^2}} \right| \tag{10.48}$$

Case G. Transmissibility Across a Clamped Plate, Mass-Loaded and Driven at the Center at which a Dynamic Absorber is Attached

It directly follows from the above discussion that if a mass M is attached at the center of the plate in addition to the dynamic absorber, the expressions for the total impedance and transmissibility across the plate become

$$Z = Z_0 + Z_m + Z_a \tag{10.49}$$

and

$$T_{am} = T_0 \left| \frac{Z_0}{Z_0 + i\Omega M + \frac{i\Omega M_a}{1 - \left(\frac{\Omega}{\Omega_a}\right)^2}} \right| \tag{10.50}$$

XI. DISCUSSION OF RESULTS

The numerical results and graphs presented in this work are obtained by using the IBM 360 Model 50 digital computer system and the Calcomp 566 digital incremental plotter which are available in the Computer Center of the University of Missouri - Rolla.

A general discussion of the results of this investigation follows.

A. Frequency Spectra (see figures 23-32 and tables I-VIII)

Each curve in these figures is drawn through a minimum of 60 data points. It is seen that virtually no similarity exists between the frequency spectra as predicted by the classical and improved theories, with the possible exception of very thin plates. Improved theory frequencies are bounded for increasing thickness to radius ratio (figures 23 and 24), while the corresponding frequencies in the classical theory increase linearly for increasing thickness to radius ratio (figures 31 and 32).

The frequency spectra for axisymmetric vibration predicted by the improved theory result from the coupling of two different systems. The first system consists of flexural modes whose frequency spectrum may be visualized as an extension into the region $\Omega > \bar{\Omega}$, of the curves in the region $\Omega < \bar{\Omega}$. In figures 23-26, these are ascending curves which flatten out for large values of $\frac{h}{a}$. In figure 29 these can be discerned as ascending straight lines. The second system consists of the fundamental thickness-shear mode and its overtones. Their spectrum, in figure 29, is formed by the loci of the flat, nearly horizontal portion of the resonance curves in the region above the thickness-shear frequencies. In figures 23-26, these can be discerned as the loci of the descending portion of the resonance curves. For the free plate the higher thickness-shear overtones are not clearly defined as for the clamped and simply supported plates (figure 25). This is also the case for the disk mounted on a shaft where the edges of the plate are free.

For vibration with one diametral node the frequency spectra result from the coupling of three different systems of motion (figures 27 and 28). In addition to the flexural and thickness-shear modes discussed earlier, the thickness-twist mode also is present here. It it seen that the frequency spectrum for the thickness-twist mode almost coincides with the spectrum for the thickness-shear mode. In other words, the thickness-twist modes have frequencies very close to the corresponding thickness-shear modes. This is evident in figure 30, where the two resonance curves are seen as parallel lines close to one another in the region above the thickness-shear frequencies.

It is seen that the suppression of the thickness-shear mode in the classical theory serves as a constraint in the system, making frequencies larger than those predicted by the improved theory. As a result, according to the improved theory, there are more resonances in a given frequency range than are predicted by the classical theory. For example, for a clamped plate with $\frac{h}{a} = 0.125$, in the frequency range $0 < \frac{\Omega}{\bar{\Omega}} < 1$, there are 10 resonances according to the improved theory, whereas the classical theory gives only 6. For $\frac{h}{a} = 0.25$, the corresponding values are 5 and 3.

The most striking difference between the two theories occurs at frequencies above that of the fundamental thickness-shear mode as is seen from figures 23-26. In the frequency range from 0 to 25, for a clamped plate with $\frac{h}{a} = 0.125$, there are 20 resonances according to the improved theory compared to 8 predicted by the classical theory. For $\frac{h}{a} = 0.25$, the corresponding values are 22 and 5.

Since for a given $\frac{h}{a}$ value the frequencies predicted by the improved theory are lower than those given by the classical theory, it is evident that for a given frequency of vibration in a particular mode the improved theory requires a higher value for $\frac{h}{a}$, and hence a smaller plate. Hence in designing a plate to vibrate at a certain frequency in a particular mode, considerable error will be introduced if the classical theory is used in place of the improved theory. This discrepancy will be higher for higher modes. For example, considering a clamped plate vibrating in its fundamental mode, for a frequency of 0.29 the classical theory gives $\frac{h}{a}$ as 0.10 compared to 0.1025 predicted by the improved theory. For a given plate thickness the radius predicted by the classical theory will be larger by 2.5 percent. Considering the third mode of vibration, for a frequency of 2.57, the radius predicted by the classical theory will be in error by 27 percent. Hence it is very important that in designing plates to resonate at particular frequencies the improved theory should always be used in place of the classical theory.

B. Effect of Poisson's Ratio on Frequencies (see figure 33 and tables IX and X)

Figure 33 and tables IX and X show the variation of the frequencies of a free circular plate with change in Poisson's ratio from 0.25 to 0.35, the usual range of variation encountered in most applications. The differences in frequencies are not obvious in the figure and can best be observed in the tables. In general, it can be observed that in the frequency range below that of the fundamental thickness-shear mode the frequencies increase with increase in Poisson's ratio. Above this range, the frequencies are found to decrease with an increase in Poisson's ratio. Thus from table IX it is observed that for a plate with $\frac{h}{a} = 0.125$, as ν increases from 0.25 to 0.35, the fundamental frequency changes from 0.32326 to 0.34161, an increase of 5.67 percent. The tenth frequency changes from 15.4196 to 15.1032, a decrease of 2.05 percent. For a plate with $\frac{h}{a} = 0.25$, table X shows that for the same range of ν, the fundamental frequency increases by 5.15 percent and the tenth frequency decreases by 1.48 percent. To summarize the effect of Poisson's ratio it can be stated that: (1) For plates vibrating at fixed frequencies, plates with larger values of ν will be larger in diameter, provided $\Omega < \bar{\Omega}$. (2) For plates of the same dimensions, those with larger values of ν will be vibrating at higher frequencies, provided $\Omega < \bar{\Omega}$. For $\Omega < \bar{\Omega}$, the opposite of the conditions stated above will prevail.

C. Mode Shapes and Profiles of Deflected Plate (see figures 34-41)

A clear picture of the boundary conditions involving W and ψ can be obtained from the mode shapes and the profiles of the deflected plate. These curves are plotted through a minimum of 50 data points equally spaced along the abscissa. The first 20 modes are considered in obtaining the profiles of the deflected plate.

For the clamped and simply supported plates it is seen that for all modes $\frac{dW}{dR}$ is zero at the center of the plate and not zero at the support. For the simply supported plate, the W nodal circles are closer to the edge of the plate compared with the corresponding nodal circles for the clamped plate. For the clamped plate it is observed that ψ is zero at the center and at the edge, whereas for the simply supported plate ψ is zero at the center and not zero at the edge. As in the case of the W nodes, the ψ nodal circles are closer to the edge of the plate for the simply supported plate compared with the corresponding nodal circles for the clamped plate.

From the profiles of the deflected plate shown in figures 39-41, it is observed that the deflections predicted by the classical theory are generally smaller than the deflections obtained by using the improved theory. For a concentrated load the classical theory gives a finite deflection at the center, whereas according to the improved theory the deflection becomes infinite at the center.

D. Response of Plate to Rapidly Applied Steady Loads (see figures 42-58)

The response curves are drawn through a minimum of 200 data points equally spaced along the abscissa. One hundred terms are taken in the modal series to obtain the response for the improved theory, whereas due to the more rapid convergence of the modal series for the classical theory, only 25 modes are considered for the response of the classical theory. For the disk mounted on a shaft, 25 terms are included in the series expansions. Table XVI shows the response data from figures 42-54, 57 and 58. The portions of the total response contributed by each mode for different cases of loading are given in tables XVII - XX. From the graphs and tables mentioned above, the following observations are made:

1. The improved theory predicts a larger static deflection than does the classical theory for all types of loading and boundary conditions considered. The difference between the predictions of the two theories increases as the value of $\frac{h}{a}$ is increased.

2. As in Reissner-Goodier theory [74, 77-81], for axisymmetrical loading the static bending moments given by the improved and classical theories are identical. For unsymmetrical loading the improved theory will give a different bending moment than the classical theory. This is also the case in the Reissner-Goodier theory.

3. The maximum total displacement predicted by the improved theory is always greater than the corresponding value obtained by using the classical theory. Hence, in problems dealing with displacement analysis the improved theory is always to be preferred. The difference in the total displacements predicted by the two theories is found to become greater for larger values of $\frac{h}{a}$.

4. The Williams-type modal series is found to converge rapidly (tables XVII - XX) so that only about 25 modes are required to insure an accuracy of the calculated results to two significant figures. However, to obtain accuracy to at least three significant figures, it was found that at least one-hundred modes were required.

5. For the cases considered, the classical theory gives a larger maximum bending moment at the outer edge of the plate, whereas, except for case 1, the improved theory gives larger maximum bending moment at the center of the plate (table XVI).

6. For the cases where the load is uniformly distributed over a circular area, the bending moment response curves are found to be smoother than the curves for the other types of load distribution considered. This can be explained from tables XVIII-XX, wherein it is observed that for a load uniformly distributed over an area, compared with the other two types of distribution, only a small number of modes contribute substantially to the response.

7. In general, the response predicted by the improved theory is slower (less cycles per unit time) than the response of the classical theory. This is evidently a consequence of the lower values of natural frequencies predicted by the improved theory.

8. Under the same loading conditions a thicker plate vibrates faster

than a thinner plate of the same radius. Also, a clamped plate is found to vibrate faster than a simply supported plate of the same dimensions under identical loading.

E. Response of Plate to Pulse Loads (figures 59-65)

These response curves are drawn through 200 data points, equally spaced along the time axis. In each case 20 modes are used in the series expansion. The maximum response data for a clamped plate are tabulated in table XXI.

It is seen that the ramp-platform load with unit rise time has achieved a dynamic overshoot factor (ratio of maximum response to maximum static response) of 1.935 compared to 1.945 for the step load. It is to be noted that if the responses of the four pulse loads are to be compared on the basis of equal input impulse, the response of the blast pulse must be doubled and the response of the half-sine pulse must be multiplied by $\pi/4$. On this basis, for both the classical and the improved theories, the blast pulse causes the largest deflection, followed by the square pulse and the triangular pulse, with the half-sine pulse producing the least deflection. For the pulse loads, the maximum deflection predicted by the improved theory is always larger than the corresponding maximum deflection given by the classical theory.

F. Effect of Load Distribution and Duration of Pulse on the Response of Plates (see figures 66-72)

The effect of changing the area of load distribution on the center deflection of a clamped circular plate is shown in figure 66 and table XXII. For a ring loading, figure 67 and table XXIII show the effect of changing the radius of the load on the deflection at the center. 100 modes are used in the series expansions and the curves are drawn through 200 equally spaced data points. Figures 68-72 and table XXIV show the variations of the center deflection of a clamped circular plate due to changes in the duration of the pulse for different pulse shapes. For these curves 20 modes and 240 equally spaced data points are used.

It is seen that spreading the load over a larger area or over a larger circle about the center obviously reduces the center deflection, but increases the dynamic overshoot factor. It is also evident that for the same total load, increasing the radius of the loading circle for a ring load increases the overshoot factor by a greater amount than that produced by a corresponding radius increase for the load distributed over a circular area. These may be explained by the fact that as the load is removed farther from the center, the higher modes get a proportionately larger amount of the total energy input and thereby contribute more to the deflection at the center.

For the same load distributed over a circular area or over a circle of the same radius or concentrated at the center, the first one achieves the lowest dynamic overshoot factor and the last one the highest. It can be observed from tables XVII -XX that in the last two cases of loading the higher modes contribute substantially greater amounts to the total response than in the first case of loading. So in general, it may be stated that the greater the contribution of the higher modes of vibration to the total response, the higher will be the dynamic overshoot factor, the less smooth the response curves and the slower the convergence of the modal series.

Table XXIV and figures 68-72 show that on the basis of equal input impulse, for the durations considered, increasing the duration of the pulse or the rise time of the load reduces the dynamic overshoot factor, the highest reduction occuring for the half-sine pulse and the lowest for the blast pulse. It is also observed that reducing the duration of the pulse increases the frequency of the resulting vibration of the plate. Moreover, for a pulse of longer duration, it is found that the deflection response curves are smoother than those for shorter pulse durations. It is to be expected that for shorter pulses, the higher modes contribute a substantially larger amount to the total response than they do for pulses of longer durations. Also it is reasonable to conclude that if the duration of the pulse is reduced to zero (an impulse) the contribution of the higher modes becomes so predominant that the question of convergence of the modal series will be in doubt or the series may not converge at all (see reference 9, p. 25 for a similar statement on beam response).

For pulse loads of very short durations figure 73 shows that on the basis of equal input impulse, the deflection response is almost independent of the duration of the pulse and the shape of the pulse.

G. Acceleration Response of the Center of Plate under Pulse Loads (see figures 74-78 and table XXV)

The response curves shown are drawn through a minimum of 200 data points, equally spaced along the time axis. 50 modes are considered for the series expansions.

For the displacement of the plate, we have [see equation (8.79)]

$$\frac{q_i(T)}{P_0} = \left[\frac{A_1 J_1(\delta_1 \gamma)}{\delta_1} + \frac{A_2 I(\bar{\delta}_2 \gamma)}{\bar{\delta}_2}\right] \frac{\cos \Omega_i T}{\pi \gamma \Omega_i^2} \tag{11.1}$$

Differentiating this twice with respect to time, one obtains

$$\frac{\ddot{q}_i(T)}{P_0} = - \left[\frac{A_1 J_1(\delta_1 \gamma)}{\delta_1} + \frac{A_2 I_1(\bar{\delta}_2 \gamma)}{\bar{\delta}_2}\right] \frac{\cos \Omega_i T}{\pi \gamma} \tag{11.2}$$

The total acceleration response is given by

$$\ddot{W}(R,T) = \ddot{W}_s(R,T) + \sum_{i=1}^{\infty} W_i(R)\ddot{q}_i(T) \tag{11.3}$$

Since equation (11.2) does not contain Ω_i^2 in the denominator as in equation (11.1) the convergence of the acceleration modal series will be much slower than that of the displacement modal series. Hence a larger number of modes must be considered to insure satisfactory accuracy in the results. The 50 modes used in this investigation for the acceleration modal series is found to give an accuracy of the results to only one significant figure.

From table XXV it is seen that on the basis of equal input impulse the blast pulse produces the highest acceleration of the center of the plate, followed by the square and triangular pulses, with the half-sine pulse producing the least acceleration. It is further observed that for gradually rising loads (triangular, half-sine and ramp-platform) the acceleration curves are smoother compared with those obtained for suddenly rising loads (blast and square pulses).

H. Frequency Spectra for Constrained Plates (see figures 79-84 and tables XII-XV)

The closed-form frequency equation is used in obtaining the resonance curves which are drawn through a minimum of 40 points.

It is observed that attaching a concentrated mass to the center of the plate reduces the values of the resonant frequencies of the plate up to a certain mass ratio after which the frequencies remain nearly constant irrespective of the magnitude of the attached mass. On the other hand, attaching a spring to the center of the plate has the effect of increasing the frequencies of the plate up to a certain value of the spring stiffness after which the frequencies are not greatly affected by an increase in the spring stiffness. For a very large mass or a very stiff spring attached to the center of the plate, the frequencies are almost identical and these frequencies can be shown to coincide with those of a plate fixed at the center. At higher modes of vibration, the effect of coupling between flexural and thickness-shear modes of vibration can be clearly seen in the frequency spectra. For modes which are affected by such coupling, the behavior of the response curves is found to be different from that of the low mode curves. Here, for a mass-loaded plate the frequencies are found to increase with an increase in mass ratio up to the point of coupling after which they maintain almost constant values for the remaining portion of the frequency spectrum. It is also seen that the frequencies calculated using the closed-form frequency equation are very close to the frequencies obtained using 20 modes in the series solution. Also the classical theory predicts higher frequency values than the improved theory.

I. Impedance and Transmissibility of Plates with No Mass or Spring Loading (see figures 85-88)

The impedance and transmissibility curves presented in this work are drawn through a minimum of 500 data points equally spaced along the frequency axis.

Between zero frequency and the first resonance (low impedance point) it is seen that the impedance is almost entirely springlike: that is to say, $|Z_n|$ decreases essentially in proportion to frequency (see appendix E). Between the first resonance and the first antiresonance (high impedance point) the impedance is almost entirely masslike in character and increases as the frequency increases. The impedance then becomes alternately springlike and masslike as the frequency increases through successive antiresonant and resonant frequencies. This behavior is typical of any continuous system such as string, rod or beam (see reference 67, p. 107). The figures show that the antiresonances occur approximately midway between successive resonances.

The transmissibility across the system exhibits a series of resonant peaks which can be shown to coincide in frequencies with the resonant frequencies of the system. The mean level of transmissibility is seen to be greater than 1, the troughs of the curves (low transmissibility points) showing a value of approximately 2, with this value falling off after the first few resonances.

J. Impedance and Transmissibility of Plates with Mass and Spring Loading (see figures 89-98)

The curves show that by attaching a mass to the center of the plate the resonant frequencies of the system are moved to lower values by an amount that will depend on the magnitude of the attached mass but will not exceed the original frequency separation of the particular mode of vibration and the next lower antiresonance. The fundamental resonant frequency is not restricted in this way because there is not a further antiresonance at a lower frequency. After the first few modes, it is seen that the resonant frequencies almost approach the next lower antiresonances, the portion of the impedance curve between each resonance and the next higher antiresonance lying almost parallel to the abscissa for almost the entire bandwidth. It is also observed that the antiresonant frequencies are essentially unchanged by the presence of the loading mass.

Attaching a spring to the center of the plate is seen to move the resonant frequencies of the system to higher values by an amount that will not exceed the original frequency separation of the particular mode of vibration and the next higher antiresonance, the proportionate increase of frequency decreasing at higher modes of vibration. Between zero frequency and the first resonance, the impedance behaves almost springlike. Between the first resonance and the first antiresonance, the impedance is predominantly masslike and the increase is very sudden. As in the case of mass-loaded plates, the antiresonant frequencies of the spring-loaded plates are not affected by the presence of the spring loading.

The transmissibility of a mass-loaded plate decreases rapidly with frequency following the first plate resonance, in contrast to the transmissibility of the unloaded plate. The maxima in the transmissibility curves are found to occur at lower frequencies than the corresponding maxima for the unloaded plate. This is clearly a consequence of the fact that an unloaded plate has higher resonant frequencies than a mass-loaded plate.

It is seen that the mean level of transmissibility for a mass-loaded plate is much lower than that for an unloaded plate, the proportionate decrease in mean level values being higher at higher magnitudes of the attached mass. The troughs of the transmissibility curves are found to fall off uniformly after the first resonance. A spring-loaded plate also exhibits a lower level of transmissibility compared to an unloaded plate, but the troughs of each transmissibility curve are found to rise successively for the first few modes after which they maintain a constant value. The maxima in the transmissibility curve occur at higher frequencies than the corresponding maxima for the unloaded plate.

From figure 97 it can be seen that the main factor contributing to a lower transmissibility level is the mounted mass and that the higher resonant frequencies of the system are not greatly affected by the magnitude of the attached mass or spring.

K. Transmissibility of Plates to which Dynamic Absorbers are Attached (see figures 99-106)

The curves show that a particular frequency of the plate can be isolated by mounting a dynamic absorber at the center of the plate, the absorber being tuned in the neighborhood of that frequency. It is to be noted that in isolating a certain frequency by a dynamic absorber, this resonant frequency is replaced by two resonances, one on each side of it so that there will be one more resonance in the system than in a similar system without the absorber. The pronounced maxima of transmissibility that occur at the resonant frequencies at which the absorbers are tuned are replaced by broad bands of relatively low transmissibility. For a plate with no mass or spring loading at the center, this band of low transmissibility level extends almost equally to both sides of the resonant frequency which is isolated by the absorber (see figures 99-102), the bandwidth being greater for larger absorber masses. Thus the bandwidth of low transmissibility level about a certain frequency can be controlled by proper choice of the absorber mass. This is of special interest in designing foundations for machines which operate over a certain range of frequencies. Isolating a particular resonance is also found to change the values of the resonant frequencies which are close to it on either side of the transmissibility curve.

For a mass-loaded plate, the fundamental resonant frequency can be isolated satisfactorily by an absorber which is tuned to that frequency, the isolated low transmissibility level bandwidth being greater for larger absorber masses (figure 103). But as is evident from figures 104 and 105, if the load mass ratio is large ($\Lambda = 5$ in these figures) the higher resonant frequencies cannot be isolated completely by a simple undamped dynamic absorber. This is true because for large load masses the second and higher resonant frequencies are not appreciably changed by changes in the values of the load masses so that one of the two resonances by which the absorber replaces the original resonance still coincides with it. However, it is seen that the transmissibility level can be considerably reduced by using the proper absorber mass. Moreover, since all dynamic absorbers used in practice will have some damping present in them, the amplitude of transmissibility at the resonance is considerably reduced by using the absorber, even though the position of resonance is not appreciably shifted by it. For lower values of load masses, the higher resonance frequencies are more sensitive to changes in the magnitude of the load masses and hence the positions of higher resonances can also be shifted considerably by the use of dynamic absorbers (see figure 106).

The impedance and transmissibility curves for the classical theory behave in a manner similar to those of the improved theory, except that in the case of the classical theory the resonant frequencies occur at higher values of frequencies than the corresponding resonant frequencies for the improved theory. Moreover, the classical theory predicts a slightly higher mean transmissibility level for a given frequency range, compared to the improved theory.

XII. CONCLUSIONS AND RECOMMENDATIONS

The main objectives of this investigation outlined in Chapter III have been achieved. Using both the improved and classical theories, natural frequencies and mode shapes are obtained for circular plates under different boundary conditions. Extensive frequency spectra have been compiled for various cases of axisymmetric and one diametral node vibrations. The effect of Poisson's ratio on the natural frequencies of plates is also presented in the form of graphs and tables. These will enable the use of the frequency spectra to be extended to materials with Poisson's ratio in the range 0.25 to 0.35. In designing circular plates to resonate at fixed frequencies, these graphs and tables should be of considerable value.

The Williams-type normal-mode solution has been successively applied to a wide variety of transient loading problems. The results are presented mostly in the form of graphs for quick visualization and ease of comparison between the results of the two theories. Moreover, nondimensional quantities are used for more generality of the results. Even though circular plate structures have limited use in practice, these results are still of great value due to the fact that the graphs and tables provide an indication of the amount of error involved in using the classical theory in place of the improved theory for the dynamic response of plates of other geometry. Also, from a knowledge of the dynamic overshoot factor obtained in this investigation for different types of loading and boundary conditions the dynamic response of similar systems can be predicted without appreciable error from a knowledge of the static response of the system.

In addition to two series forms of frequency equations, a closed-form frequency equation has been developed for the frequencies of circular plates loaded at the center with arbitrary load impedances. Using this equation frequency spectra have been compiled for mass-loaded and spring-loaded plates, for both the classical and improved theories. These spectra should be of considerable value in the analysis of noise emitted from loaded plate structures and in devising means to reduce or isolate the noise.

Treating the plate as a foundation structure, closed-form expressions have been derived for the impedance and transmissibility of plates loaded and driven at the center and using these expressions impedance and transmissibility curves have been presented for various combinations of load mass ratio, absorber mass ratio and spring stiffness. These graphs will serve to give an insight into the behavior of the circular plate as a foundation structure and thereby assist in the design and vibration isolation of plates used as machine foundations. It should be noted that in view of the dual significance of the expression for transmissibility [see equation (E.6)] the transmissibility curves can be used to predict the motion transmitted to a machine from the vibration of the floor or alternately the force transmitted from a machine to the floor.

One of the main objectives of this investigation has been an evaluation of the improved theory compared to the classical theory. Regarding this, the following conclusions can be drawn on the basis of the results of this study:

1. For correct determination of the resonant frequencies of plates the improved theory which takes into account the effect of transverse shear and rotary inertia should always be used. The classical theory is found

to give rather good results only for very thin plates and then for only the first few modes of vibration. For plates loaded with masses or springs the improved theory is to be preferred for similar reasons.

2. Since the deflections predicted by the improved theory are always higher than those given by the classical theory, for problems concerned with dynamic deflections, the improved theory is preferable to classical theory.

3. In many cases the dynamic bending moments given by the classical theory are found to be greater than those obtained on the basis of the improved theory. In those cases the classical theory is conservative. Extreme caution should be exercised in using the classical theory for the evaluation of dynamic bending moment, since in certain cases the bending moments predicted by the classical theory are much lower than those obtained using the improved theory.

4. Since the mean transmissibility levels predicted by the classical theory are generally slightly higher than those of the improved theory, in cases concerned with the determination of the force transmitted from a machine to the floor or the motion transmitted from the floor to the machine, the classical theory can be used to advantage.

5. In the design of plates as foundations for machines the classical theory should not be used as the frequencies predicted on the basis of this theory are greatly in error compared to those obtained by the improved theory.

In spite of the general principles outlined above, for actual dynamic response problems one should choose between the two theories by considering the importance of the problem and the degree of accuracy desired in the results. In general, computations using the improved theory are more difficult and time consuming and these may not be justified unless a high degree of accuracy in results is desired for the problem under investigation.

The investigations in this work have been mainly devoted to the study of axisymmetrical vibrations of uniform circular plates under axisymmetric loading. It is felt that the same procedure can be extended to nonuniform plates as well as arbitrarily placed loads. Only clamped circular plates driven at the center have been considered in detail in the study of impedance and transmissibility. But the procedure can be readily applied to other boundary conditions as well. It may also be possible to obtain similar solutions for the impedance and transmissibility of plates under other types of axisymmetric distribution of the driving force. Even though the method of including internal damping has been treated in general, no numerical results for damped plate are presented in this investigation, since such detailed treatment of damping is considered to be beyond the scope of this work. If desired, results with damping considered can be obtained by treating δ as a complex quantity as explained in appendix F. Furthermore, the improved methods and procedures established in this investigation can be used for the analysis of many other types of plate vibration problems including the effect of transverse shear and rotary inertia.

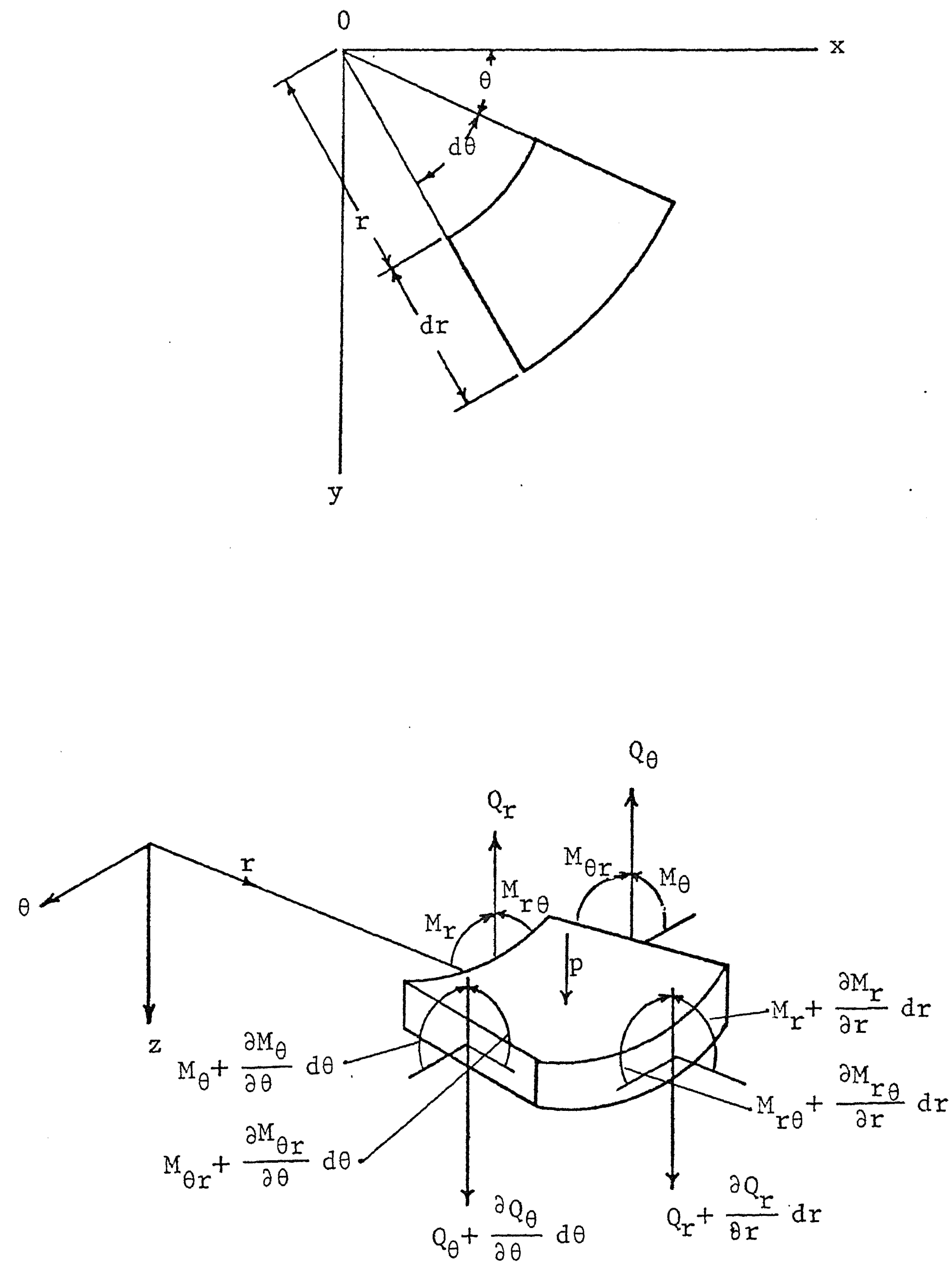

Figure 1 Typical Circular Plate Element

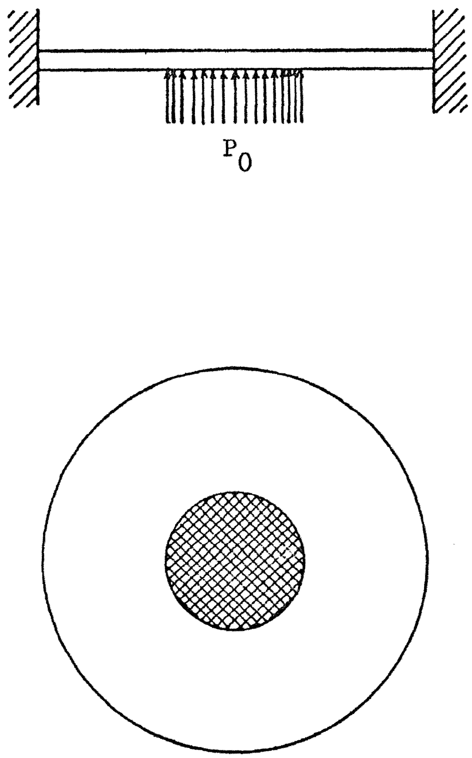

Figure 2 Clamped Circular Plate, Load Distributed over a Circular Area

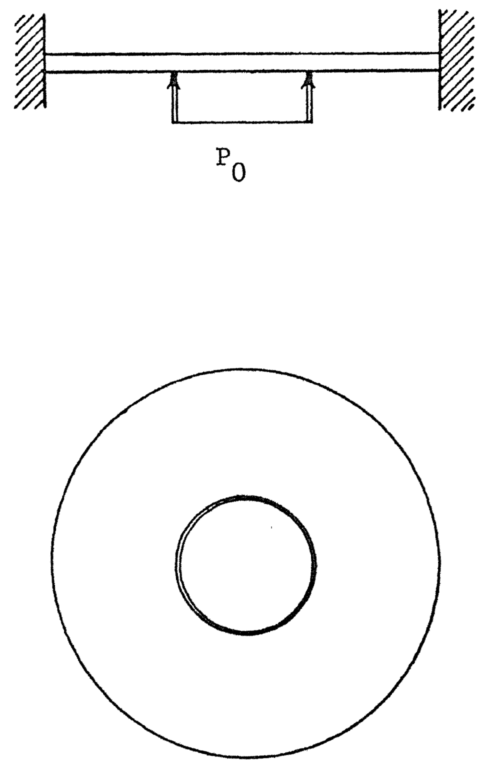

Figure 3 Clamped Circular Plate, Load Distributed over a Circle

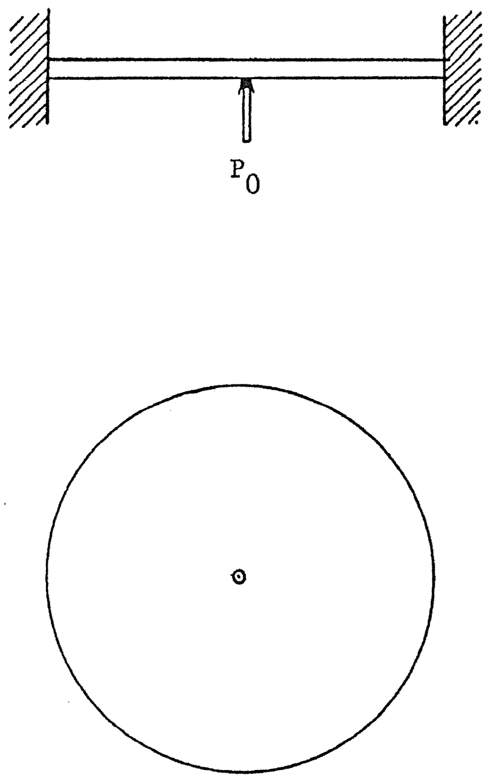

Figure 4 Clamped Circular Plate, Load Concentrated at the Center

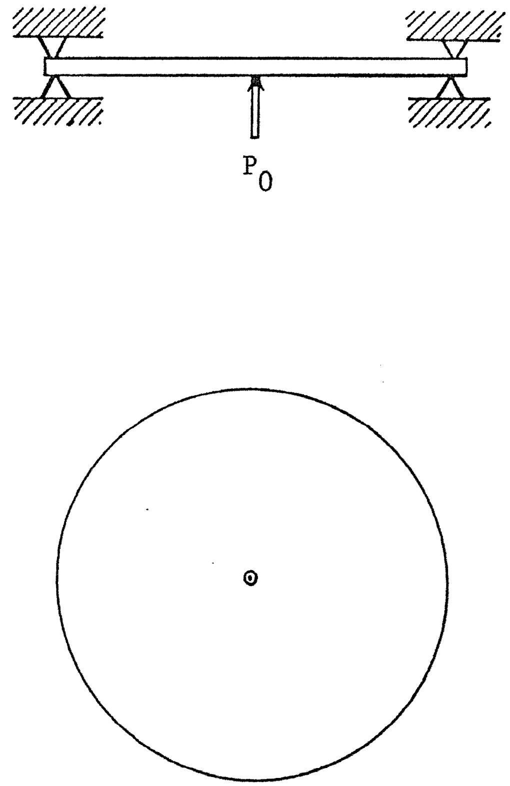

Figure 5 Simply Supported Circular Plate, Load Concentrated at the Center

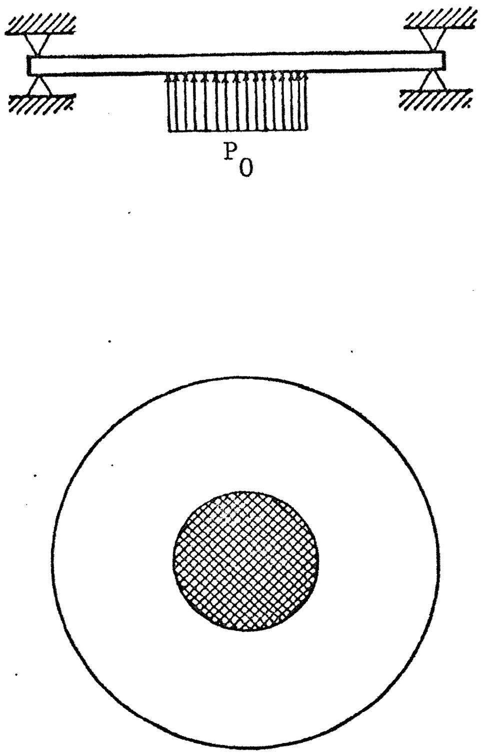

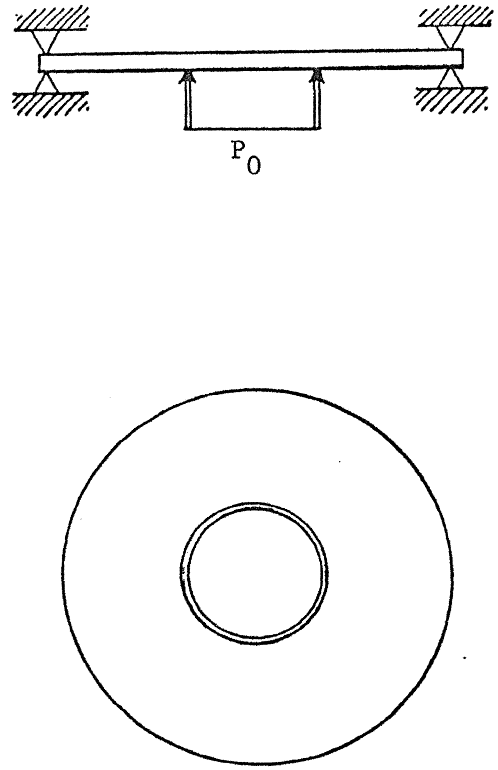

Figure 6 Simply Supported Circular Plate, Load Distributed over a Circular Area

Figure 7 Simply Supported Circular Plate, Load Distributed over a Circle

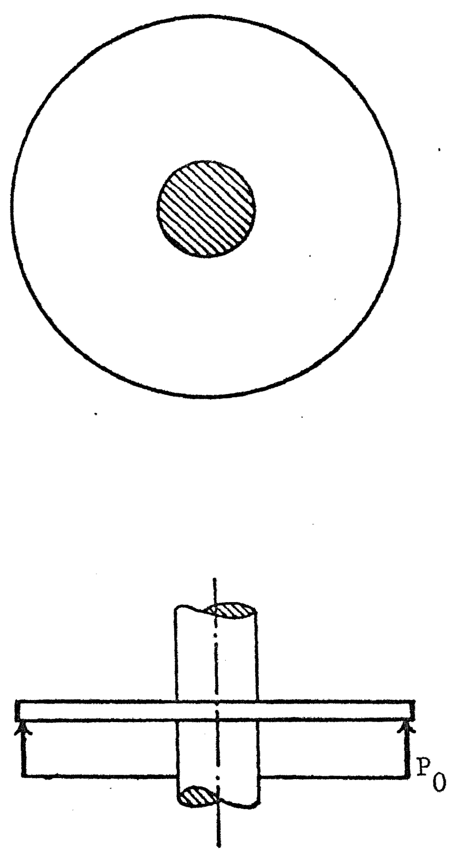

Figure 8 Disk Mounted on a Shaft, Loaded at the Outer Edge

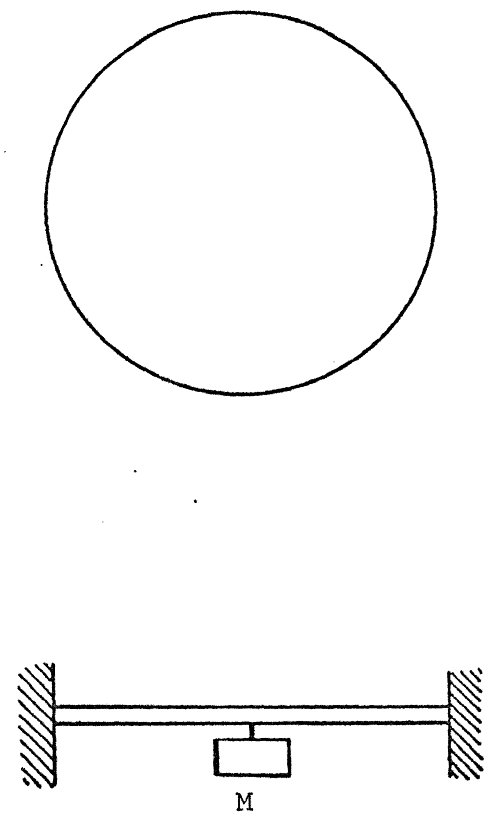

Figure 9 Clamped Circular Plate, Concentrated Mass Attached at the Center

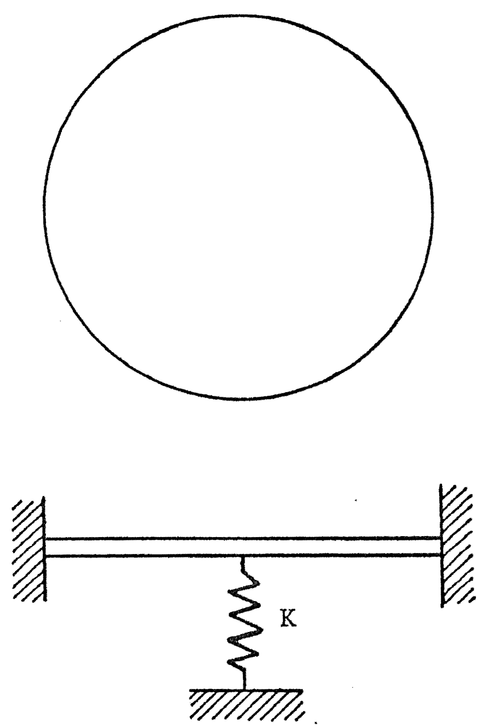

Figure 10 Clamped Circular Plate, Spring Attached at the Center

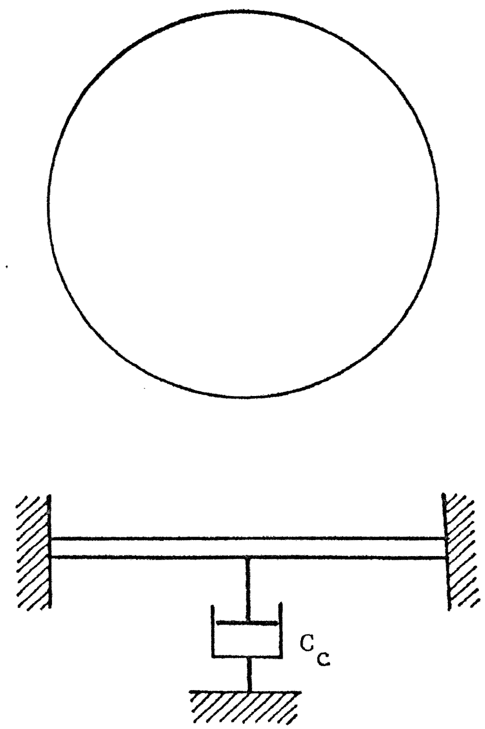

Figure 11 Clamped Circular Plate, Dashpot Attached at the Center

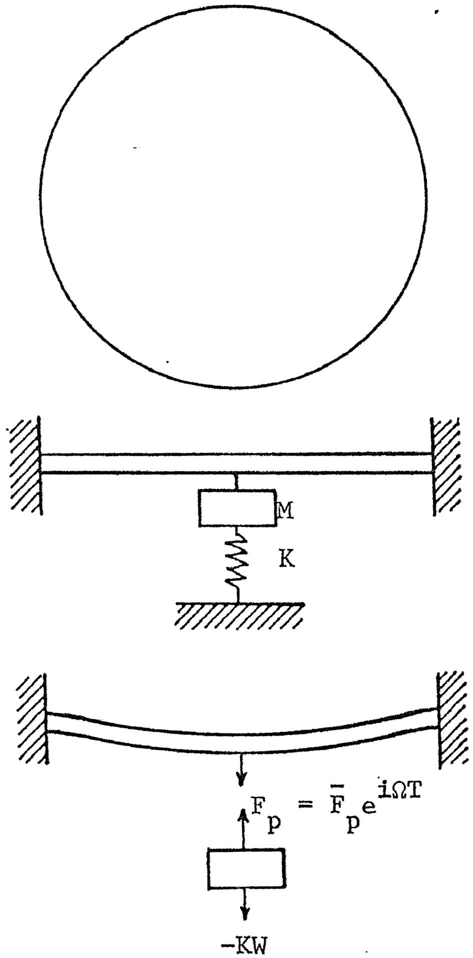

Figure 12 Clamped Circular Plate, Concentrated Mass and Spring Attached at the Center

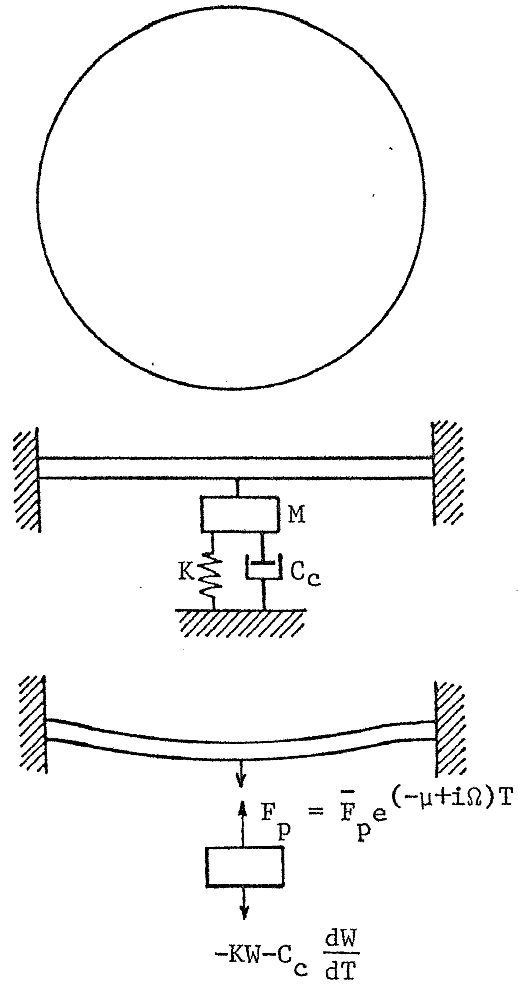

Figure 13 Clamped Circular Plate, Concentrated Mass, Spring and Dashpot Attached at the Center

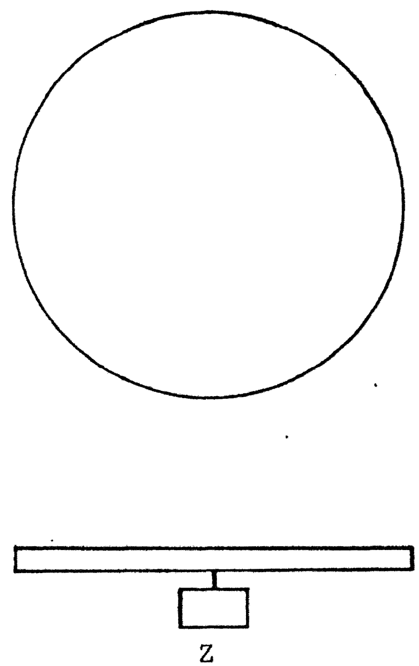

Figure 14 Circular Plate with
Arbitrary Load Impedance at the Center

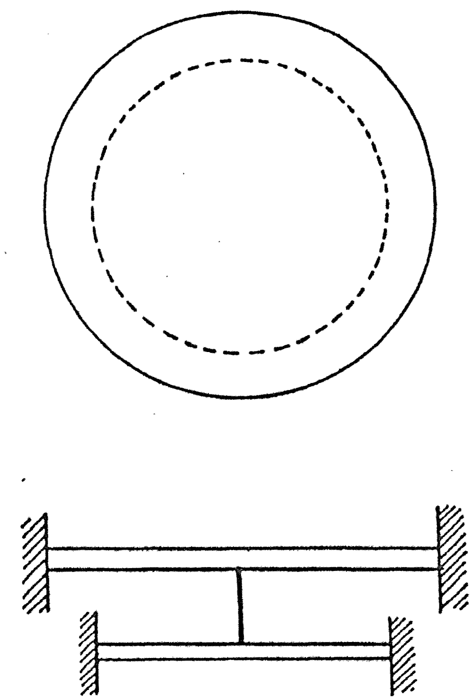

Figure 15 Two Clamped Circular Plates,
Rigidly Connected Together at the Centers

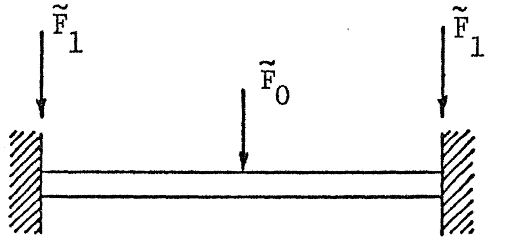

Figure 16 Clamped Circular Plate, Driven at the Center

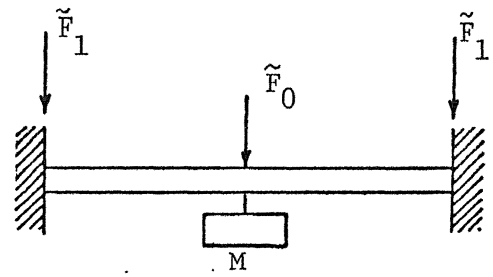

Figure 17 Clamped Circular Plate, Mass-Loaded and Driven at the Center

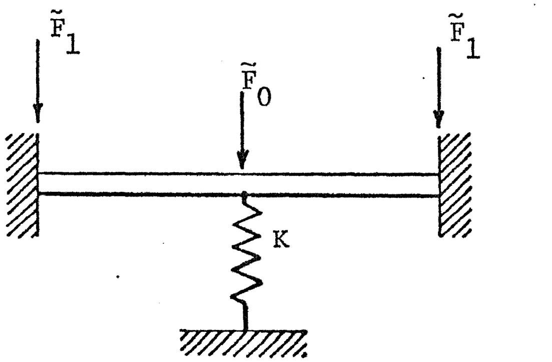

Figure 18 Clamped Circular Plate, Spring-Loaded and Driven at the Center

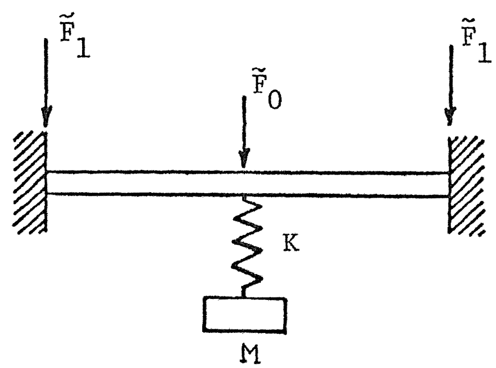

Figure 19 Clamped Circular Plate with Dynamic Absorber at the Center and Driven at the Center

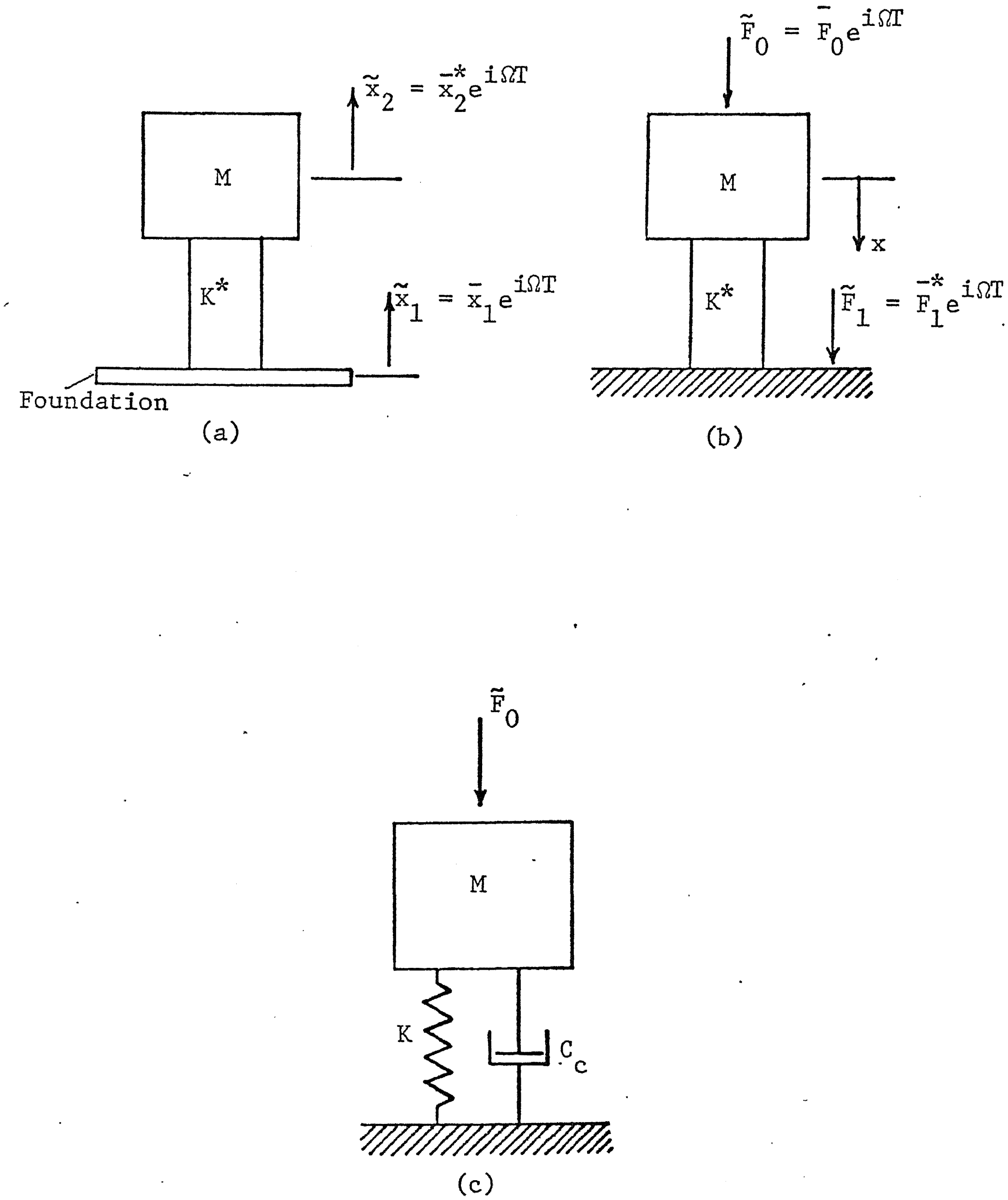

Figure 20 Simple Mounting System

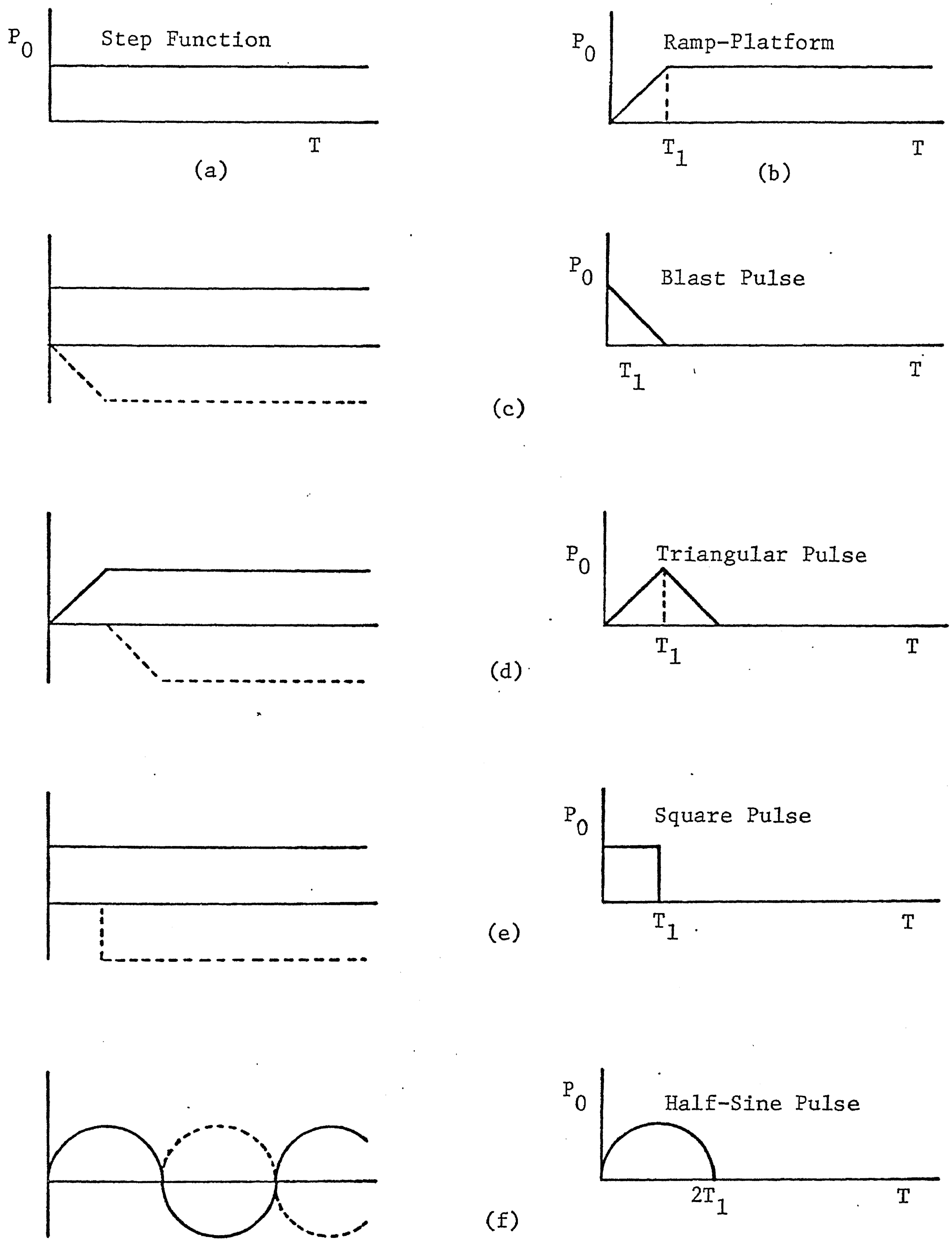

Figure 21 Some Load Time Histories

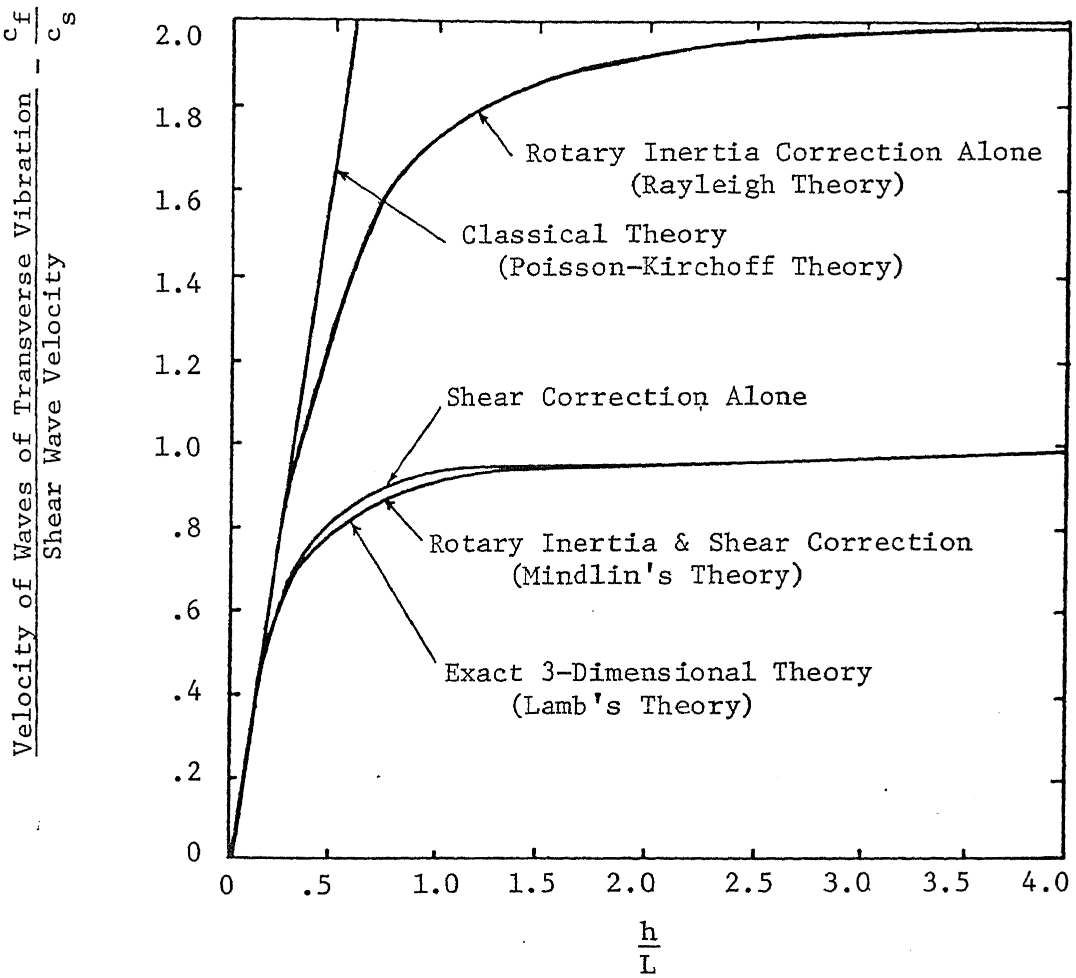

Figure 22 Phase Velocity of Transverse Waves in Plate

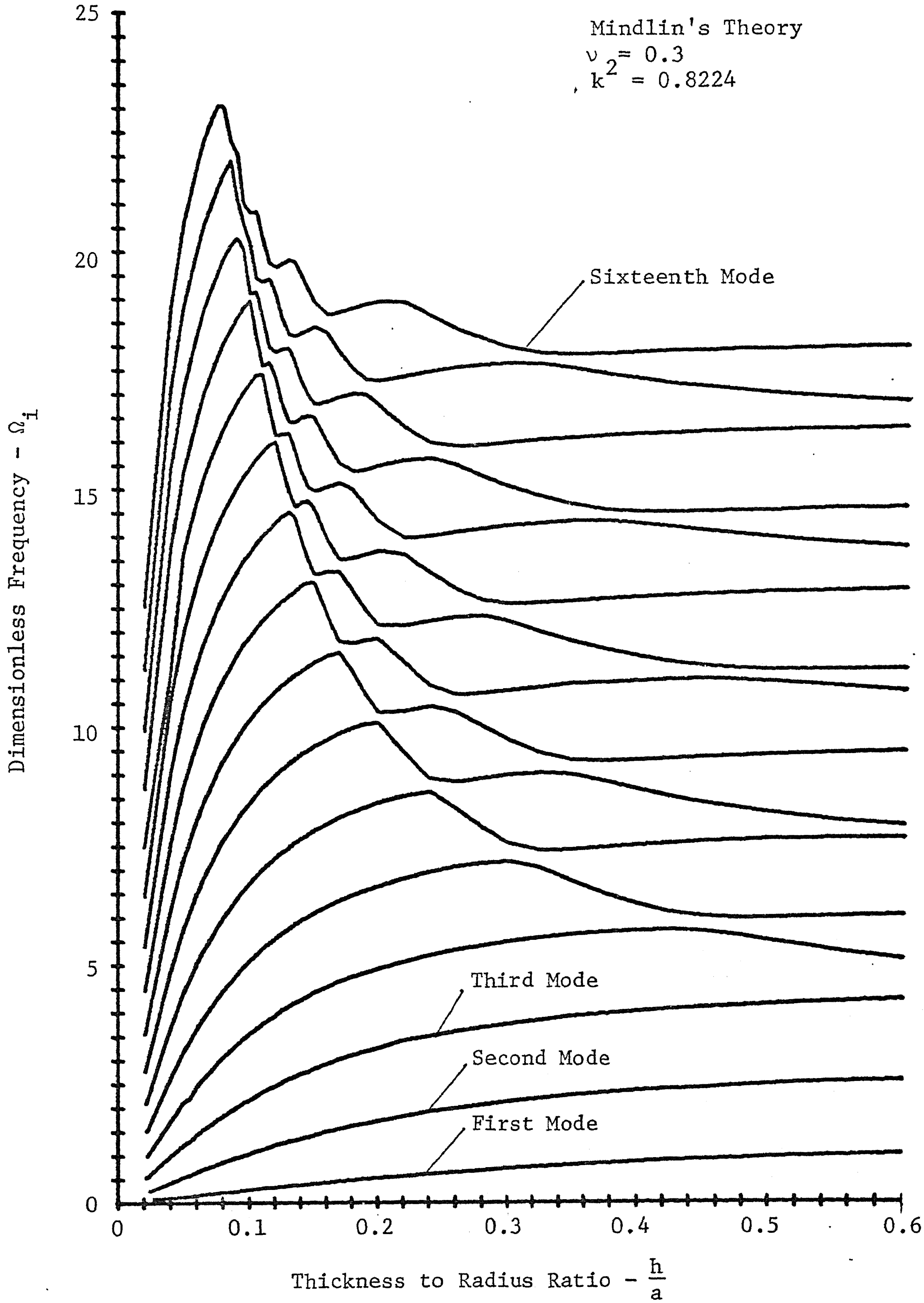

Figure 23 Clamped Circular Plate Frequency Spectrum

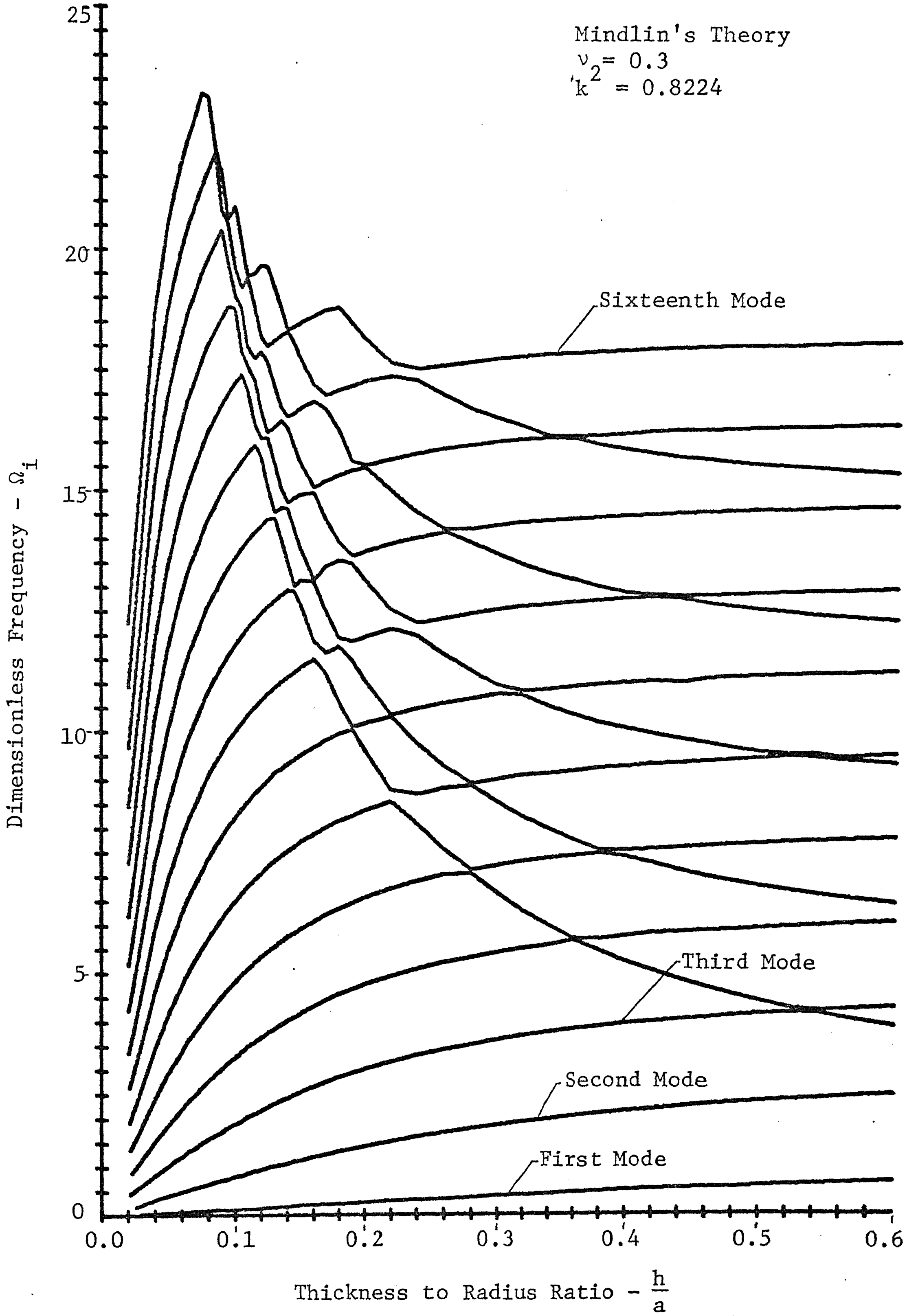

Figure 24 Simply Supported Circular Plate Frequency Spectrum

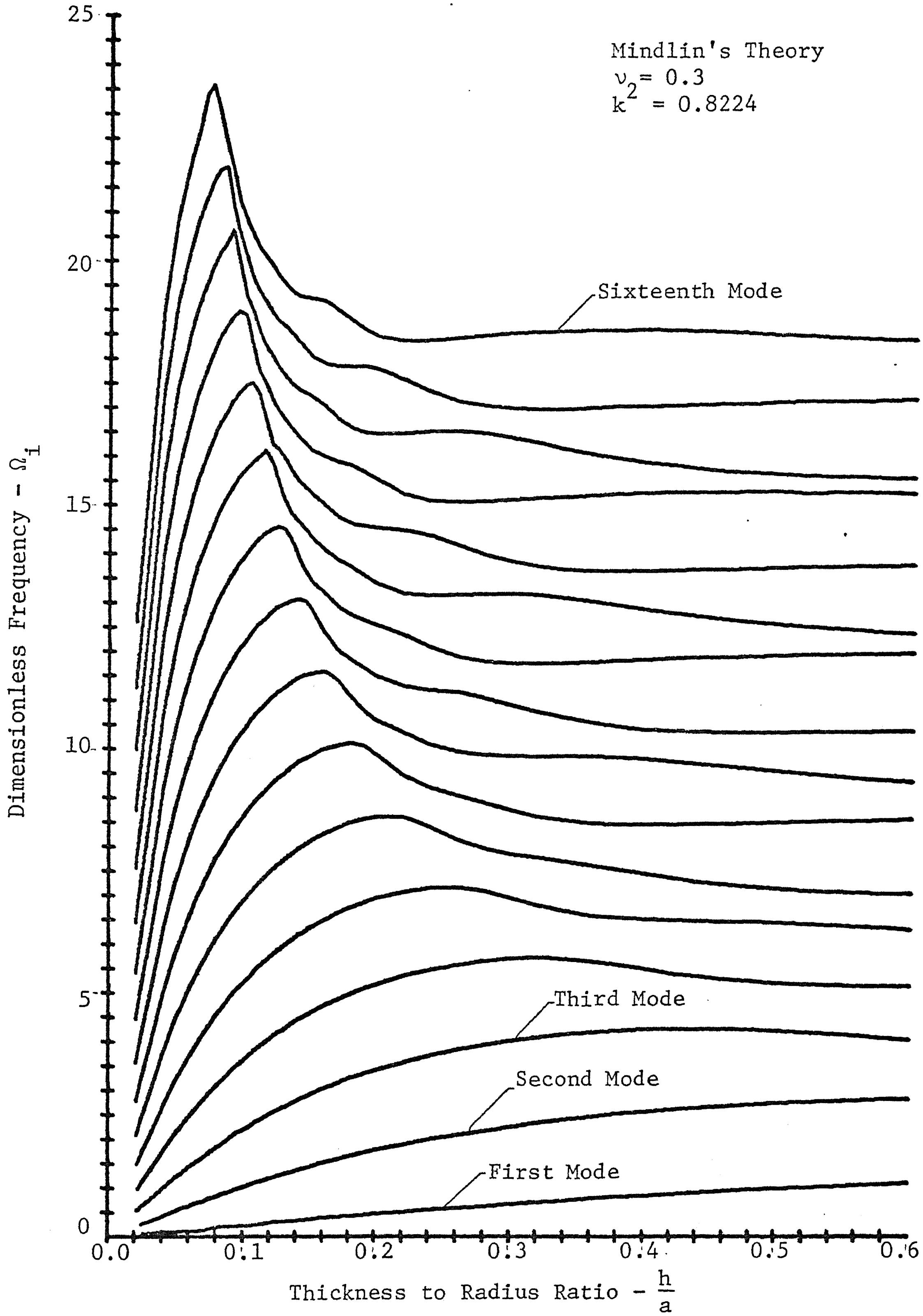

Figure 25 Free Circular Plate Frequency Spectrum

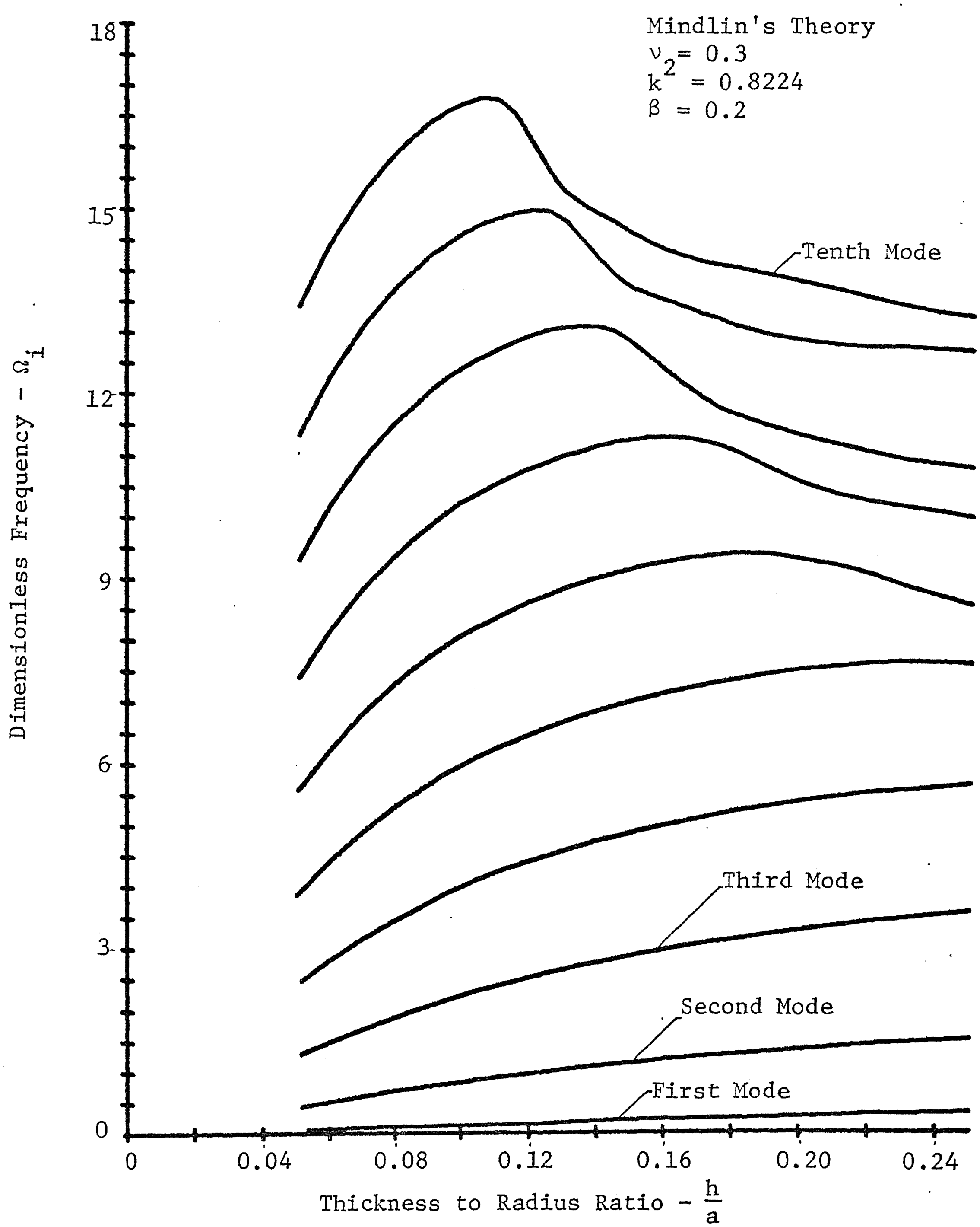

Figure 26 Frequency Spectrum for Disk Mounted on a Shaft

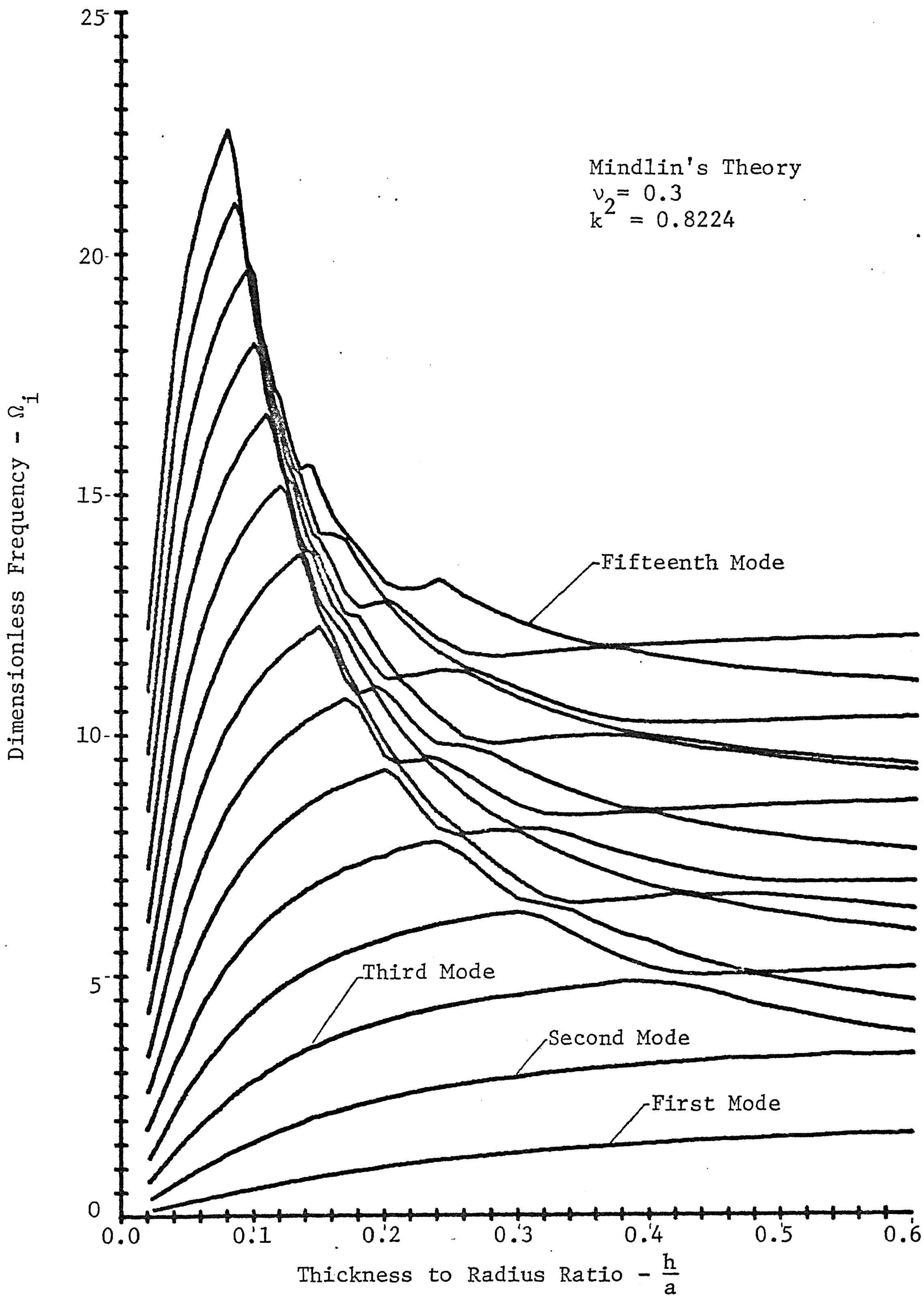

Figure 27 One Diametral Node Frequency Spectrum for Clamped Circular Plate

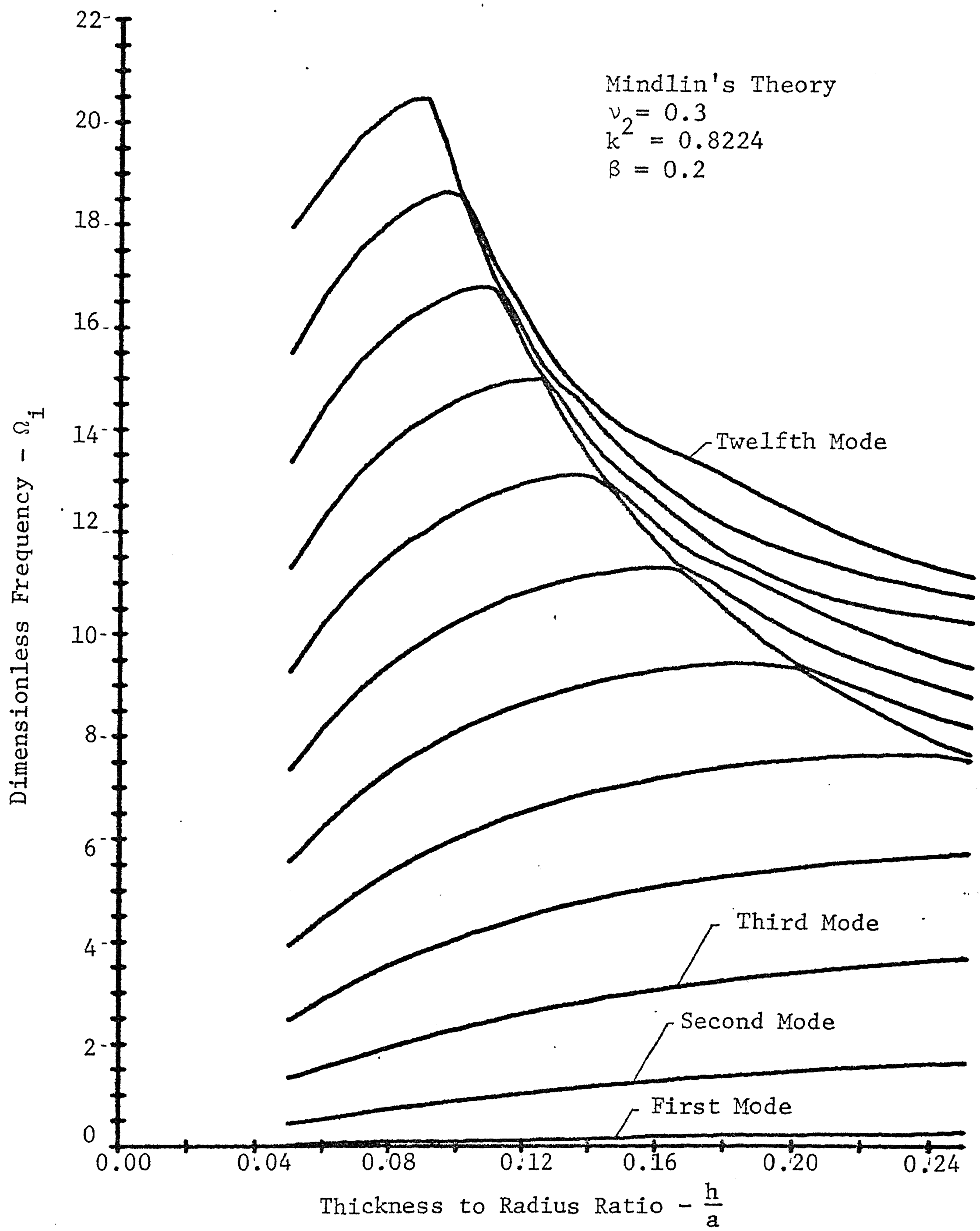

Figure 28 One Diametral Node Frequency Spectrum for Disk Mounted on a Shaft

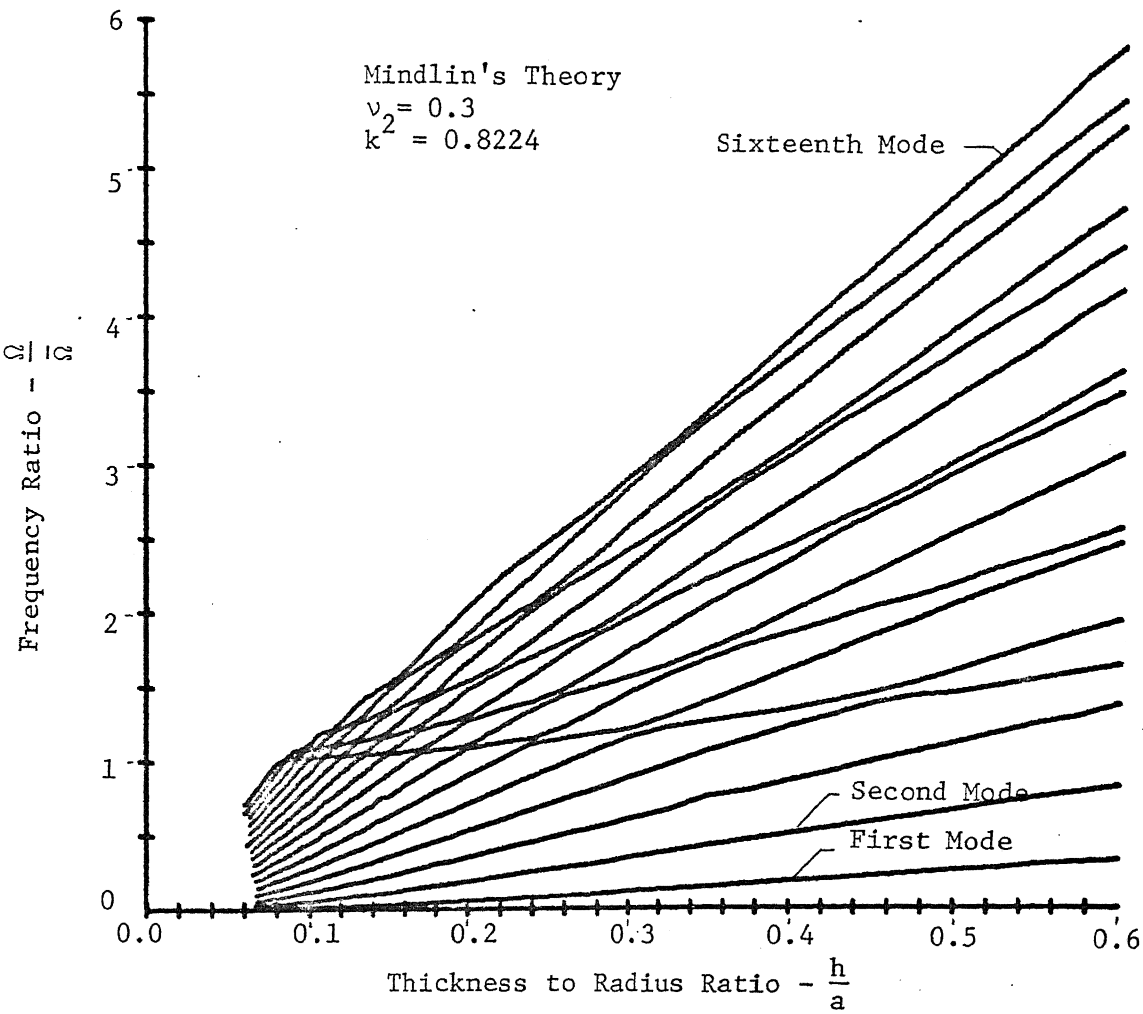

Figure 29 Clamped Circular Plate Frequency Ratio Spectrum

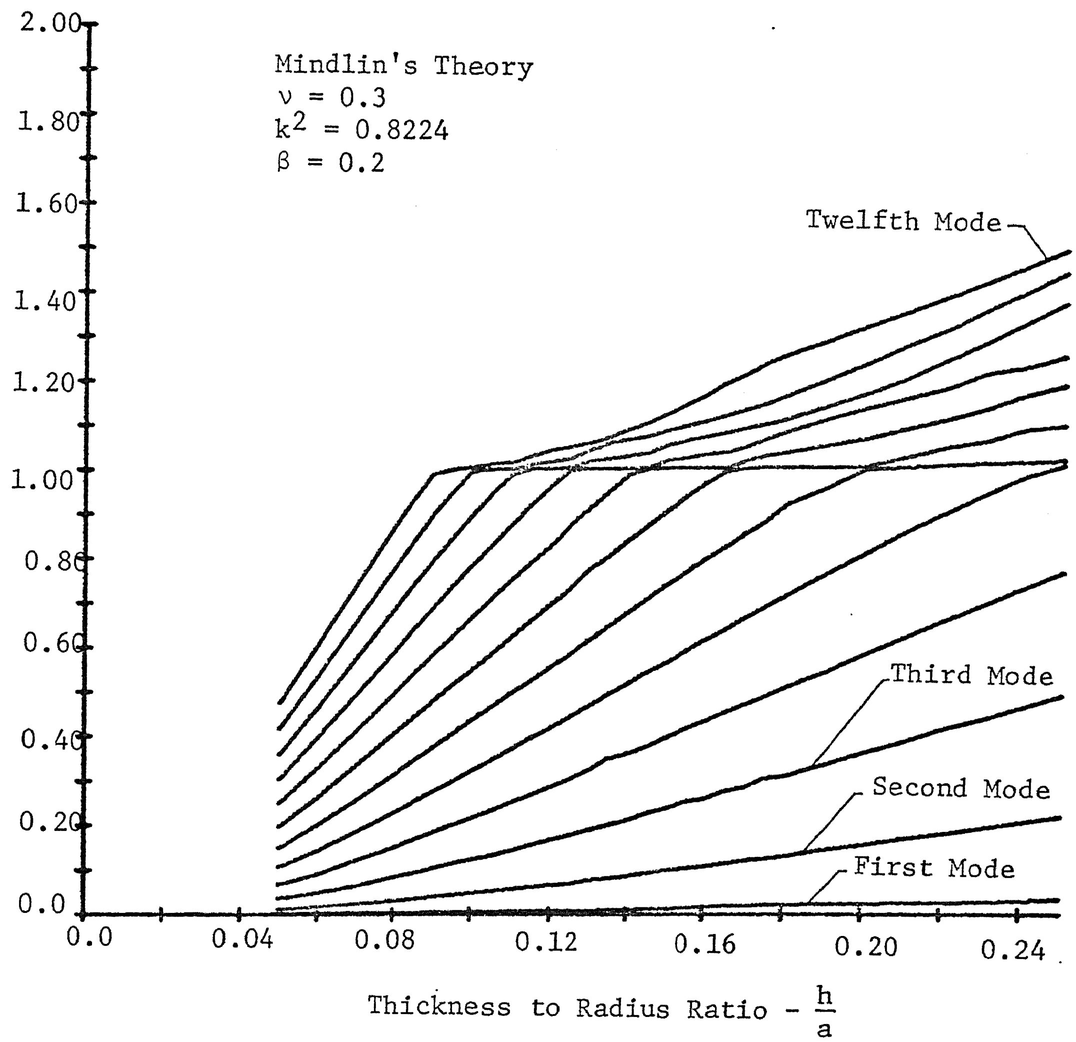

Figure 30 One Diametral Node Frequency Ratio Spectrum for Disk Mounted on a Shaft

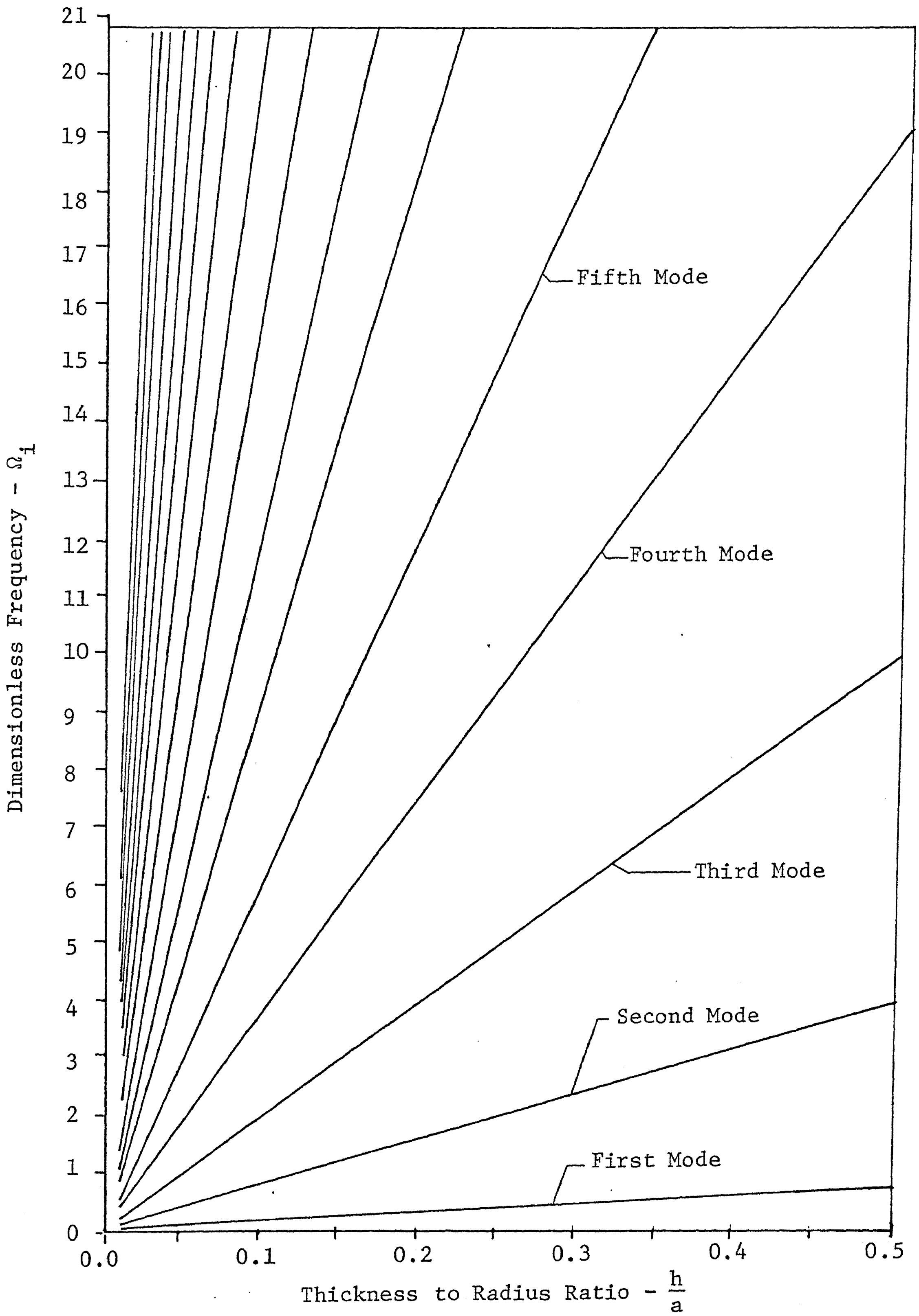

Figure 31 Clamped Circular Plate Frequency Spectrum, Classical Theory

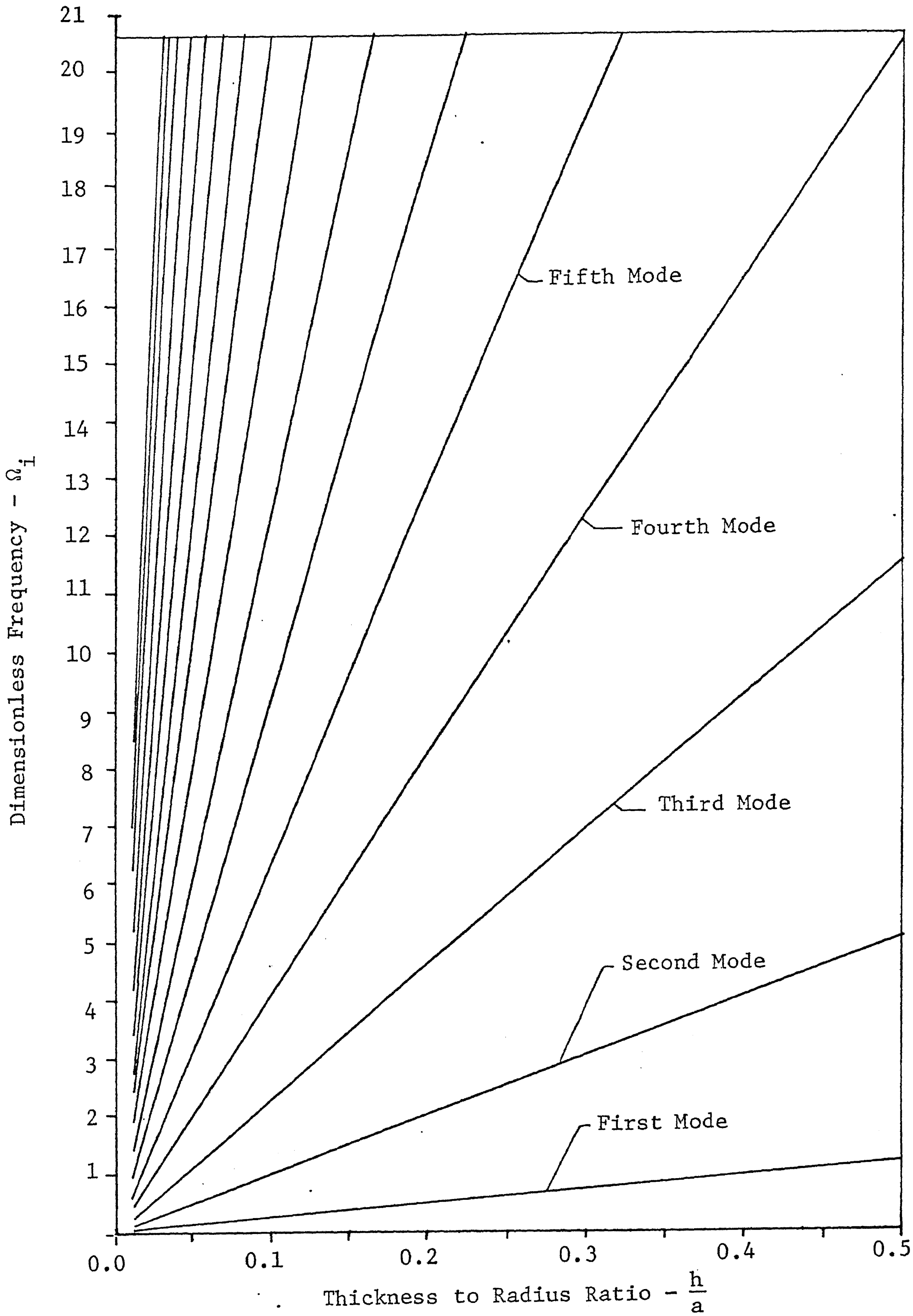

Figure 32 Simply Supported Circular Plate Frequency Spectrum, Classical Theory

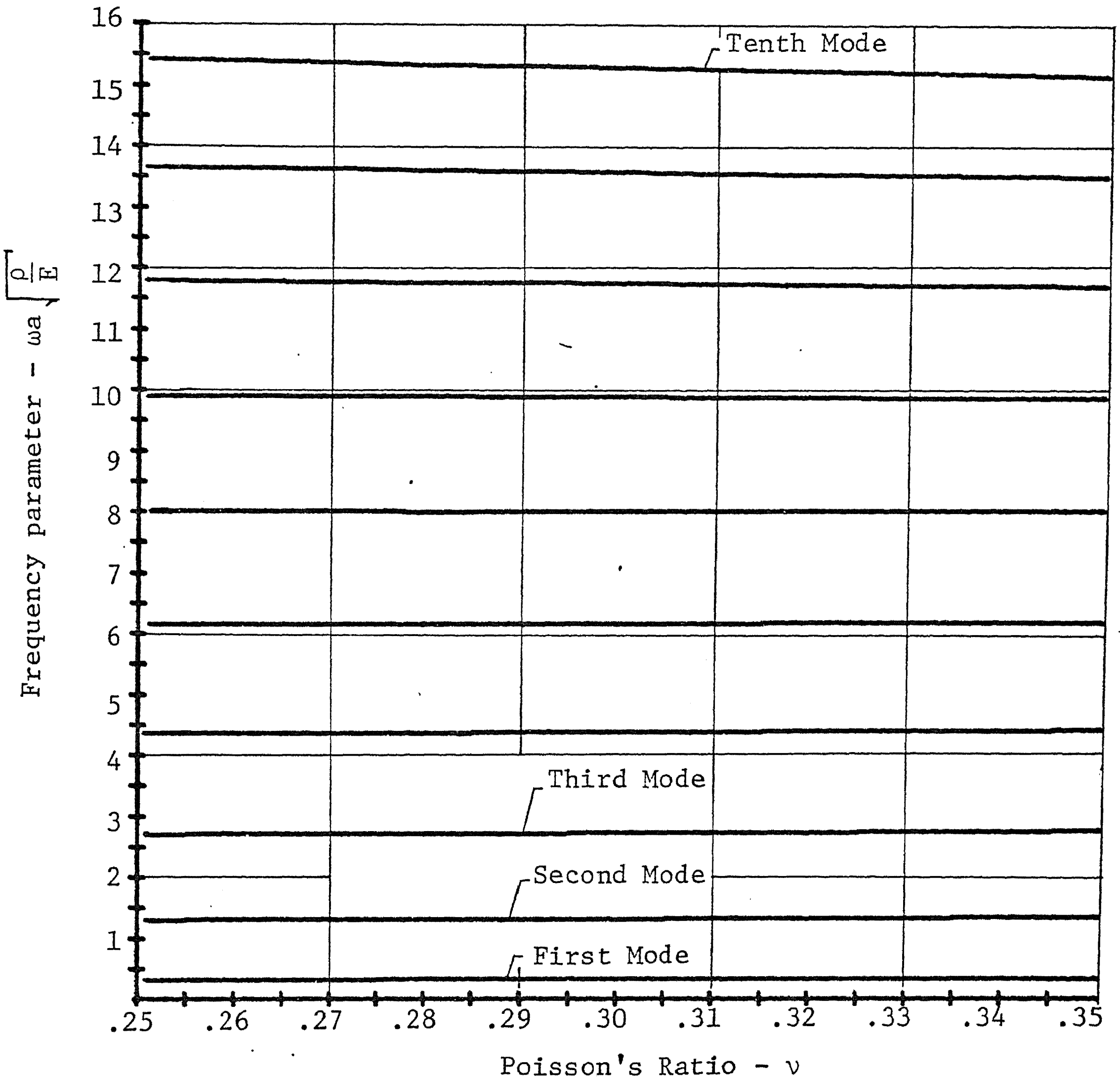

Figure 33 Frequency versus Poisson's Ratio, Free Circular Plate, $\frac{h}{a}$ = .125

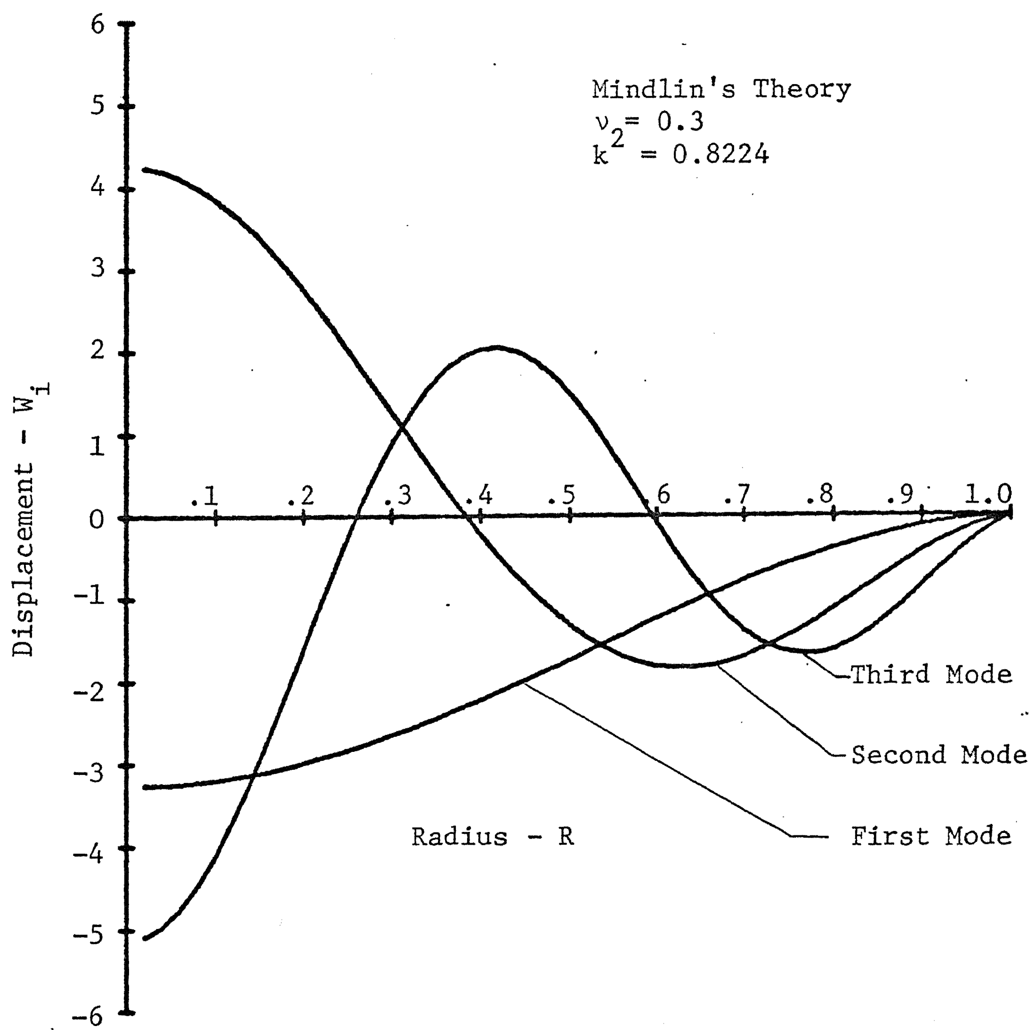

Figure 34 First Three W Mode Shapes for a Clamped Circular Plate

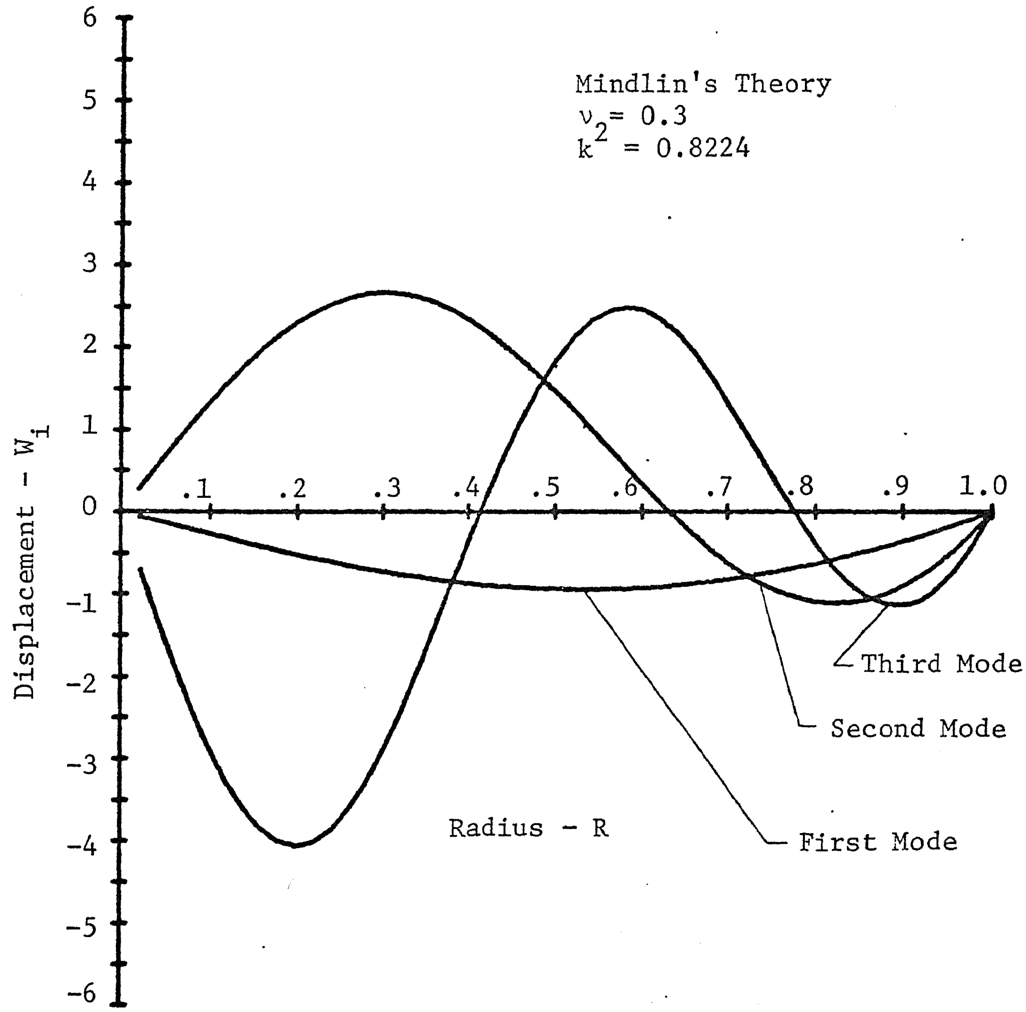

Figure 35 First Three W Mode Shapes for a Simply Supported Circular Plate

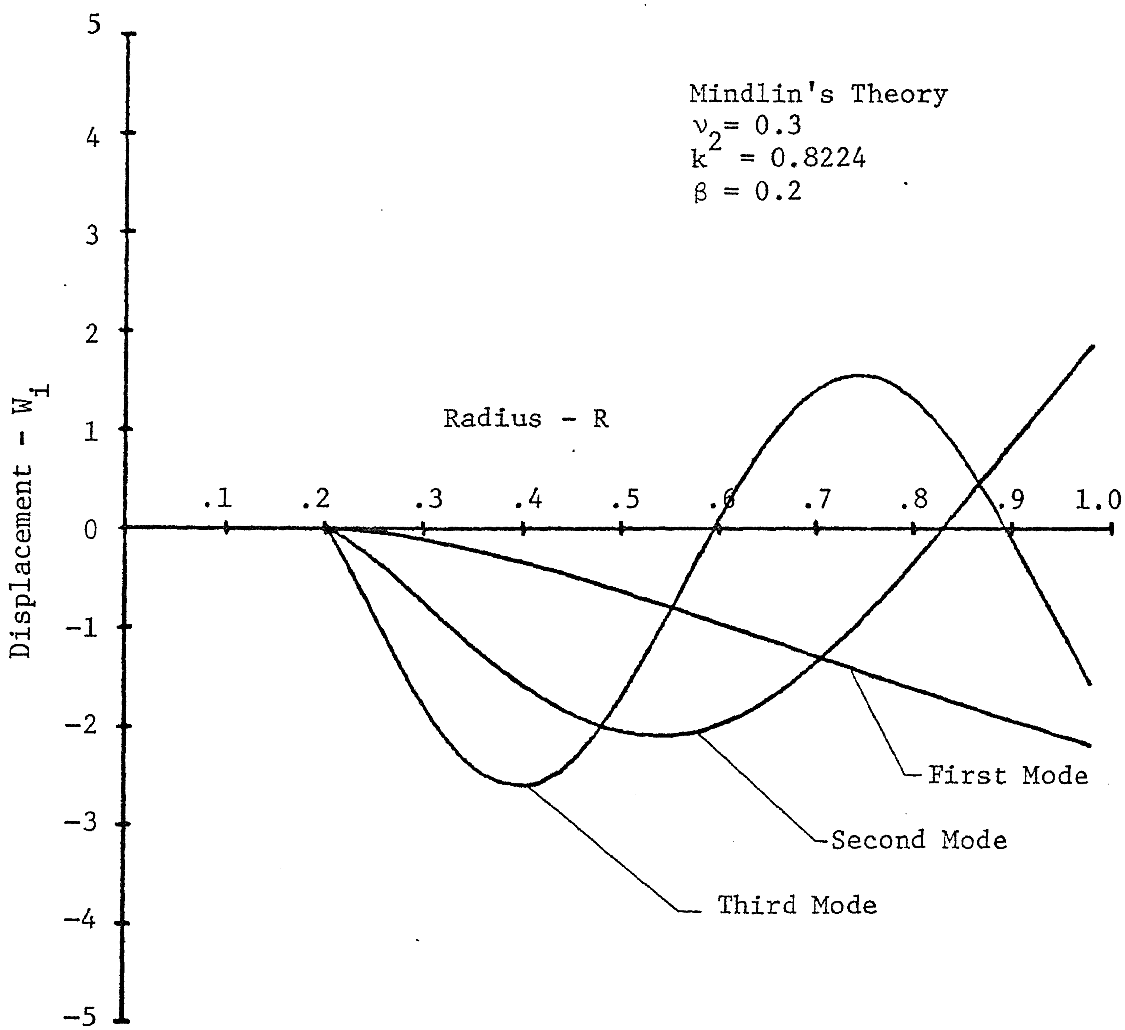

Figure 36 First Three W Mode Shapes for a Disk Mounted on a Shaft

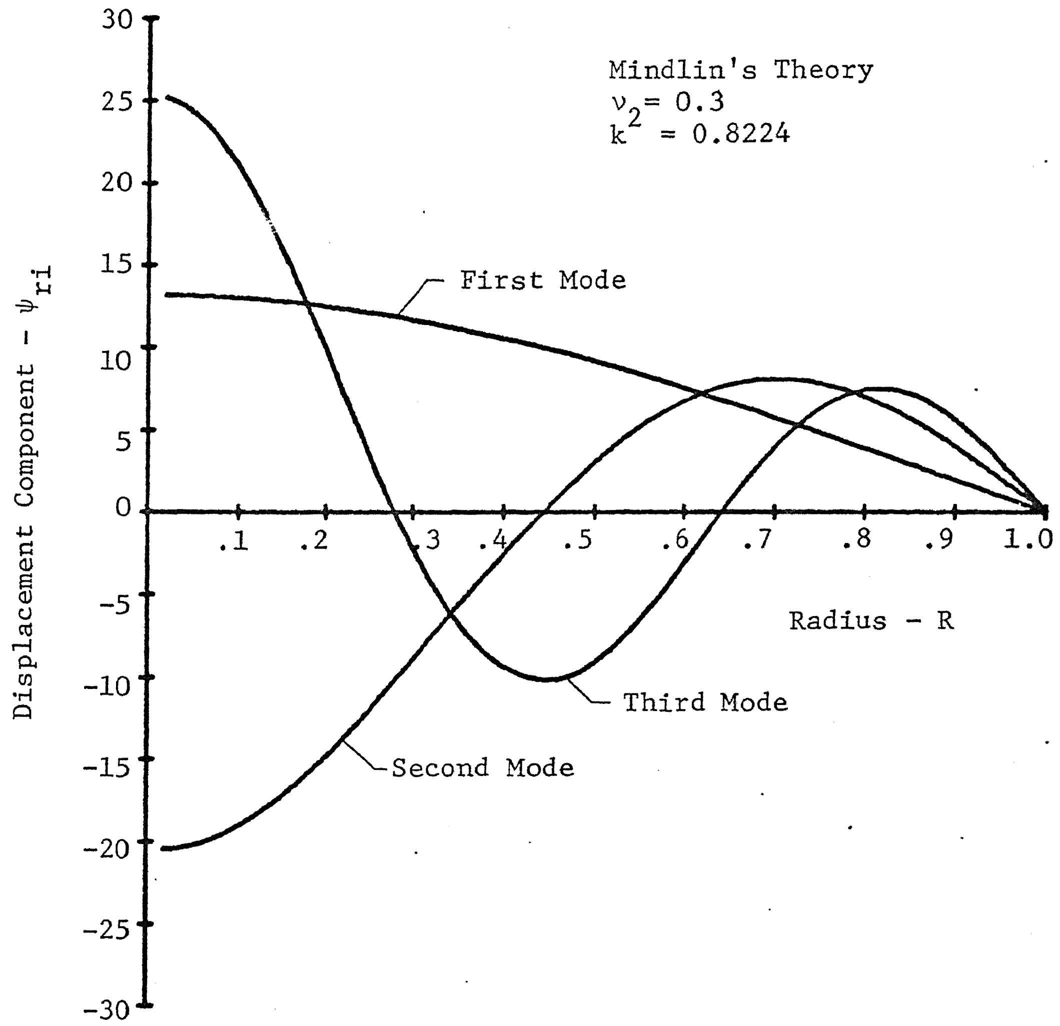

Figure 37 First Three ψ_r Mode Shapes for a Clamped Circular Plate

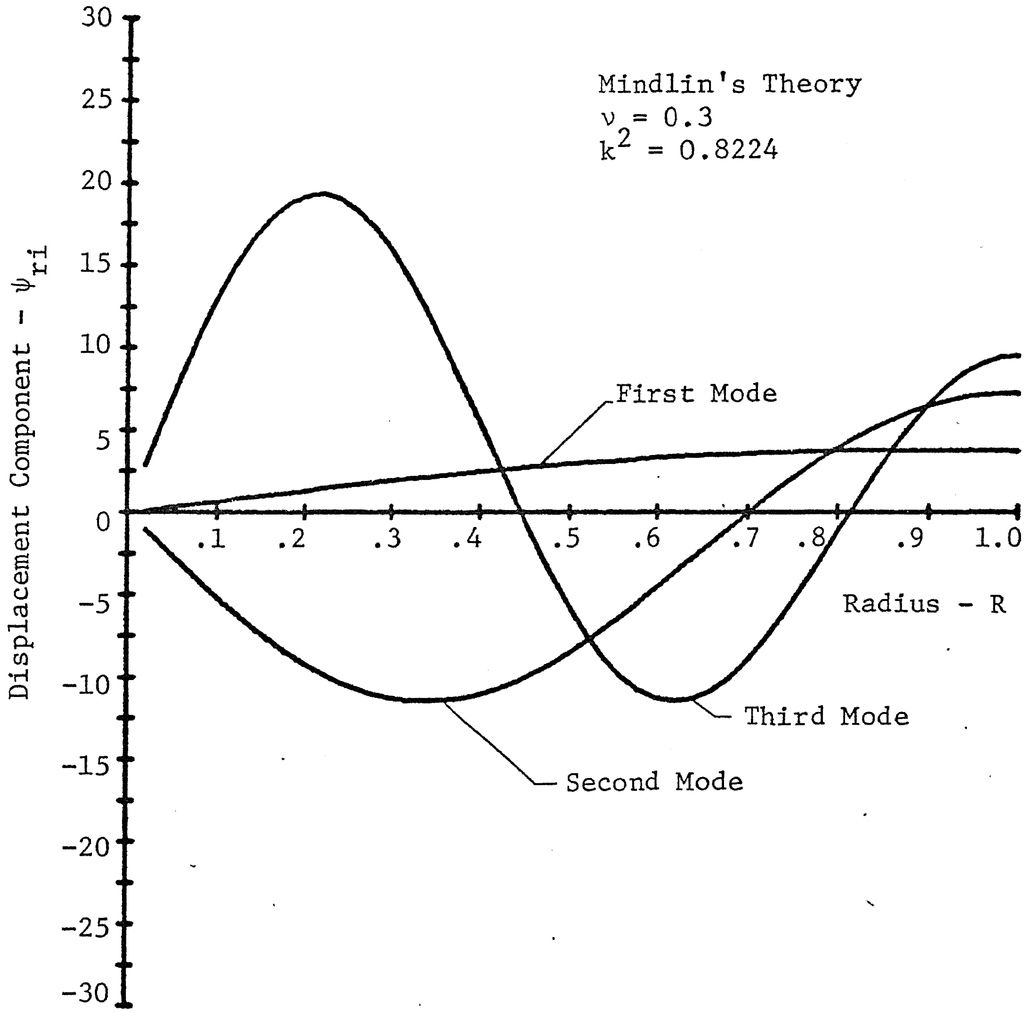

Figure 38 First Three ψ_r Mode Shapes for a Simply Supported Circular Plate

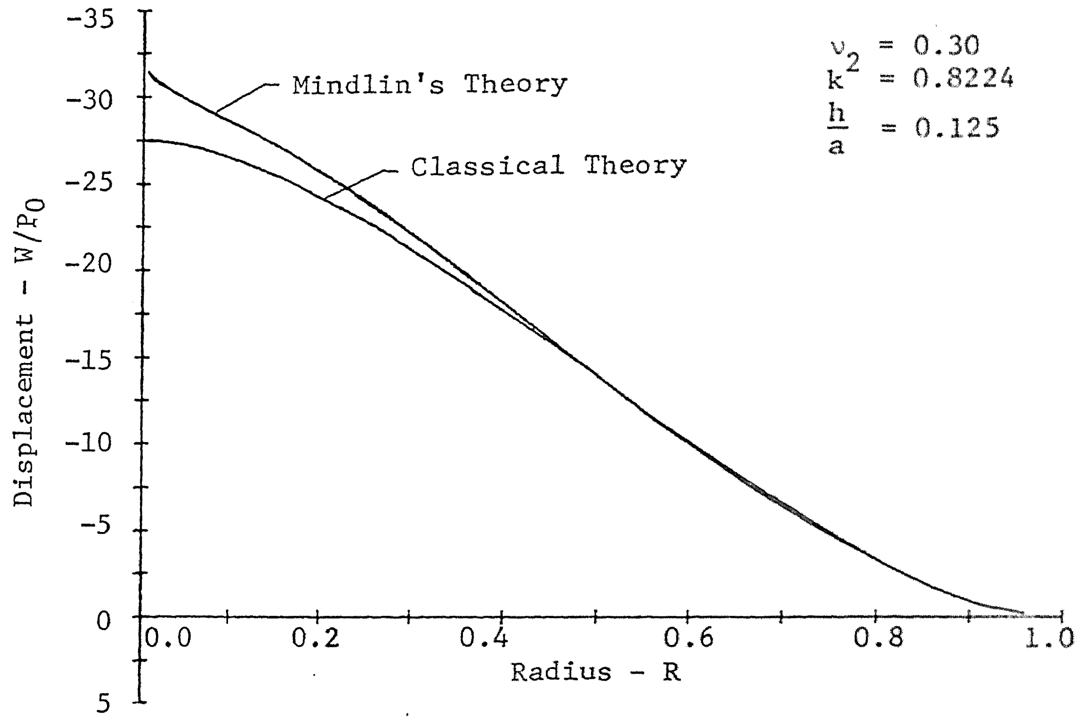

Figure 39 Plate Profile at Maximum Deflection, Case 3 - Section VIII.C

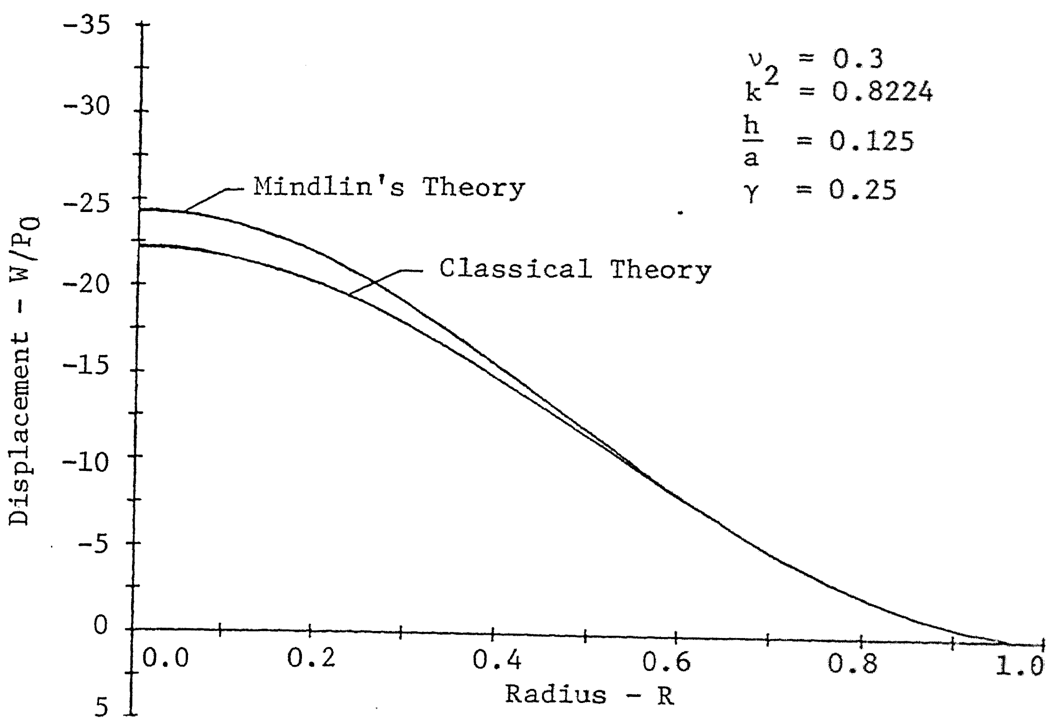

Figure 40 Plate Profile at Maximum Deflection, Case 2 - Section VIII.C

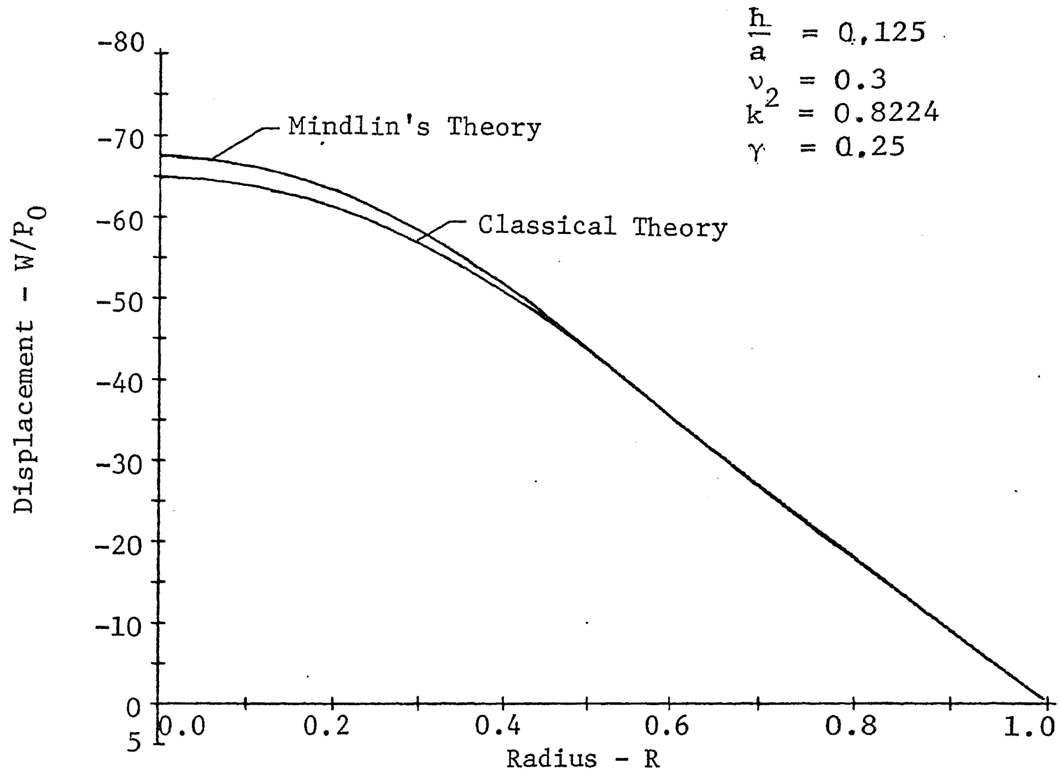

Figure 41 Plate Profile at Maximum Deflection, Case 5 - Section VIII.C

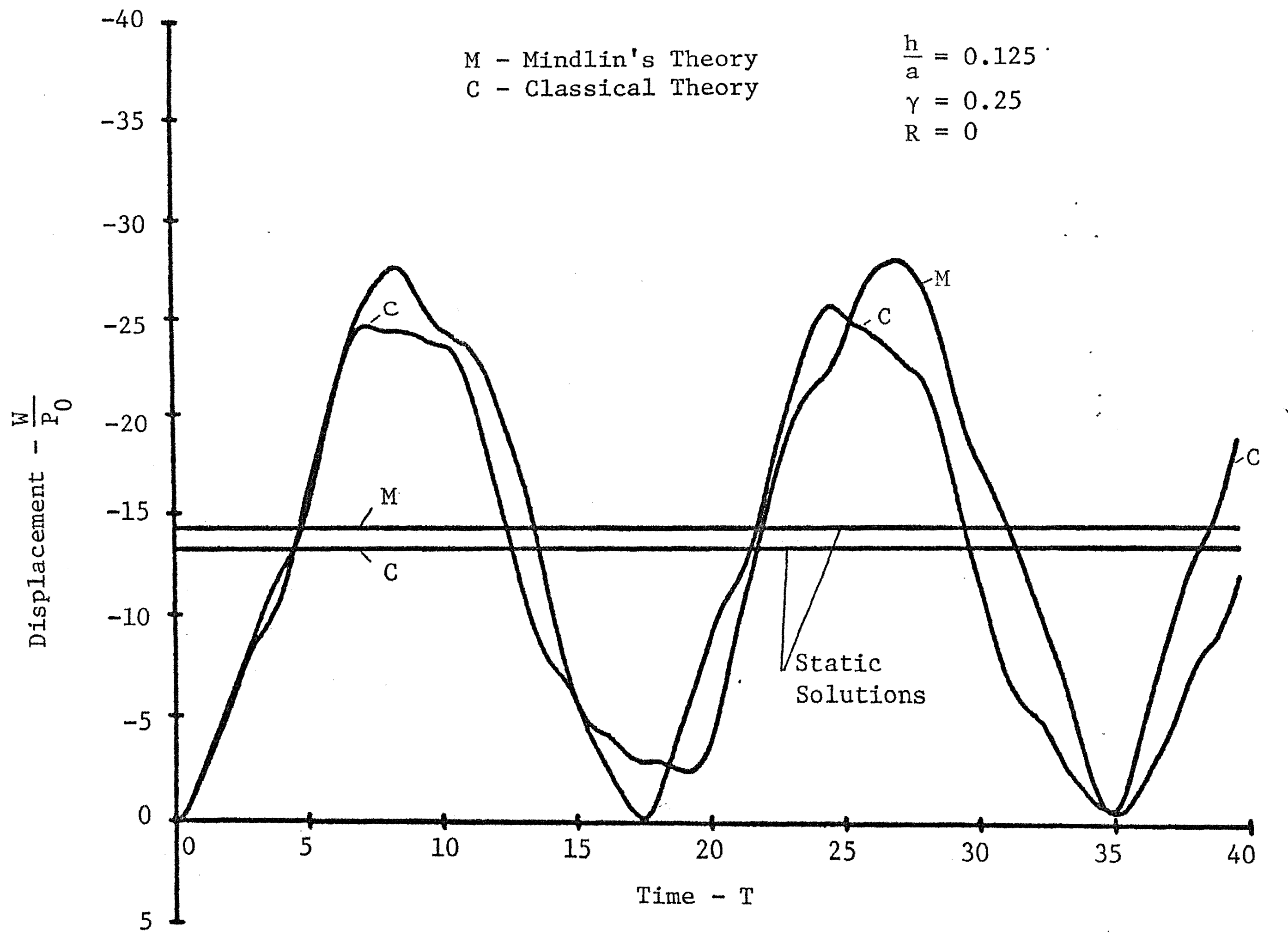

Figure 42 Deflection at Center versus Time, Case 1 - Section VIII.C

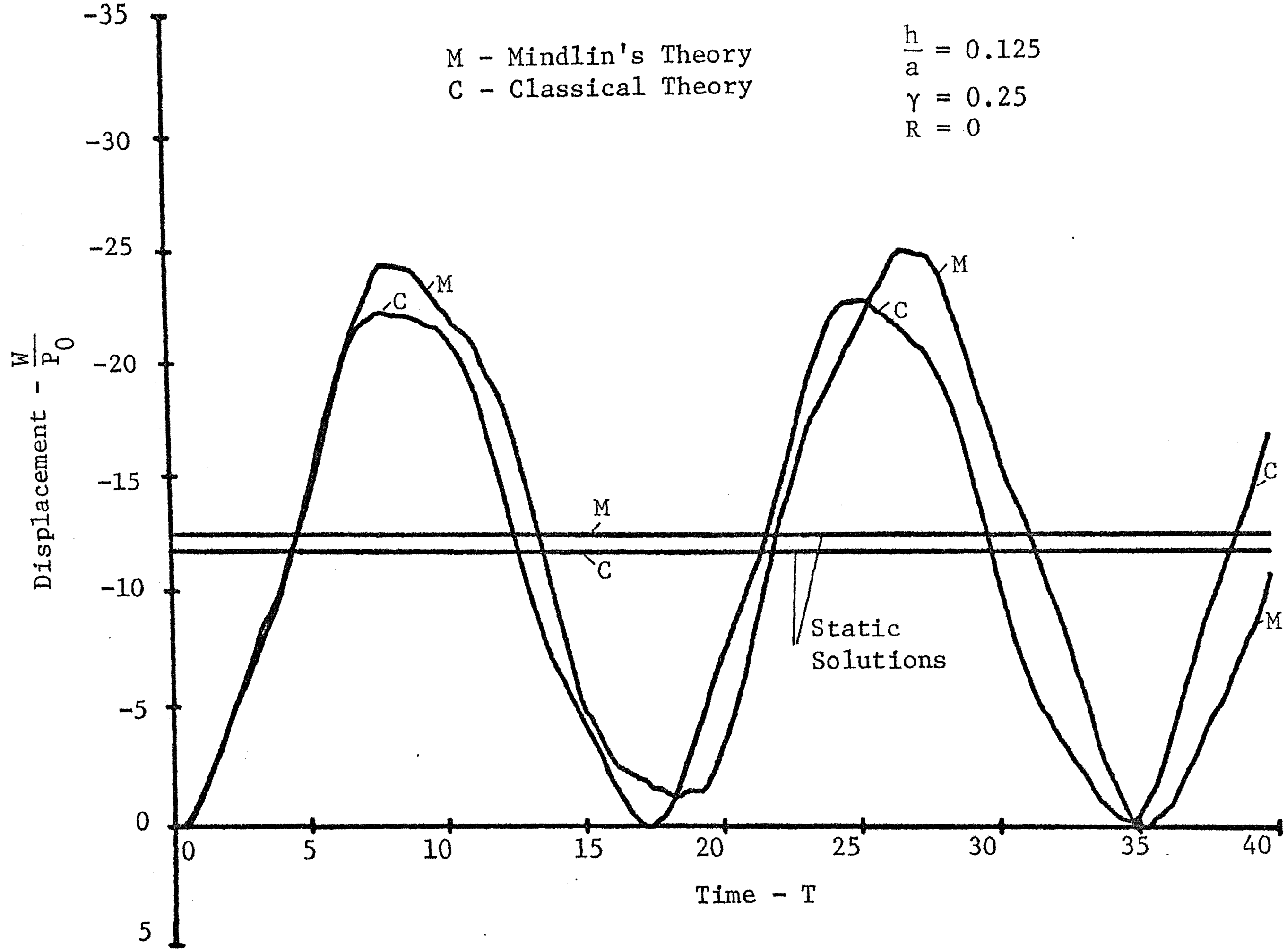

Figure 43 Deflection at Center versus Time, Case 2 - Section VIII.C

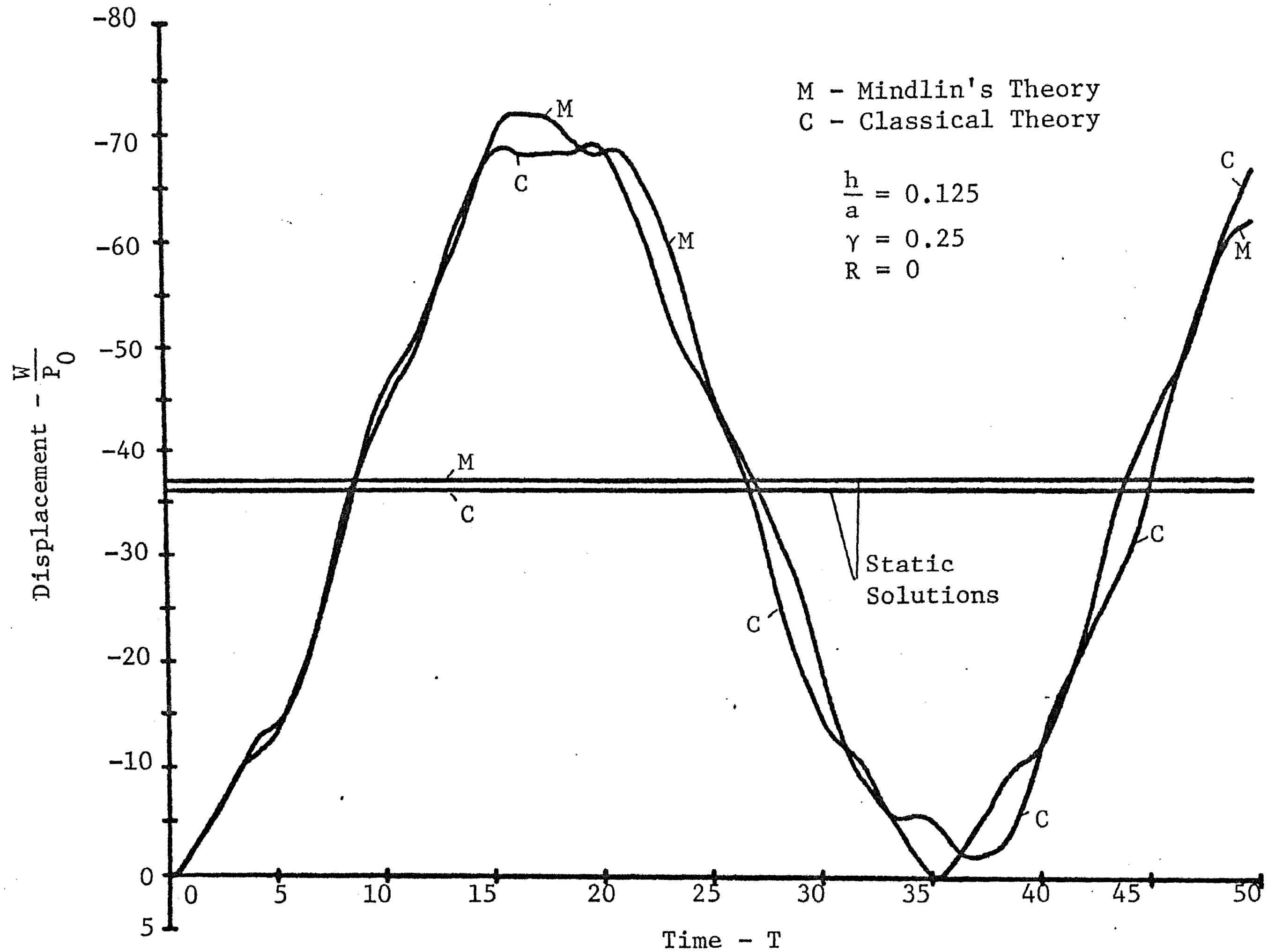

Figure 44 Deflection at Center versus Time, Case 4 - Section VIII.C

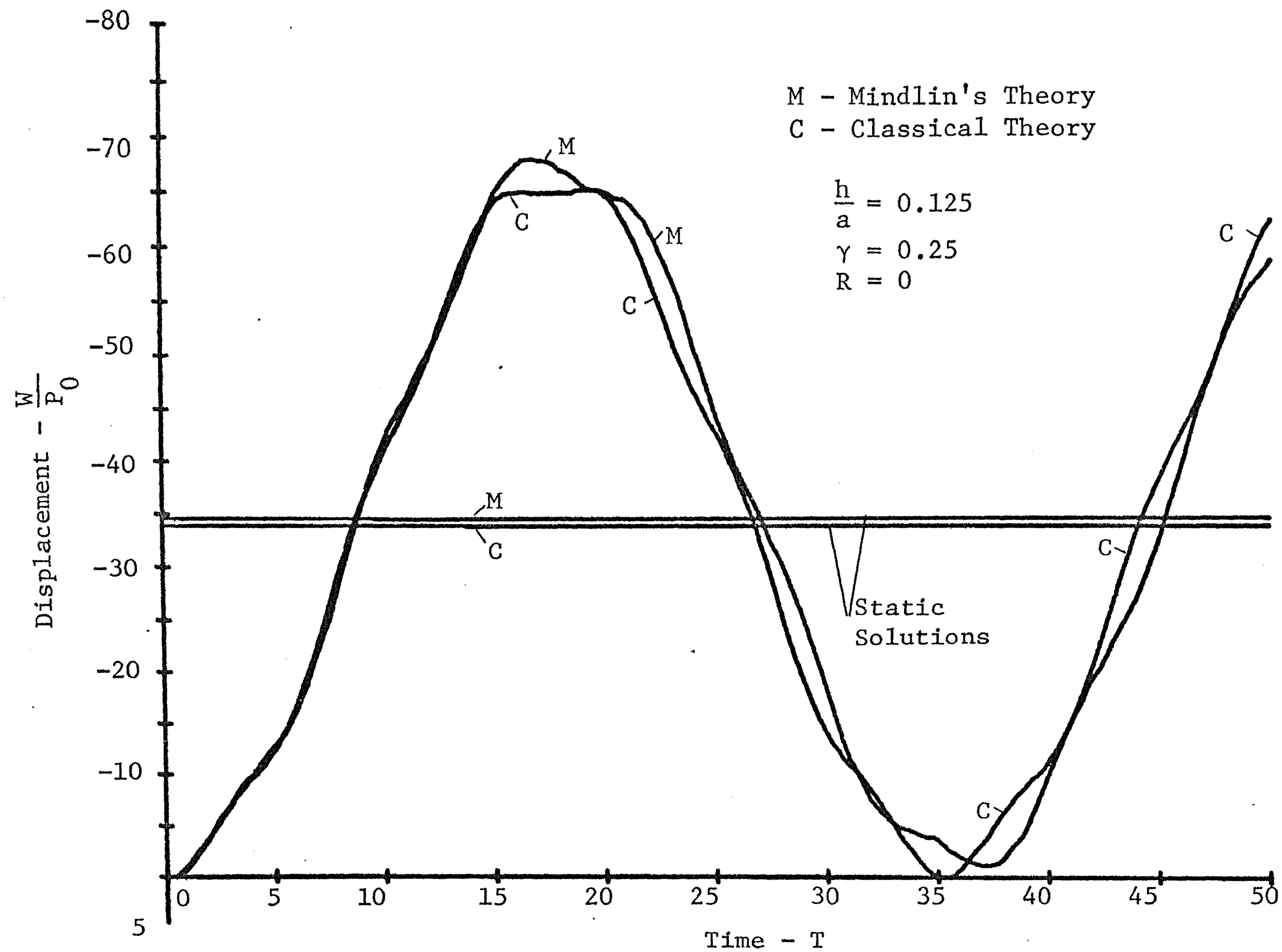

Figure 45 Deflection at Center versus Time, Case 5 - Section VIII.C

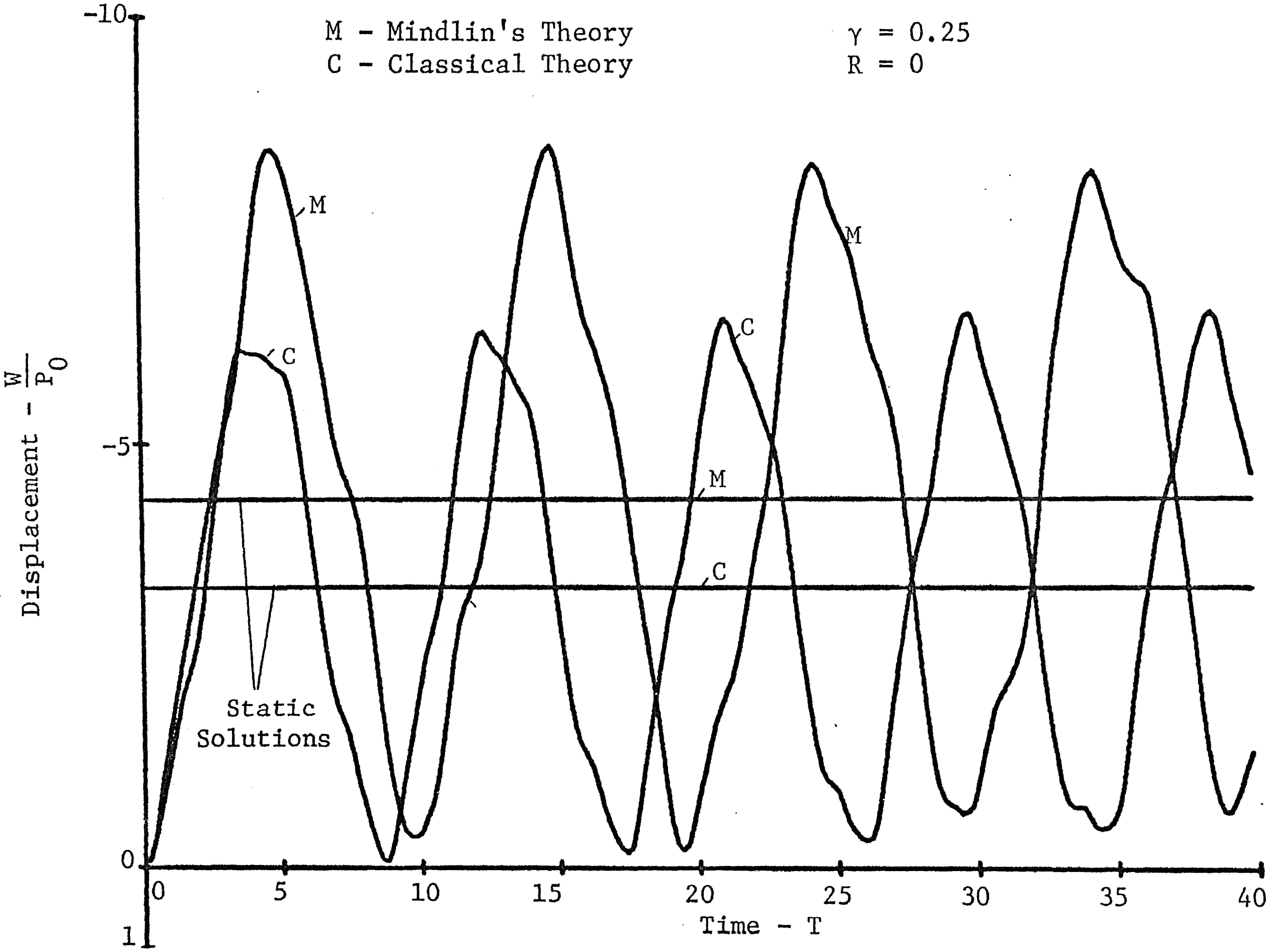

Figure 46 Deflection at Center versus Time, Case 1 - Section VIII.C, $\frac{h}{a} = 0.25$

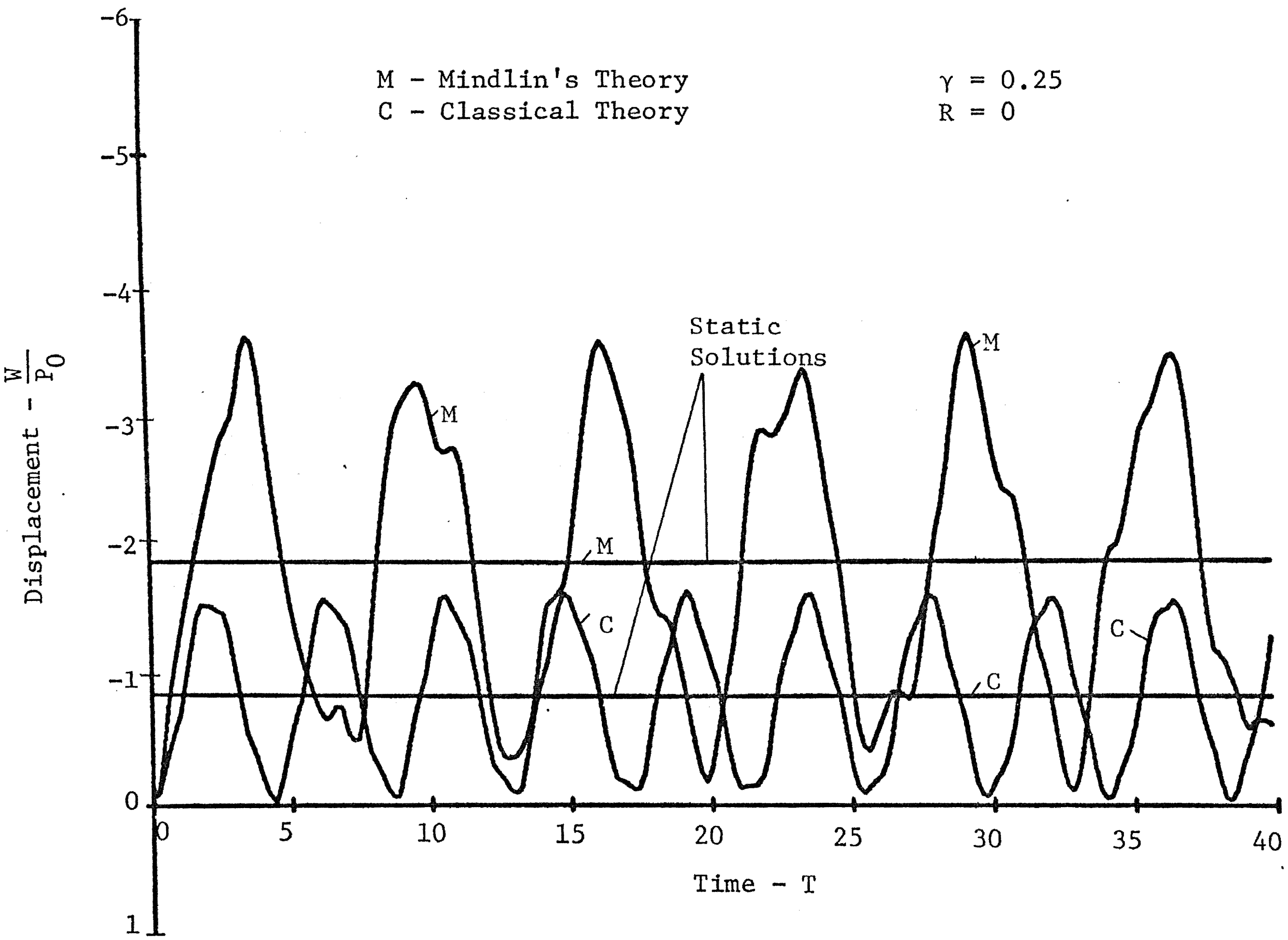

Figure 47 Deflection at Center versus Time, Case 1 - Section VIII.C, $\frac{h}{a} = 0.5$

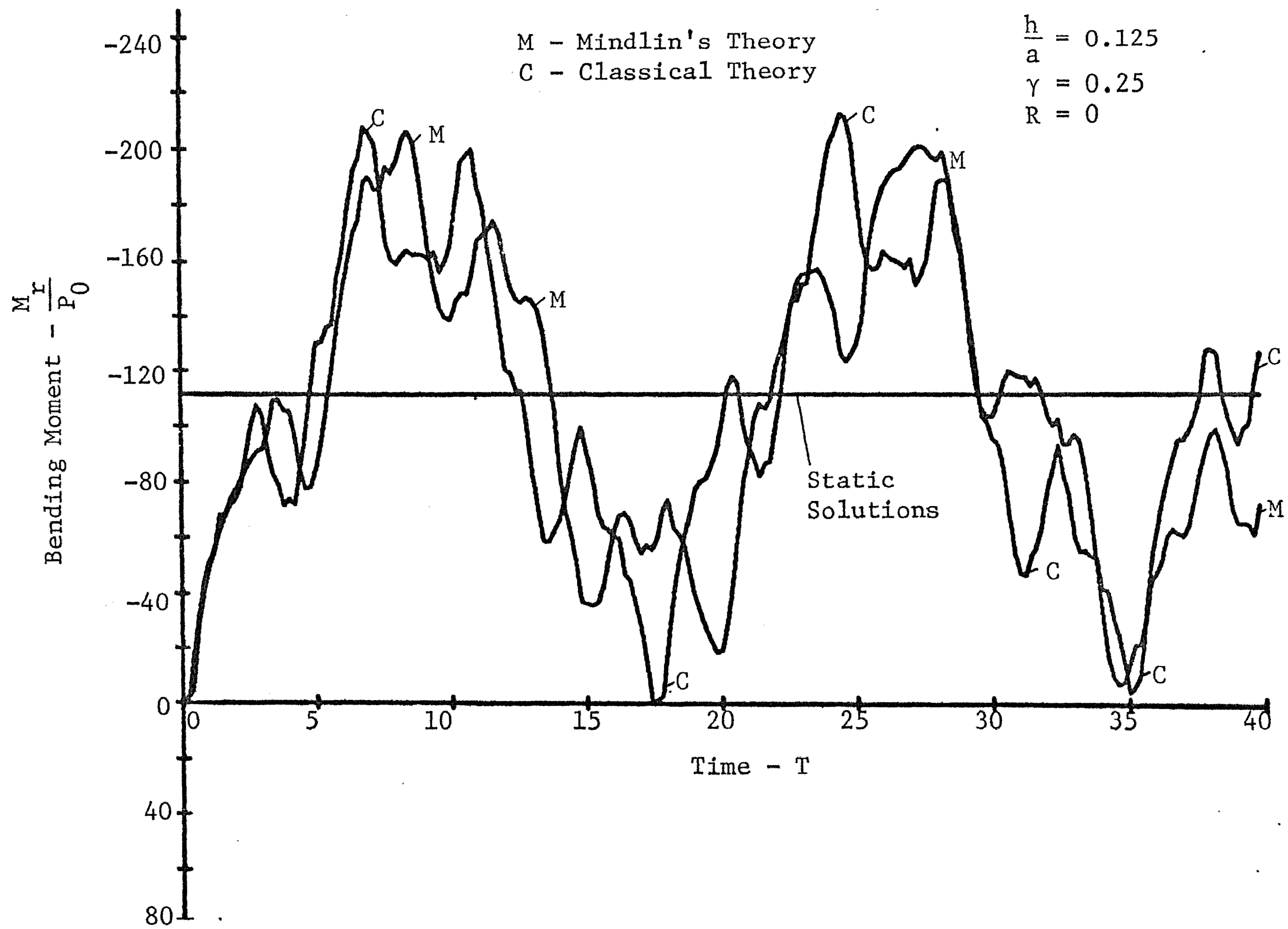

Figure 48 Bending Moment at Center versus Time, Case 1 - Section VIII.C

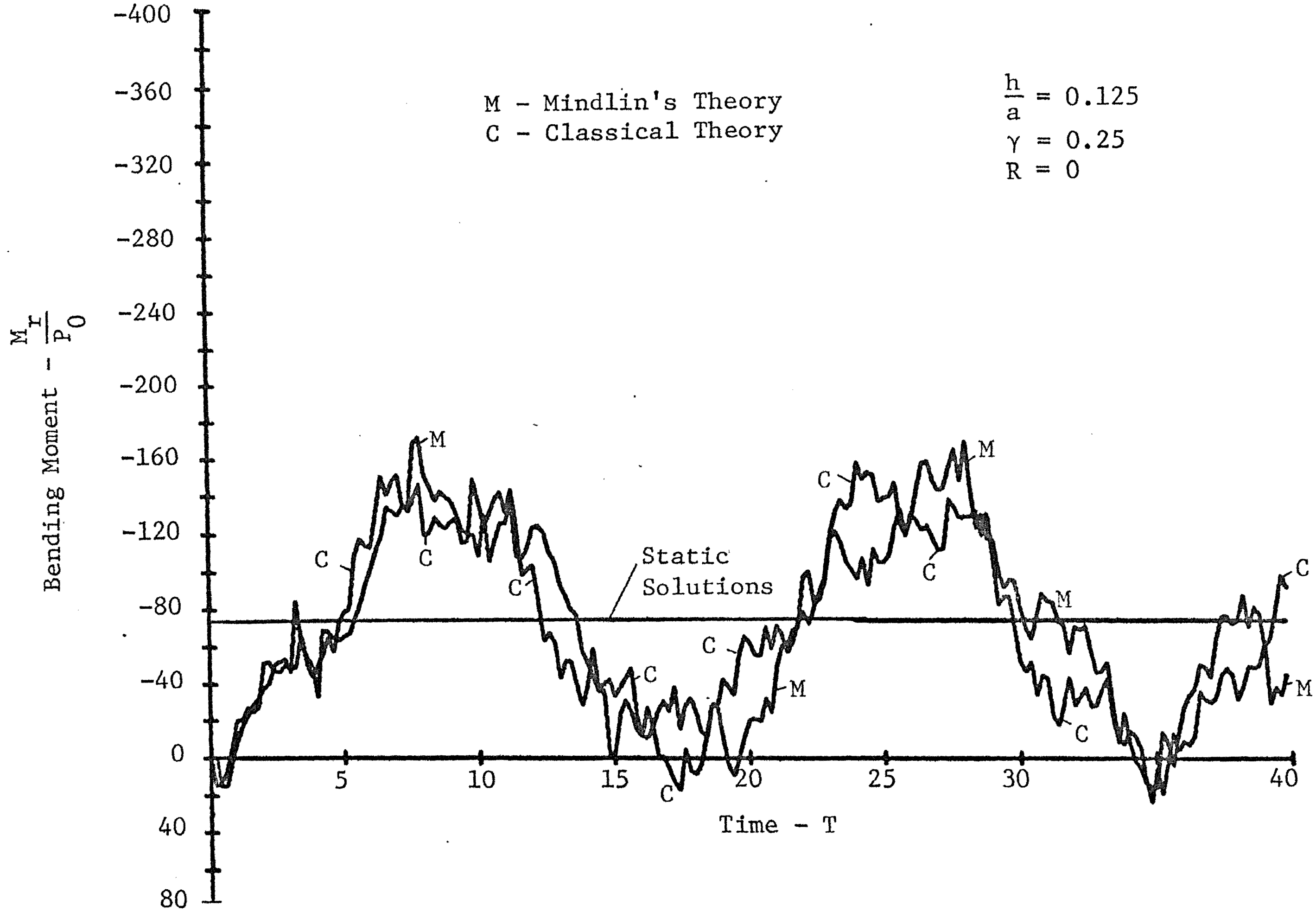

Figure 49 Bending Moment at Center versus Time, Case 2 - Section VIII.C

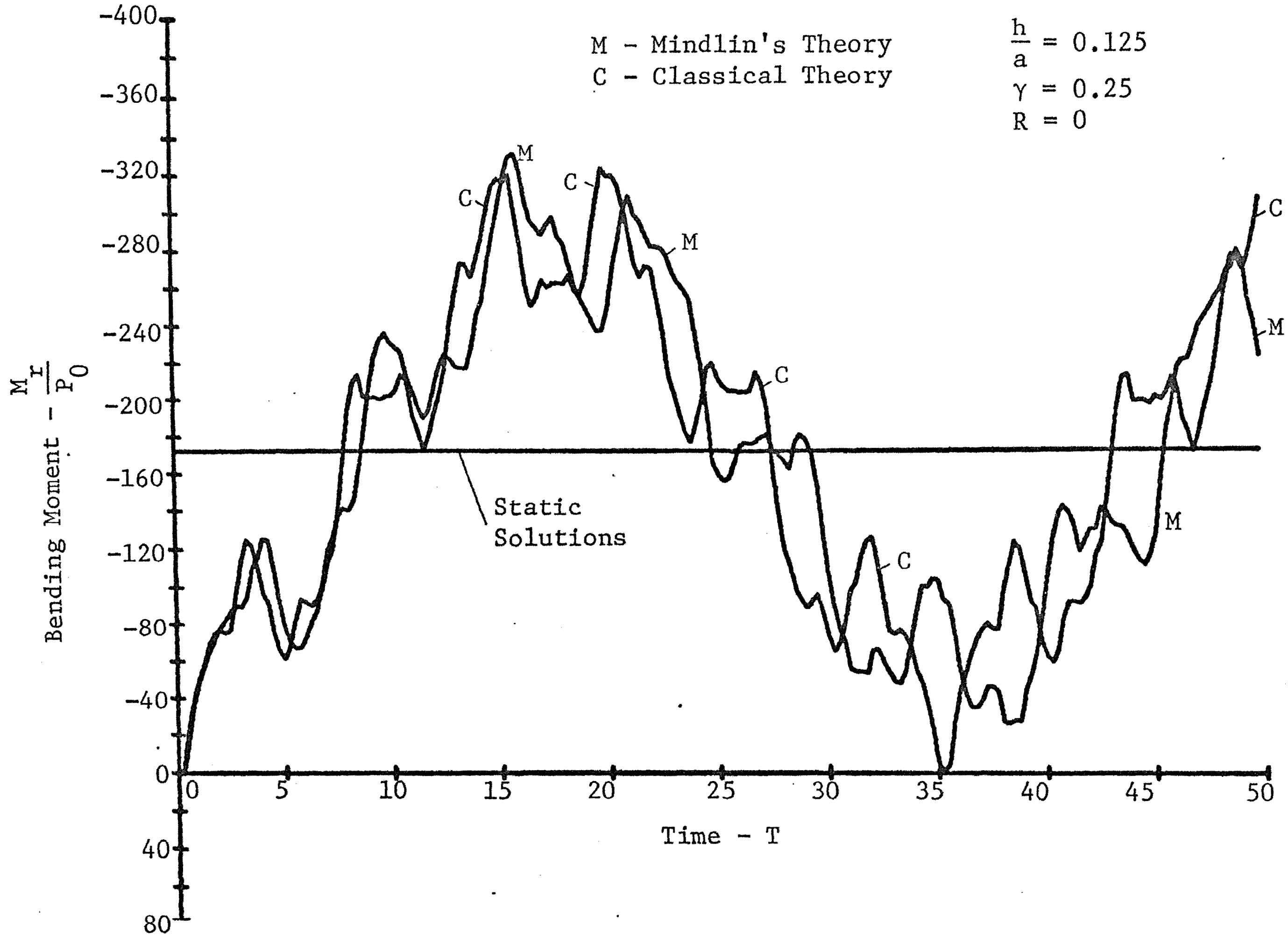

Figure 50 Bending Moment at Center versus Time, Case 4 - Section VIII.C

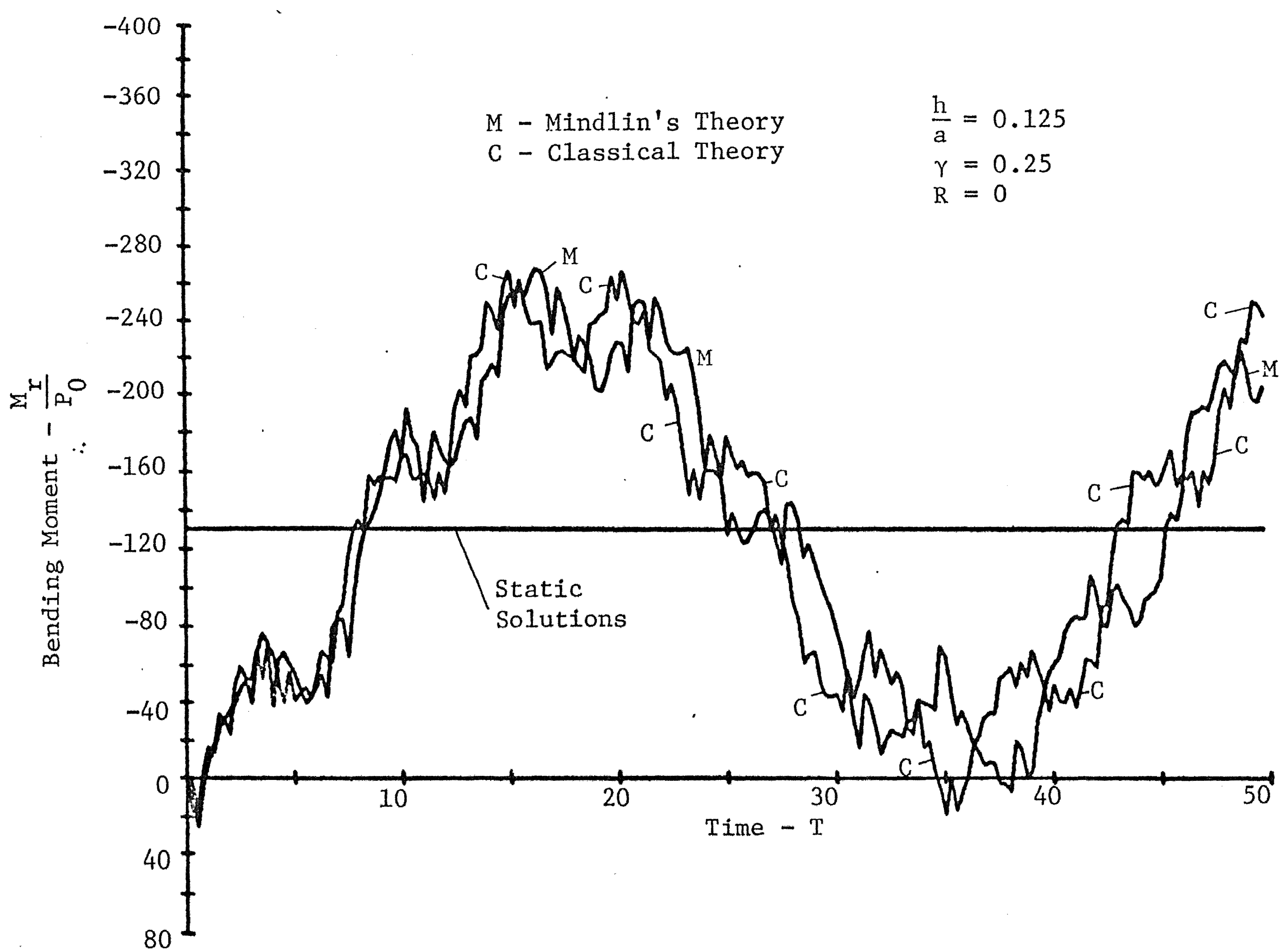

Figure 51 Bending Moment at Center versus Time, Case 5 - Section VIII.C

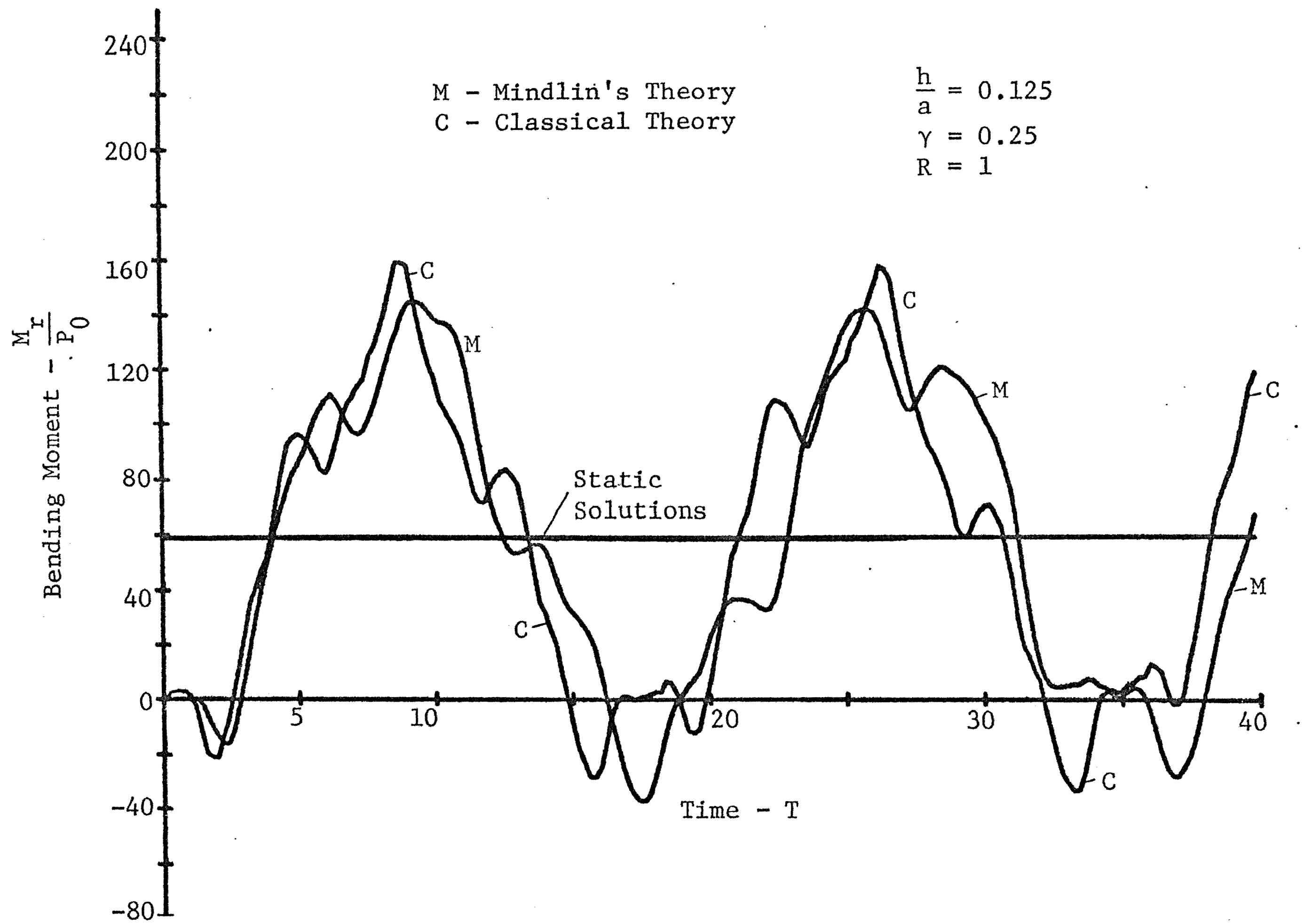

Figure 52 Bending Moment at Edge versus Time, Case 1 - Section VIII.C

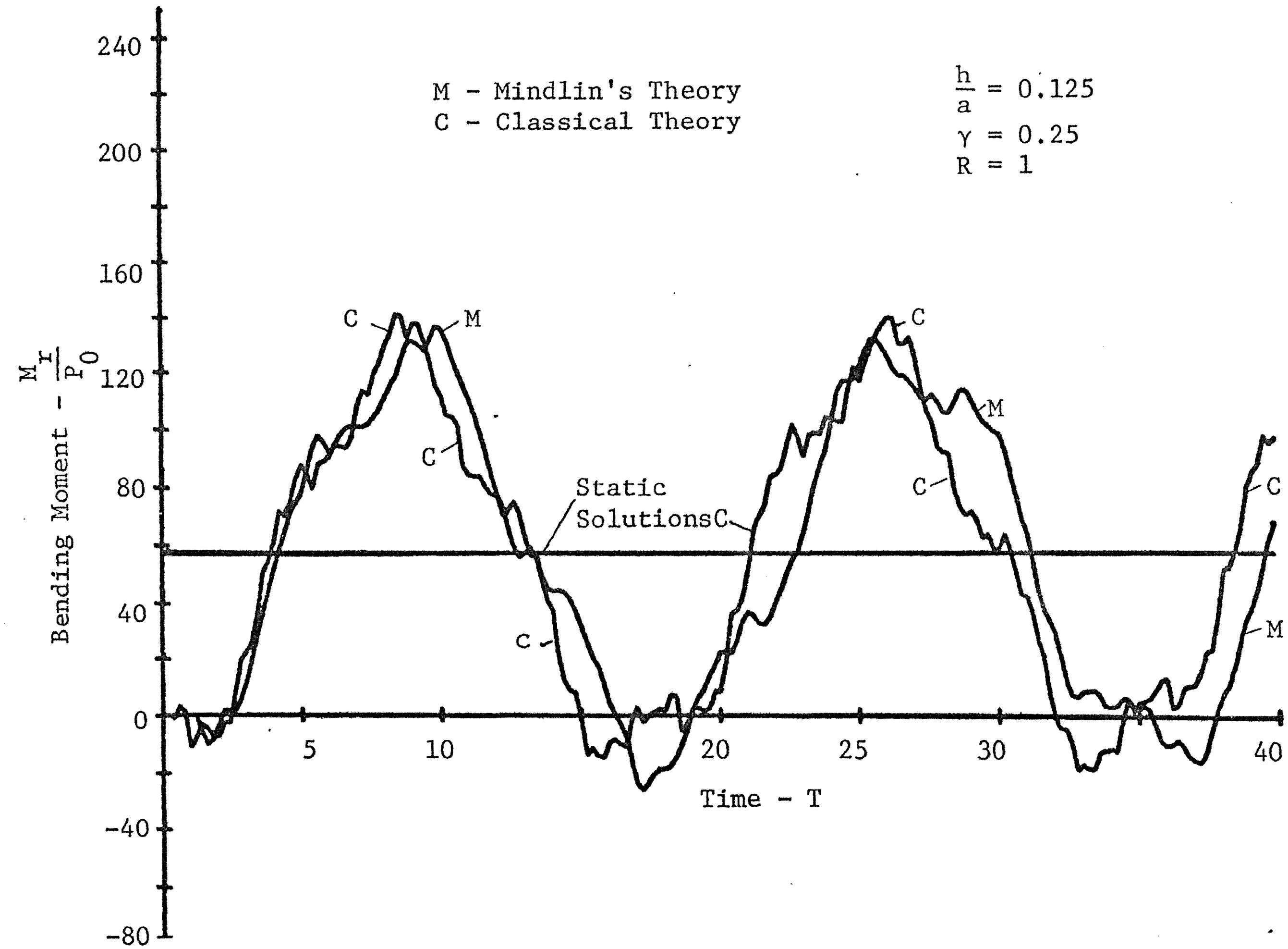

Figure 53 Bending Moment at Edge versus Time, Case 2 - Section VIII.C

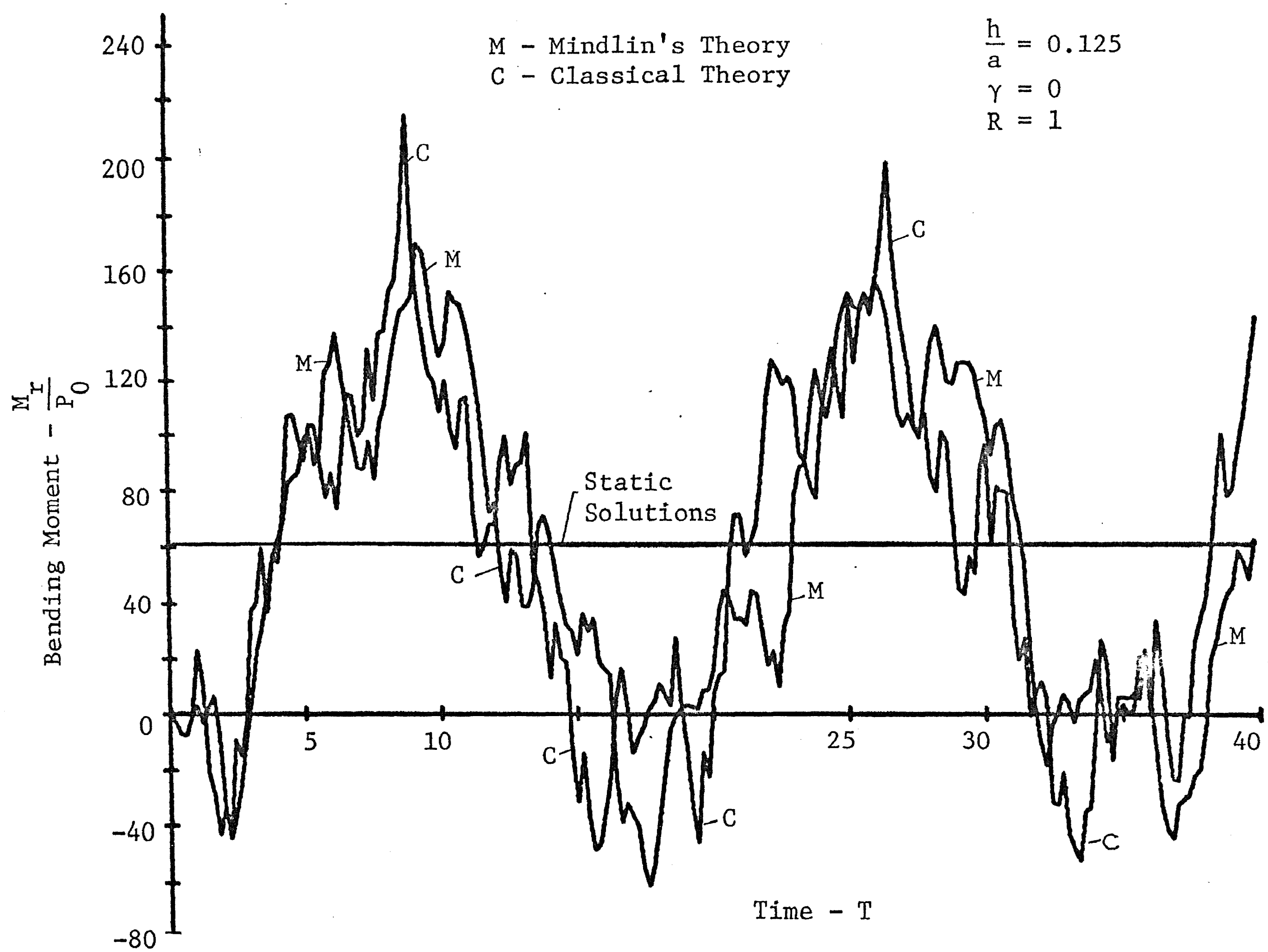

Figure 54 Bending Moment at Edge versus Time, Case 3 - Section VIII.C

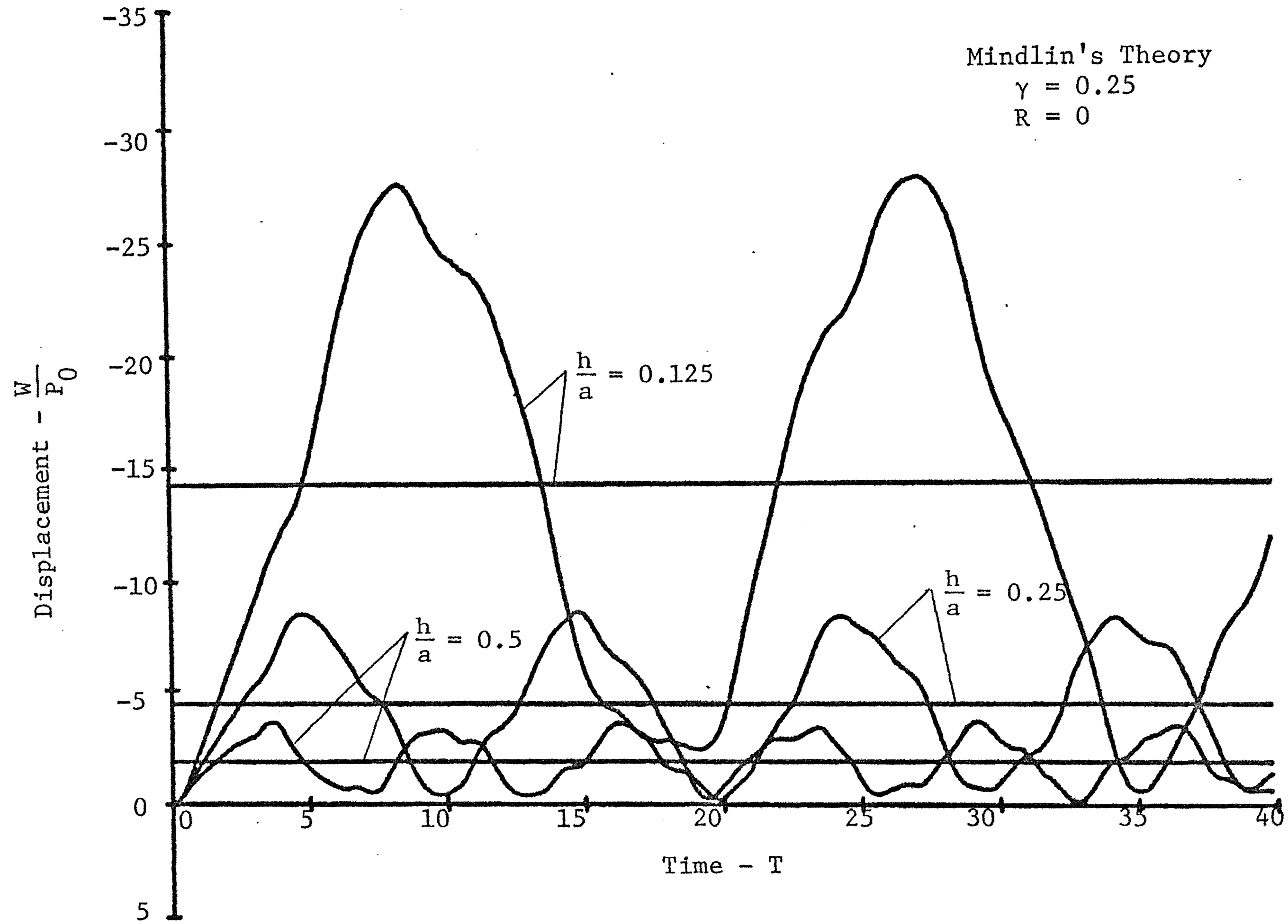

Figure 55 Effect of $\frac{h}{a}$ on Deflection at Center, Case 1 - Section VIII.C

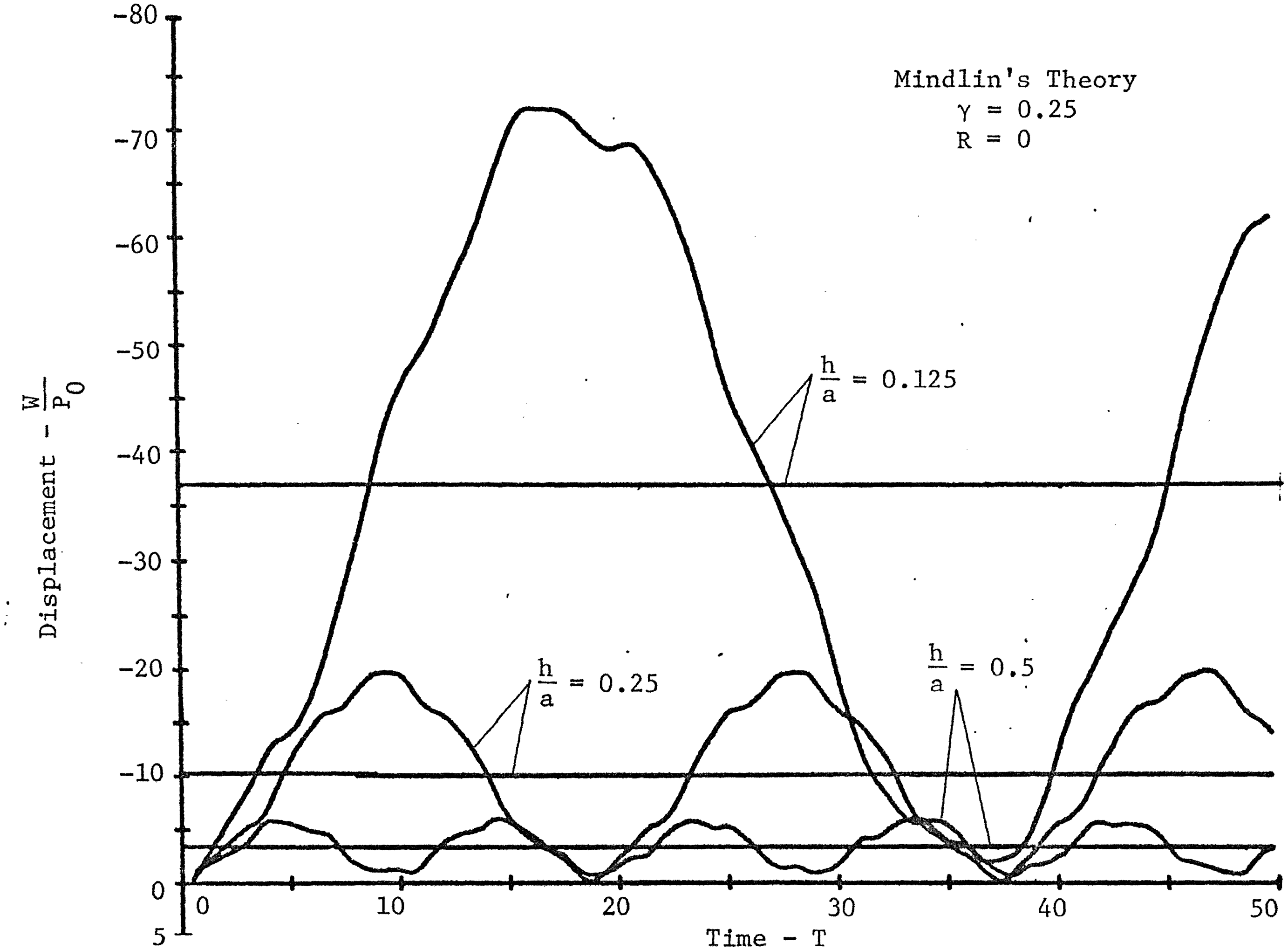

Figure 56 Effect of $\frac{h}{a}$ on Deflection at Center, Case 4 - Section VIII.C

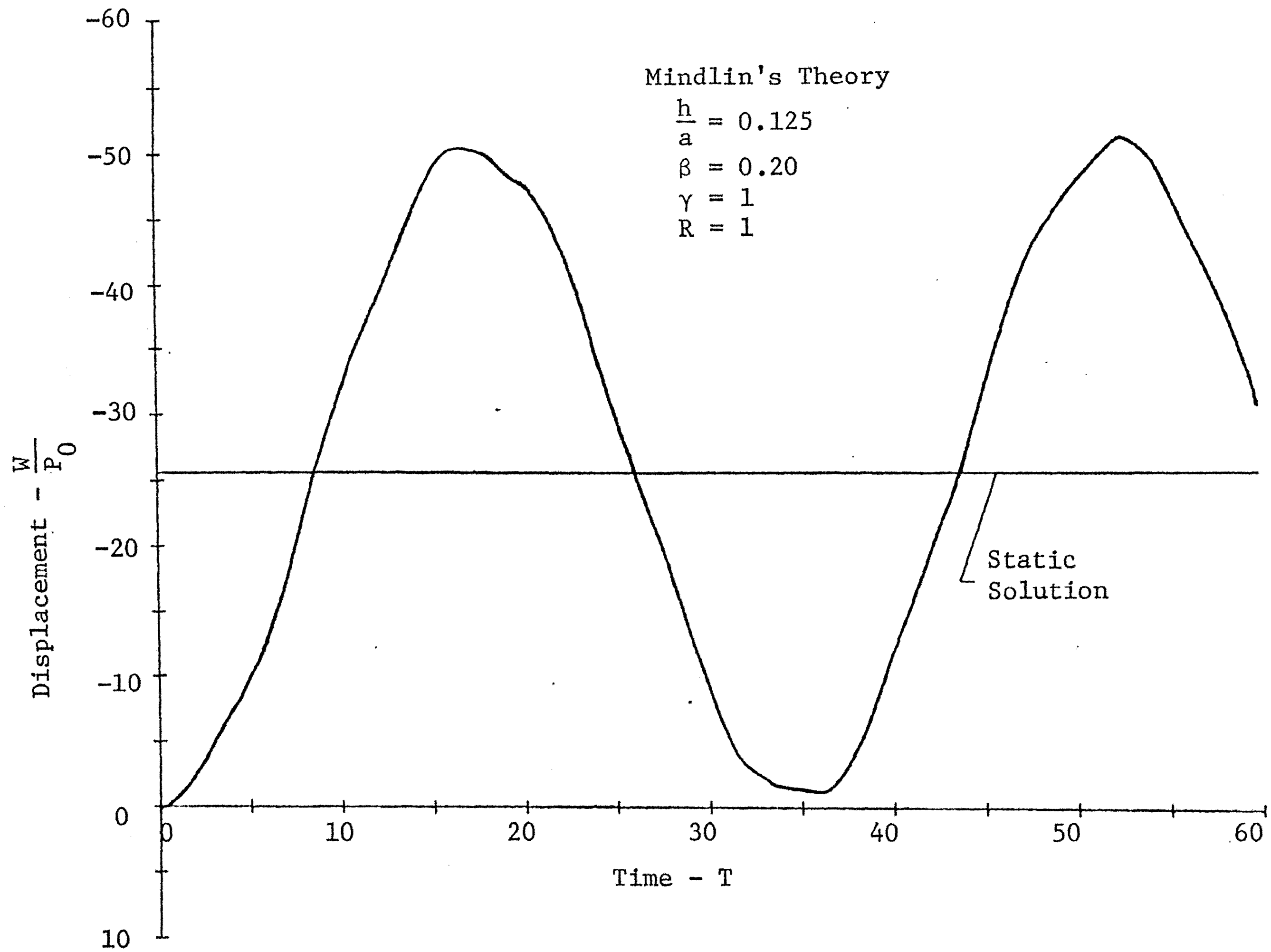

Figure 57 Deflection at Edge versus Time, Case 7 - Section VIII.C

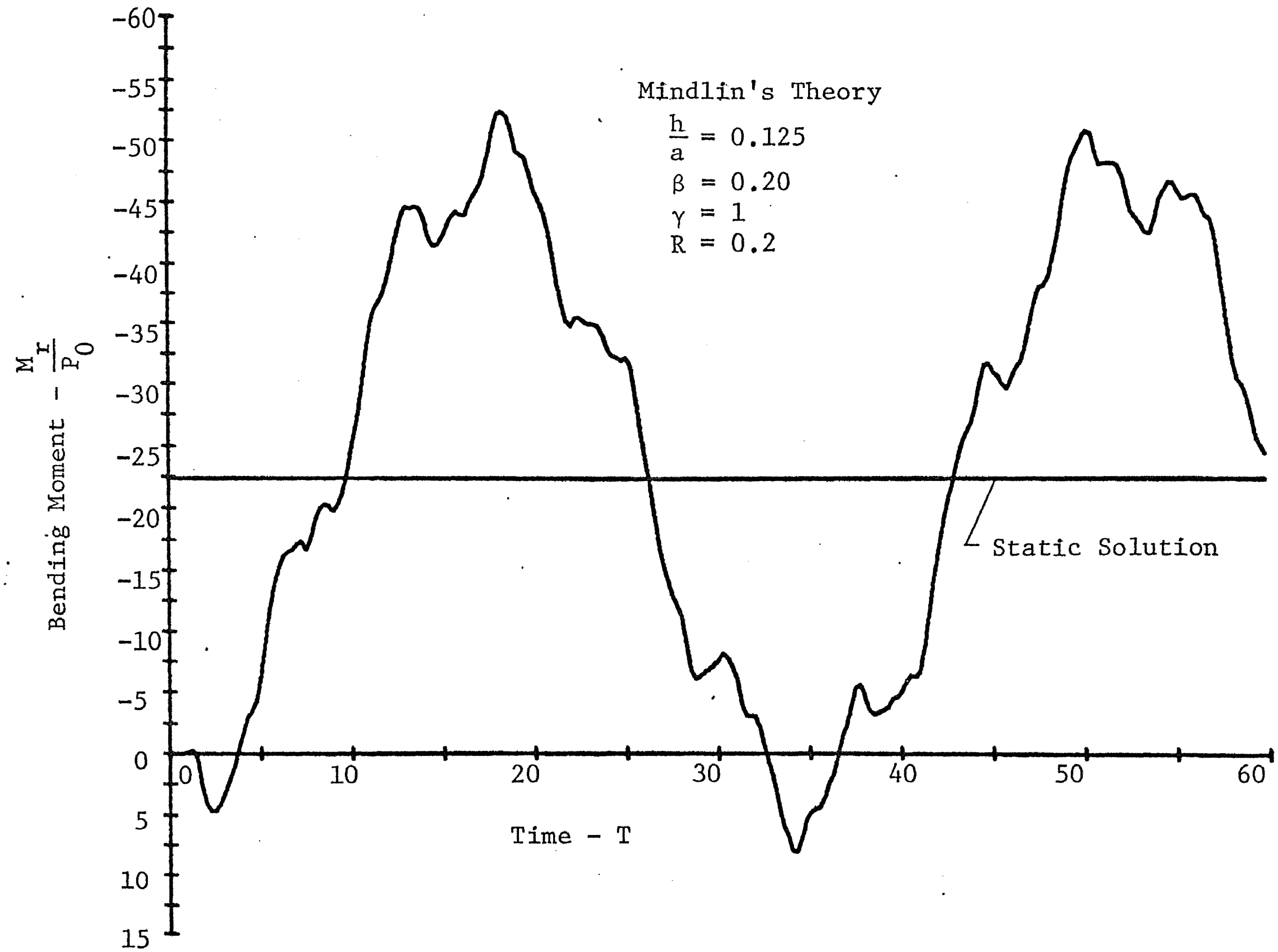

Figure 58 Bending Moment at Support versus Time, Case 7 - Section VIII.C

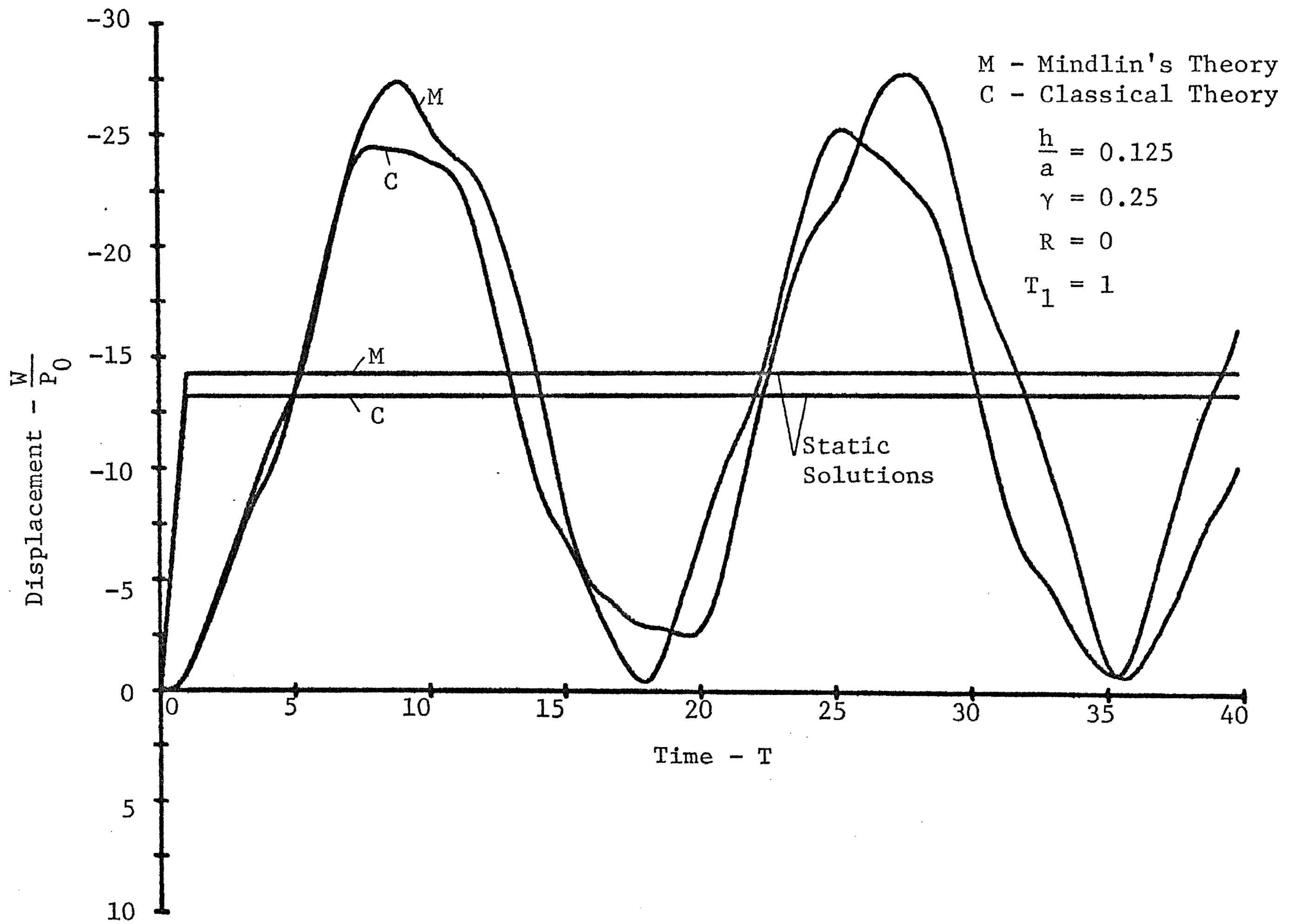

Figure 59 Deflection at Center versus Time, Clamped Plate, Ramp-Platform Load

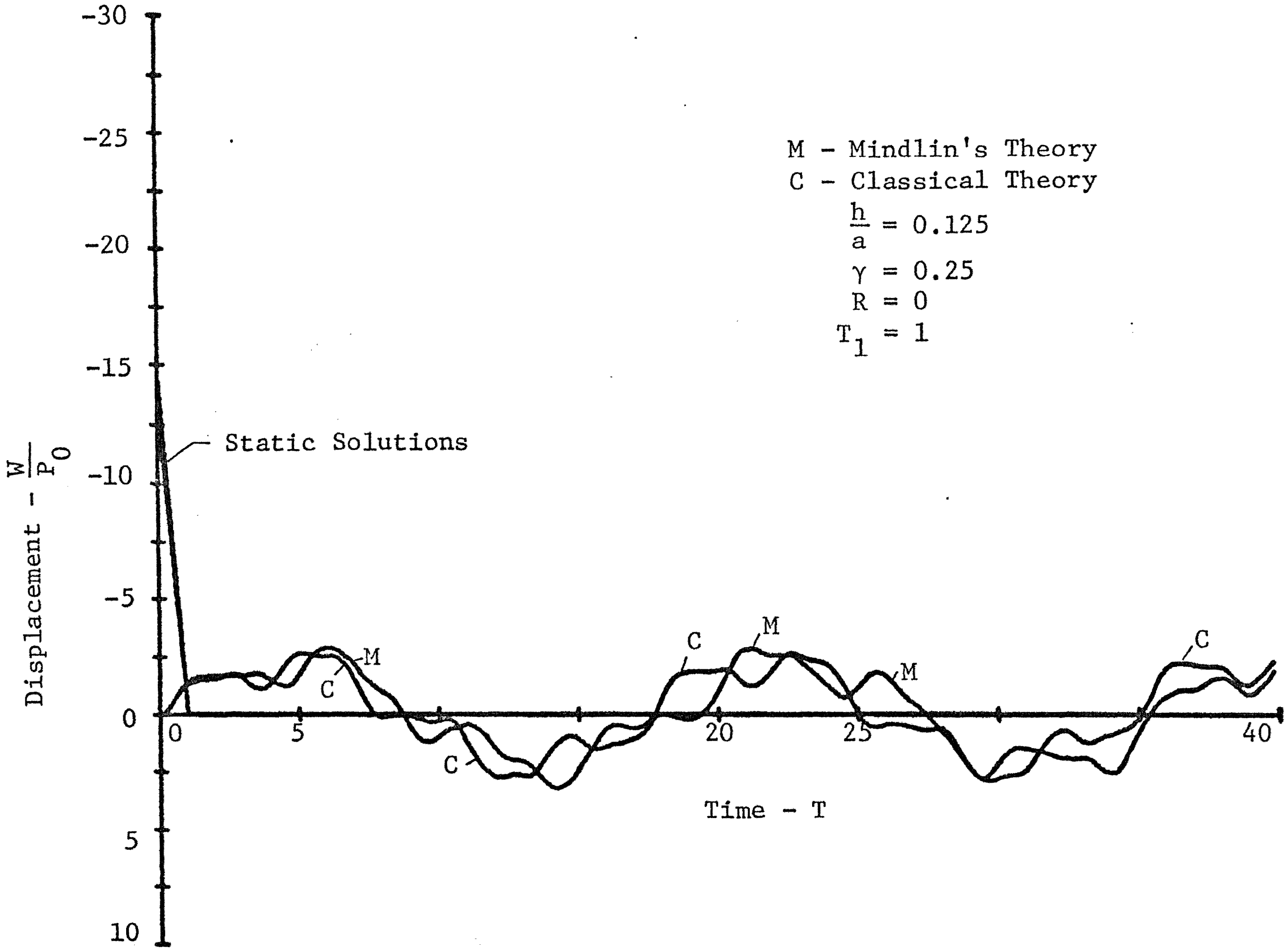

Figure 60 Deflection at Center versus Time, Clamped Plate, Blast Pulse

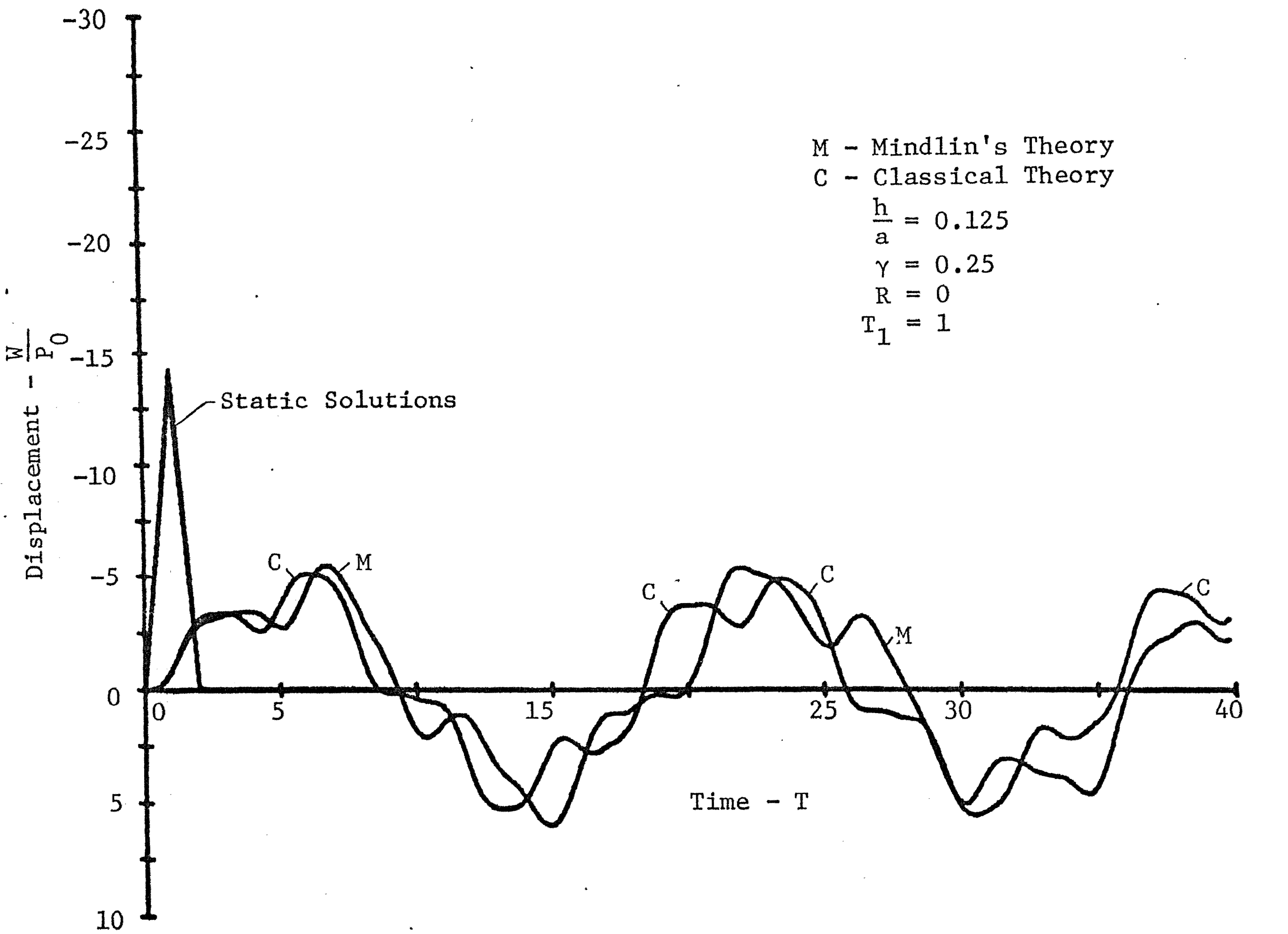

Figure 61 Deflection at Center versus Time, Clamped Plate, Triangular Pulse

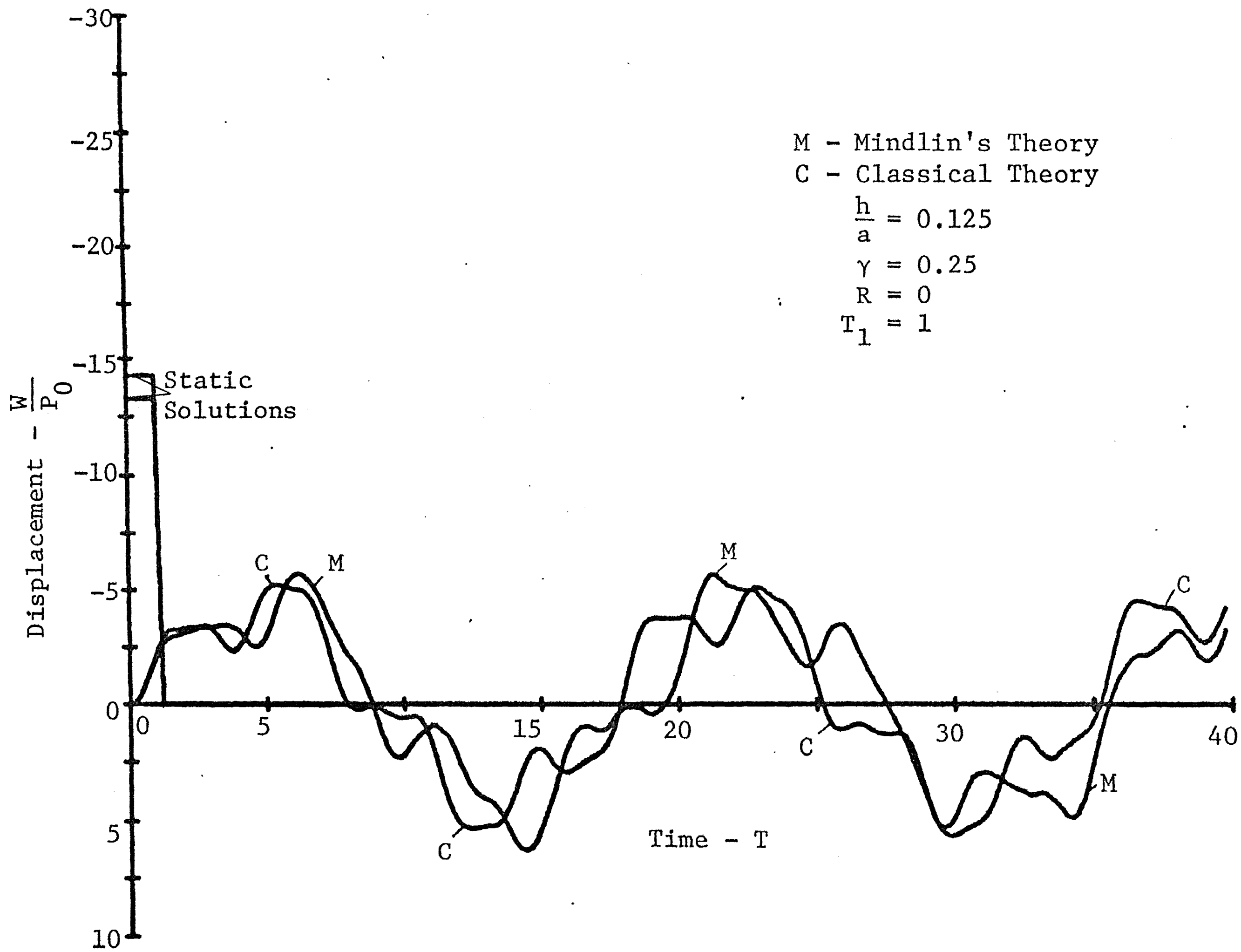

Figure 62 Deflection at Center versus Time, Clamped Plate, Square Pulse

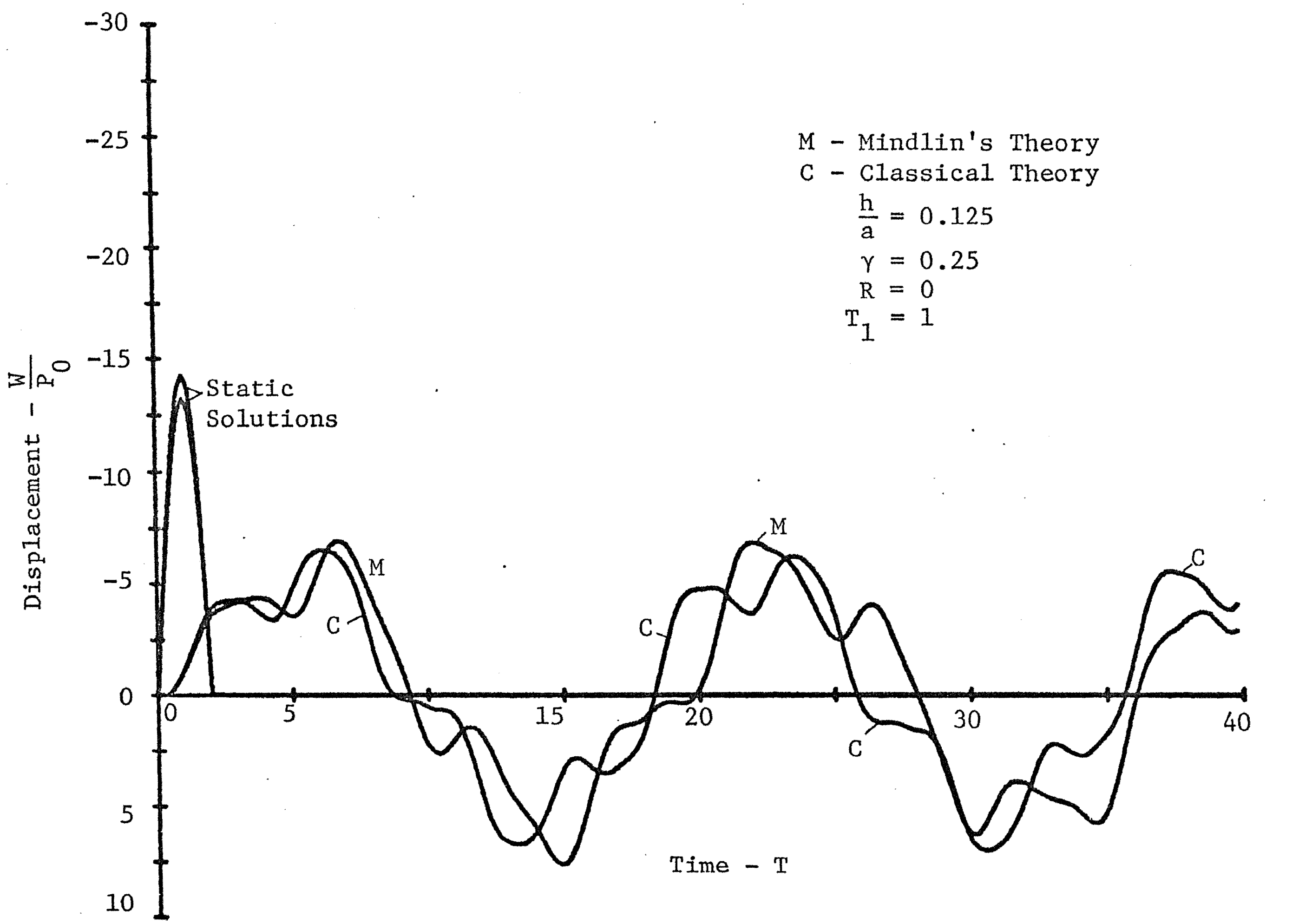

Figure 63 Deflection at Center versus Time, Clamped Plate, Half-Sine Pulse

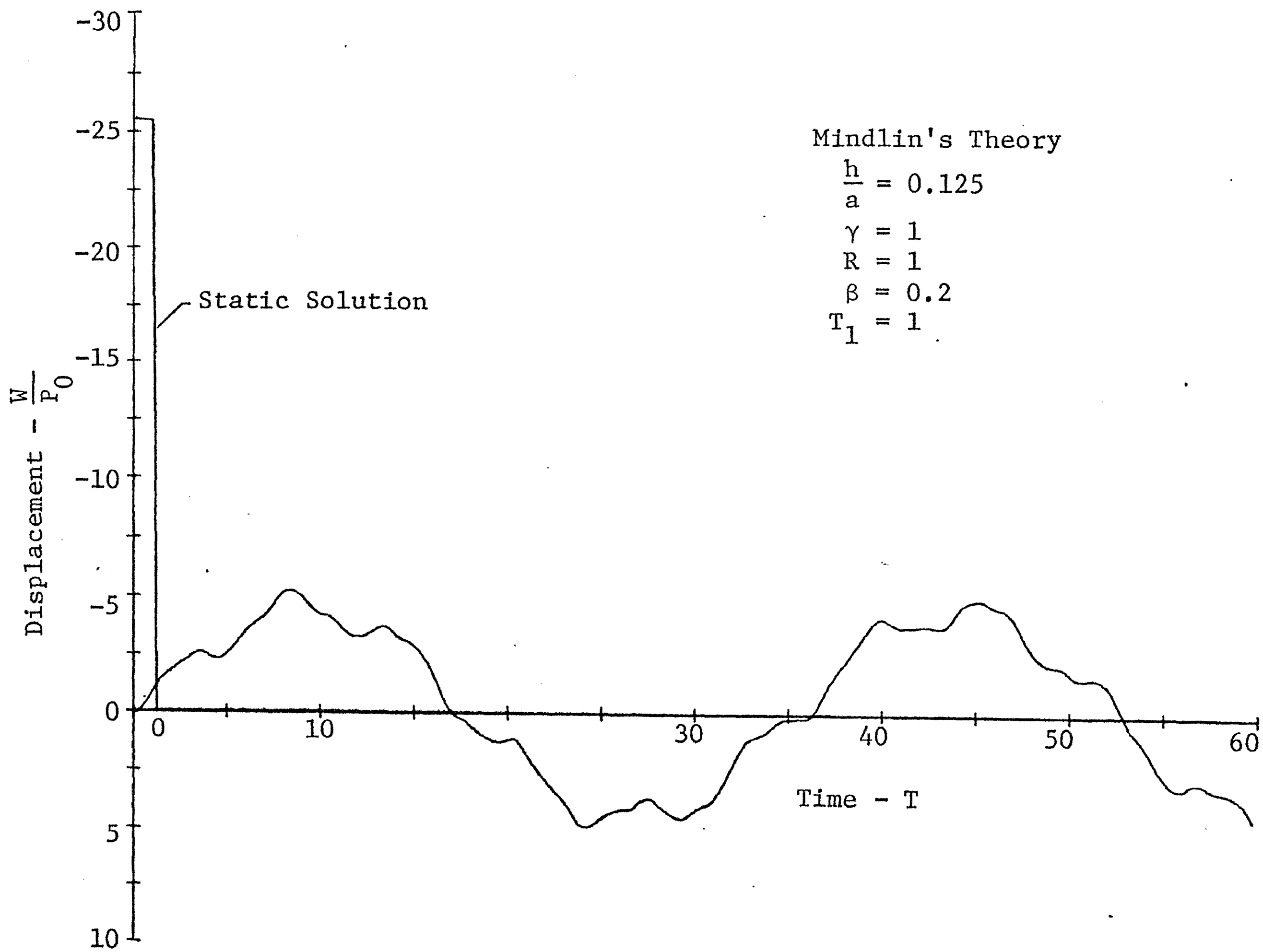

Figure 64 Deflection at Edge versus Time, Disk Mounted on a Shaft, Square Pulse

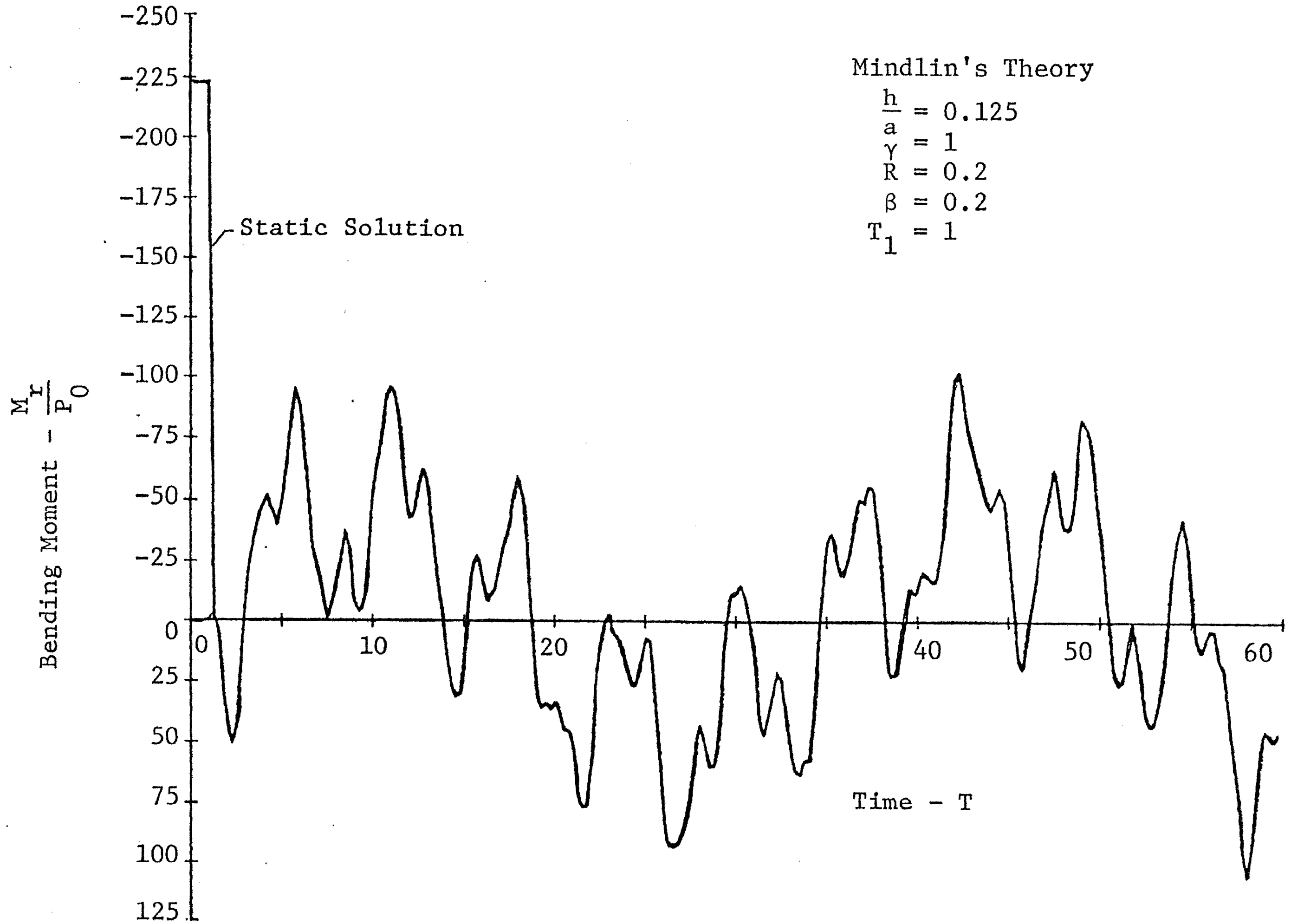

Figure 65 Bending Moment at Support versus Time, Disk Mounted on a Shaft, Square Pulse

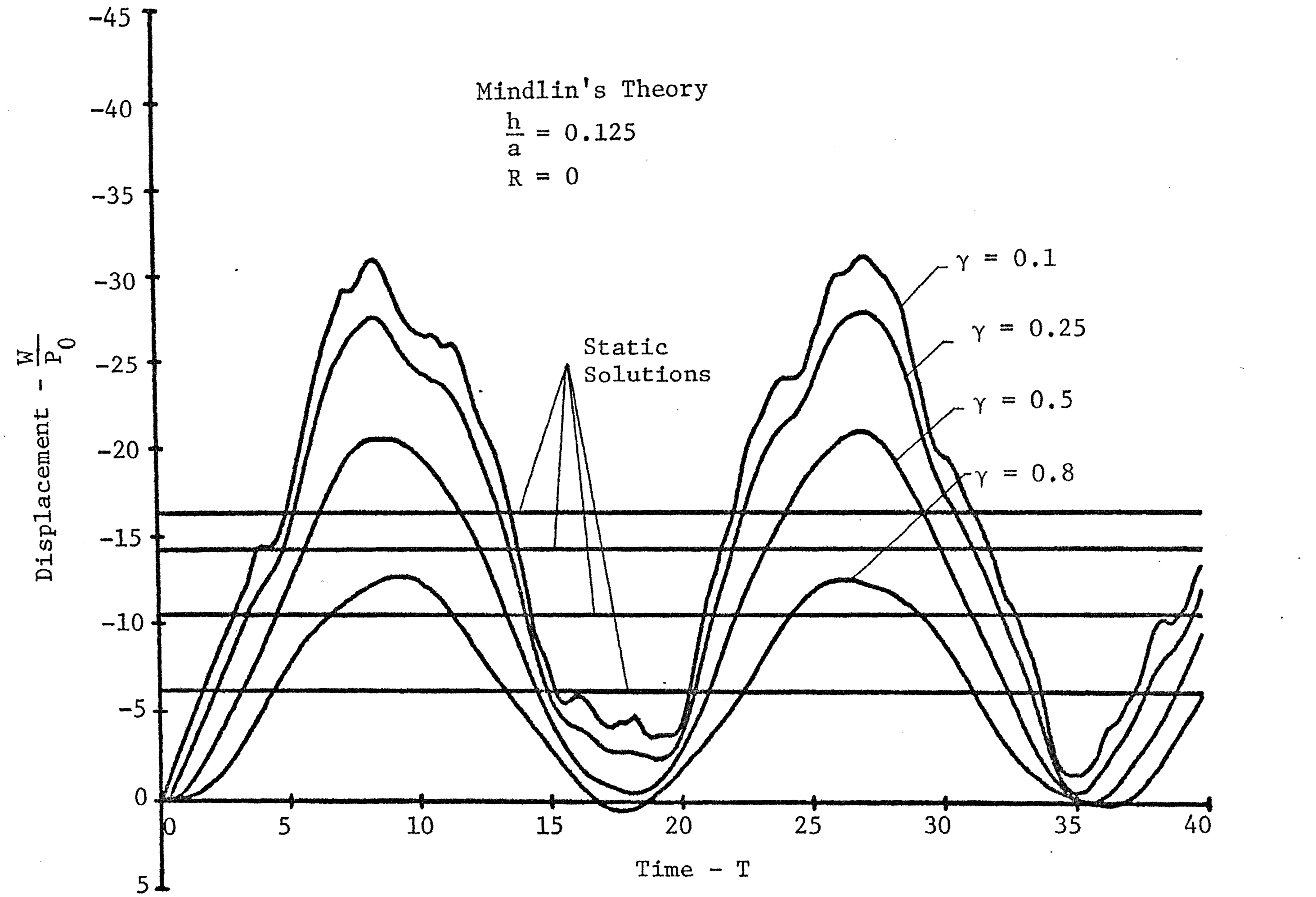

Figure 66 Effect of Area of Load on Deflection at Center, Case 1 - Section VIII.C

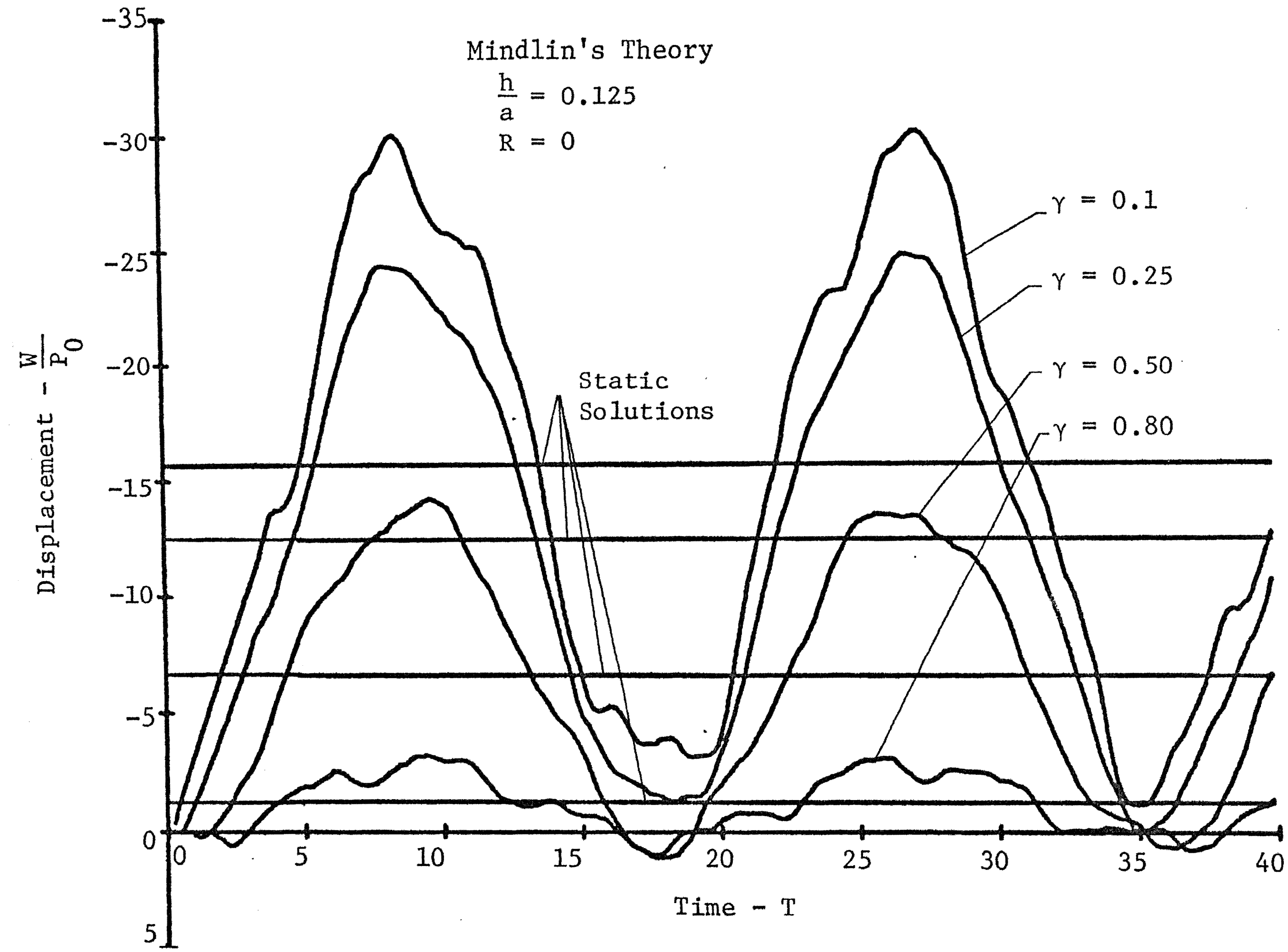

Figure 67 Effect of Radius of Load on Deflection at Center, Case 2 - Section VIII.C

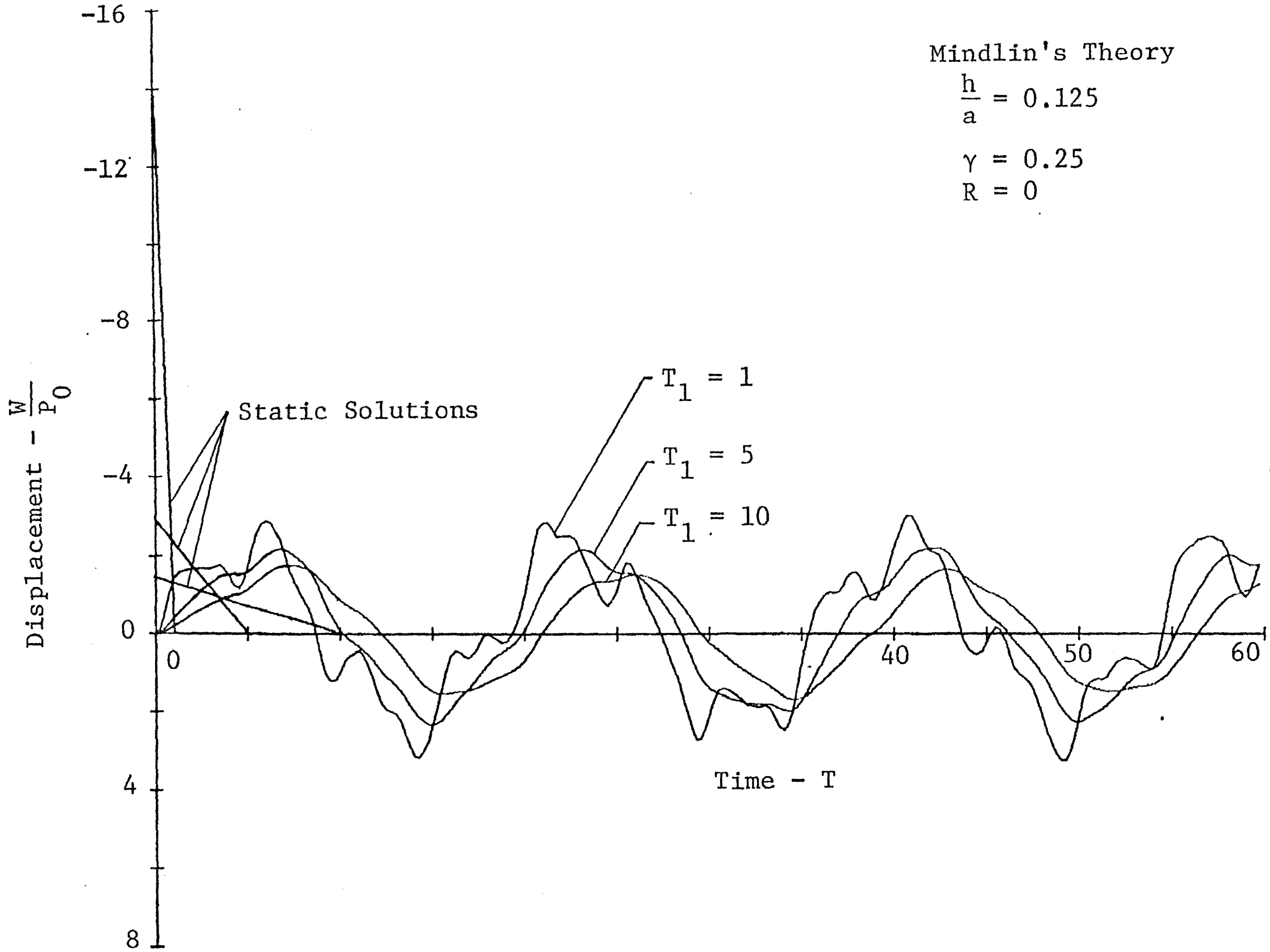

Figure 68 Effect of Duration of Pulse on Deflection at Center, Clamped Circular Plate, Blast Pulse

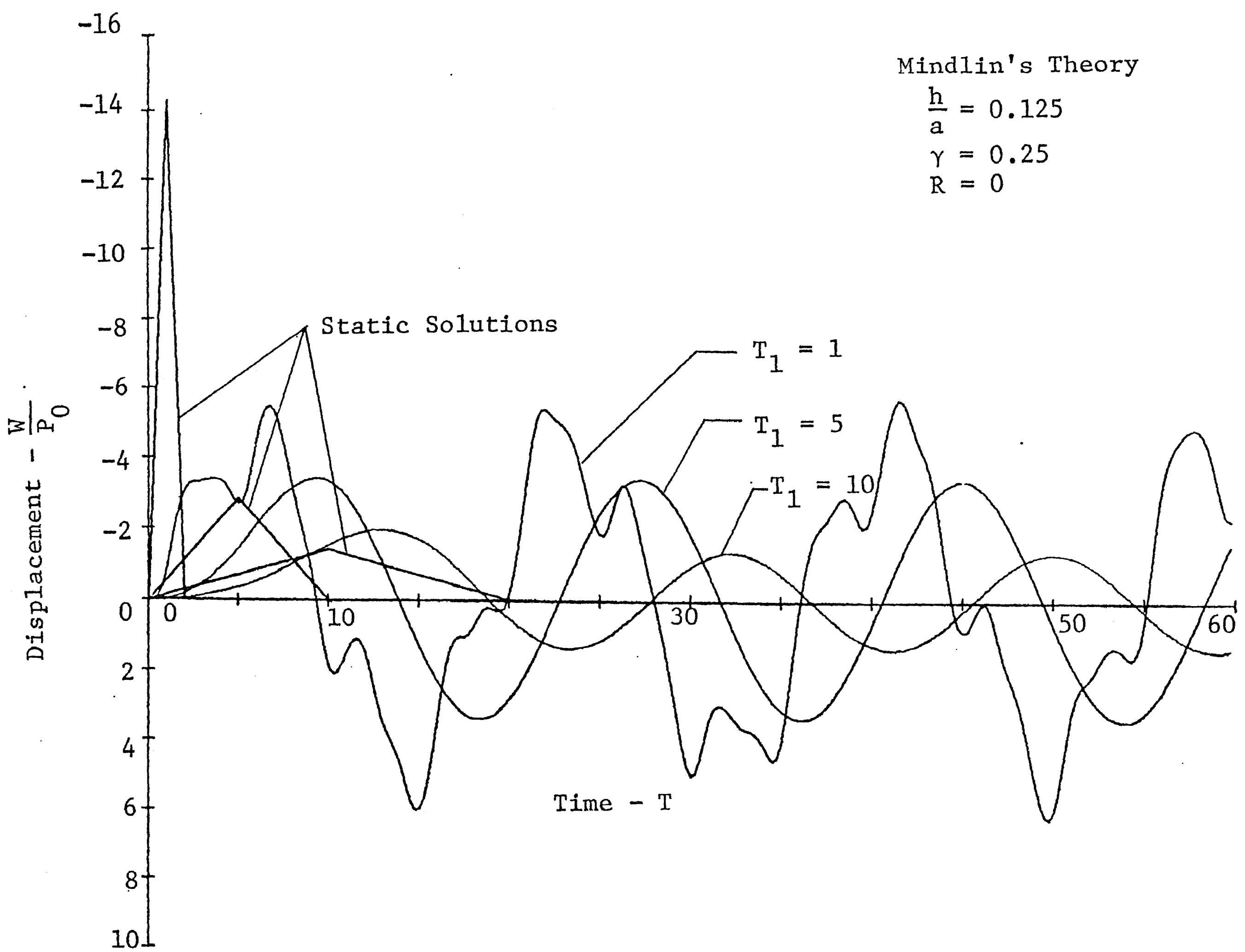

Figure 69 Effect of Time of Rise of Pulse on Deflection at Center, Clamped Circular Plate, Triangular Pulse

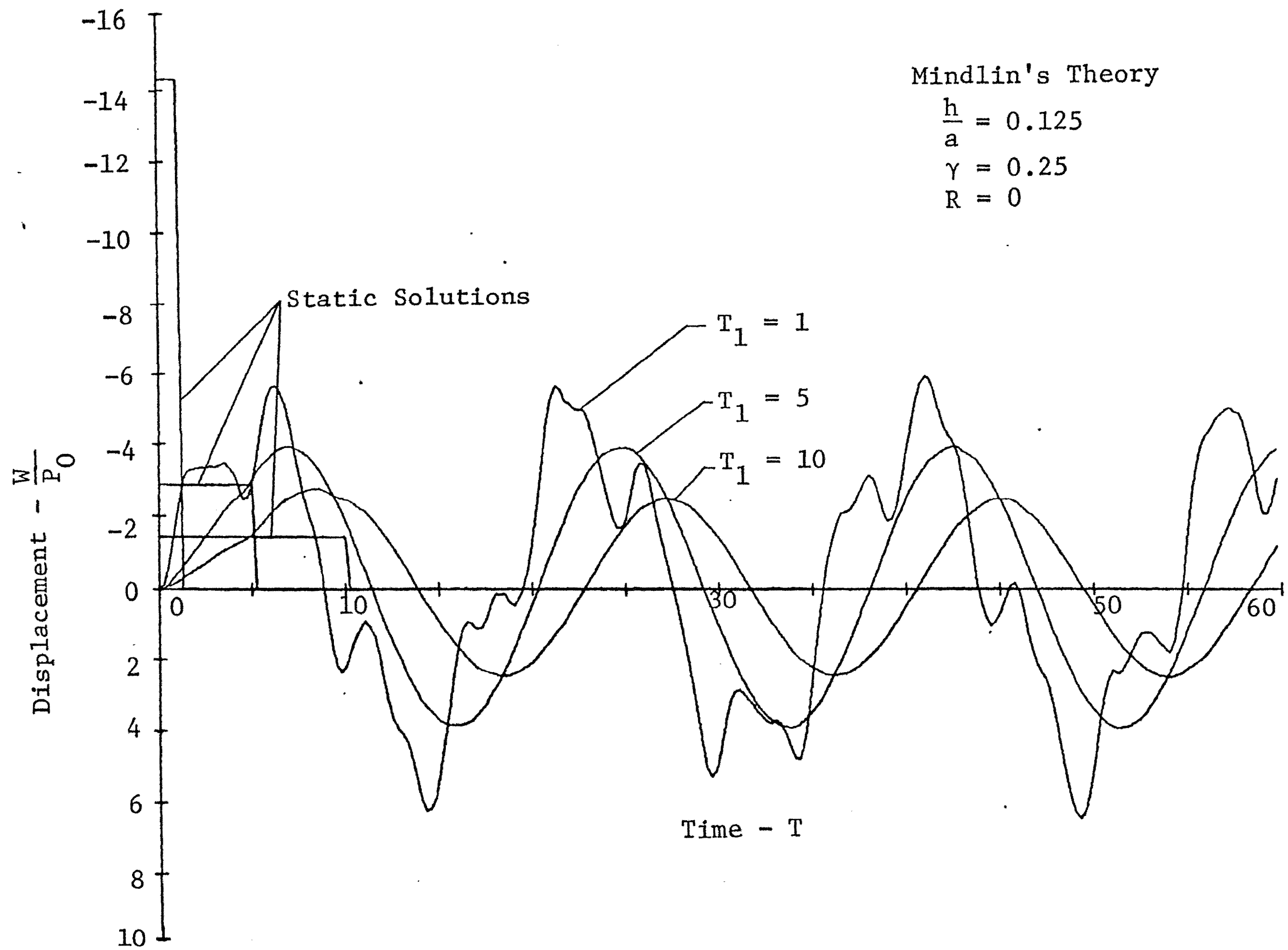

Figure 70 Effect of Duration of Pulse on Deflection at Center, Clamped Circular Plate, Square Pulse

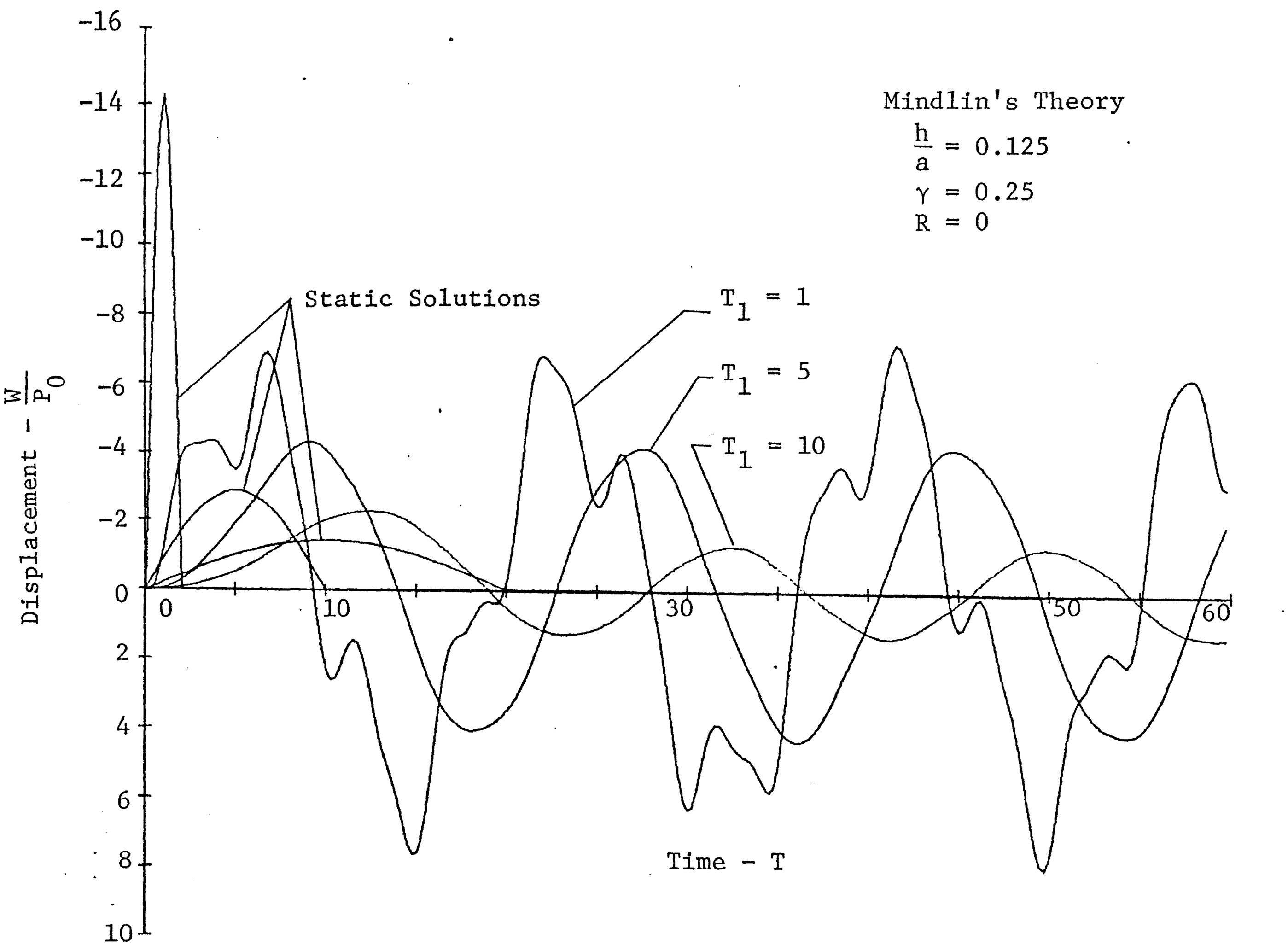

Figure 71 Effect of Time of Rise of Pulse on Deflection at Center, Clamped Circular Plate, Half-Sine Pulse

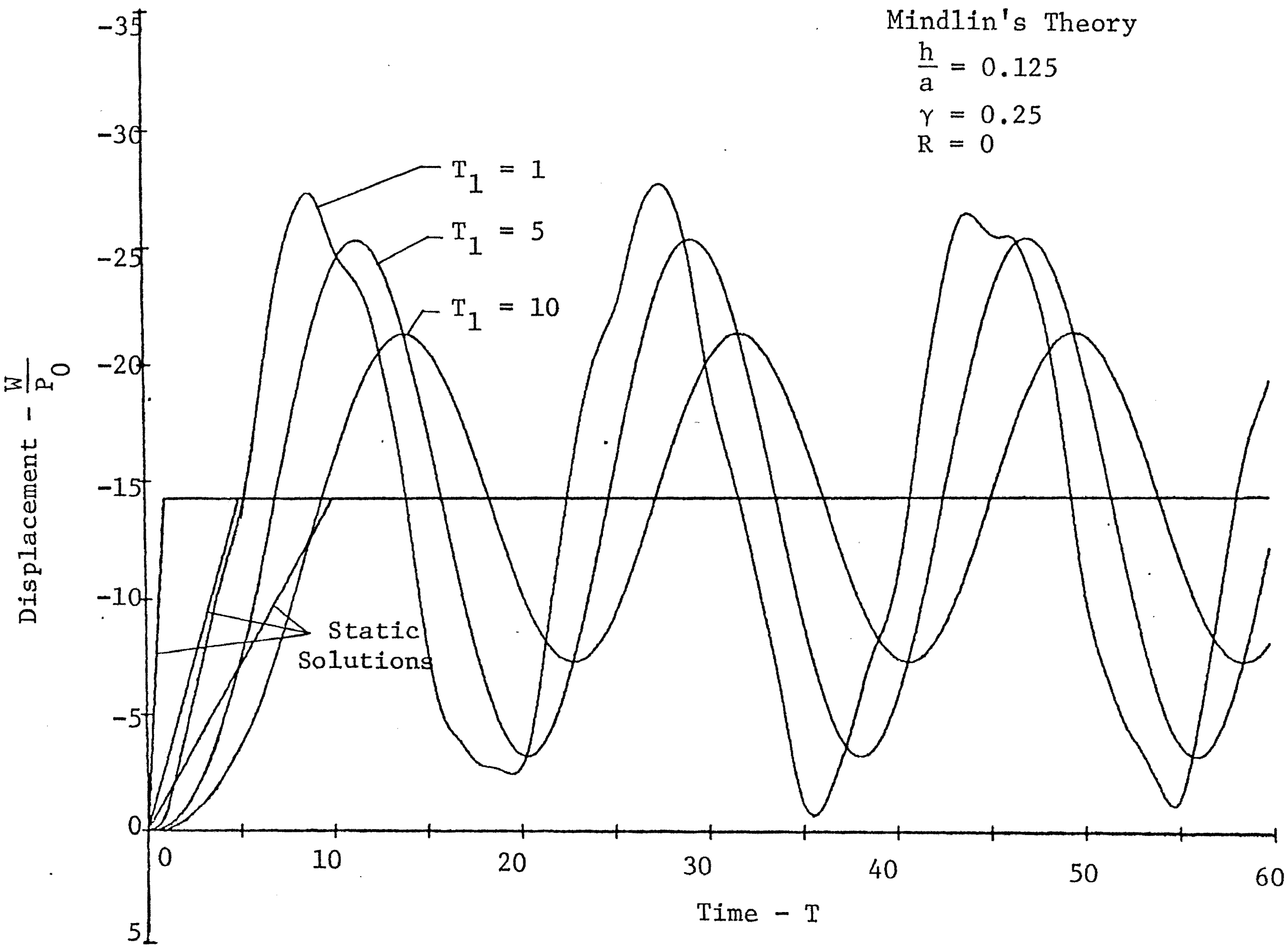

Figure 72 Effect of Time of Rise of Load on Deflection at Center, Clamped Circular Plate, Ramp-Platform Load

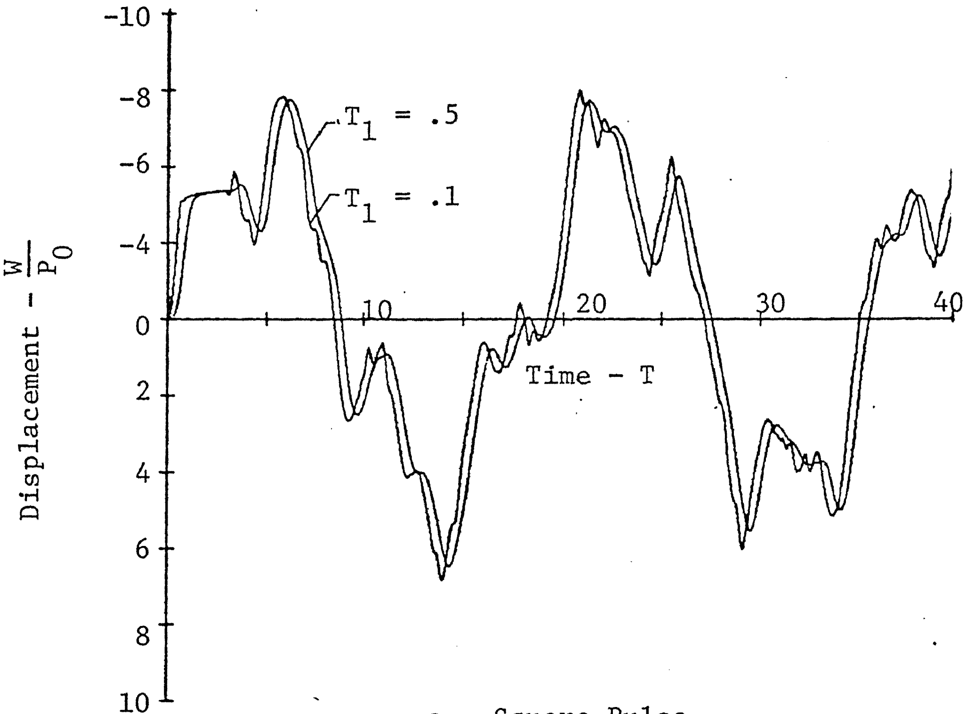

a. Square-Pulse

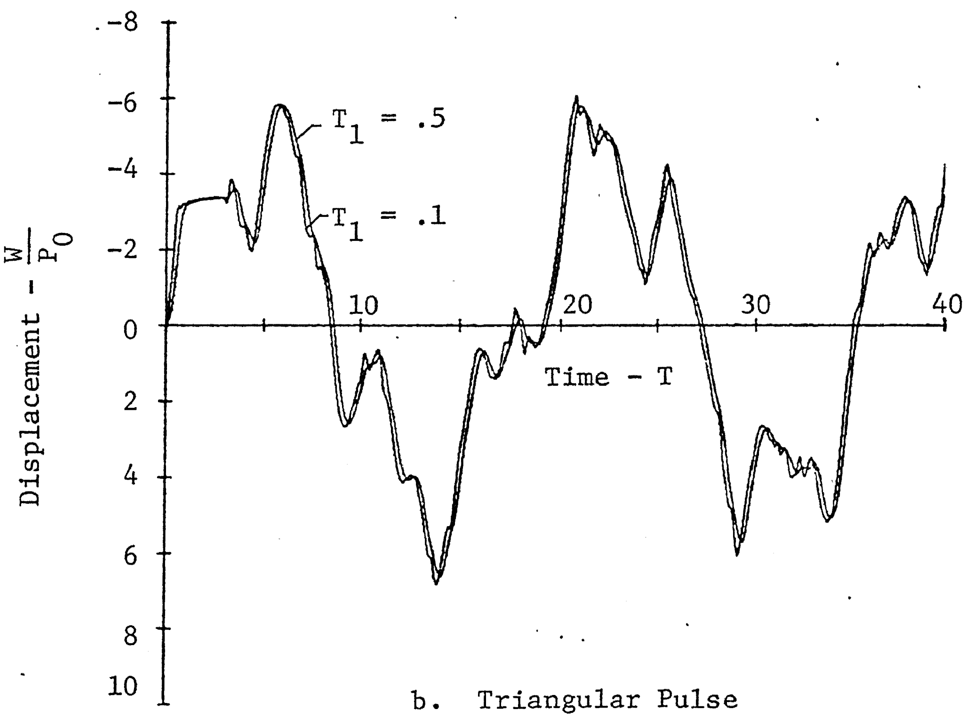

b. Triangular Pulse

Figure 73 Effect of Duration of Pulse on Deflection at the Center, Clamped Circular Plate

(continued on next page)

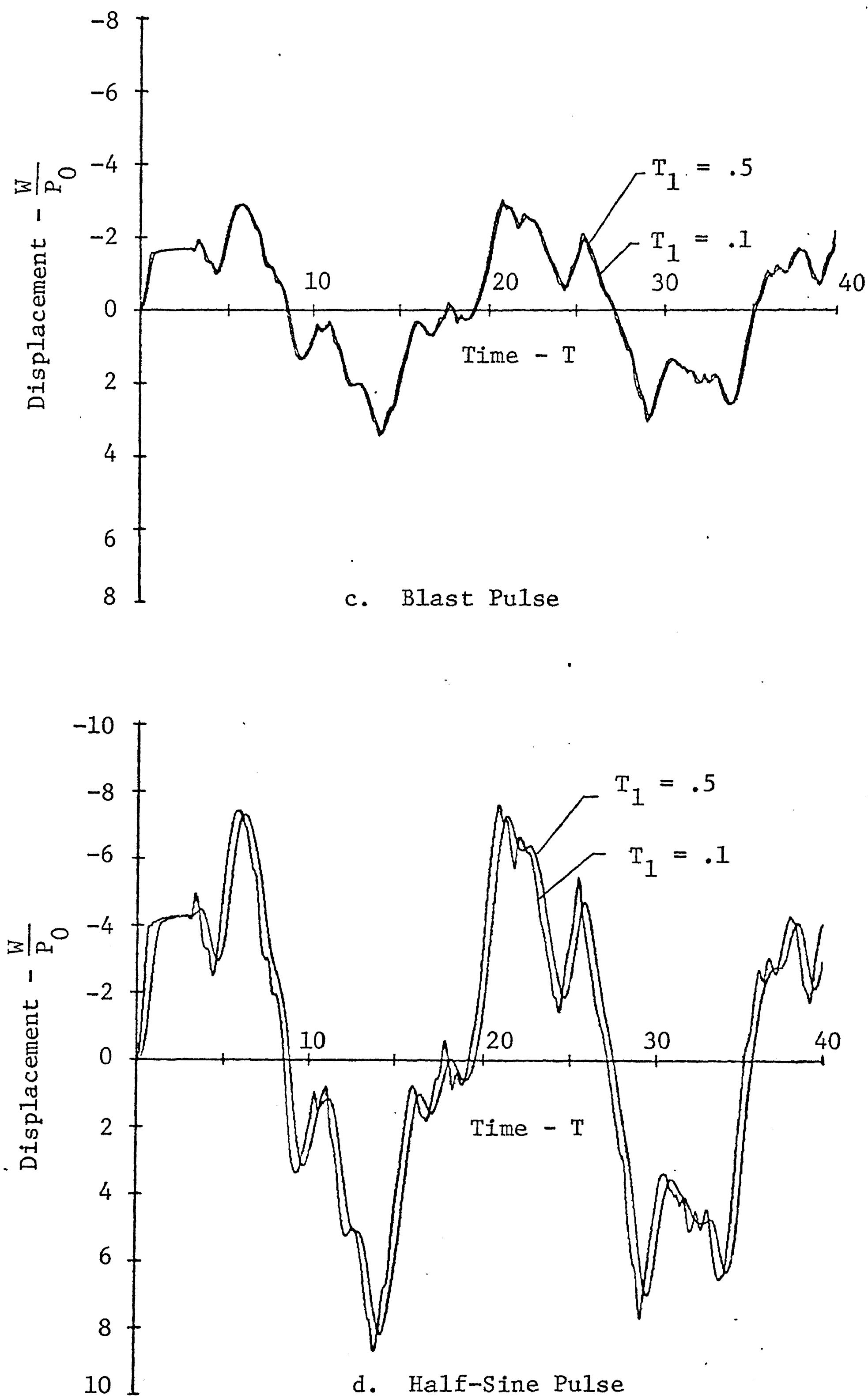

Figure 73. Effect of Duration of Pulse on Deflection at the Center, Clamped Circular Plate

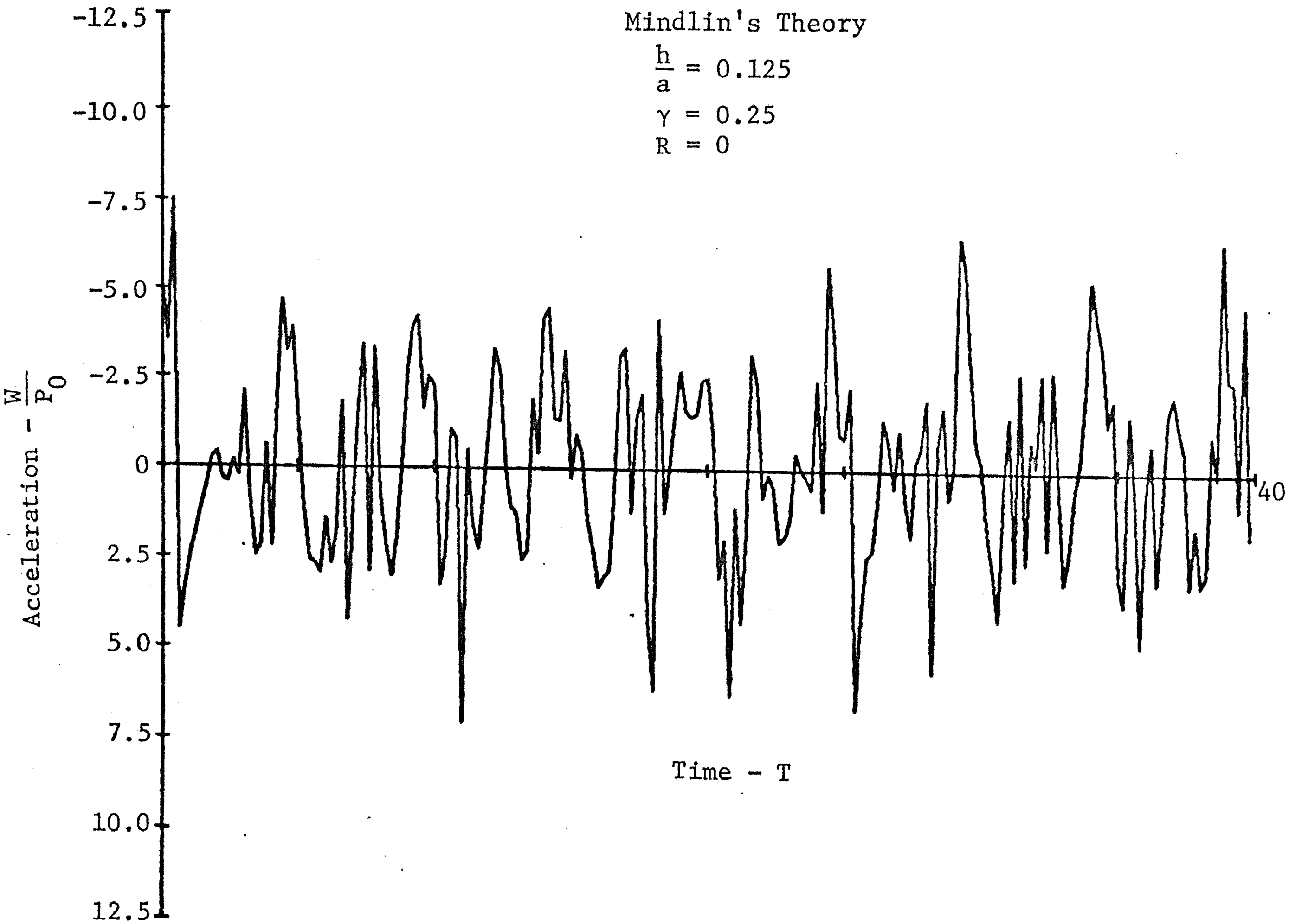

Figure 74 Acceleration at Center versus Time, Clamped Circular Plate, Blast Pulse, $T_1 = 1$

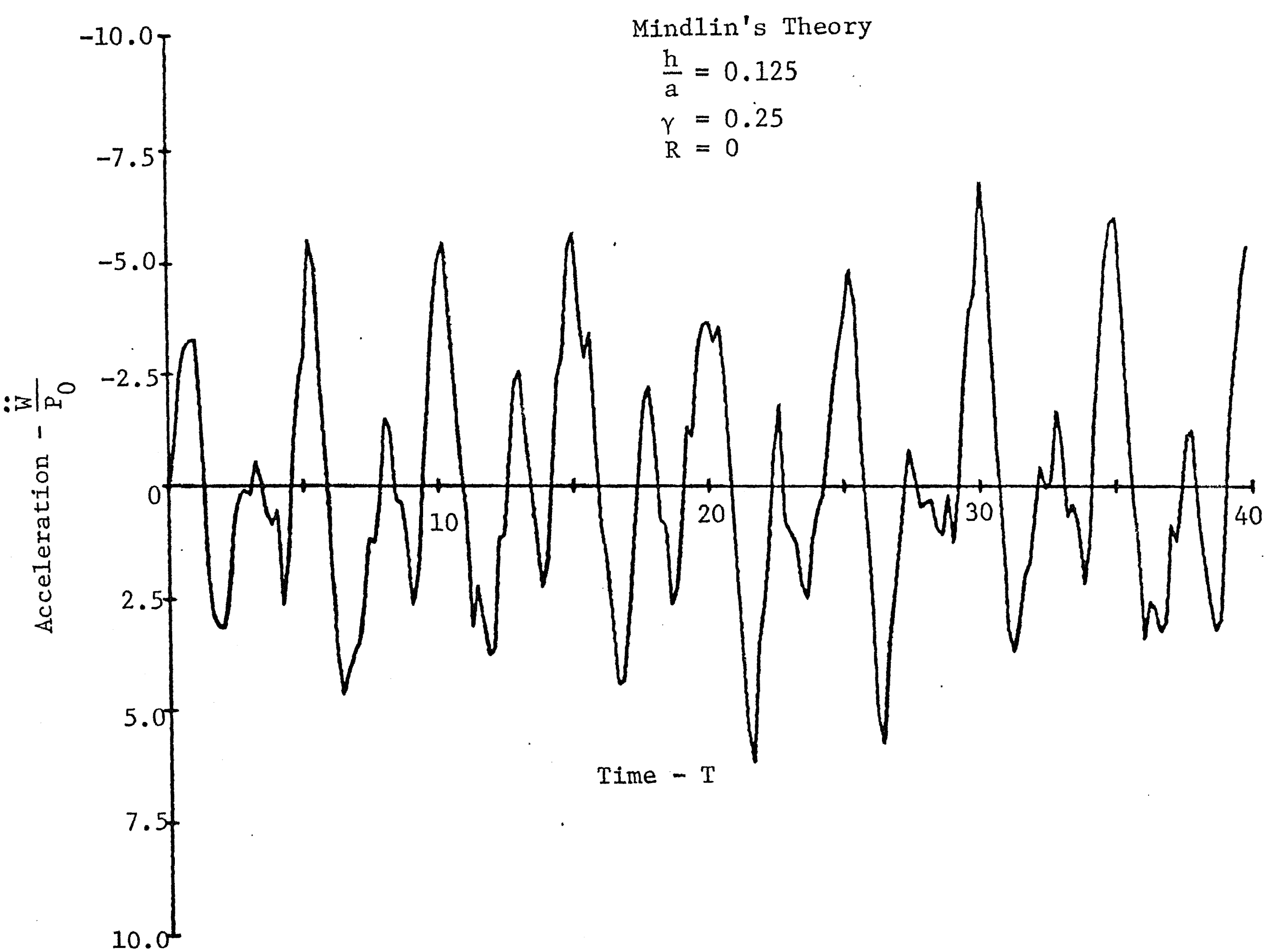

Figure 75 Acceleration at Center versus Time, Clamped Circular Plate, Triangular Pulse, $T_1 = 1$

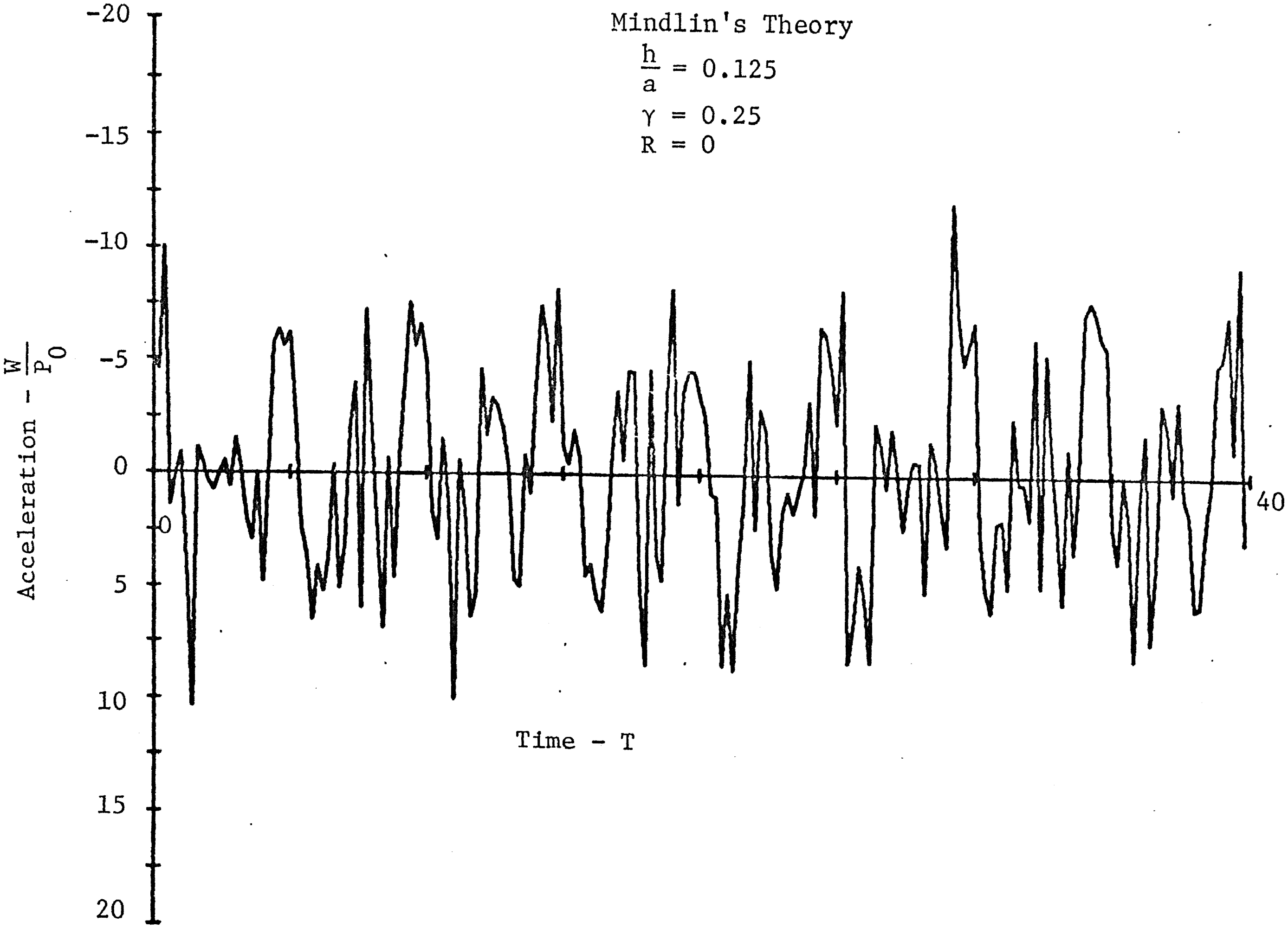

Figure 76 Acceleration at Center versus Time, Clamped Circular Plate, Square Pulse, $T_1 = 1$

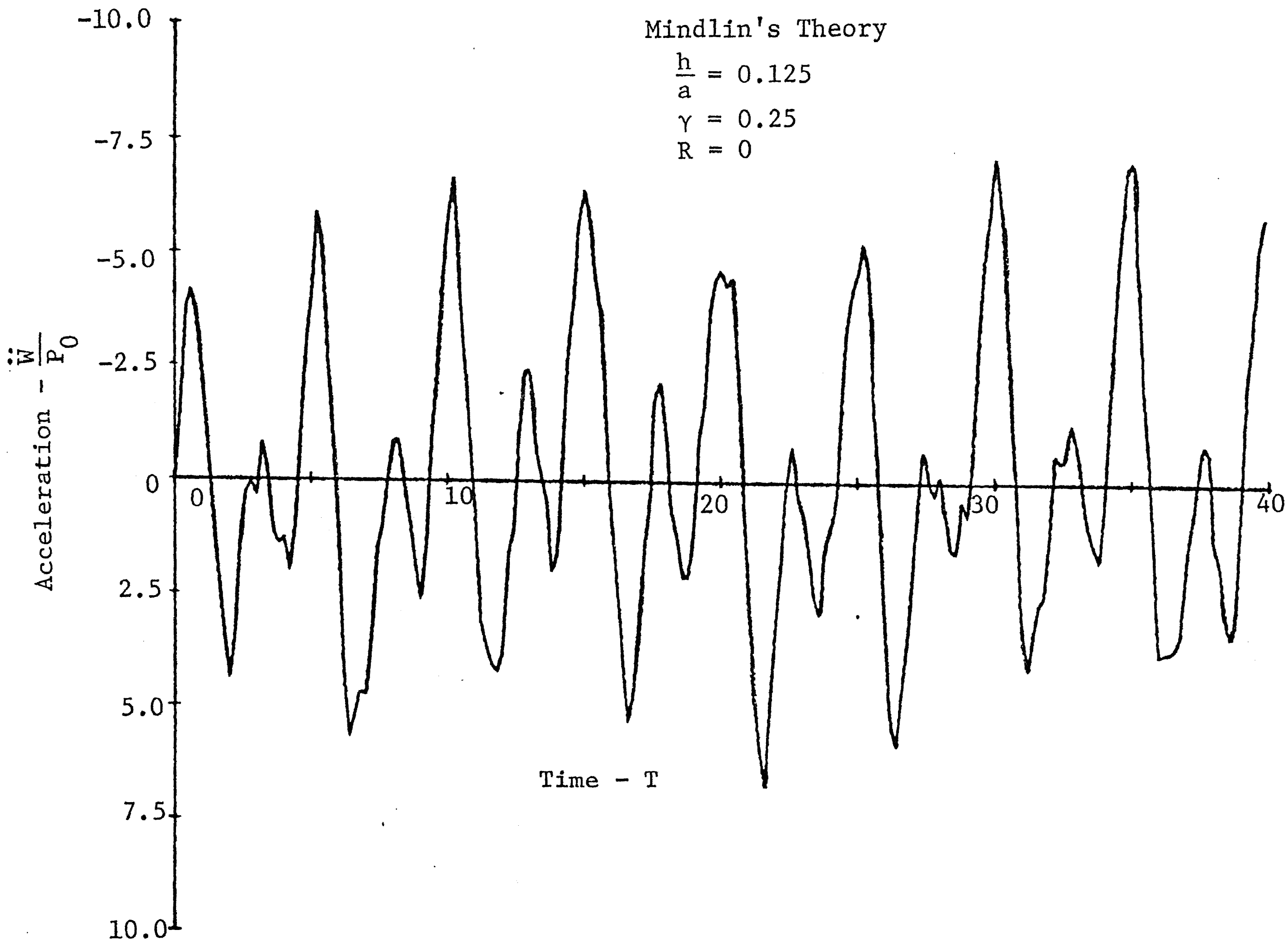

Figure 77 Acceleration at Center versus Time, Clamped Circular Plate, Half-Sine Pulse, $T_1 = 1$

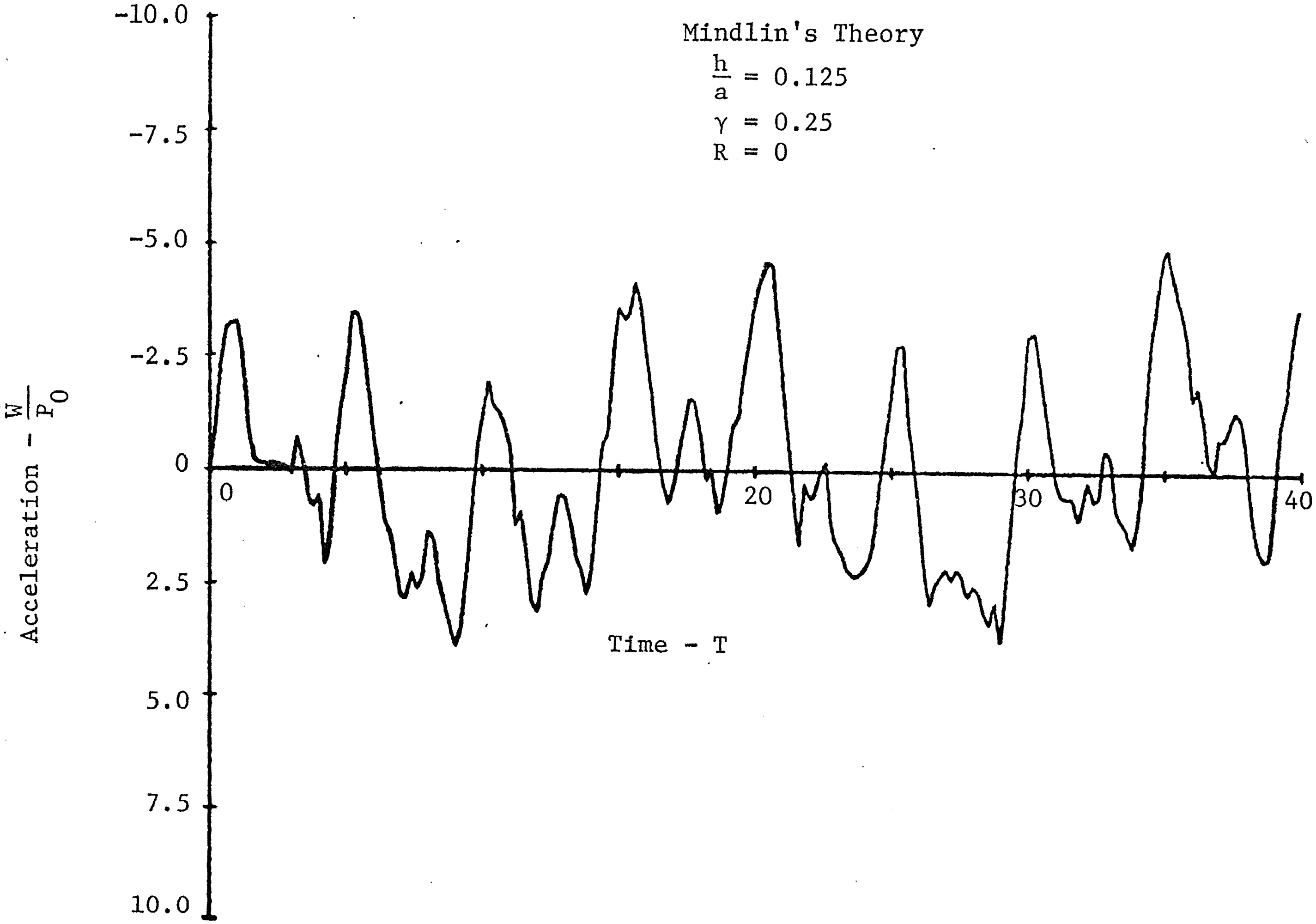

Figure 78 Acceleration at Center versus Time, Clamped Circular Plate, Ramp-Platform Load, $T_1 = 1$

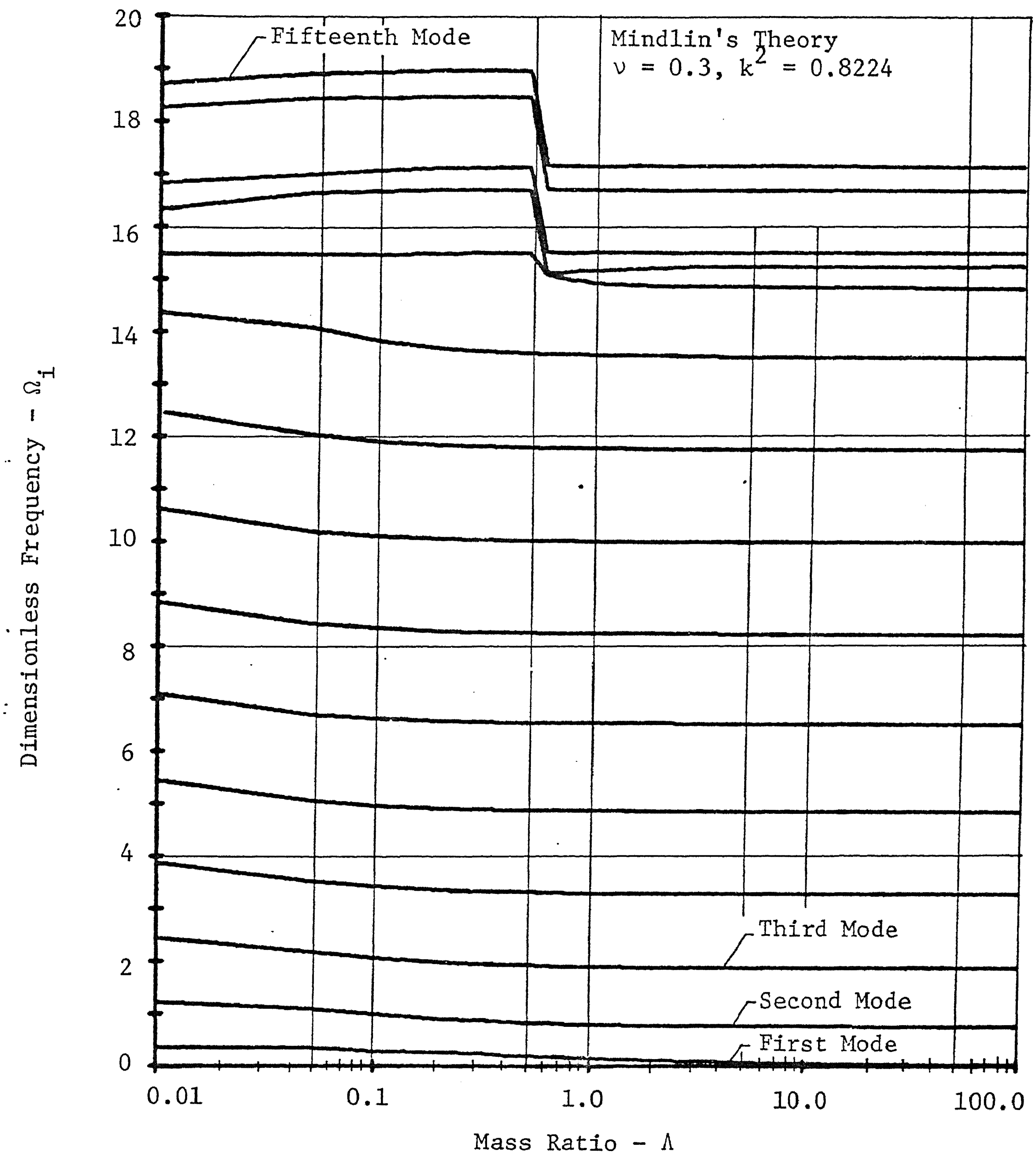

Figure 79 Frequency Spectrum of Mass-Loaded Clamped Circular Plate, $\frac{h}{a} = 0.125$

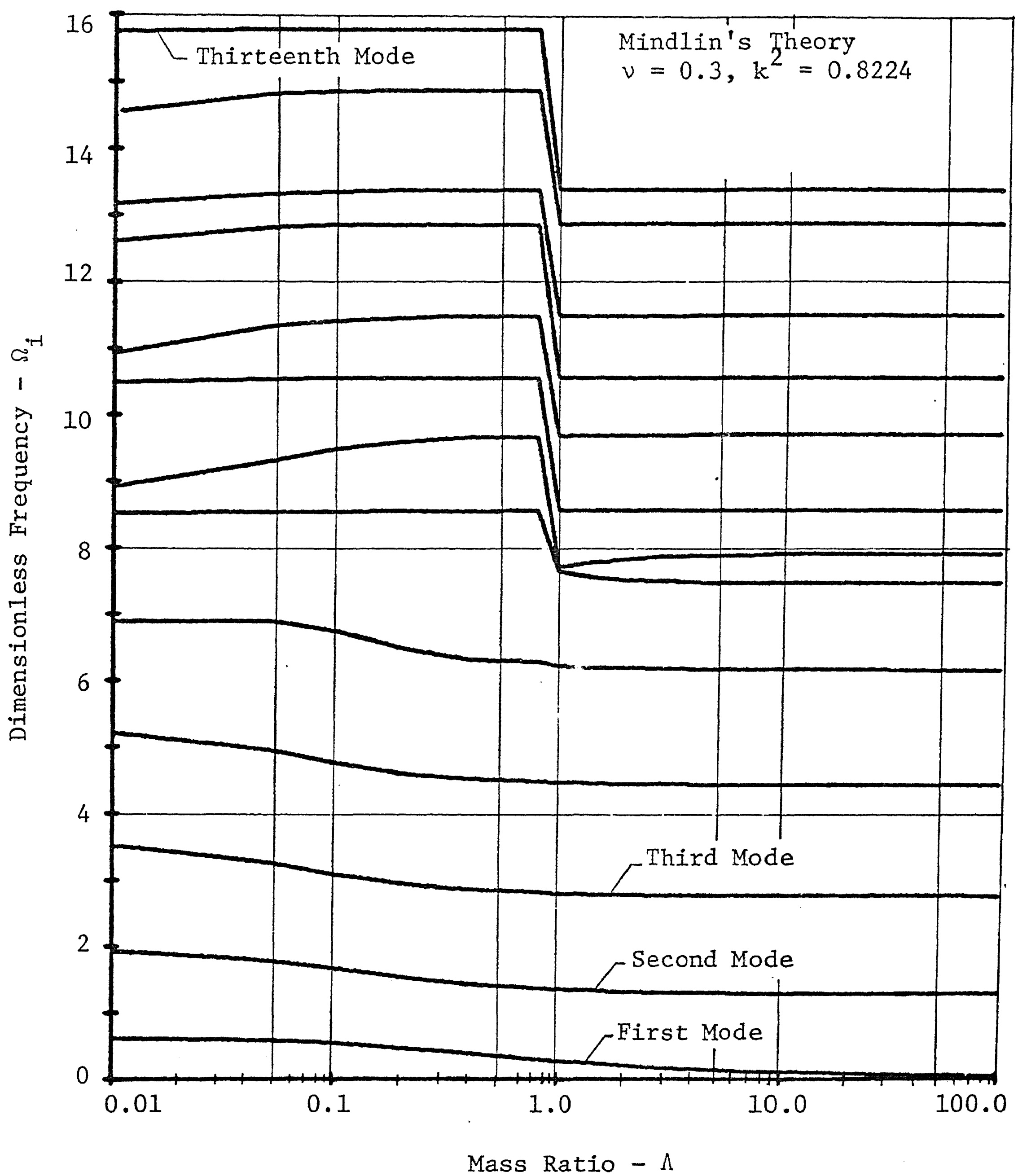

Figure 80 Frequency Spectrum of Mass-Loaded Clamped Circular Plate, $\frac{h}{a} = 0.25$

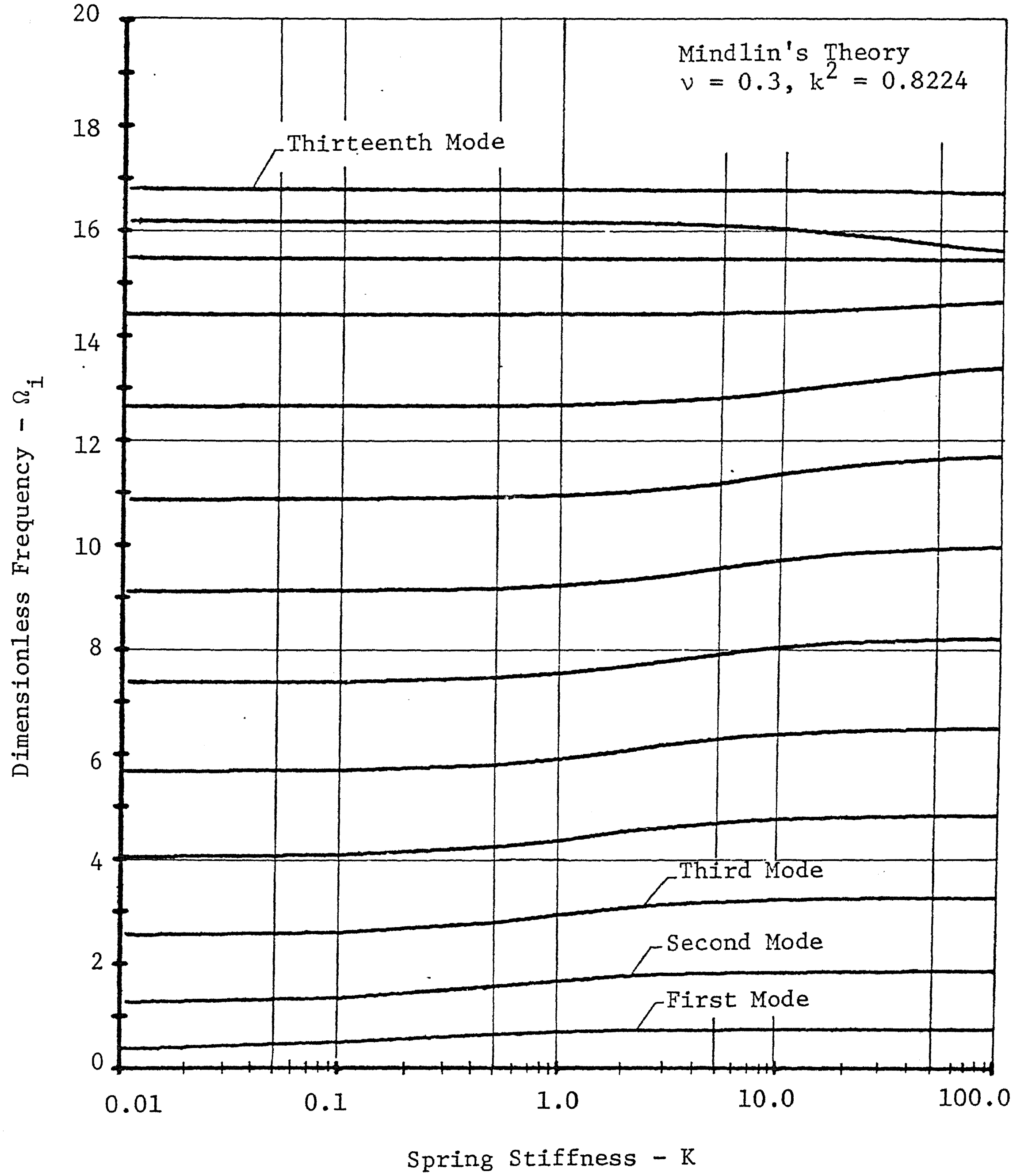

Figure 81 Frequency Spectrum of Spring-Loaded Clamped Circular Plate, $\frac{h}{a} = 0.125$

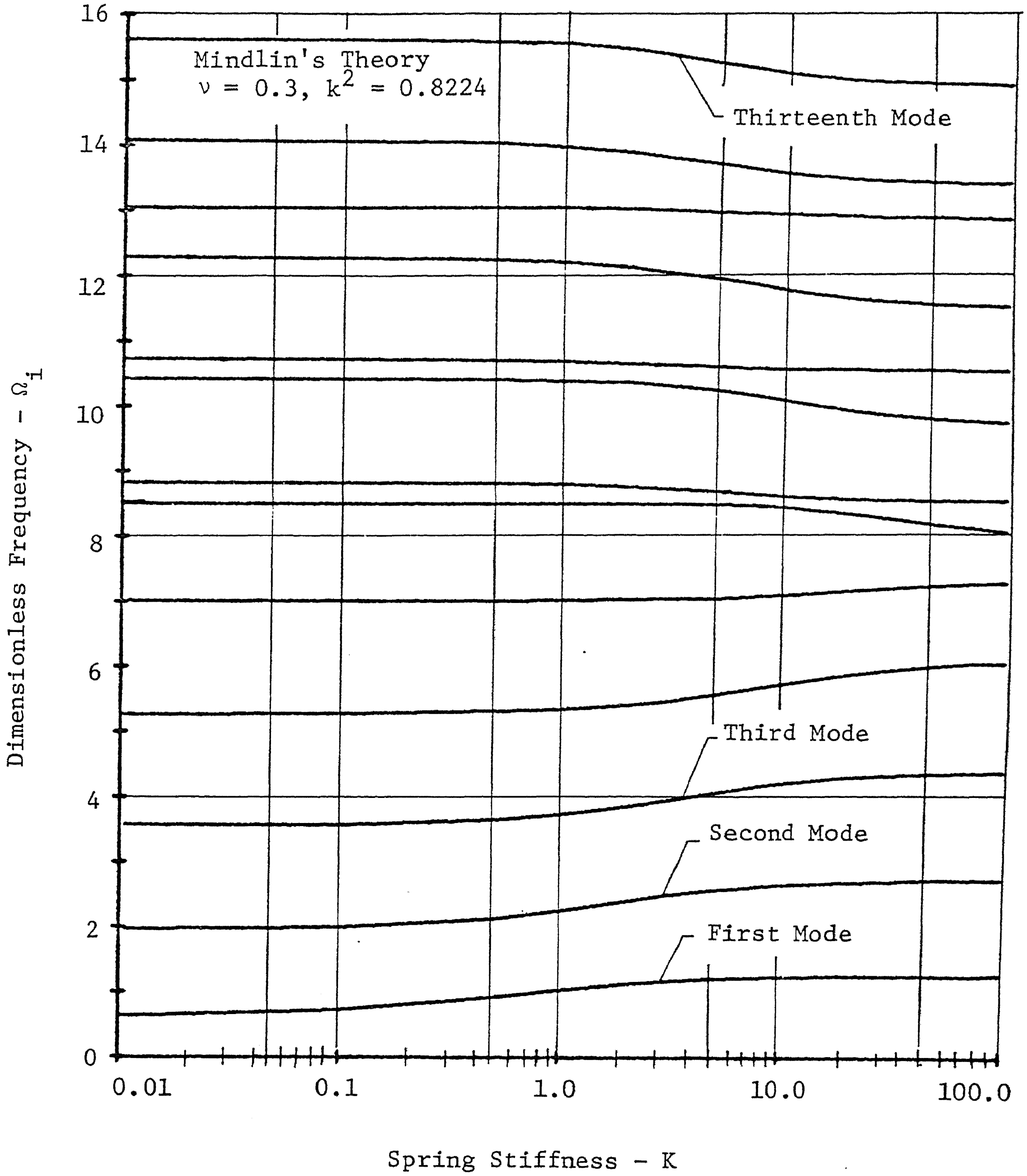

Figure 82 Frequency Spectrum of Spring-Loaded Clamped Circular Plate, $\frac{h}{a} = 0.25$

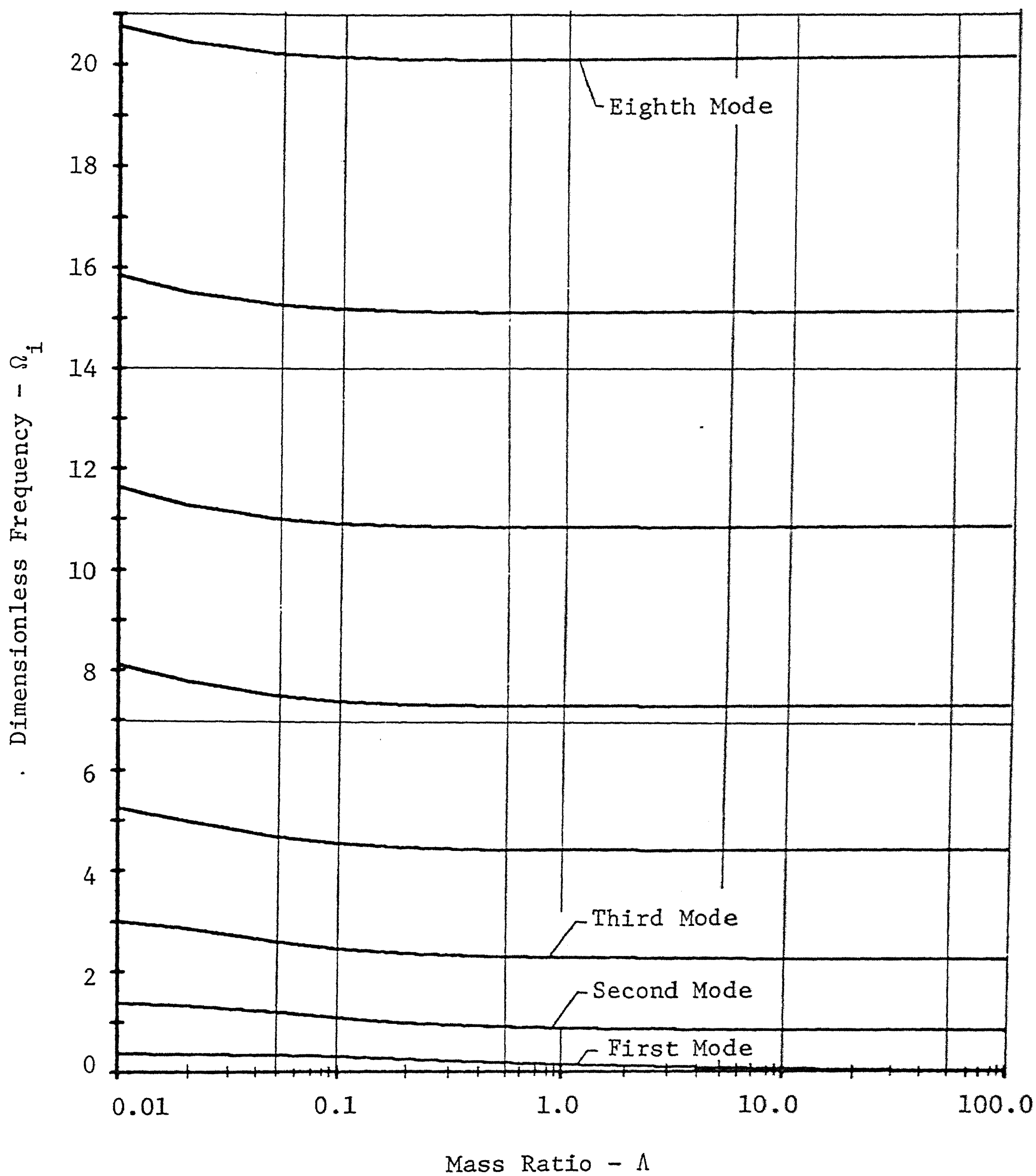

Figure 83 Frequency Spectrum of Mass-Loaded Clamped Circular Plate, Classical Theory, $\frac{h}{a} = .125$

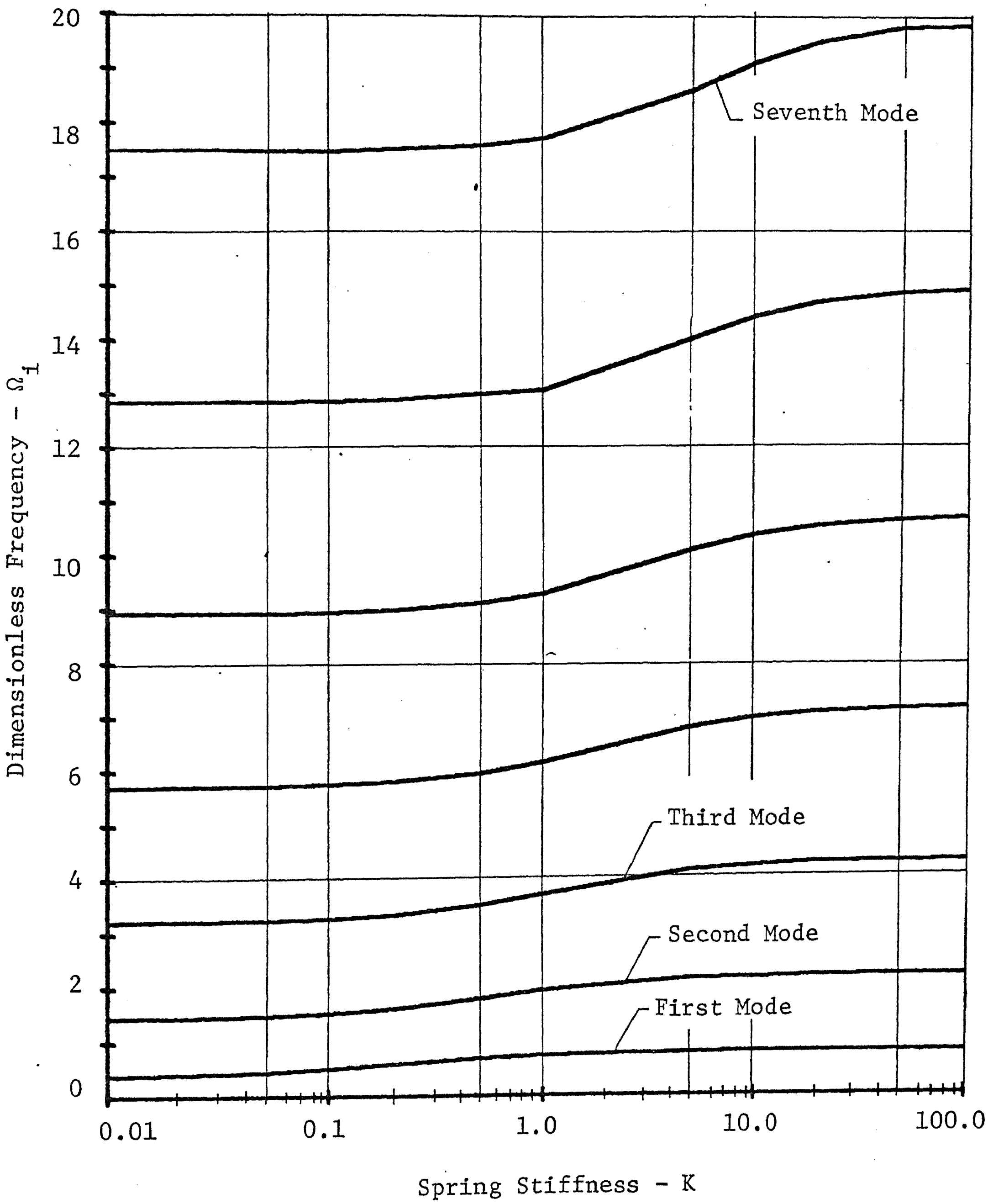

Figure 84 Frequency Spectrum of Spring-Loaded Clamped Circular Plate, Classical Theory, $\frac{h}{a}$ = 0.125

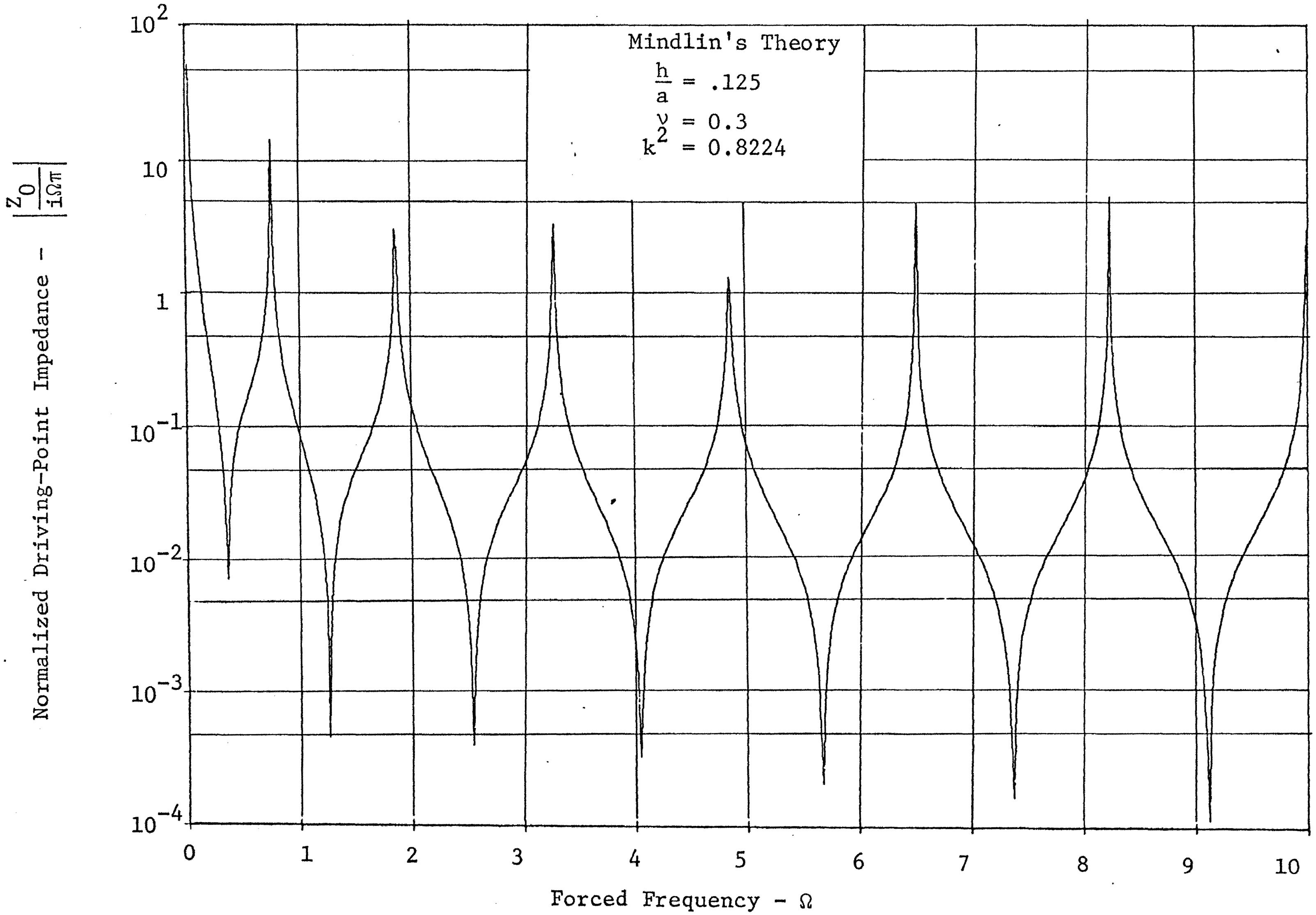

Figure 85 Normalized Driving-Point Impedance of Clamped Circular Plate Driven at the Center

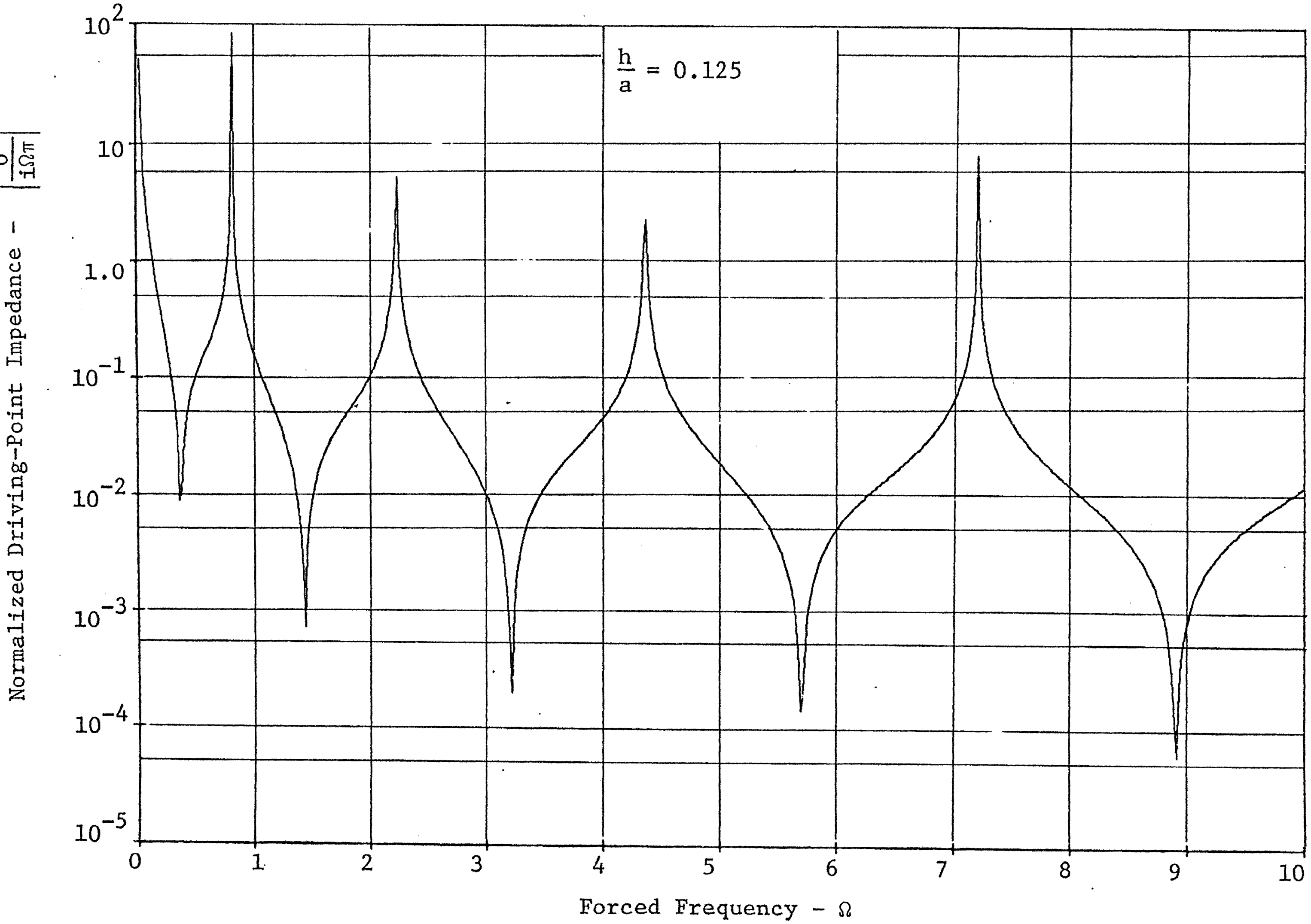

Figure 86 Normalized Driving-Point Impedance of Clamped Circular Plate Driven at the Center, Classical Theory

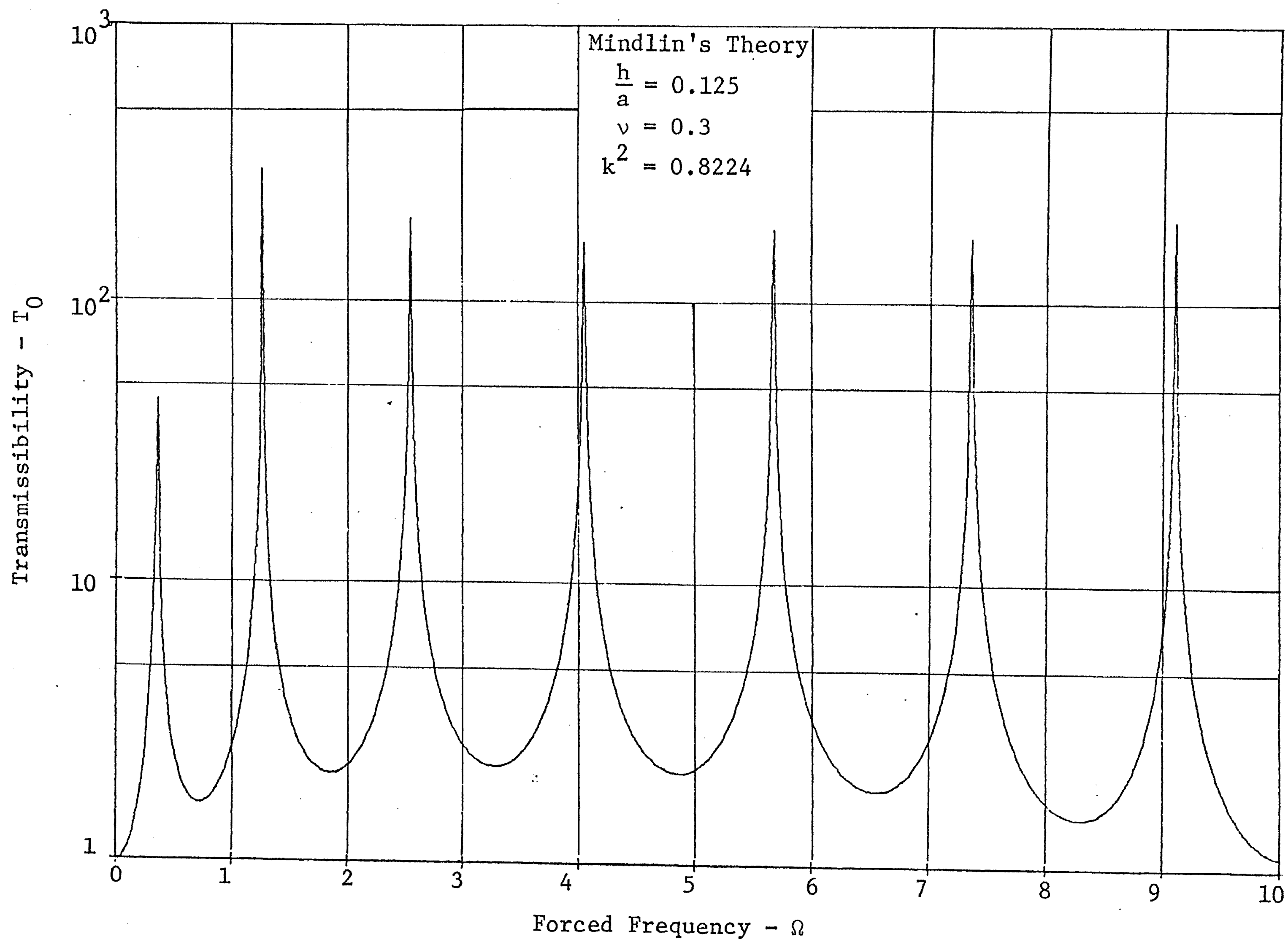

Figure 87 Transmissibility Across Clamped Circular Plate Driven at the Center

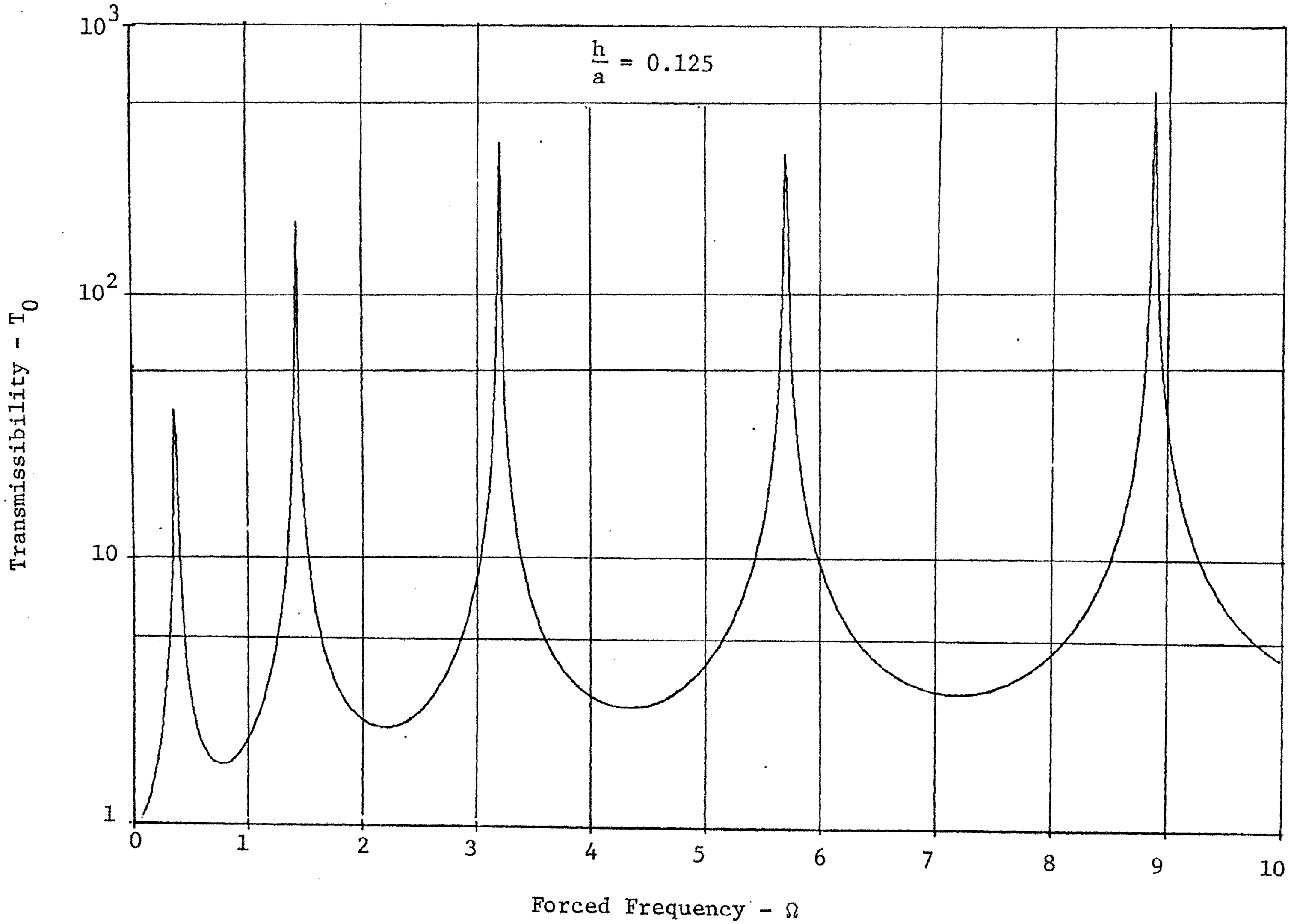

Figure 88 Transmissibility Across Clamped Circular Plate Driven at the Center, Classical Theory

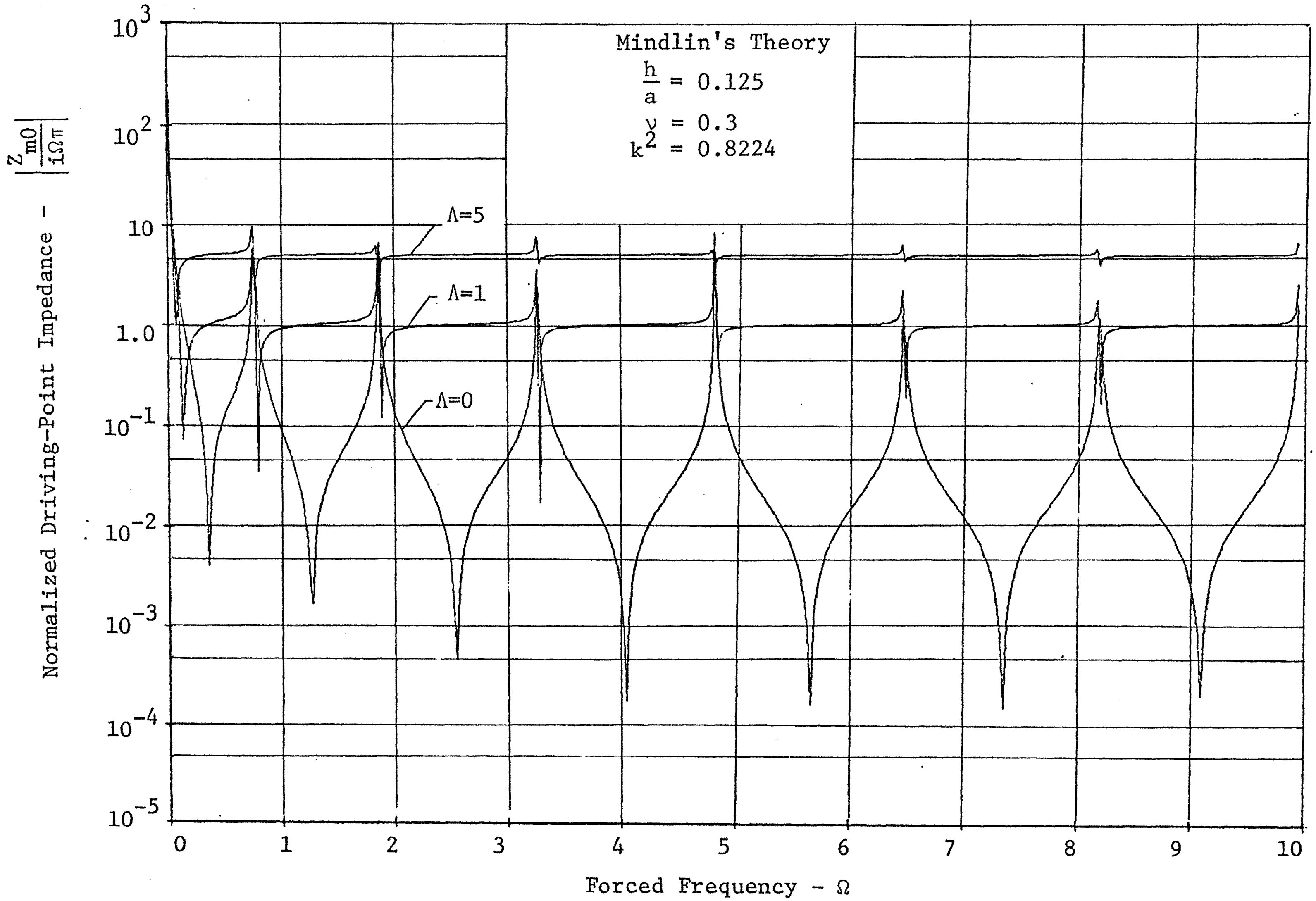

Figure 89 Normalized Driving-Point Impedance of Mass-Loaded Clamped Circular Plate Driven at the Center

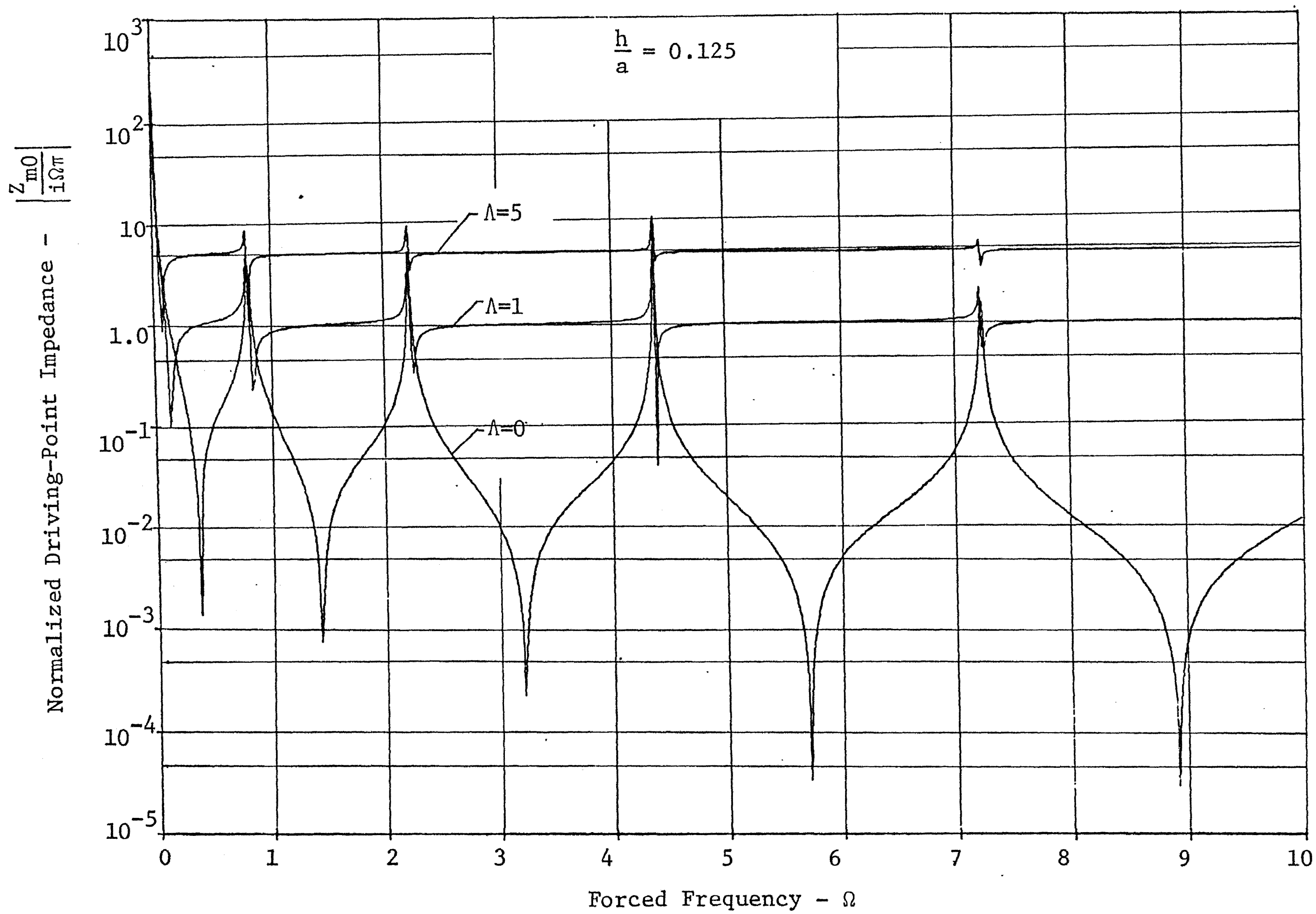

Figure 90 Normalized Driving-Point Impedance of Mass-Loaded Clamped Circular Plate Driven at the Center, Classical Theory

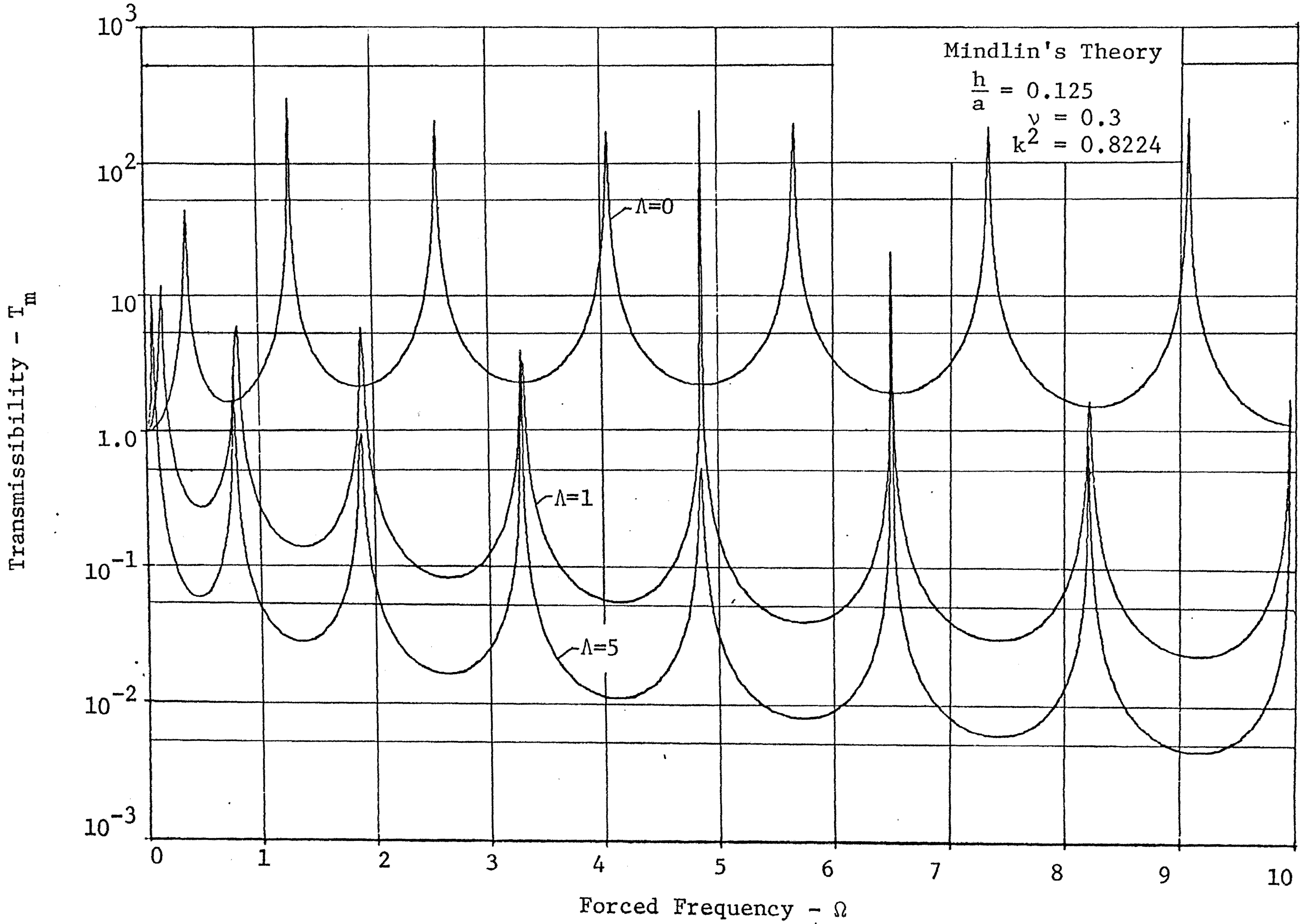

Figure 91 Transmissibility Across Mass-Loaded Clamped Circular Plate Driven at the Center

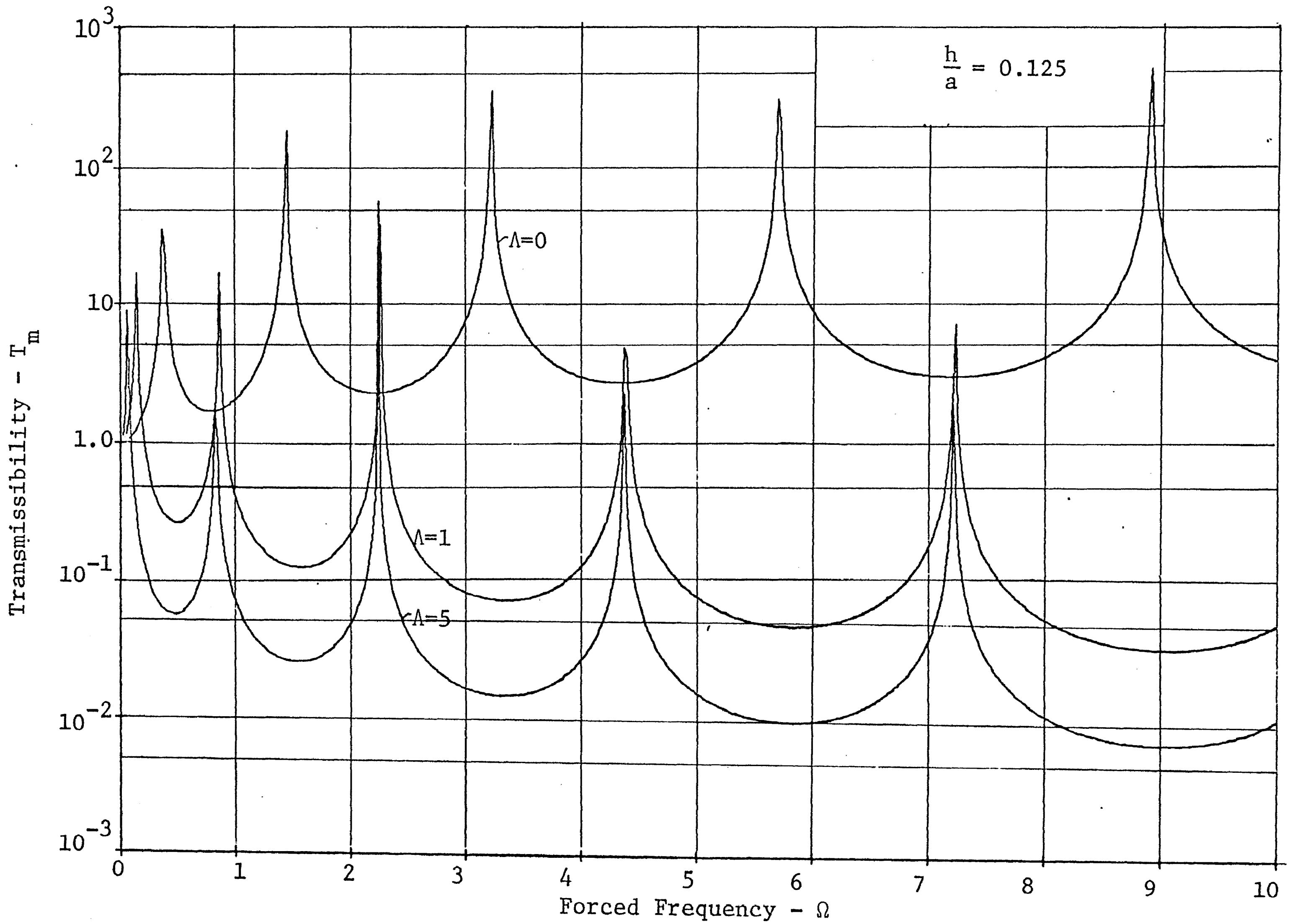

Figure 92 Transmissibility Across Mass-Loaded Clamped Circular Plate Driven at the Center, Classical Theory

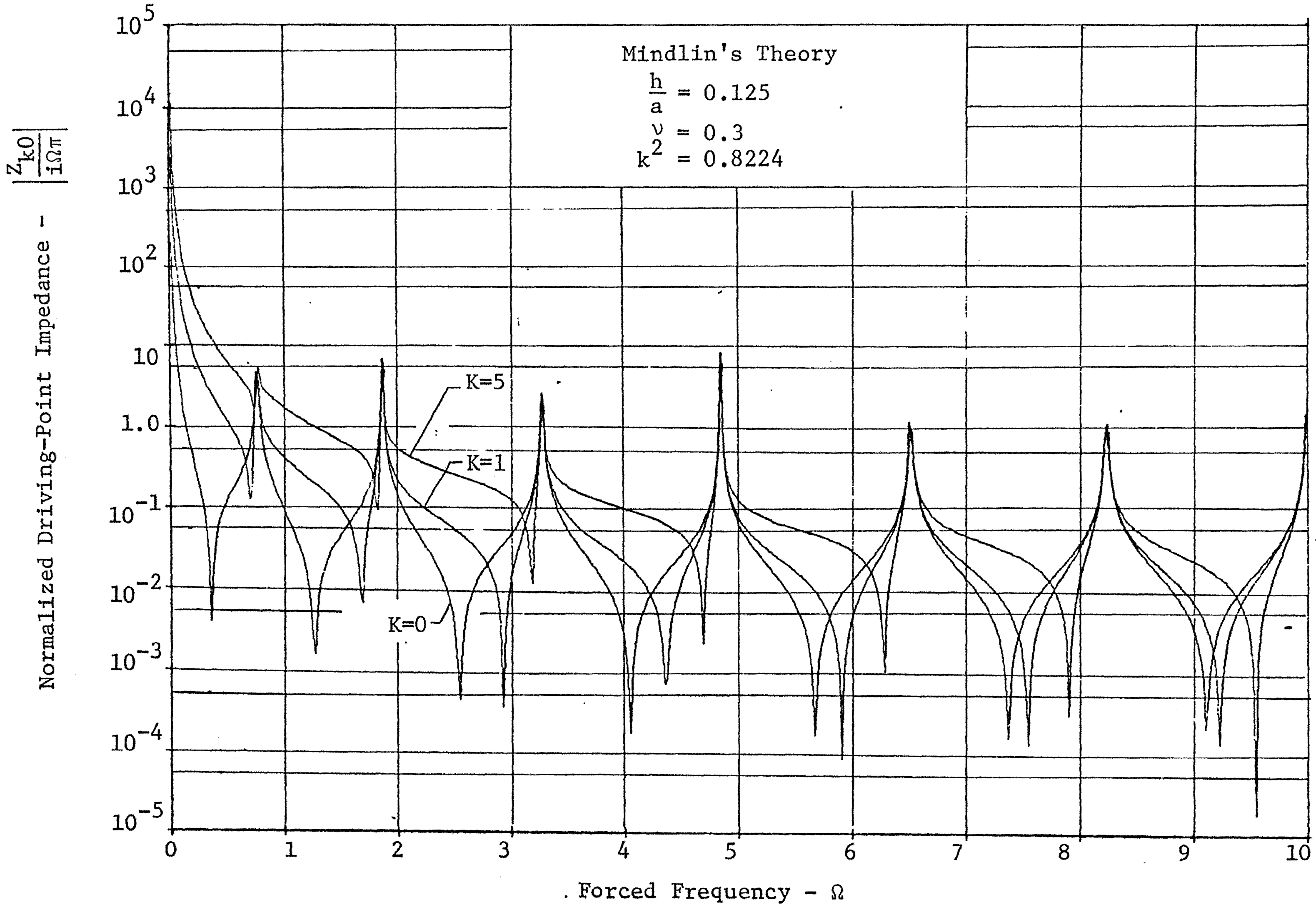

Figure 93 Normalized Driving-Point Impedance of Spring-Loaded Clamped Circular Plate Driven at the Center

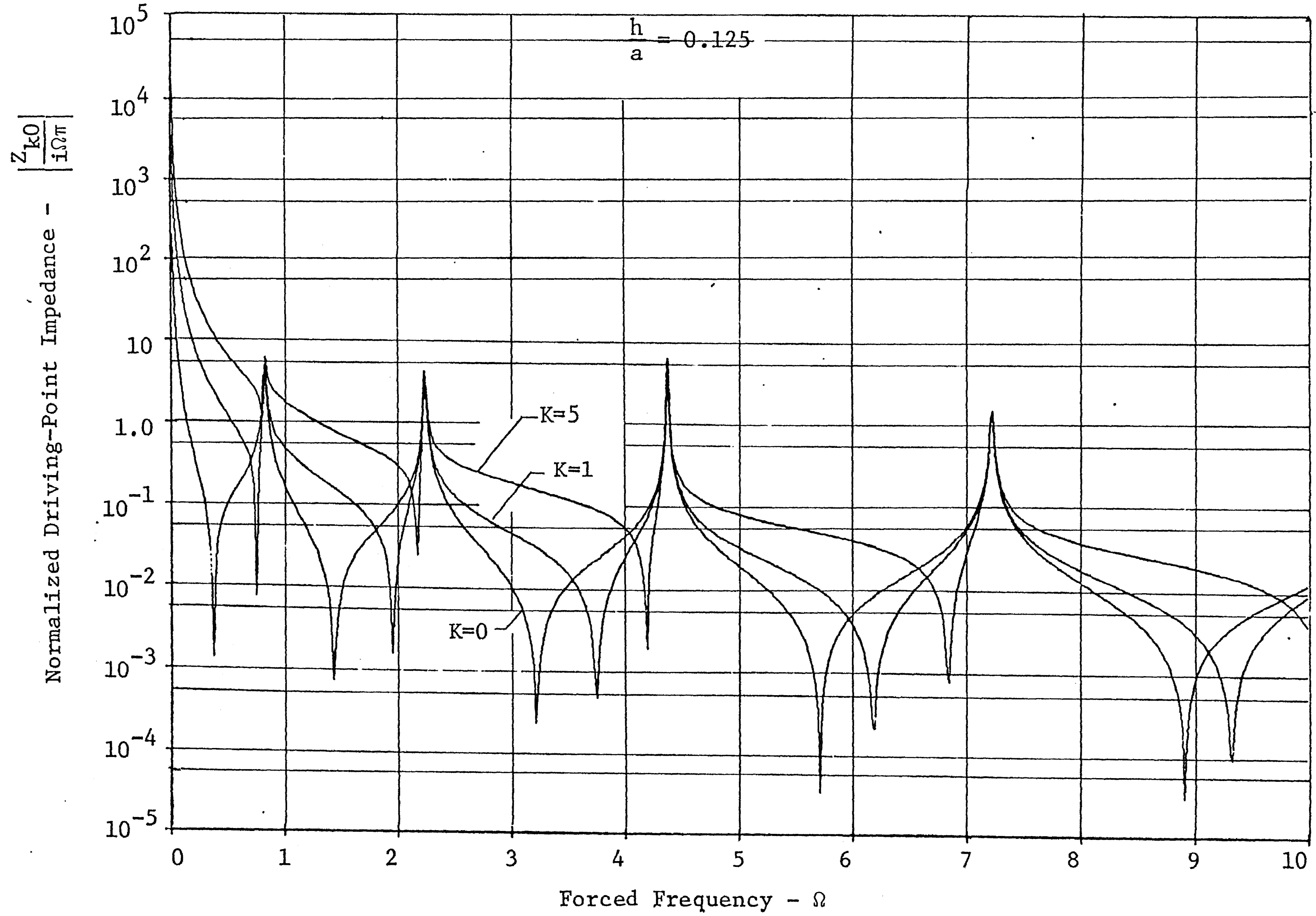

Figure 94 Normalized Driving-Point Impedance of Spring-Loaded Clamped Circular Plate Driven at the Center, Classical Theory

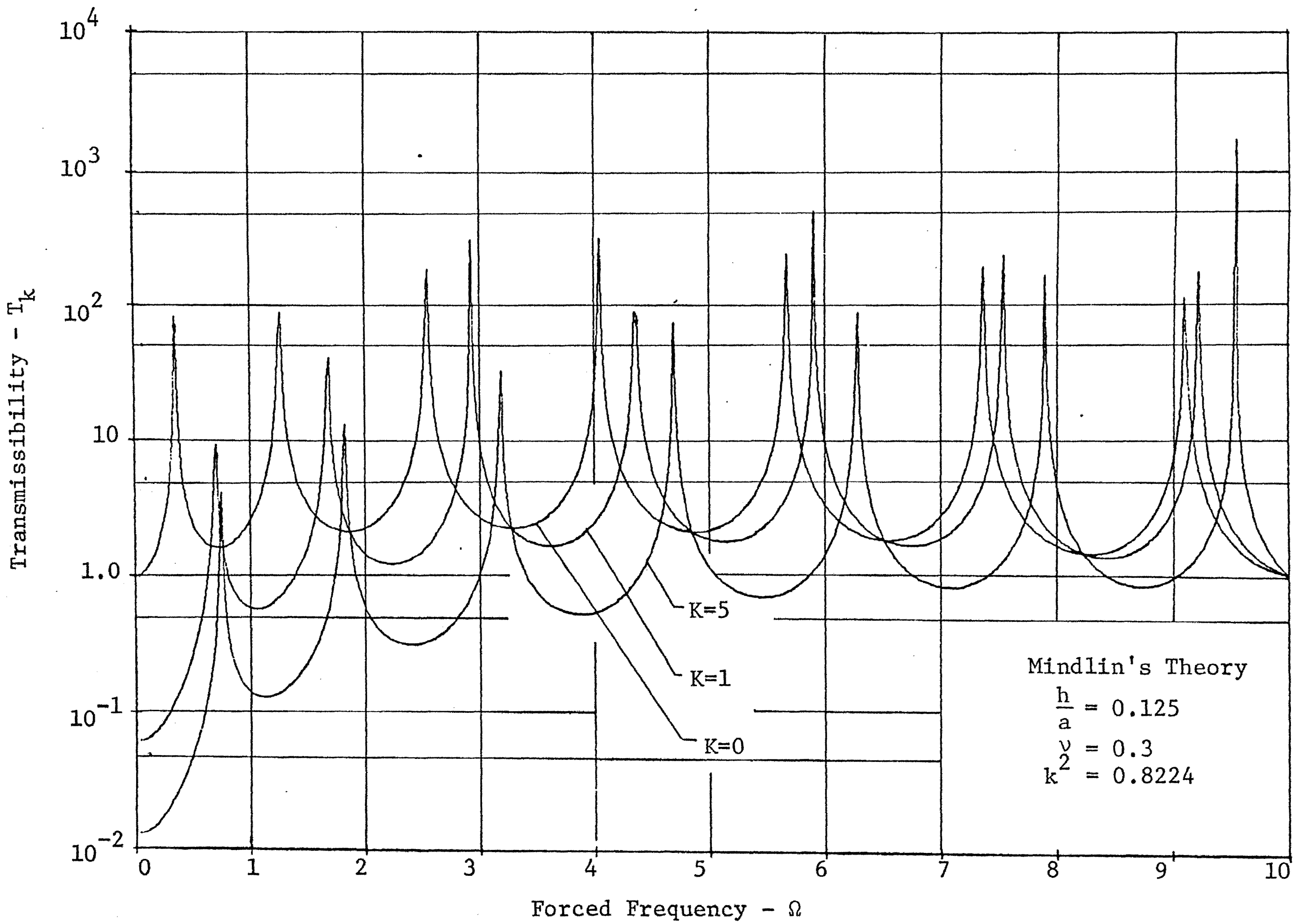

Figure 95 Transmissibility Across Spring-Loaded Clamped Circular Plate Driven at the Center

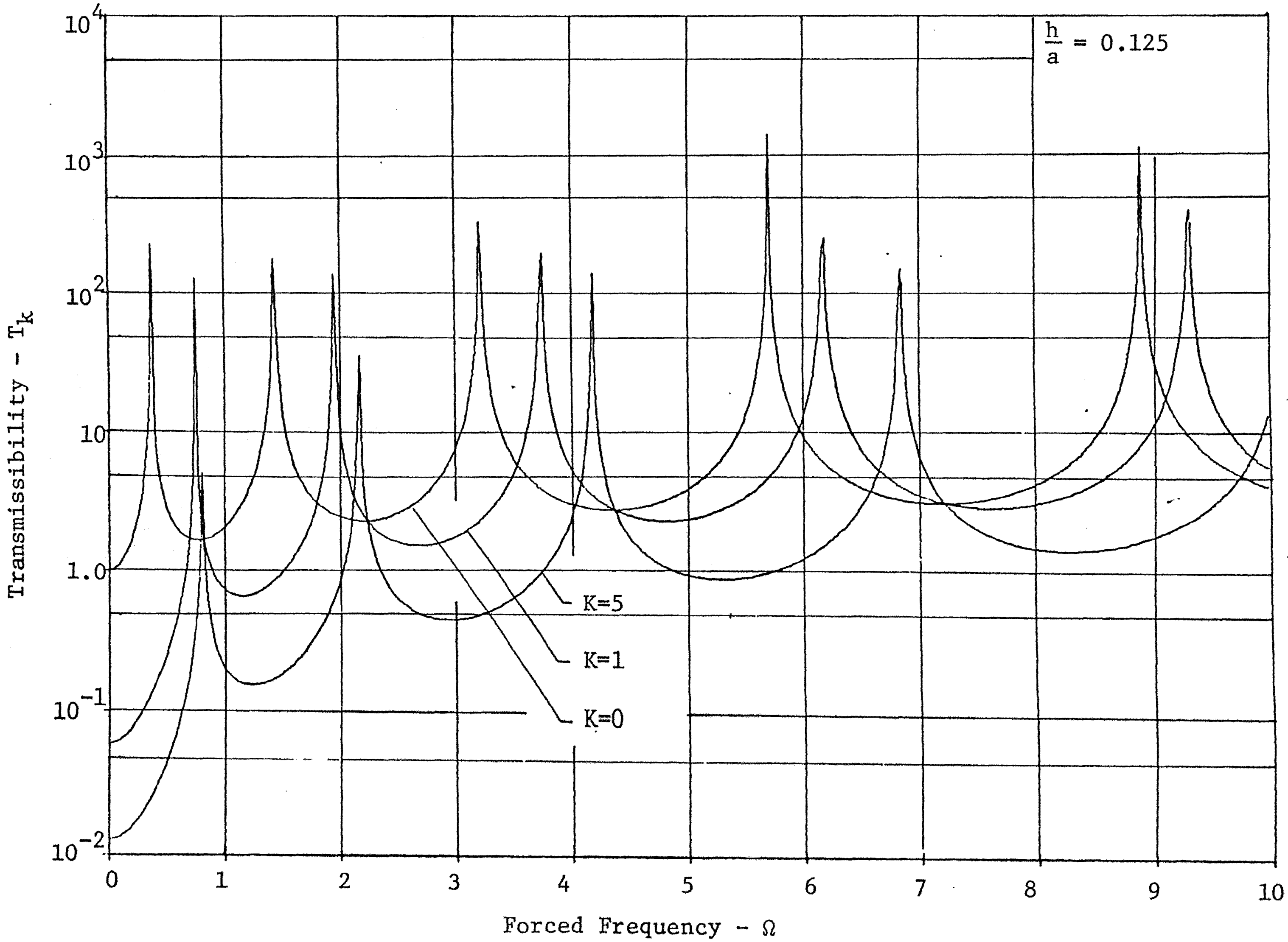

Figure 96 Transmissibility Across Spring-Loaded Clamped Circular Plate Driven at the Center, Classical Theory

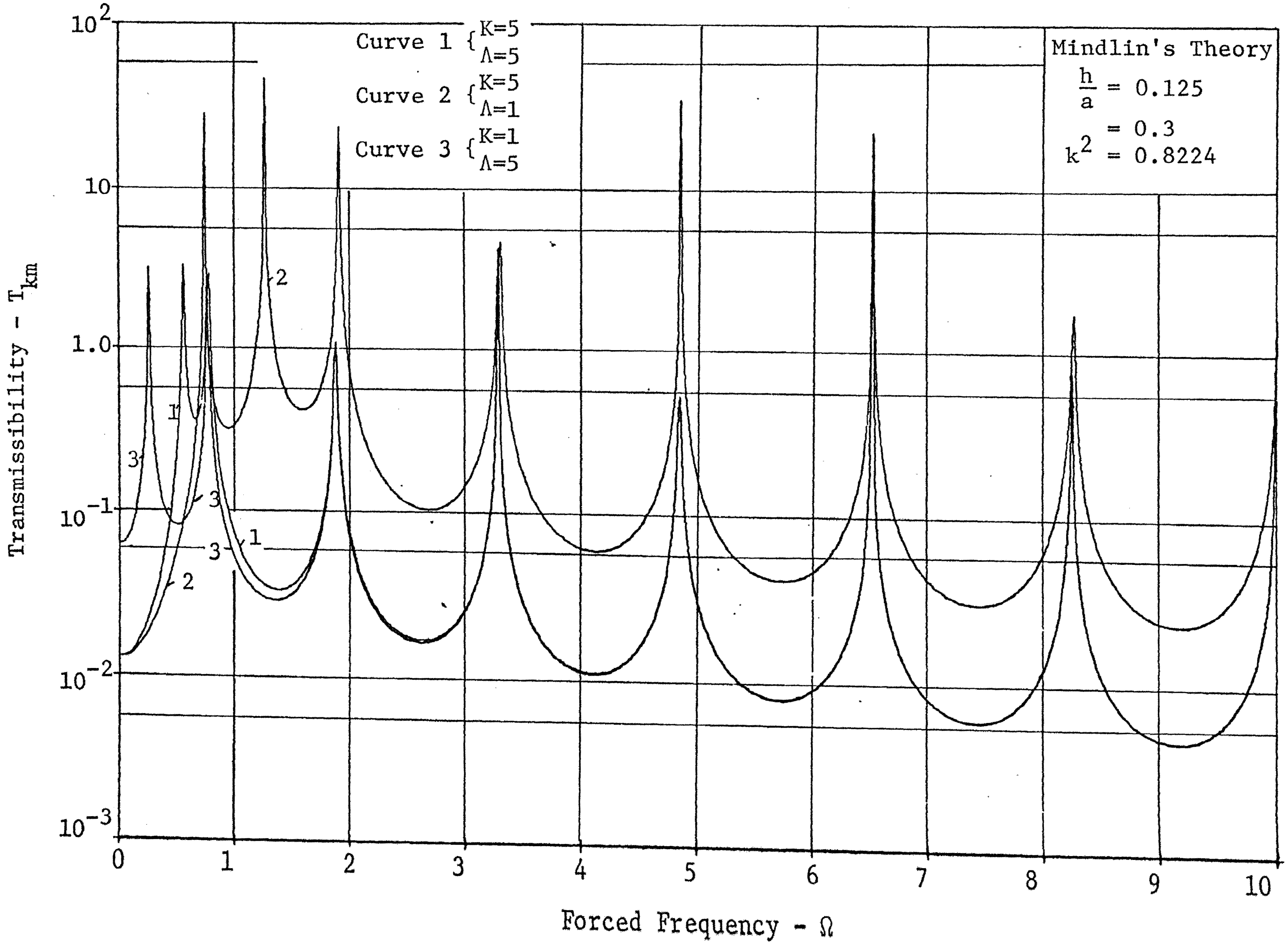

Figure 97 Transmissibility Across Clamped Circular Plate with Mass and Spring Attached to the Center and Driven at the Center

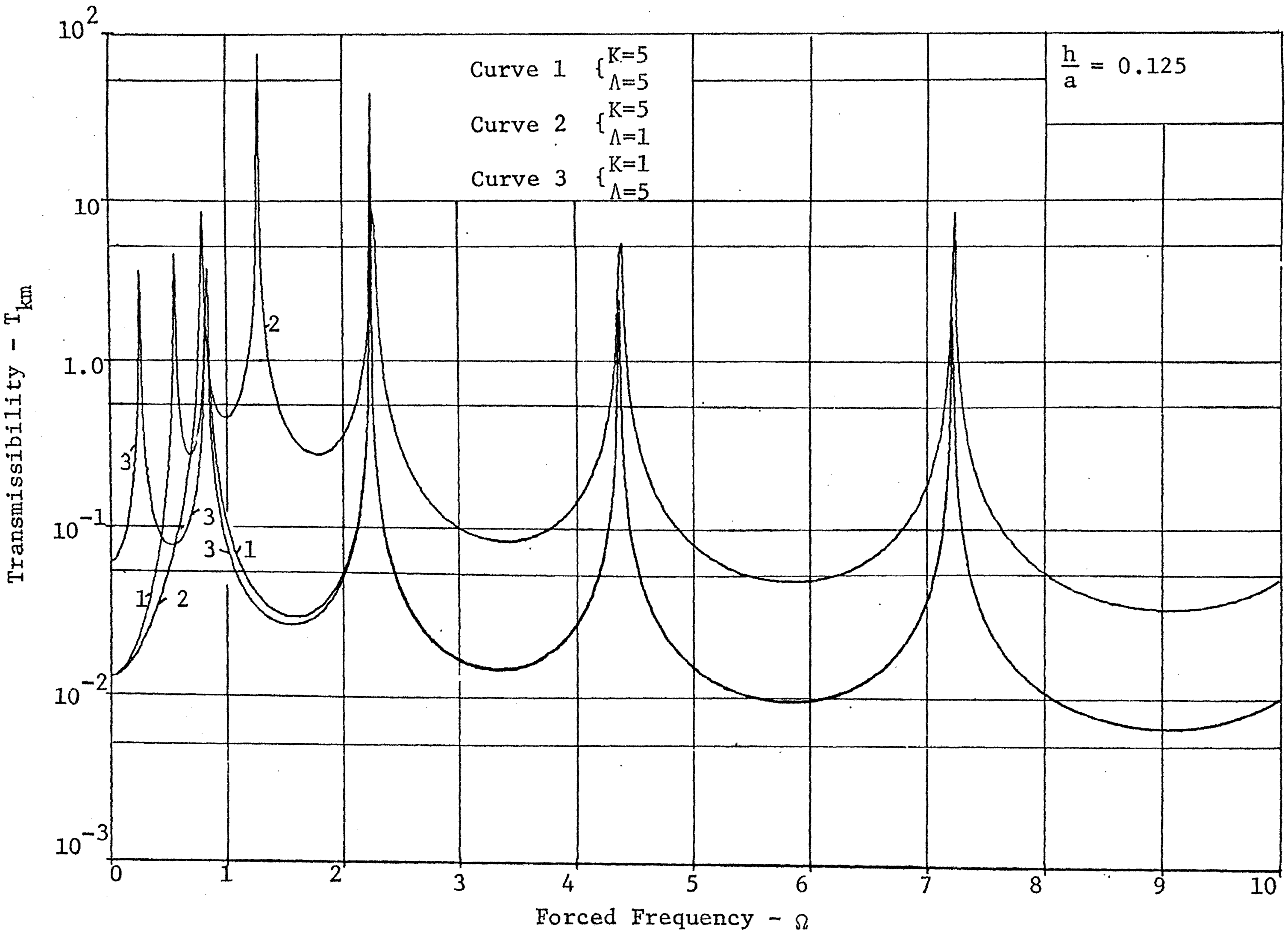

Figure 98 Transmissibility Across Clamped Circular Plate with Mass and Spring Attached to the Center and Driven at the Center, Classical Theory

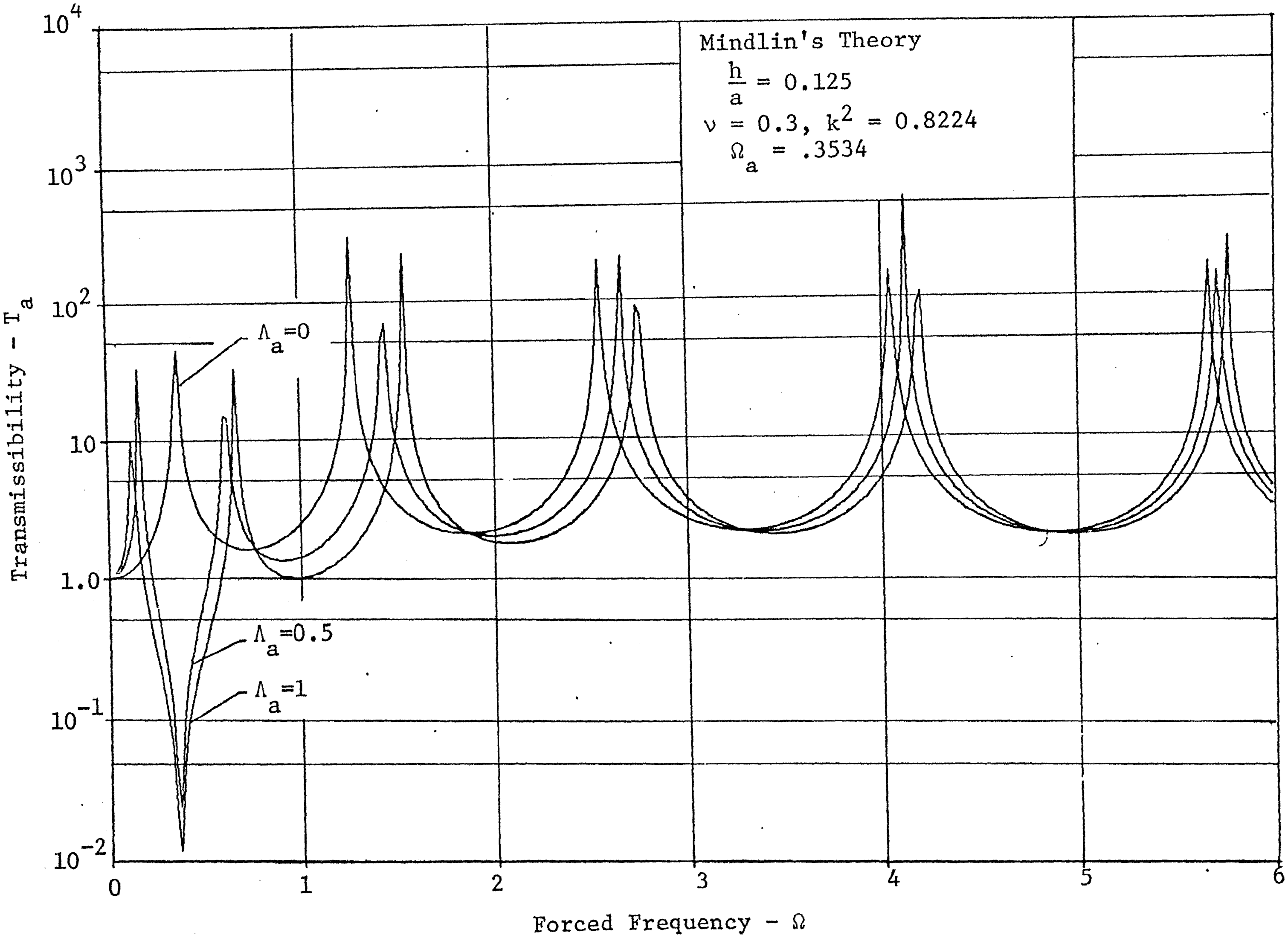

Figure 99 Transmissibility Across Clamped Circular Plate with Absorber Tuned to the First Resonant Frequency of the Plate

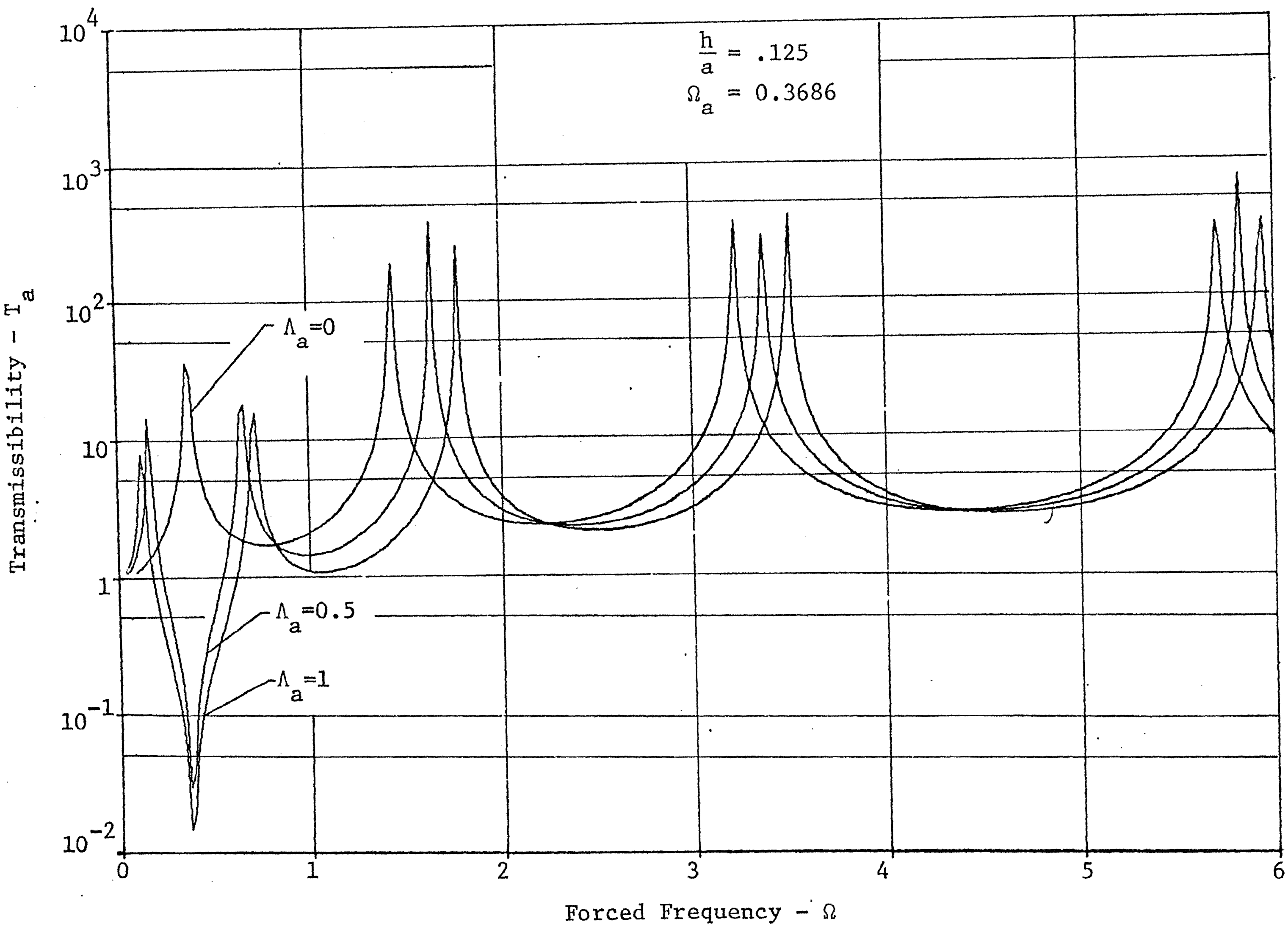

Figure 100 Transmissibility Across Clamped Circular Plate with Absorber Tuned to the First Resonant Frequency of the Plate, Classical Theory

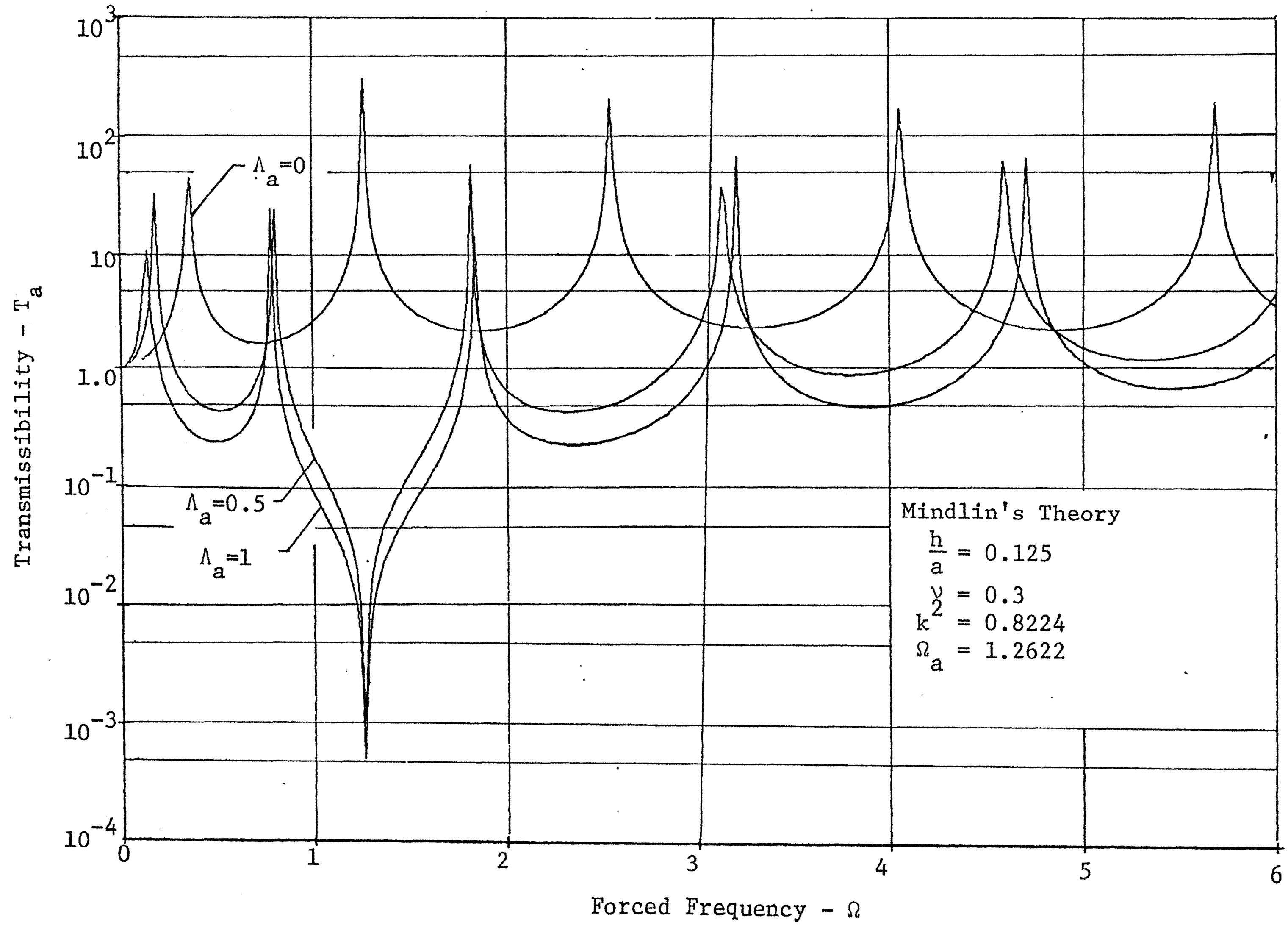

Figure 101 Transmissibility Across Clamped Circular Plate with Absorber Tuned to the Second Resonant Frequency of the Plate

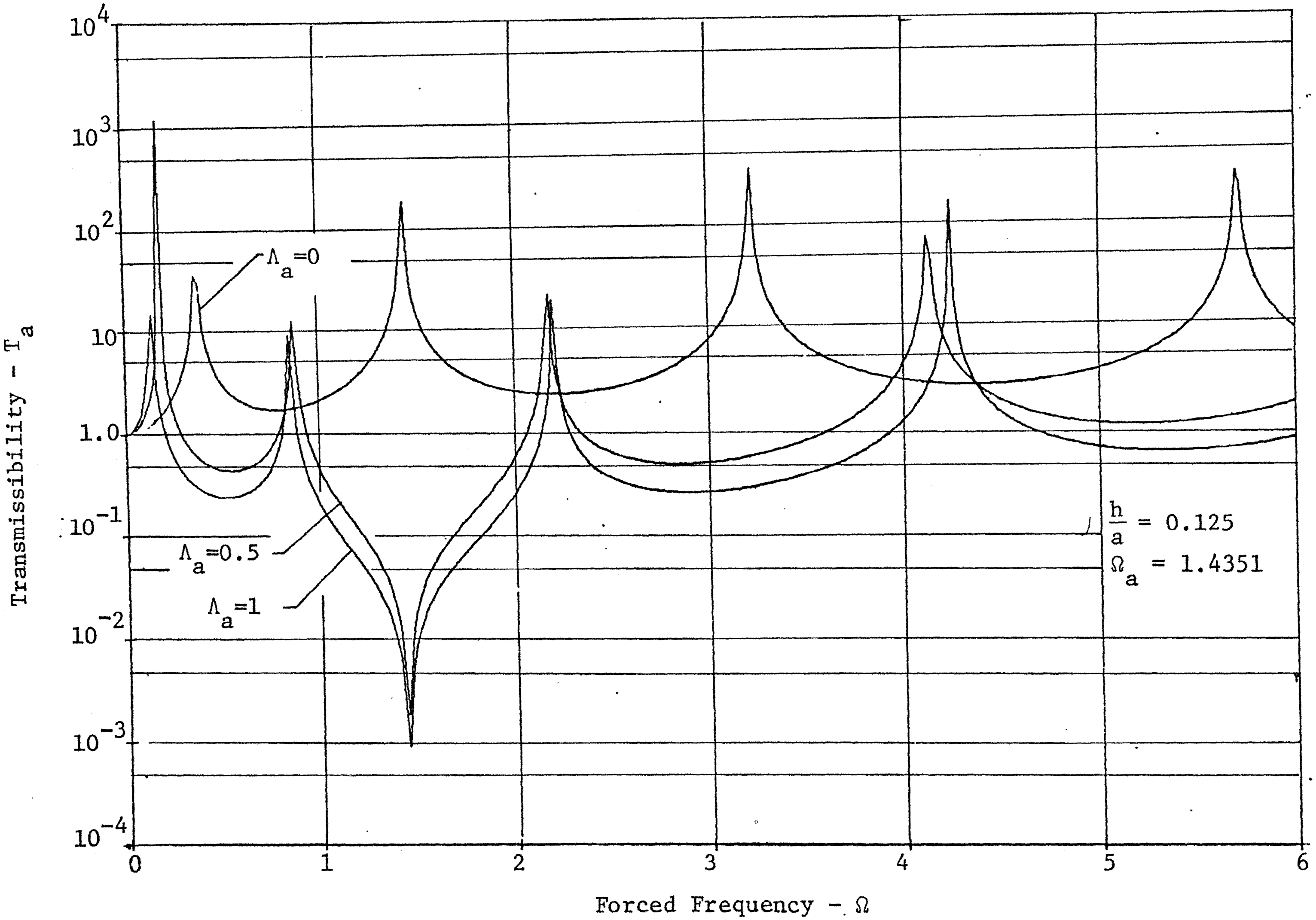

Figure 102 Transmissibility Across Clamped Circular Plate with Absorber Tuned to the Second Resonant Frequency of the Plate, Classical Theory

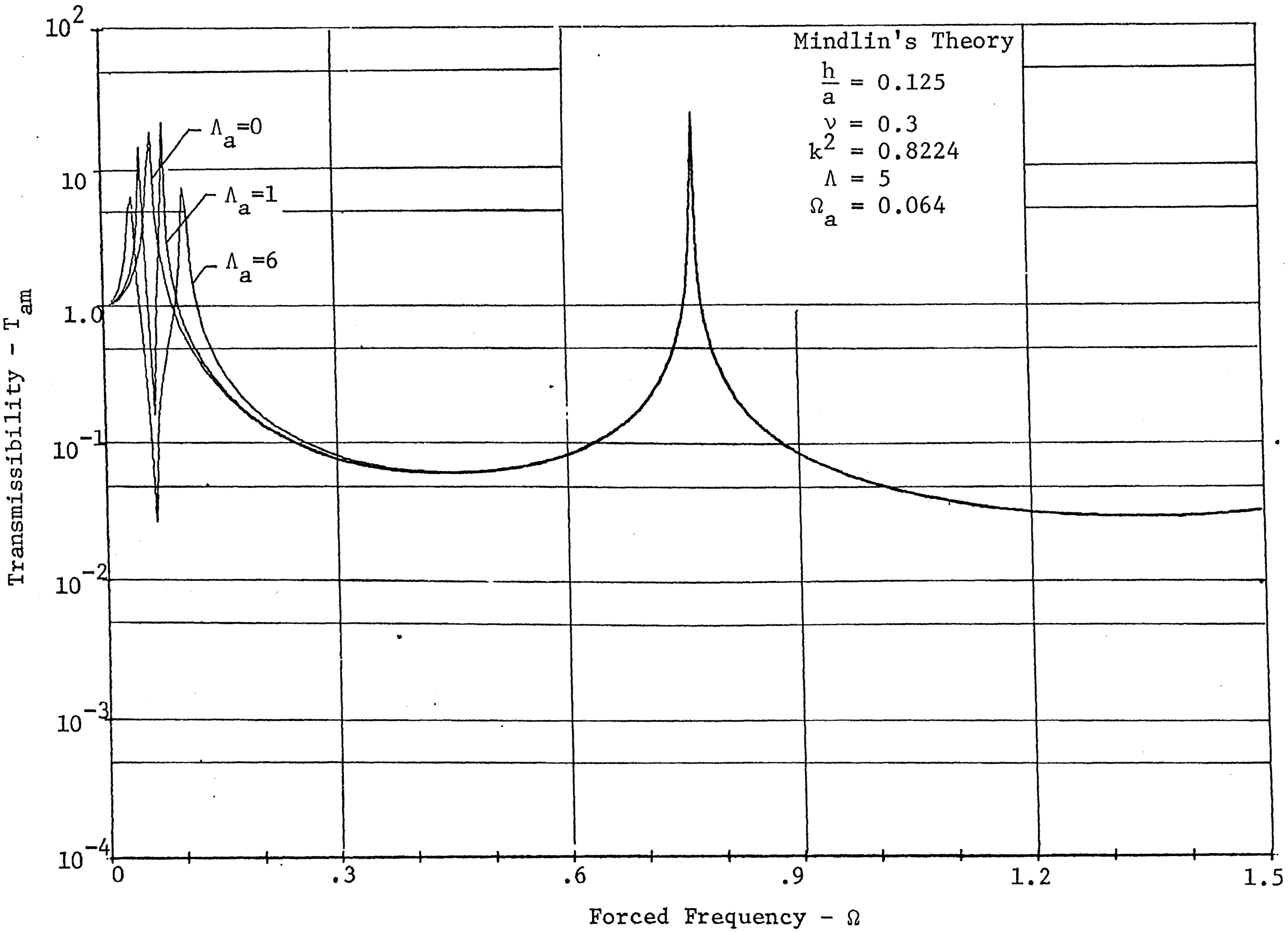

Figure 103 Transmissibility Across Mass-Loaded Clamped Circular Plate with Absorber Tuned to the First Resonant Frequency of the Loaded Plate

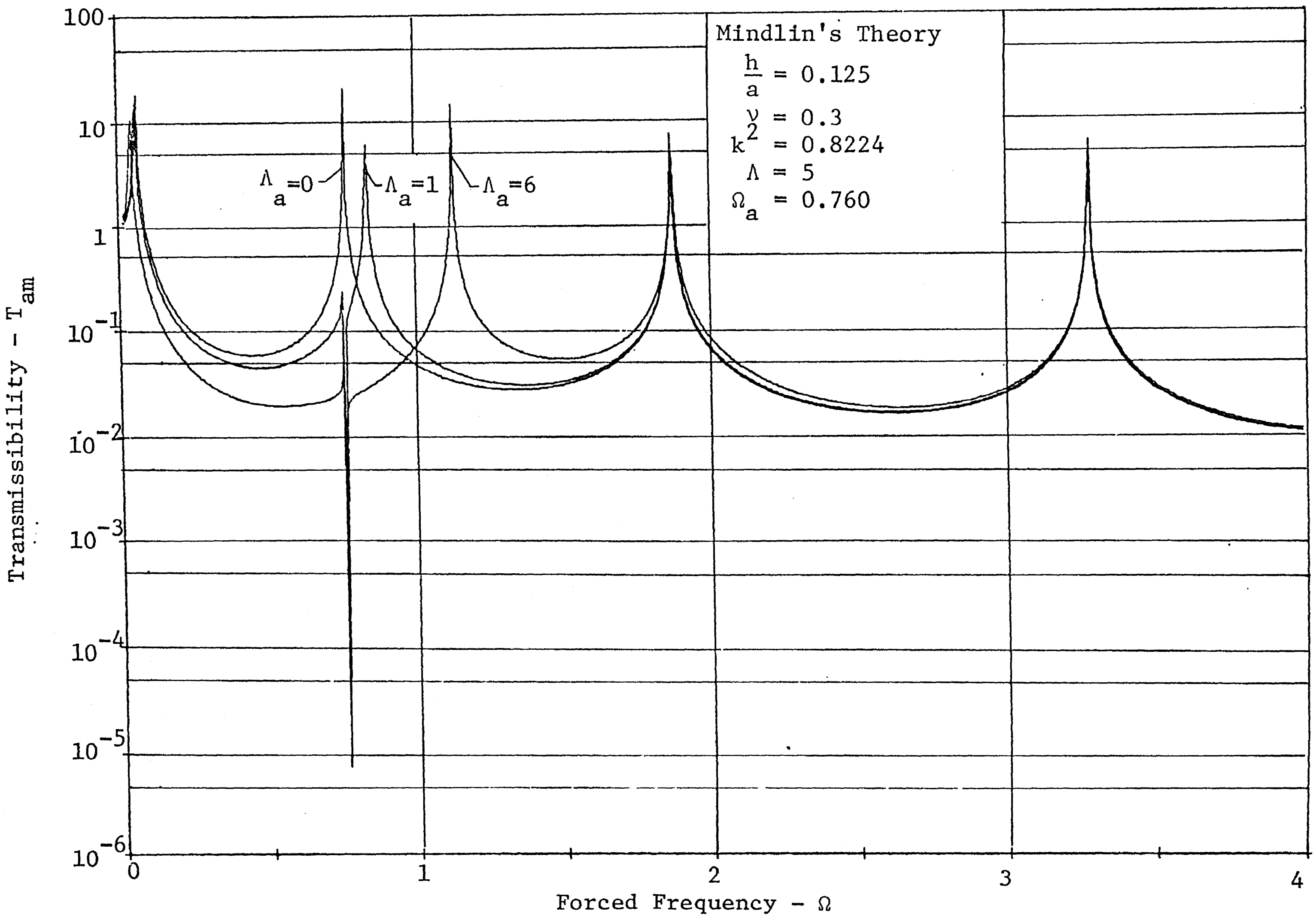

Figure 104 Transmissibility Across Mass-Loaded Clamped Circular Plate with Absorber Tuned to the Second Resonant Frequency of the Loaded Plate

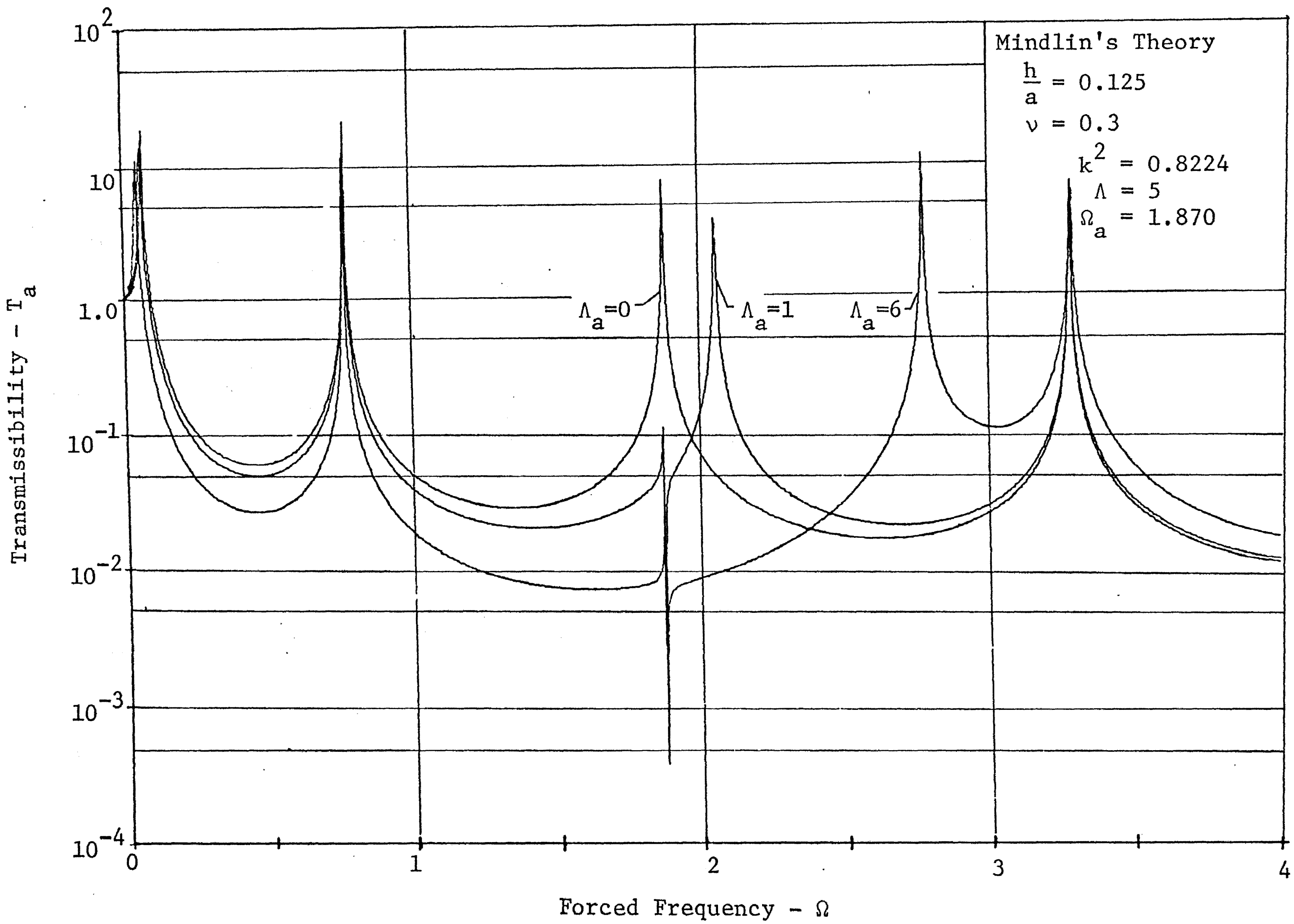

Figure 105 Transmissibility Across Mass-Loaded Clamped Circular Plate with Absorber Tuned to the Third Resonant Frequency of the Loaded Plate

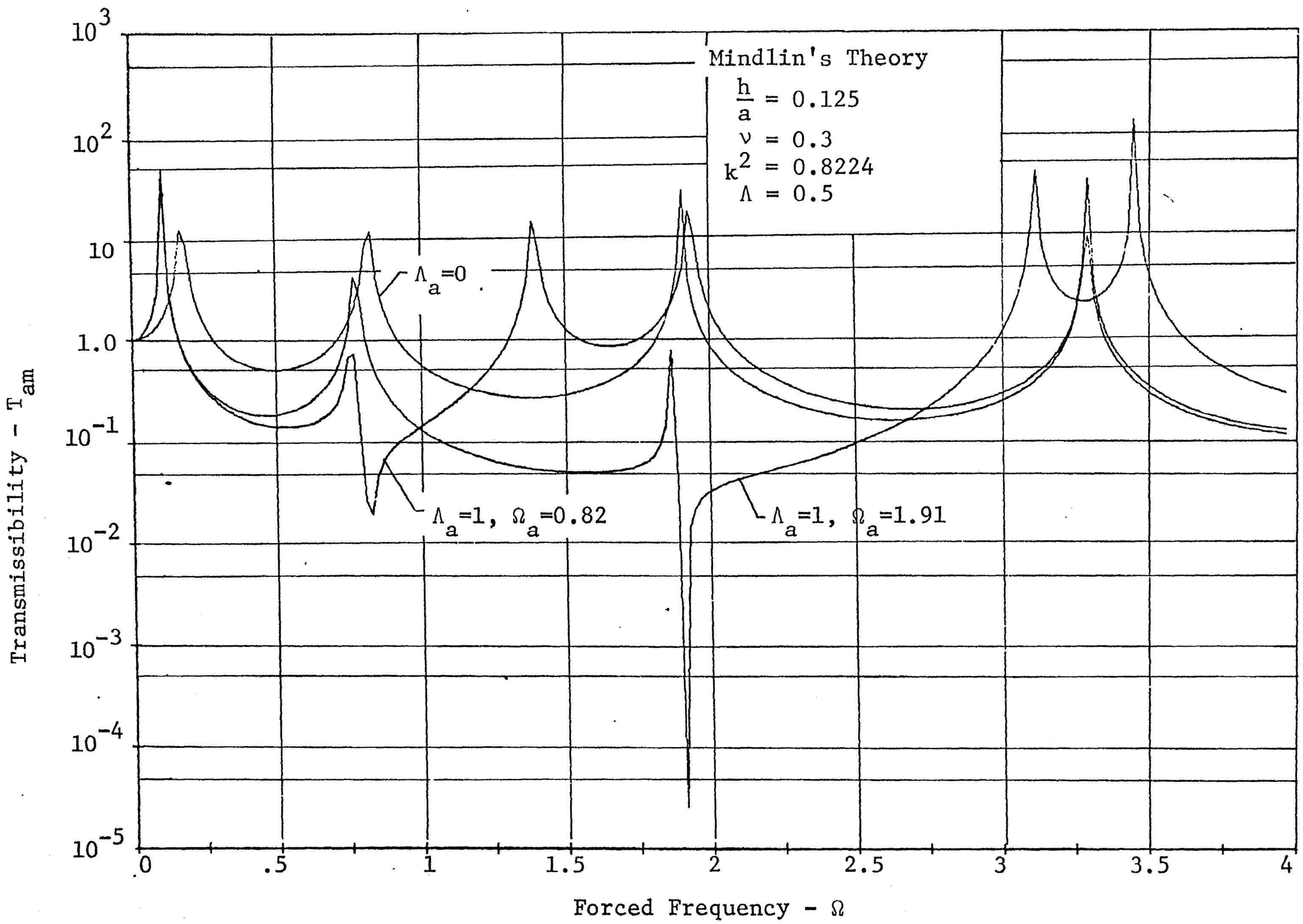

Figure 106 Transmissibility Across Mass-Loaded Clamped Circular Plate with Absorber Tuned to the Second and Third Resonant Frequencies of the Loaded Plate

TABLE I

First 100 Natural Frequencies of Clamped Circular Plate, $\frac{h}{a} = .125$

(Mindlin's Theory, $\nu = .3$, $k^2 = .8224$

0.3534	30.281	56.884	84.290
1.2622	30.829	57.839	85.032
2.5447	32.062	59.515	86.716
4.0464	33.490	59.908	87.373
5.6742	33.857	61.243	88.419
7.3746	35.512	62.837	90.100
9.1162	36.356	63.018	90.462
10.8797	37.268	64.645	91.806
12.6526	38.924	65.928	93.454
14.4236	39.258	66.365	93.584
15.4812	40.704	68.045	95.193
16.192	42.053	68.981	96.615
16.806	42.464	69.757	96.900
17.967	44.134	71.440	98.578
18.605	45.002	72.038	99.716
19.761	45.872	73.151	100.278
20.698	47.546	74.825	101.962
21.557	47.968	75.108	102.815
22.967	49.291	76.545	103.660
23.378	50.837	78.110	105.345
25.025	51.068	78.282	105.917
25.555	52.706	79.937	107.043
26.824	53.872	81.209	108.724
28.080	54.435	81.646	109.023
28.615	56.116	83.328	110.426

TABLE II

First 100 Natural Frequencies of Clamped Circular Plate, $\frac{h}{a} = .25$

(Mindlin's Theory, $\nu = .3$, $k^2 = 8.224$)

0.6355	29.547	56.692	83.725
1.9668	30.315	57.989	85.410
3.5666	31.266	58.390	86.055
5.2722	32.945	60.073	87.100
7.0146	33.357	61.101	88.785
8.5087	34.665	61.768	89.182
8.8355	36.296	63.453	90.476
10.4224	36.455	64.214	92.156
10.7352	38.064	65.147	92.314
12.2957	39.437	66.831	93.851
13.066	39.773	67.330	95.426
14.081	41.451	68.525	95.547
15.617	42.520	70.207	97.226
15.919	43.156	70.451	98.561
17.538	44.840	71.903	98.916
18.510	45.606	73.535	100.601
19.293	46.541	73.620	101.693
20.967	48.225	75.281	102.290
21.421	48.700	76.679	103.975
22.720	49.926	76.975	104.824
24.260	51.601	78.658	105.664
24.500	51.805	79.804	107.349
26.138	53.310	80.349	107.955
27.294	54.868	82.034	109.038
27.866	55.023	82.929	110.732

TABLE III

First 100 Natural Frequencies of Clamped Circular Plate, $\frac{h}{a} = .5$

(Mindlin's Theory, $\nu = .3$, $k^2 = .8224$)

0.9618	29.371	56.834	83.823
2.4978	29.832	57.496	85.508
4.1876	31.516	58.526	85.718
5.4954	32.486	60.211	87.195
5.9950	33.209	60.630	88.846
7.6565	34.894	61.899	88.890
8.1982	35.605	63.583	90.568
9.4300	36.587	63.766	91.992
10.9617	38.271	65.273	92.255
11.2202	38.727	66.890	93.940
12.855	39.963	66.967	95.130
13.996	41.645	68.646	95.626
14.581	41.854	70.032	97.312
16.263	43.339	70.334	98.269
17.036	44.958	72.019	98.998
17.975	45.043	73.168	100.684
19.657	46.715	73.706	101.408
20.104	48.100	75.299	102.370
21.365	48.406	76.305	104.056
23.031	50.090	77.078	104.547
23.203	51.231	78.764	105.742
24.752	51.779	79.442	107.427
26.255	53.464	80.451	107.686
26.460	54.363	82.136	109.114
28.135	55.152	82.580	110.794

TABLE IV

First 100 Natural Frequencies of Simply Supported Circular Plate, $\frac{h}{a} = .125$

(Mindlin's Theory, $\nu = .3$, $k^2 = .8224$)

0.1757	29.443	56.125	83.331
0.9928	30.318	57.832	85.027
2.2560	32.058	58.380	85.828
3.7850	32.163	59.537	86.722
5.4099	33.794	61.241	88.417
7.2079	34.942	61.395	88.908
8.9931	35.526	62.945	90.111
10.7935	37.255	64.422	91.806
12.5974	37.770	64.647	91.890
14.3988	38.982	66.349	93.499
15.065	40.637	67.458	95.080
16.058	40.705	68.050	95.193
16.196	42.426	69.750	96.887
17.635	43.538	70.503	98.171
17.984	44.145	71.449	98.580
19.606	45.861	73.148	100.272
19.765	46.466	73.556	101.265
21.540	47.576	74.847	101.965
21.839	49.289	76.544	103.658
23.307	49.417	76.616	104.362
24.254	51.000	78.242	105.350
25.068	52.389	79.681	107.042
26.799	52.710	79.939	107.462
26.825	54.419	81.635	108.734
28.573	55.377	82.752	110.425

TABLE V

First 100 Natural Frequencies of Simply Supported Circular Plate, $\frac{h}{a} = .25$

(Mindlin's Theory, $\nu = .3$, $k^2 = .8224$)

0.3389	28.890	56.438	83.724
1.6782	29.556	56.693	84.489
3.3789	31.260	58.384	85.412
5.1675	31.819	59.544	87.100
6.9721	32.962	60.075	87.614
7.8139	34.663	61.765	88.788
8.7684	34.858	62.654	90.476
9.5009	36.362	63.455	90.741
10.5490	37.914	65.145	92.163
11.7854	38.060	65.767	93.851
12.315	39.758	66.835	93.869
14.068	40.981	68.525	95.539
14.360	41.454	68.833	96.997
15.812	43.149	70.214	97.226
17.098	44.059	71.903	98.914
17.548	44.844	72.001	100.126
19.276	46.538	73.592	100.601
19.938	47.145	75.120	102.288
20.990	48.232	75.281	103.257
22.717	49.925	76.970	103.975
22.848	50.237	78.242	105.663
24.431	51.617	78.659	106.387
25.806	53.310	80.347	107.350
26.142	53.335	81.365	109.037
27.850	55.001	82.035	109.519

TABLE VI

First 100 Natural Frequencies of Simply Supported Circular Plate, $\frac{h}{a} = .5$

(Mindlin's Theory, $\nu = .3$, $k^2 = .8224$)

0.6620	28.136	55.926	83.823
2.3473	29.827	56.839	84.146
4.1517	30.924	58.526	85.509
4.4043	31.517	59.059	87.195
5.9381	33.207	60.212	87.283
6.7904	34.039	61.899	88.882
7.6905	34.896	62.193	90.421
9.4230	36.585	63.586	90.568
9.5688	37.158	65.270	92.254
11.1456	38.269	65.327	93.559
12.498	39.963	66.959	93.940
12.859	40.281	68.462	95.626
14.566	41.651	68.646	96.698
15.504	43.339	70.332	97.312
16.270	43.406	71.598	98.998
17.970	45.027	72.019	99.836
18.551	46.534	73.705	100.684
19.668	46.715	74.734	102.370
21.364	48.402	75.392	102.975
21.625	49.663	77.078	104.056
23.058	50.090	77.871	105.742
24.714	51.777	78.764	106.114
24.752	52.794	80.450	107.428
26.444	53.464	81.008	109.114
27.815	55.152	82.137	109.253

TABLE VII

First 25 Natural Frequencies of Clamped Circular Plate, Classical Theory, $\nu = .3$

h/a = .125	h/a = .250	h/a = .50
0.3686	0.7372	1.4744
1.4351	2.8702	5.7403
3.2152	6.4305	12.8610
5.7079	11.4159	22.8318
8.9130	17.8260	35.6522
12.8305	25.6610	51.3220
17.4602	34.9204	69.8408
22.8022	45.6045	91.2090
28.8565	57.7130	115.4262
35.6230	71.2462	142.4926
43.102	86.204	172.408
51.293	102.586	205.172
60.196	120.393	240.786
69.812	139.624	279.250
80.140	160.280	320.561
91.180	182.361	364.722
102.933	205.866	411.732
115.398	230.797	461.592
128.575	257.150	514.300
142.464	284.929	569.858
157.066	314.132	628.265
172.380	344.760	689.520
188.406	376.813	753.626
205.144	410.290	820.580
222.595	445.191	890.382

TABLE VIII

First 25 Natural Frequencies of Simply Supported Circular Plate, Classical Theory, $\nu = .3$

h/a = .125	h/a = .250	h/a = .50
0.1780	0.3561	0.7123
1.0724	2.1447	4.2896
2.6757	5.3516	10.7034
4.9910	9.9821	19.9644
8.0183	16.0370	32.0738
11.7580	23.5160	47.0322
16.2090	32.4197	64.8395
21.3740	42.7480	85.4958
27.2502	54.5005	109.0010
33.838	67.6777	135.3555
41.139	82.279	164.559
49.152	98.305	196.611
57.878	115.756	231.513
67.316	134.632	269.264
77.466	154.931	309.864
88.328	176.656	353.313
99.902	199.805	399.611
112.189	224.379	448.758
125.188	250.377	500.754
138.899	277.799	555.599
153.323	306.647	613.294
168.459	336.919	673.838
184.307	368.615	737.230
200.868	401.736	803.472
218.140	436.281	872.562

TABLE IX

Frequency versus Poisson's Ratio for Free Circular Plate,

h/a = .125, Mindlin's Theory

(Values given are $\omega a\sqrt{\frac{\rho}{E}}$)

Poisson's Ratio	Mode Number 1	2	3	4	5
.25	0.32326	1.30132	2.70902	4.36562	6.15856
.26	0.32518	1.30488	2.71331	4.36926	6.15880
.27	0.32715	1.30860	2.71690	4.37239	6.15977
.28	0.32812	1.31250	2.71287	4.37604	6.16146
.29	0.33019	1.31553	2.72720	4.38128	6.16283
.30	0.33231	1.31979	2.73183	4.38497	6.16496
.31	0.33448	1.32423	2.73682	4.39028	6.16785
.32	0.33565	1.32782	2.74324	4.39510	6.17045
.33	0.33793	1.33265	2.74899	4.40051	6.17385
.34	0.34027	1.33662	2.75513	4.40651	6.17698
.35	0.34161	1.34187	2.76167	4.41313	6.18095

Poisson's Ratio	Mode Number 6	7	8	9	10
.25	8.01862	9.90761	11.79556	13.65562	15.41964
.26	8.01567	9.89841	11.78013	13.63285	15.38615
.27	8.01258	9.89032	11.76494	13.61049	15.35321
.28	8.01000	9.88229	11.75104	13.58854	15.32083
.29	8.00709	9.87433	11.73739	13.56806	15.28920
.30	8.00575	9.86750	11.72401	13.54698	15.25778
.31	8.00432	9.86077	11.71092	13.52635	15.22608
.32	8.00281	9.85415	11.69811	13.50724	15.19499
.33	8.00228	9.84871	11.68368	13.48756	15.16450
.34	8.00169	9.84341	11.67450	13.46837	15.13357
.35	8.00212	9.83827	11.66373	13.44969	15.10328

TABLE X

Frequency versus Poisson's Ratio for Free Circular Plate

h/a = .25, Mindlin's Theory

(Values given are $\omega a \sqrt{\frac{\rho}{E}}$)

Poisson's Ratio	Mode Number				
	1	2	3	4	5
.25	0.61038	2.14718	3.97626	5.84665	7.60034
.26	0.61308	2.14993	3.97573	5.84087	7.58589
.27	0.61587	2.15296	3.97565	5.83573	7.57119
.28	0.61875	2.15625	3.97604	5.83020	7.55729
.29	0.62172	2.15981	3.97690	5.82429	7.54420
.30	0.62478	2.16366	3.97719	5.82008	7.53088
.31	0.62793	2.16779	3.97902	5.81549	7.51732
.32	0.63119	2.17116	3.97818	5.81053	7.50461
.33	0.63455	2.17589	3.98101	5.80626	7.49167
.34	0.63801	2.17986	3.98224	5.80269	7.47853
.35	0.64158	2.18414	3.98399	5.79877	7.46624

Poisson's Ratio	Mode Number				
	6	7	8	9	10
.25	8.78702	9.65044	10.60681	11.81105	12.67240
.26	8.76235	9.63123	10.58192	11.78945	12.64798
.27	8.73647	9.61198	10.55604	11.76806	12.62488
.28	8.71250	9.59375	10.53229	11.74791	12.60312
.29	8.68732	9.57549	10.50754	11.72276	12.58168
.30	8.66407	9.55721	10.48390	11.70829	12.56264
.31	8.64066	9.54102	10.46136	11.68883	12.54395
.32	8.61816	9.52484	10.43890	11.67067	12.52668
.33	8.59551	9.50866	10.41652	11.65171	12.51190
.34	8.57271	9.49357	10.39529	11.63303	12.49753
.35	8.55191	9.47851	10.37523	11.61463	12.48465

TABLE XI

First 25 Natural Frequencies of Disk Mounted on a Shaft, $\frac{h}{a} = .125$

(Mindlin's Theory, $\nu = .3$, $\beta = .2$, $k^2 = .8224$)

Axisymmetric vibration	Vibration with one diametral node
0.181	0.164
1.008	1.075
2.601	2.674
4.506	4.581
6.582	6.653
8.731	8.789
10.898	10.953
13.017	13.065
14.932	14.910
15.611	14.988
16.865	15.289
17.578	15.690
19.057	16.077
19.975	16.857
21.473	17.045
22.431	17.700
24.110	18.238
24.842	19.089
26.846	19.658
27.356	20.073
29.289	21.166
30.303	21.604
31.666	22.471
33.182	22.943
34.330	24.190

TABLE XII

Frequencies of Clamped Circular Plate with Concentrated Mass Attached at the Center, $\frac{h}{a} = .125$

(Mindlin's Theory, $\Lambda = 1$, $\nu = .3$, $k^2 = .8224$)

Closed-form solution	20 modes series solution
0.134	0.128
0.790	0.731
1.887	1.747
3.289	3.090
4.859	4.635
6.527	6.303
8.252	8.043
10.007	9.828
11.779	11.637
13.567	13.460
14.944	15.248
15.189	15.528
15.523	16.721
16.715	17.210
17.167	18.490
18.473	19.089
18.989	20.522
20.435	21.035
20.921	22.615
22.339	23.168
23.113	

TABLE XIII

Frequencies of Clamped Circular Plate with Spring Attached at the Center, $\frac{h}{a} = .125$

(Mindlin's Theory, $K = 1$, $\nu = .3$, $k^2 = .8224$)

Closed-form solution	20 modes series solution
0.701	0.658
1.682	1.617
2.933	2.900
4.359	4.390
5.913	6.016
7.546	7.717
9.234	9.465
10.953	11.238
12.689	13.023
14.431	14.805
15.479	15.500
16.176	16.529
16.804	16.885
17.934	18.290
18.589	18.723
19.712	20.165
20.686	20.790
21.489	22.063
22.935	23.088
23.324	24.308

TABLE XIV

Frequencies of Constrained Clamped Circular Plate, Classical Theory

($\frac{h}{a}$ = .125, ν = .3, Closed-Form Solution)

Mass attached to center Mass ratio = 1	Spring attached to center Spring constant = 1
0.135	0.751
0.857	1.954
2.258	3.744
4.388	6.181
7.235	9.322
10.789	13.183
15.065	17.767
20.049	23.073
25.747	29.089
32.149	35.827
39.255	43.262
47.055	51.389

TABLE XV

Frequencies of Two Identical Circular Plates Rigidly Connected at the Centers, $\frac{h}{a}$ = .125

(Mindlin's Theory, ν = .3, k^2 = .8224, Closed-Form Solution)

0.757	17.178
1.867	18.475
3.275	18.989
4.848	20.438
6.517	20.922
8.242	22.341
9.990	23.113
11.765	24.157
13.540	25.533
15.271	25.945
15.530	27.703
16.717	28.102

TABLE XVI

Maximum Response Under Suddenly Applied Steady Loads

Figure Number	Maximum Static Response		Maximum Total Response	
	Mindlin's Theory	Classical Theory	Mindlin's Theory	Classical Theory
42	14.281	13.238	27.763	25.404
43	12.442	11.676	24.790	22.637
44	37.053	36.010	71.932	69.064
45	34.479	33.713	67.942	65.055
46	4.352	3.309	8.541	6.540
47	1.870	0.827	3.615	1.641
48	111.382	111.382	206.004	211.950
49	72.899	72.899	170.954	156.610
50	170.588	170.588	330.518	322.331
51	130.194	130.194	267.578	266.232
52	59.205	59.205	144.893	159.189
53	57.295	57.295	136.566	140.828
54	61.115	61.115	169.938	214.873
57	25.523	*	50.405	*
58	223.501	*	523.484	*

*Not investigated

TABLE XVII

Relative Amplitudes of Response Contributed by Different Modes,

Displacement at the Center for Case 1 - Section VIII.C

Mode Number	Mindlin's Theory	Classical Theory
1	12.63977	11.92512
2	1.30685	1.08945
3	0.30258	0.20426
4	0.06852	0.03477
5	0.00026	-0.00194
6	-0.01673	-0.00684
7	-0.01504	-0.00477
8	-0.00772	-0.00163
9	-0.00081	0.00007
10	0.00301	0.00066
11	0.00289	0.00058
12	0.00274	0.00026
13	0.00144	-0.00001
14	0.00143	-0.00014
15	0.00122	-0.00014
16	-0.00000	-0.00007
17	0.00030	0.00000
18	-0.00114	0.00004
19	-0.00062	0.00005
20	-0.00105	0.00002

TABLE XVIII

Relative Amplitudes of Response Contributed by Different Modes, Bending Moment at the Center for Case 1 - Section VIII.C

Mode Number	Mindlin's Theory	Classical Theory
1	70.10714	70.82226
2	28.34576	28.30638
3	12.36873	11.82775
4	4.17434	3.57586
5	0.02102	-0.31246
6	-1.60917	-1.58312
7	-1.66175	-1.40876
8	-0.94778	-0.66993
9	-0.10894	0.04038
10	0.42856	0.42761
11	0.43715	0.45440
12	0.44883	0.24799
13	-0.09057	-0.01116
14	0.26642	-0.18185
15	-0.14305	-0.20915
16	-0.00156	-0.12203
17	-0.06230	0.00437
18	-0.23883	0.09627
19	0.08411	0.11580
20	-0.29112	0.07027

TABLE XIX

Relative Amplitudes of Response Contributed by Different Modes, Bending Moment at the Center for Case 2 - Section VIII.C

Mode Number	Mindlin's Theory	Classical Theory
1	65.14060	65.70799
2	18.66241	18.34582
3	1.34443	0.63056
4	-5.77673	-6.04773
5	-6.79968	-6.36267
6	-4.35281	-3.51120
7	-0.73349	-0.08047
8	2.11887	2.18938
9	3.13660	2.64459
10	2.30506	1.62078
11	0.78654	0.02633
12	0.42794	-1.20052
13	-0.03594	-1.52477
14	-1.28129	-0.97513
15	0.15649	-0.01221
16	-2.06711	0.78250
17	0.46605	1.01999
18	-1.58004	0.66750
19	0.32331	0.00676
20	-0.09159	-0.56107

TABLE XX

Relative Amplitudes of Response Contributed by Different Modes, Bending Moment at the Outer Edge for Case 3 - Section VIII.C

Mode Number	Mindlin's Theory	Classical Theory
1	-78.53144	-79.13867
2	25.96948	27.23114
3	-13.47175	-14.92794
4	8.04204	9.70897
5	-5.13127	-6.95193
6	3.36823	5.29060
7	-2.22353	-4.19912
8	1.43779	3.43735
9	-0.86122	-2.88097
10	0.34560	2.45986
11	0.27456	-2.13239
12	0.08638	1.97114
13	-0.61689	-1.65951
14	-0.27666	1.48512
15	0.90120	-1.33914
16	0.09838	1.21551
17	-1.00445	-1.10999
18	0.21978	1.01885
19	1.35704	-0.93946
20	-0.82202	0.86983

TABLE XXI

Maximum Response Data for Ramp-Platform and Pulse Loads
from Figures 42 and 59-63

(On the basis of equal input impulse for pulse loads)

Loading Description	Maximum Response		Dynamic Overshoot Factor	
	Mindlin's Theory	Classical Theory	Mindlin's Theory	Classical Theory
Step Function	27.763	25.404	1.945	1.920
Ramp-Platform	27.661	25.206	1.935	1.900
Blast Pulse	6.477	5.764	0.450	0.435
Triangular Pulse	6.058	5.503	0.424	0.416
Square Pulse	6.264	5.657	0.438	0.427
Half-Sine Pulse	6.000	5.450	0.420	0.412

TABLE XXII

Maximum Response Data for Different Areas of Load Distribution
from Figure 66

Radius of Load	Static Response	Total Response	Dynamic Overshoot Factor
0.10	16.362	31.005	1.895
0.25	14.281	27.763	1.940
0.50	10.426	20.893	2.005
0.80	6.162	12.718	2.060

TABLE XXIII

Maximum Response Data for Different Radii of Load Distribution from Figure 67

Radius of Load	Static Response	Total Response	Dynamic Overshoot Factor
0.10	15.695	30.083	1.910
0.25	12.442	24.790	1.980
0.50	6.547	14.230	2.18
0.80	1.259	3.235	2.56

TABLE XXIV

Maximum Response Data for Pulse Loads with Different Durations or Rise Times from Figures 68-72

Rise Time or Duration of Load	Maximum Center Deflection				
	Blast Pulse	Triangular Pulse	Square Pulse	Half-Sine Pulse	Ramp-Platform Load
1	3.223	6.058	6.264	7.615	27.763
5	2.352	3.425	3.932	4.321	25.336
10	1.748	1.974	2.751	2.279	21.297

TABLE XXV

Maximum Acceleration Data from Figures 74-78

(On the basis of equal input impulse for pulse loads)

Blast Pulse	Triangular Pulse	Square Pulse	Half-Sine Pulse	Ramp-Platform Load
22.897	6.775	13.880	5.540	4.9585

XIII. APPENDICES

APPENDIX A

Assumptions and Approximations Used in the Development of Mindlin's Theory of Plate Vibration

The development of an exact solution for plate vibration is very difficult. The stresses vary over the thickness of the plate, and the problem is a three-dimensional one. For bodies having at least one small dimension, the usual procedure in elasticity theory is to reduce the number of variables in the differential equations of the system at the start by omitting certain variables considered to be unimportant and employing average values or restricted regions of others. In this way an approximate theory is formed in which some of the boundary conditions are satisfied identically and some or all of the remaining ones may be satisfied exactly. The classical plate theory, for example, simplifies the derivations considerably by neglecting the variations of the stresses over the thickness of the plate; the shear deformation and rotary inertia are also neglected. It also employs the Kirchoff hypothesis that (1) the linear elements of the plate initially perpendicular to the middle surface remain straight and perpendicular to the deformed middle surface and suffer no extensions and (2) the transverse normal stresses are negligible in comparison with the other stress components. The motion of the plate is described by the deflection of its central plane.

In the improved theory due to Mindlin, the Kirchoff hypothesis is replaced by a more judicious alternative which takes into account the effect of transverse shear deformation. Details of the assumptions and approximations used in the development of Mindlin's theory will now be given.

Since the displacements u_r, u_θ, and u_z are functions of (r,θ,z), we may expand them in power series of z:

$$u_r(r,\theta,z) = u_r(r,\theta,0) + \left(\frac{\partial u_r}{\partial z}\right)_{z=0} z + \frac{1}{2!}\left(\frac{\partial^2 u_r}{\partial z^2}\right)_{z=0} z^2 + -----$$
$$u_\theta(r,\theta,z) = u_\theta(r,\theta,0) + \left(\frac{\partial u_\theta}{\partial z}\right)_{z=0} z + \frac{1}{2!}\left(\frac{\partial^2 u_\theta}{\partial z^2}\right)_{z=0} z^2 + ----- \qquad (A.1)$$
$$u_z(r,\theta,z) = u_z(r,\theta,0) + \left(\frac{\partial u_z}{\partial z}\right)_{z=0} z + \frac{1}{2!}\left(\frac{\partial^2 u_z}{\partial z^2}\right)_{z=0} z^2 + -----$$

Since we are interested in a small displacement theory, the most natural and simplest expressions for the displacements to include the effect of transverse shear deformation may be given by retaining only the first two terms in the above equations. Considering only bending of the plate, $u_r(r,\theta,0)$ and $u_\theta(r,\theta,0)$ which are related to the stretching of the plate can be dropped from the above equations. In plates, the component of the strain in the thickness direction is small compared to the strains in the other directions and is, therefore, neglected from the last of the above equations. Hence for the small deflection theory of bending of circular plates, we have

$$u_r(r,\theta,z) = z\left(\frac{\partial u_z}{\partial z}\right)_{z=0} = z\psi_r(r,\theta)$$
$$u_\theta(r,\theta,z) = z\left(\frac{\partial u_\theta}{\partial z}\right)_{z=0} = z\psi_\theta(r,\theta) \qquad (A.2)$$
$$u_z(r,\theta,z) = u_z(r,\theta) = w(r,\theta)$$

Equations (A.2) state that the linear elements perpendicular to the undeformed middle surface remain straight and suffer no strains although they are no longer perpendicular to the deformed middle surface. The functions u_r and u_θ can be considered as the Taylor series representation up to the linear terms of the exact solution. The function $u_z(r,\theta,z)$ must also depend on z. Because we neglect the z-dependence

u_z and use only the linear terms in the expressions for u_r and u_θ, we have to make certain corrections in the expressions for the plate-stress components to make the results comparable to those of the exact theory.

In plates, the change in thickness because of load on the plate is of no importance. This change and, consequently, the component of the strain in the thickness direction is usually eliminated. (In fact, this is the standard procedure for plate and shell computations). Eliminating ε_z, we obtain equations (4.10). In view of equations (4.1), equations (4.10) yield

$$
\begin{aligned}
M_r &= \frac{E}{1-\nu^2}\,[\int \varepsilon_r z dz + \nu \int \varepsilon_\theta z dz] + \frac{\nu}{1-\nu} \int \sigma_z \, z dz \\
M_\theta &= \frac{E}{1-\nu^2}\,[\nu \int \varepsilon_r z dz + \int \varepsilon_\theta z dz] + \frac{\nu}{1-\nu} \int \sigma_z z dz \\
Q_r &= k^2 G \int \gamma_{rz} dz \\
Q_\theta &= k^2 G \int \gamma_{\theta z} dz
\end{aligned}
\qquad (A.3)
$$

where

$$
\begin{aligned}
\gamma_{rz} &= \frac{\partial u_r}{\partial z} + \frac{\partial w}{\partial r} \\
\gamma_{\theta z} &= \frac{\partial u_\theta}{\partial z} + \frac{\partial w}{r \partial \theta}
\end{aligned}
\qquad (A.4)
$$

If the plate surfaces are free of normal load, σ_z is zero at the surfaces and small as compared to σ_r and σ_θ everywhere else. But even if the plate is loaded, σ_z will be relatively small. The contribution of σ_z, which is represented by the last terms in the first two of equations (A.3) will be a very small quantity as σ_z does not change sign over the thickness of the plate and can therefore be neglected from equations (A.3). This procedure reveals that only a linearly weighted, average effect of σ_z is neglected, rather than σ_z itself as is done in the classical theory.

k^2G is identical with the shear modulus G if the exact expression for γ_{rz} and $\gamma_{\theta z}$ are used in the integrals of equations (A.3). But the exact solution is not available and we are replacing u_r and u_θ by their linear approximations and neglecting the z-dependence of u_z. To compensate for the error due to these approximations and assumptions, G is replaced by k^2G where k^2 can be determined by comparing the present solution with the exact solutions that have been derived for special cases (see appendix B).

APPENDIX B

Comparison of the Two-Dimensional Classical and Mindlin's Theories of Plate Vibration to the Three-Dimensional Theory

The classical Poisson-Kirchoff plate theory has served for many years as the accepted mathematical model to be used for the calculation of frequencies, mode shapes and dynamic response under applied loads. However, in the course of exploring the validity and limitations of this model, certain important deficiencies were discovered. In particular: (1) Because the basic partial differential equation of motion is of the fourth order, only two boundary conditions can be imposed at an edge of the plate to satisfy the requirements of mathematical consistency. In some cases, this gives rise to situations which are contrary to "physical intuition", for example, the Kirchoff boundary conditions at the free edge (see Langhaar [82], p. 170). (2) Even if a solution is obtained which satisfies the differential equation as well as the (mathematically correct) associated boundary conditions, it is possible to find sub-regions of the plate which are clearly not in a state of equilibrium (see Langhaar [82], p. 172). This inconsistency may be attributed to the initial assumption, $\tau_{rz} = \tau_{\theta z} = 0$, upon which the classical theory is based. (3) In the area connected with dynamic response, classical plate theory predicts unrealistically large phase velocities in the plate for short wave lengths (see Mindlin [4], p. 31).

According to the classical theory of plate flexural vibration, which leads to the equation

$$D\nabla^4 w + \rho h \frac{\partial^2 w}{\partial t^2} = p(r,\theta,t) \tag{B.1}$$

the velocities of waves of transverse vibration are inversely proportional to the wave-lengths. The exact solution by Rayleigh [83], Lamb [84] and Timoshenko [85] of the three-dimensional theory of elasticity, for the case of straight-crested flexural waves, confirms this result only for waves which are long in comparison with the thickness of the plate. As the wave length diminishes, the velocity in the three-dimensional theory has as its upper limit the velocity of Rayleigh surface waves. Hence the classical theory cannot be expected to give good results for sharp transients or for the frequencies of modes of vibrations of higher order. A detailed comparison between the classical theory, three-dimensional theory and Mindlin's theory will now be given.

Three-Dimensional Theory:

In the three-dimensional theory, for an infinite plate, the wave velocity c_f of wave length L is given in the form of the transcendental equation [83-85]

$$\frac{4c_s^2\sqrt{(c_s^2 - \alpha c_f^2)(c_s^2 - c_f^2)}}{(2c_s^2 - c_f^2)^2} = \frac{\tanh \frac{\pi h}{Lc_s}\sqrt{c_s^2 - \alpha c_f^2}}{\tanh \frac{\pi h}{Lc_s}\sqrt{c_s^2 - c_f^2}}, \quad 0 < \frac{c_f}{c_s} < 1 \qquad \text{(B.2)}$$

where

c_f is the phase velocity of waves of transverse vibration

$c_s = \sqrt{\frac{G}{\rho}}$, velocity of waves of distortion (shear waves)

$$\alpha = \frac{c_s^2}{c_1^2} = \frac{1-2\nu}{2(1-\nu)}$$

$c_1 = \sqrt{\frac{\lambda+2G}{\rho}} = \sqrt{\frac{E(1-\nu)}{(1+\nu)(1-2\nu)\rho}}$, velocity of waves of dilation.

For long waves (L >>h), equation, (B.2) reduces to

$$\frac{c_f^2}{c_s^2} = \frac{2\pi^2}{3(1-\nu)} \left(\frac{h}{L}\right)^2 \qquad \text{(B.3)}$$

while for short waves ($L \to 0$), equation (B.2) yields

$$4c_s^2\sqrt{(c_s^2 - \alpha c_f^2)(c_s^2 - c_f^2)} = (2c_s^2 - c_f^2)^2, \quad 0 < \frac{c_f}{c_s} < 1 \tag{B.4}$$

In the case of long waves, equation (B.3) shows that the wave velocity c_f is inversely proportional to the wave length L.

Equation (B.4) is the equation for the velocity of Rayleigh surface waves (see Timoshenko [86], p. 458). For short waves, therefore, the velocity c_f approaches the velocity of Rayleigh surface waves. Since the velocity of Rayleigh surface waves is always less than the velocity of shear waves (see Kolsky [87], p. 16), it is evident that the ratio $\frac{c_f}{c_s}$ is always less than 1.

Classical Theory:

Assume a solution for equation (B.1) in the form of

$$w = \cos \frac{2\pi}{L} (x-c_f t) \tag{B.5}$$

Substituting equation (B.5) into equation (B.1), one obtains

$$\frac{c_f^2}{c_s^2} = \frac{D}{\rho h c_s^2} \left(\frac{2\pi}{L}\right)^2 = \frac{2\pi^2}{3(1-\nu)} \left(\frac{h}{L}\right)^2 \tag{B.6}$$

This is identical with equation (B.3). Hence for long waves, the predictions of the classical theory and 3-dimensional theory are identical.

Mindlin's Theory:

The governing differential equation for this theory is (see Mindlin [4], p. 36)

$$\left(\nabla^2 - \frac{\rho}{k^2 G} \frac{\partial^2}{\partial t^2}\right)\left(D\nabla^2 - \frac{\rho h^3}{12} \frac{\partial^2}{\partial t^2}\right)w + \rho h \frac{\partial^2 w}{\partial t^2} = \left(1 - \frac{D\nabla^2}{k^2 G h} + \frac{\rho h^2}{12 k^2 G} \frac{\partial^2}{\partial t^2}\right)p \tag{B.7}$$

If rotary inertia terms are omitted, equation (B.7) reduces to

$$D\left(\nabla^2 - \frac{\rho}{k^2 G} \frac{\partial^2}{\partial t^2}\right) \nabla^2 w + \rho h \frac{\partial^2 w}{\partial t^2} = \left(1 - \frac{D\nabla^2}{k^2 G h}\right)p \tag{B.8}$$

If transverse shear deformation is neglected, but rotary inertia retained, equation (B.7) yields

$$\left(D\nabla^2 - \frac{\rho h^3}{12}\frac{\partial^2}{\partial t^2}\right)\nabla^2 w + \rho h\frac{\partial^2 w}{\partial t^2} = p \tag{B.9}$$

When both shear deformation and rotary inertia are neglected, equation (B.7) reduces to equation (B.1) of the classical theory.

Rotary Inertia Correction:

Substituting equation (B.5) into equation (B.9) with p = 0, one obtains

$$\frac{c_f^2}{c_s^2} = \frac{2\pi^2}{3(1-\nu)}\left(\frac{h}{L}\right)^2\left[1 + \frac{\pi^2}{3}\left(\frac{h}{L}\right)^2\right]^{-1} \tag{B.10}$$

For L>>h, equation (B.10) reduces to equation (B.3) as it should. But as $L \to 0$, $\frac{c_f^2}{c_s^2} = \frac{2}{(1-\nu)}$, which is much larger in comparison to the value of $\frac{c_f^2}{c_s^2}$ given by equation (B.4).

Rotary Inertia and Shear Corrections: (Mindlin's Theory)

Substituting equation (B.5) into equation (B.7) with p = 0, we obtain

$$\frac{\pi^2}{3}\left(\frac{h}{L}\right)^2\left(1 - \frac{c_f^2}{k^2 c_s^2}\right)\left(\frac{c_p^2}{c_f^2} - 1\right) = 1 \tag{B.11}$$

where

$$c_p = \sqrt{\frac{E}{\rho(1-\nu^2)}} \tag{B.12}$$

There are two roots for this equation. With the smaller root, equation (B.11) reduces to equation (B.3) for long waves as it should. As $L \to 0$, equation (B.11) yields

$$\frac{c_f^2}{c_s^2} = k^2 \tag{B.13}$$

According to the three-dimensional theory, this should be the velocity of Rayleigh surface waves. Substituting equation (B.13) into equation (B.4), one gets

$$k^8 - 8k^6 + (24 - 16\alpha)k^4 - 16(\alpha - 1)k^2 = 0 \tag{B.14}$$

If Mindlin's theory is to be identical with the 3-dimensional theory, the appropriate values of k^2 are the roots of equation (B.14). It can be shown that k^2 varies almost linearly from 0.76 for $\nu = 0$ to 0.91 for $\nu = \frac{1}{2}$.

Shear Correction Only:

Substituting equation (B.5) into equation (B.8) with p = 0, one obtains

$$\frac{c_f^{\,2}}{c_s^{\,2}} = \frac{2\pi^2}{3(1-\nu)} \left(\frac{h}{L}\right)^2 \left[1 + \frac{2\pi^2}{3k^2(1-\nu)} \left(\frac{h}{L}\right)^2\right]^{-1} \tag{B.15}$$

For large values of L this reduces to equation (B.3) as it should. As $L \to 0$, equation (B.15) yields

$$\frac{c_f^{\,2}}{c_s^{\,2}} = k^2 \tag{B.16}$$

which is identical to equation (B.13).

Thickness-Shear Motion:

The validity of Mindlin's theory should also be investigated in the case of thickness-shear motion. The circular frequency of the first axisymmetric mode of thickness-shear vibration, according to the exact theory is given by Lamb [84]. It is given as

$$\bar{\omega} = \frac{\pi c_s}{h} \tag{B.17}$$

The corresponding solution of Mindlin's theory is obtained by setting

$$\psi_\theta = w = 0, \; \psi_r = e^{i\omega t} \tag{B.18}$$

in equation (4.15). This yields

$$\bar{\omega} = kc_s \frac{\sqrt{12}}{h}$$

If Mindlin's theory is to be identical with the three-dimensional theory, equations (B.17) and (B.19) must be equal. This condition yields

$$k^2 = \frac{\pi^2}{12} \tag{B.20}$$

It is to be noted that this value of k^2 is very close to Reissner's $\frac{5}{6}$ (see reference 78). Reissner obtained this value by assuming a parabolic variation of transverse shear stress across the thickness of the plate.

Substituting $k^2 = \frac{\pi^2}{12}$, into equation (B.14), one obtains $\nu = .176$.

Thus in a material with $\nu = .176$, there is no conflict between equations (B.20) and (B.14). For other values of ν, one must compromise between equations (B.14) and (B.20) or choose a particular value.

Using equations (B.2), (B.6), (B.10) and the smaller root of equation (B.11), $\frac{c_f}{c_s}$ versus $\frac{h}{L}$ are plotted in figure 22.

From the figure it may be seen that as the wave length L becomes smaller, the classical theory departs considerably from the three-dimensional theory. It is also seen that the results predicted by the three-dimensional theory and Mindlin's theory are almost the same. It is interesting to note that the shear deformation accounts almost entirely for the discrepancy between the classical theory and the three-dimensional theory over the whole wave length spectrum.

To summarize:

1. Classical plate theory is applicable only for large wave lengths, i.e., L>>h. So, for very thin plates, classical theory gives rather good results.

2. Mindlin's improved theory gives results which are identical to those given by the three-dimensional theory, if k^2 is chosen in accordance with

equations (B.14) or (B.20).

3. Transverse shear deformation accounts almost entirely for the discrepancy between the classical and three-dimensional theories over the entire wave length spectrum.

APPENDIX C

Discussion of Boundary Conditions for Classical and Mindlin's Theories of Plate Vibration

The classical Poisson-Kirchoff theory of plate vibration leads to a differential equation of the fourth order [see equation (B.1)] for the deflection and, accordingly, to two boundary conditions which can and must be satisfied at each edge. For a plate of finite thickness, it appears more natural to require the satisfaction of three boundary conditions than of two. For instance, along a free edge of a plate one has the three conditions of vanishing vertical force, bending moment and twisting moment. The assumptions underlying the classical theory allow for a contraction of the three conditions mentioned to two conditions, which are the vanishing bending moment and the vanishing of the sum of vertical force and edgewise rate of change of twisting moment. The physical significance of this reduction in the number of boundary conditions has been explained by Kelvin and Tait (see Timoshenko [89], p.84). The simplifying assumptions made in the development of the classical theory often lead to several puzzling inconsistencies (see Langhaar [82], p. 172 and Reissner [77], p. 69).

The improved theory of plate vibration due to Mindlin [see equations (5.19)] makes it possible to satisfy three boundary conditions at each edge of the plate, and hence is consistent with the physical requirements of the problem. In the improved theory, the line integral in the expression for the total energy of the plate is [see equation (6.15)]

$$\oint (M_r \frac{\partial \psi_r}{\partial t} + M_{r\theta} \frac{\partial \psi_\theta}{\partial t} + Q_r \frac{\partial w}{\partial t}) dS \tag{C.1}$$

where $dS = r\, d\theta$.

In the refined formulation of the plate vibration problem there are three mechanical boundary conditions M_r, $M_{r\theta}$ and Q_r which are independent quantities and three geometrical boundary conditions w, ψ_r and ψ_θ which are dependent on M_r, $M_{r\theta}$ and Q_r [see equations (4.13)]. From equations (4.13) it is clear that one member of each of the pairs of terms $M_r\psi_r$, $M_{r\theta}\psi_\theta$ and $Q_r w$ must be known for the others to be determined uniquely. Hence the necessary boundary conditions for the refined theory of plate vibration can be stated as follows: Any combination which contains one member of each of the three pairs of terms in equations (C.1) must be specified at the edge of the plate.

The possible combinations of the six quantities are:

$$\begin{array}{ll} \psi_r, \psi_\theta, w & M_r, M_{r\theta}, w \\ \psi_r, \psi_\theta, Q_r & M_r, M_{r\theta}, Q_r \\ \psi_r, M_{r\theta}, w & M_r, \psi_\theta, w \\ \psi_r, M_{r\theta}, Q_r & M_r, \psi_\theta, Q_r \end{array} \tag{C.2}$$

The three quantities in any of the above sets must be specified at the edge of the plate to assure a unique solution for the plate vibration problem.

The boundary conditions applicable to the classical theory can be deduced from the equations of the improved theory as follows:

From equations (4.13) we have

$$Q_\theta = k^2 Gh(\psi_\theta + \frac{\partial w}{\partial S}) \tag{C.3}$$

This gives

$$\psi_\theta = \frac{Q_\theta}{k^2 Gh} - \frac{\partial w}{\partial S} \tag{C.4}$$

In the classical theory, since the transverse shear deformation term vanishes, this becomes

$$\psi_\theta = - \frac{\partial w}{\partial S} \tag{C.5}$$

In view of the above relation we obtain

$$M_{r\theta} \frac{\partial \psi_\theta}{\partial t} = - M_{r\theta} \frac{\partial^2 w}{\partial S \partial t} \tag{C.6}$$

Hence one obtains

$$\oint M_{r\theta} \frac{\partial \psi_\theta}{\partial t} dS = -\oint M_{r\theta} \frac{\partial}{\partial S} (\frac{\partial w}{\partial t}) dS \tag{C.7}$$

Integrating by parts, the above yields

$$\oint \frac{\partial w}{\partial t} \frac{\partial M_{r\theta}}{\partial S} dS \tag{C.8}$$

Hence the second and third terms in equation (C.1) can be combined to yield

$$\oint [M_r \frac{\partial \psi_r}{\partial t} + (\frac{\partial M_{r\theta}}{\partial S} + Q_r) \frac{\partial w}{\partial t}] dS \tag{C.9}$$

This leaves the two edge conditions prescribed by Kirchoff in the classical theory. The above procedure to reduce the boundary conditions from three to two is not necessary in the improved theory as it can satisfy three boundary conditions.

APPENDIX D

Variational Formulation of the Plate Vibration Problem

Whenever a strain-energy function, W_s, exists, we may deduce the equations of motion from the Hamilton Principle [88]. For the expression of this principle, we take $\bar{T}$ to be the total kinetic energy of the body, and V to be the potential energy of deformation, so that $\bar{V}$ is the volume integral of W_s. We form by the rules of the calculus of variations, the variation of the integral $\int(\bar{T} - \bar{V})dt$, taken between fixed initial and final values of time, t_0 and t_1. In varying the integral we assume that the displacement alone is subject to variation, and that its values at the initial and final instants are given. We denote by W_1, the work done by the external forces when the displacement is varied. Then by the principle mentioned above, we get (see Love [88]

$$\delta\int_{t_0}^{t_1}(\bar{T} - \bar{V})dt = \int_{t_0}^{t_1}\delta W_1 dt = 0 \qquad \text{(D.1)}$$

For the plate problem under consideration, equation (D.1) can be written as

$$\begin{aligned}\int_{t_0}^{t_1}\Big\{ &\delta\int\int[(\frac{\partial u_r}{\partial t})^2 + (\frac{\partial u_\theta}{\partial t})^2 + (\frac{\partial u_z}{\partial t})^2]\ \frac{\rho}{2}\ r d\theta dr \\ &- \int\int \delta\bar{W} r d\theta dr + \int\int p\delta w r d\theta dr\Big\}\ dt = 0\end{aligned} \qquad \text{(D.2)}$$

where $\bar{W}$ is the strain energy per unit area of the plate.

Now in view of equations (6.11 - 6.14) one obtains

$$\delta\bar{W} = \frac{\partial\bar{W}}{\partial\Gamma_r}\ \delta\Gamma_r + \frac{\partial\bar{W}}{\partial\Gamma_\theta}\ \delta\Gamma_\theta + \frac{\partial\bar{W}}{\partial\Gamma_{r\theta}}\ \delta\Gamma_{r\theta} + \frac{\partial\bar{W}}{\partial\Gamma_{rz}}\ \delta\Gamma_{rz} + \frac{\partial\bar{W}}{\partial\Gamma_{\theta z}}\ \delta\Gamma_{\theta z} \qquad \text{(D.3)}$$

This gives

$$\delta\bar{W} = [M_r \frac{\partial}{\partial_r} + \frac{M_\theta}{r} + M_{r\theta} \frac{\partial}{r\partial\theta} + Q_r]\ \delta\psi_r$$
$$+ [M_\theta \frac{\partial}{r\partial\theta} + M_{r\theta} \frac{\partial}{\partial r} - \frac{M_{r\theta}}{r} + Q_\theta]\delta\psi_\theta \qquad \text{(D.4)}$$
$$+ [Q_r \frac{\partial}{\partial r} + Q \ \frac{\partial}{r\partial\theta}]\ \delta w$$

Integrating the terms containing space derivatives by parts, we get

$$\iint \delta\bar{W} r d\theta dr = \oint [M_r \delta\psi_r + M_{r\theta}\delta\psi_\theta + Q_r \delta w] dS$$
$$- \Big\{ [\frac{\partial M_r}{\partial r} + \frac{M_r}{r} - \frac{M_\theta}{r} - Q_r + \frac{\partial M_{r\theta}}{r\partial\theta}]\ \delta\psi_r$$
$$+ [\frac{\partial M_{r\theta}}{\partial r} + \frac{M_{r\theta}}{r} - Q_\theta + \frac{M_{r\theta}}{r} + \frac{\partial M_\theta}{r\partial\theta}]\ \delta\psi_\theta \qquad \text{(D.5)}$$
$$+ [\frac{\partial Q_r}{\partial r} + \frac{\partial Q_\theta}{r\partial\theta} + \frac{Q_r}{r}]\ \delta w \Big\}\ r d\theta dr$$

where $dS = rd\theta$.

The first integral in equation (D.2) becomes

$$\delta\iint \Big\{ \frac{\rho h^3}{24} [(\frac{\partial\psi_r}{\partial t})^2 + (\frac{\partial\psi_\theta}{\partial t})^2] + \frac{\rho h}{2} (\frac{\partial w}{\partial t})^2 \Big\}\ r d\theta dr \qquad \text{(D.6)}$$

Integrating by parts between t_0 and t_1, the above yields

$$\int_{t_0}^{t_1} dt \iint \Big\{ \frac{\rho h^3}{12} [\frac{\partial\psi_r}{\partial t} \frac{\partial}{\partial t} \delta\psi_r + \frac{\partial\psi_\theta}{\partial t} \frac{\partial}{\partial t} \delta\psi_\theta] + \rho h (\frac{\partial w}{\partial t} \frac{\partial}{\partial t} \delta w) \Big\}\ r d\theta dr$$
$$= \iint \Big\{ \frac{\rho h^3}{12} [\frac{\partial\psi_r}{\partial t} \delta\psi_r + \frac{\partial\psi_\theta}{\partial t} \delta\psi_\theta] + \rho h (\frac{\partial w}{\partial t} \delta w) \Big\}\ r d\theta dr \Big]_{t_0}^{t_1} \qquad \text{(D.7)}$$
$$- \int_{t_0}^{t_1} dt \iint \Big\{ \frac{\rho h^3}{12} [\frac{\partial^2\psi_r}{\partial t^2} \delta\psi_r + \frac{\partial^2\psi_\theta}{\partial t^2} \delta\psi_\theta] + \rho h (\frac{\partial^2 w}{\partial t^2} \delta w) \Big\}\ r d\theta dr$$

Here t_0 and t_1 are the initial and final values of time, and $\delta\psi_r$, $\delta\psi_\theta$ and δw vanish for both these values. Hence the first integral on the right hand side of equation (D.7) vanishes.

Now combining equations (D.5) and (D.7), equation (D.2) can be written as

$$\int_{t_0}^{t_1} \iint \Big\{ \Big[-\frac{\rho h^3}{12} \frac{\partial^2 \psi_r}{\partial t^2} + \frac{\partial M_r}{\partial r} + \frac{\partial M_{r\theta}}{r\partial\theta} + \frac{M_r - M_\theta}{r} - Q_r \Big] \delta\psi_r$$

$$+ \Big[-\frac{\rho h^3}{12} \frac{\partial^2 \psi_\theta}{\partial t^2} + \frac{\partial M_{r\theta}}{\partial r} + \frac{\partial M_\theta}{r\partial\theta} + \frac{2M_{r\theta}}{r} - Q_\theta \Big] \delta\psi_\theta \tag{D.8}$$

$$+ \Big[-\rho h \frac{\partial^2 w}{\partial t^2} + \frac{\partial Q_r}{\partial r} + \frac{\partial Q_\theta}{r\partial\theta} + \frac{Q_r}{r} + p \Big] \delta w \Big\} \, r d\theta dr$$

$$\int_{t_0}^{t_1} \oint [M_r \delta\psi_r + M_{r\theta}\delta\psi_\theta + Q_r \delta w] \, dS dt = 0$$

The three bracketed terms in the surface integral of the above equation, each equated to zero, give the three equations of motion for the improved theory of plate vibration. As boundary conditions, one member of each of the groups $M_r \psi_r$, $M_{r\theta}\psi_\theta$ and $Q_r w$ is to be specified.

APPENDIX E

Definitions of Certain Terms Used in Chapter X

1. Internal Damping

The strain produced in a purely elastic material is proportional to the stress that produces the deformation. The stresses are related to the strain by simple constants of proportionality, E or G. However, when the material is linearly viscoelastic and when it is subjected to time-dependent variations of stress and strain, the stress is not related to the strain by a simple constant of proportionality, E or G. In this case internal damping must be taken into account. Thus we have (see Snowdon [68], p. 177)

$$\begin{aligned} E^*_{\omega,\theta} &= E_{\omega,\theta}\,(1 + i\delta_{E_{\omega,\theta}}) \\ G^*_{\omega,\theta} &= G_{\omega,\theta}\,(1 + i\delta_{G_{\omega,\theta}}) \end{aligned} \tag{E.1}$$

In equation (E.1), $E_{\omega,\theta}$ is the real part and $\delta_{E_{\omega,\theta}}$ is the ratio of the imaginary part to the real part of the complex Young's modulus. The imaginary part (the product $\delta_{E_{\omega,\theta}} E_{\omega,\theta}$) is a measure of the mechanical loss associated with the linear deformation of the material. The quantity $\delta_{E_{\omega,\theta}}$ is correspondingly known as the loss or damping factor [67]. The fact that $E^*_{\omega,\theta}$ is a complex quantity signifies only that the strain lags behind the stress by an angle the tangent of which is equal to $\delta_{E_{\omega,\theta}}$. The complex modulus is commonly referred to as the dynamic modulus.

In general, the dynamic modulus and damping factor are functions of temperature and frequency. For many materials such as plastics, rubber-like materials and annealed steel it is reasonable to assume that dynamic modulus and damping factor are constants in the frequency range usually encountered in vibration problems. The damping factor typically takes values of the order of 0.1. Such materials are said to possess damping of Solid Type I (see Snowdon [67], p. 27). Materials for which the loss factor and dynamic modulus are dependent on frequency are referred to as materials with damping of Solid Type II. For these materials, the damping factor may take values up to 1. Our investigation is concerned only with materials having damping of Solid Type I.

2. Impedance

The driving-point impedance at any point of a mechanical system is defined as the ratio of the force to velocity at that point when both force and velocity vary sinusoidally with time at the same frequency [67]. In general, impedance is a complex quantity.

If the velocity is monitored at a point other than the driving point, the complex ratio of force to velocity is called transfer impedance.

The characteristic impedance of a system is the driving-point impedance of a similar system having infinite dimensions.

For a mass M acted on by a force F, the impedance is $i\Omega M$. For a spring K, the impedance is $\frac{K}{i\Omega}$ and for a dashpot of strength C_c it is C_c.

The total impedance of a system of mass, spring and dashpot which experiences a common velocity is the sum of the component impedances. Thus, for the system shown in figure 20.c, we have

$$Z = i\Omega M + \frac{K}{i\Omega} + C_c \tag{E.2}$$

Neglecting damping, it is clear from the above equation that at low frequencies, $\frac{K}{\Omega} >> \Omega M$, the impedance Z is almost entirely springlike in character. At very high frequencies, $\Omega M >> \frac{K}{\Omega}$, the impedance Z is almost entirely masslike.

3. Transmissibility

Assume that a machine, represented by a mass M, is supported through an isolator of stiffness K* by a foundation which vibrates sinusoidally with angular frequency Ω (see figure 20.a). The resulting displacement of the mass is given by

$$\tilde{x}_2 = x_2^* e^{i\Omega T} \qquad \text{(E.3)}$$

The transmissibility is defined as

$$T_m = \left| \frac{x_2^*}{x_1} \right| \qquad \text{(E.4)}$$

The displacement x_2^* is taken as a complex quantity, because in general, the phase of $\tilde{x}_2$ will be different from that of x_1.

Alternatively, transmissibility can be defined as (see figure 20.b)

$$T_m = \left| \frac{F_1^*}{F_0} \right| \qquad \text{(E.5)}$$

It is to be noted that

$$T_m = \left| \frac{x_2^*}{x_1} \right| = \left| \frac{F_1^*}{F_0} \right| \qquad \text{(E.6)}$$

So any expression for transmissibility will have dual significance. Depending on the problem, whether it is isolating a machine from the vibration of the floor, or reducing the force transmitted from the machine to the floor, one may have to choose equation (E.4) or equation (E.5) for defining transmissibility.

APPENDIX F

Inclusion of Internal Damping in Plate Vibration Problems

The manner in which internal damping may be included in the expressions derived for the classical theory of plate vibration will now be considered.

The classical flexural vibration equation for a plate is

$$(\nabla^4 - \delta^4)W = 0 \qquad \text{(F.1)}$$

where

$$\delta^4 = \frac{\Omega^2}{\alpha^2} = \frac{\rho h \omega^2}{D} = \frac{12(1-\nu^2)\rho\omega^2}{Eh^2} \qquad \text{(F.2)}$$

To include internal damping, the parameter δ that appears in equation (F.1) is replaced by a complex quantity δ^* defined by (* denotes a complex quantity)

$$\delta^{*4} = \frac{12(1-\nu^2)\rho\omega^2}{E^*h^2} \qquad \text{(F.3)}$$

where

$$E^* = E(1 + i\delta_e) \qquad \text{(F.4)}$$

E^* is complex Young's modulus

δ_e is loss factor associated with linear deformation

In view of (F.4) δ^* can be expressed as

$$\delta^{*4} = \frac{12(1-\nu^2)\,\rho\omega^2}{Eh^2(1 + i\delta_e)} = \frac{\delta^4}{(1+i\delta_e)} \qquad \text{(F.5)}$$

In general, E and δ_e depend on frequency. We assume that the material has damping of the Solid Type I (see Appendix E), which enables us to assume that E and δ_e are independent of frequency. Temperature change effects are usually negligible and hence will be neglected here (see reference 67)

δ^* can be conveniently expressed in the form

$$\delta^* = \frac{\delta}{(1+i\delta_e)^{\frac{1}{4}}} = (s + ig) \tag{F.6}$$

Solving for s and g from equation (F.6), one obtains

$$\begin{aligned} s &= \delta\left[\frac{1}{2(D_e)^{\frac{1}{2}}} + \frac{(1 + D_e)^{\frac{1}{2}}}{2\sqrt{2}\,D_e}\right]^{\frac{1}{2}} \\ g &= \delta\left[\frac{1}{2(D_e)^{\frac{1}{2}}} - \frac{(1 + D_e)^{\frac{1}{2}}}{2\sqrt{2}\,D_e}\right]^{\frac{1}{2}} \end{aligned} \tag{F.7}$$

where

$$D_e = (1 + \delta_e)^{\frac{1}{2}}$$

Hence, damping can be taken into account in all expressions derived for the classical theory by using δ^* in place of δ.

APPENDIX G

Conversion Factors for Dimensional Quantities

The numerical results presented in this investigation are in terms of nondimensional quantities defined on pages 31 and 92, using a Poisson's ratio of 0.3. The results are thus applicable to all materials with this value for Poisson's ratio. The variation of frequency with Poisson's ratio is given in tables IX and X.

As an example, the following table is given for conversion of non-dimensional quantities into dimensional quantities, using $\rho = 0.282$ lbs/in^3 and $E = 30 \times 10^6$ lbs/in^2.

Nondimensional Quantity	Dimensions Required	To Convert to Dimensional Quantity Multiply by
T	Seconds	$92.23\ a\ (10^6)$
Ω	Radians per Second	$\frac{10820}{a}$
P_0	Pounds	$33\ ha\ (10^6)$
P, K	Pounds per Inch	$33\ h\ (10^6)$
P	Pounds per Square Inch	$33\ \frac{h}{a}\ (10^6)$
M_r	Pounds	$2.75\ \frac{h^3}{a}\ (10^6)$
Z	Pound Seconds per Inch	$3040\ ha$
W	Inches per Second per Second	$\frac{117.6}{a}\ (10^6)$

APPENDIX H

Some Integrals of Bessel Functions

The following integral formulas were used in this investigation:

1. $\int_a^b J_0^{\,2}(kR)RdR = \frac{R^2}{2}\left[J_1^{\,2}(kR) + J_o^{\,2}(kR)\right]\Big]_a^b$, valid for Y_0 also

2. $\int_a^b I_0^{\,2}(kR)RdR = -\frac{R^2}{2}\left[I_1^{\,2}(kR) - I_0^{\,2}(kR)\right]\Big]_a^b$, valid for K_0 also

3. $\int_a^b J_1^{\,2}(kR)RdR = \frac{R^2}{2}\left[J_1^{\,2}(kR) - J_0(kR)J_2(kR)\right]\Big]_a^b$, valid for Y_1, I_1, and K_1 also

4. $\int_a^b J_0(kR)J_0(\ell R)RdR = \frac{R}{k^2 - \ell^2}\left[kJ_0(\ell R)J_1(kR) - \ell J_1(\ell R)J_0(kR)\right]\Big]_a^b$, valid for Y_0Y_0 and J_0Y_0 also.

5. $\int_a^b J_1(kR)J_1(\ell R)RdR = \frac{R}{k^2 - \ell^2}\left[\ell J_0(\ell R)J_1(kR) - kJ_1(\ell R)J_0(kR)\right]\Big]_a^b$, valid for Y_1Y_1 and J_1Y_1 also

6. $\int_a^b J_0(kR)Y_0(kR)RdR = \frac{R^2}{2}\left[J_0(kR)Y_0(kR) + J_1(kR)Y_1(kR)\right]\Big]_a^b$, valid for I_0K_0 also

7. $\int_a^b J_1(kR)Y_1(kR)RdR = \frac{R^2}{4}\left[2J_1(kR)Y_1(kR) - J_0(kR)Y_2(kR) - J_2(kR)Y_0(kR)\right]\Big]_a^b$

8. $\int_a^b J_0(kR)I_0(\ell R)RdR = \frac{R}{k^2 + \ell^2}\left[\ell J_0(kR)I_1(\ell R) + kI_0(\ell R)J_1(kR)\right]\Big]_a^b$ valid for Y_0I_0 also

9. $\int_a^b K_0(kR)\ J_0(\ell R)RdR = \frac{R}{k^2 + \ell^2}\left[\ell K_0(kR)J_1(\ell R) - kJ_0(\ell R)K_1(kR)\right]\Big]_a^b$, valid for K_0Y_0 also

$$10.\ \int_a^b J_1(kR)I_1(\ell R)RdR = \frac{R}{k^2+\ell^2}\left[\ell J_1(kR)I_0(\ell R) - kI_1(\ R)J_0(kR)\right]_a^b$$

$$11.\ \int_a^b K_1(kR)J_1(\ell R)RdR = \frac{R}{k^2+\ell^2}\left[\ell K_1(kR)J_2(\ell R) - kK_2(kR)J_1(\ell R)\right]_a^b ,$$

valid for K_1Y_1 also

$$12.\ \int_a^b I_1(kR)K_1(kR)RdR = \frac{-R^2}{2}\Big[\frac{1}{k}K_2(kR)I_1(kR) + K_2(kR)I_2(kR)$$

$$+ I_1(kR)K_1(kR) - \frac{1}{k}K_1(kR)I_2(kR)\Big]_a^b$$

APPENDIX I

Solutions for the Classical Theory

All the derivations in chapters IV to IX have been done for the improved theory of plate vibration. Since one of the objectives of this investigation is to study the scope and limitations of the classical theory of plate vibration, homogeneous and forced motion solutions using the classical theory are also needed. Toward this end, without giving emphasis to details, the necessary solutions for the classical theory will now be given.

1. Governing Equations

The plate-stress-displacement relations are

$$\begin{aligned} M_r &= D\left(\frac{\partial \psi_r}{\partial r} + \frac{\nu}{r}\psi_r\right) \\ M_\theta &= D\left(\nu\frac{\partial \psi_r}{\partial r} + \frac{1}{r}\psi_r\right) \\ Q_r &= D\left(\frac{\partial^2 \psi_r}{\partial r^2} + \frac{1}{r}\frac{\partial \psi_r}{\partial r} - \frac{\psi_r}{r^2}\right) \end{aligned} \tag{I.1}$$

where

$$\psi_r = -\frac{\partial w}{\partial r} \qquad \text{(see Timoshenko [89], p. 51)}$$

The homogeneous equation in w is

$$\nabla^4 w - \frac{\rho h \omega^2}{D} w = 0 \tag{I.2}$$

In nondimensional form, this becomes

$$(\nabla^4 - \delta^4)W = 0 \tag{I.3}$$

where

$$\delta^4 = \frac{\Omega^2}{\alpha^2}$$

The required solution of this equation for axisymmetric vibration is

$$W(R) = A_1 J_0(\delta R) + A_2 I_0(\delta R) \tag{I.4}$$

2. Frequency Equations

a. Clamped Plate

The boundary conditions are

$$W(1) = \frac{\partial W}{\partial R}(1) = 0 \tag{I.5}$$

Substituting equation (I.5) in equation (I.4), one obtains

$$\left\| \begin{matrix} J_0 & I_0 \\ -\delta J_1 & \delta I_1 \end{matrix} \right\|_{(\delta)} = 0 \tag{I.6}$$

b. Simply Supported Plate

The boundary conditions are

$$W(1) = M_r(1) = 0 \tag{I.7}$$

This gives with equation (I.4)

$$\left\| \begin{matrix} J_0 & I_0 \\ [\delta^2 J_0 + (\nu-1)\delta J_1] & -[\delta^2 I_0 + (\nu-1)\delta I_1] \end{matrix} \right\|_{(\delta)} = 0 \tag{I.8}$$

c. Free Plate

The boundary conditions are

$$M_r(1) = Q_r(1) = 0 \tag{I.9}$$

This yields with equation (I.4)

$$\left\| \begin{matrix} [\delta^2 J_0 + (\nu-1)\delta J_1] & -[\delta^2 I_0 + (\nu-1)\delta I_1] \\ \delta^3 J_1 & \delta^3 I_1 \end{matrix} \right\|_{(\delta)} = 0 \tag{I.10}$$

3. Forced Motion Solutions

$$W(R,T) = W_s(R,T) = \sum_{i=1}^{\infty} W_i(R) q_i(T) \tag{I.11}$$

a. Generalized Coordinates q_i

$$\frac{q_i(T)}{P_0} = [A_1 J_1(\delta\gamma) + A_2 I_1(\delta\gamma)] \frac{\cos\Omega_i T}{\pi\gamma\delta\Omega_i^{\,2}} \tag{I.12}$$

where P_0 is the total load uniformly distributed over a circular area of radius γ.

$$\frac{q_i(T)}{P_0} = [A_1 J_0(\delta\gamma) + A_2 I_0(\delta\gamma)] \frac{\cos\Omega_i T}{2\pi\Omega_i^2} \tag{I.13}$$

where P_0 is the total load uniformly distributed over a circle of radius γ.

$$q_i(T) = [A_1 + A_2] \frac{\cos\Omega_i T}{2\pi\Omega_i^2} \tag{I.14}$$

where P_0 is a concentrated load at the center of the plate.

b. Static solutions

The static solutions can be obtained by putting $\frac{1}{K^2} = 0$ in the solutions for the improved theory.

c. Unique solution for A_1 and A_2

The normalization condition for the modes is given by

$$\int_\beta^1 W_i^2 R dR = 1 \tag{I.15}$$

In view of the above and the condition that $W(1) = 0$, equation (I.4) yields

$$A_2 = -\frac{J_0(\delta)}{I_0(\delta)} A_1 \tag{I.16}$$

$$A_1 = \sqrt{\frac{2}{J_0^2\left[2 + \frac{J_1^2}{J_0^2} - \frac{I_1^2}{I_0^2} - \frac{2}{\delta}\frac{I_1}{I_0} - \frac{2}{\delta}\frac{J_1}{J_0}\right](\delta)}} \tag{I.17}$$

The modal bending moment and shearing force are given by

$$M_r(R) = A_1\left[\delta^2 J_0 + \frac{\nu-1}{R}\delta J_1\right]_{(\delta R)} - A_2\left[\delta^2 I_0 + \frac{\nu-1}{R}\delta I_1\right]_{(\delta R)} \tag{I.18}$$

$$Q_r(R) = -\alpha^2\delta^3[A_1 J_1 + A_2 I_1]_{(\delta R)} \tag{I.19}$$

4. Response to Pulse Loads

For a ramp-platform load, we obtain, for $0 < T < T_1$

$$\frac{q_i(T)}{P_0} = WC \frac{\sin\Omega_i T}{T_1 \pi\gamma\Omega_i^3} \tag{I.20}$$

and for $T > T_1$

$$\frac{q_i(T)}{P_0} = WC \frac{\sin\Omega_i T - \sin\Omega_i (T-T_1)}{T_1 \pi\gamma\Omega_i^3} \tag{I.21}$$

where

$$WC = \frac{A_1 J_1(\delta\gamma) + A_2 I_1(\delta\gamma)}{\delta} \tag{I.22}$$

The values of q_i for blast, triangular, square and half-sine pulses are obtained from the results of the improved theory by replacing WJ or WI by WC.

5. Frequency Equation for Impedance Loaded Plate

The closed form frequency equation for this case is given by

$$\left\| \begin{matrix} 1 & \dfrac{8\alpha^2\delta^2}{-i\Omega z} & 1 \\ J_0 & Y_0 + \dfrac{2}{\pi} K_0 & I_0 \\ J_1 & Y_1 + \dfrac{2}{\pi} K_1 & -I_1 \end{matrix} \right\|_{(\delta)} = 0 \tag{I.23}$$

XIV. BIBLIOGRAPHY

1. ALLEN, C. H. (1969) Guidelines for Designing Quieter Equipment. Paper presented at the ASME Conference, May 5-8, New York, p. 1-7.

2. CREDE, C. E. (1951) Vibration and Shock Isolation. Wiley, New York, 328 p.

3. TIMOSHENKO, S. and D. H. YOUNG (1965) Vibration Problems in Engineering. Van Nostrand Co., Inc., New York, 337 p.

4. MINDLIN, R.D. (1951) Influence of Rotary Inertia and Shear on Flexural Motions of Isotropic, Elastic Plates. J. Appl. Mech., p. 31-38.

5. MEIROVITCH, L. (1967) Analytical Methods in Vibrations. Macmillan, New York, 555 p.

6. THOMSON, W. T. (1965) Vibration Theory and Applications. Prentice Hall, New Jersey, 384 p.

7. WILLIAMS, D. (1949) Displacement of a Linear Elastic System under a Given Transient Load. Aeronautical Quarterly, p. 123-136.

8. REISMANN, H. (1968) Forced Motion of Elastic Plates. J. Appl. Mech., p. 510-515.

9. LEONARD, R. W. (1959) On Solutions for the Transient Response of Beams. NASA Technical Report R-21.

10. POISSON, S. D. (1829) Sur le mouvement des corps elastiques. Memoires de l'Academie Royale des Sciences de l'Institut de France, Vol. 8, p. 357-370.

11. KIRCHOFF, G. (1850) Uber das Gleichgewicht und die Bewegung einer elastischen Scheibe. Journal fur die reine und angewandte Mathematik, Crelle, Vol. 40, p. 51.

12. SNEDDON, I. N. (1951) Fourier Transforms. McGraw-Hill, New York, 542 p.

13. FLYNN, P. D. (1950) Elastic Response of Simple Structures to Pulse Loadings. Ballistic Research Laboratories Memorandum Report No. 525.

14. WAH, T. (1962) Vibration of Circular Plates. J. Acous, Soc. Amer., p. 275-281.

15. ERINGEN, A. C. (1957) Response of Beams and Plates to Random Loads. J. Appl. Mech., p. 46-52.

16. MASE, G.E. (1960) Transient Response of Linear Viscoelastic Plates. J. Appl. Mech., p. 589-590.

17. BAUER, H. F. (1968) Nonlinear Response of Elastic Plates to Pulse Excitation. J. Appl. Mech., p. 47-52.

18. REISMANN, H. (1959) Forced Vibrations of a Circular Plate. J. Appl. Mech., p. 526-527.

19. KANTHAM, C. L. (1958) Bending and Vibration of Elastically Restrained Circular Plates. Journal of the Franklin Institute, Vol. 265, p. 483-491.

20. REID, W. P. (1962) Free Vibrations of a Circular Plate. J. Soc. Indus. Appl. Math., p. 668-674.

21. WEINER, R. S. (1965) Forced Axisymmetric Motions of Circular Elastic Plates. J. Appl. Mech., p. 893-898.

22. MEDICK, M. A. (1961) Classical Plate Theory and Wave Propagation. J. Appl. Mech., p. 223-228.

23. ROBERSON, R. E. (1951) Transverse Vibrations of a Clamped Circular Plate Carrying Concentrated Mass. J. Appl. Mech., p. 349-352.

24. ROBERSON, R. E. (1951) Transverse Vibrations of a Free Circular Plate Carrying Concentrated Mass. J. Appl. Mech., p. 280-282.

25. TYUTEKIN, V. V. (1961) Flexural Oscillations of a Circular Elastic Plate Loaded at the Center. (Translated from Akusticheskii Zhurnal Vol. 6, No. 3, Moscow, p. 388-391). Soviet Phys-Acoust., p. 389-392.

26. DAS, Y. C. and D. R. NAVARANTNA (1963) Vibrations of a Rectangular Plate with Concentrated Mass, Spring and Dashpot. J. Appl. Mech., p. 31-36.

27. STOKEY, W. F. and C. F. ZOROWSKI (1959) Normal Vibrations of a Uniform Plate Carrying any Number of Finite Masses. J. Appl. Mech., p. 210-216.

28. KIRK, C. L. and A. W. LEISSA (1967) Vibration Characteristics of a Circular Plate with a Concentrated Reinforcing Ring. J. Sound Vibr., p. 278-284.

29. STANISIC, M. M. (1955) Free Vibration of Rectangular Plates with Damping Considered. Quart. Appl. Math., p. 361-367.

30. GREENE, D. C. (1961) Vibration and Sound Radiation of Damped and Undamped Flat Plates. J. Acous. Soc. Amer., p. 1315.

31. LANGE, J. N. (1963) Bending Wave Propagation in Rods and Plates. J. Acous. Soc. Amer., p. 378.

32. SKUDRZYK, E. J., KAUTZ, BARBARA R., and D. C. GREENE (1961) Vibration of and Bending Wave Propagation in Plates. J. Acous. Soc. Amer., p. 36.

33. FLINN, E. A. (1958) Dispersion Curves for Longitudinal and Flexural Waves in Solid Circular Cylinders. J. Appl. Phys., p. 1261-1262.

34. HENCKY, H. (1947) Uber die Berucksichtigung der Schubverzerrung in ebenen Platten. Ingenieur Archiv, 16, p. 72-76.

35. HECKL, M. (1959) Schallabstrahlung von Platten bei punkfoermiger Anregung. Acustica, 9, p. 371.

36. HECKL, M. (1959) Schallabstrahlung von punktfoermig angeregten Hohlzylindern. Acustica, 9, p. 86.

37. CHOU, P. C. and H. A. KOENIG (1965) Flexural Waves in Elastic Circular Plates by Method of Characteristics. D.I.T. Report No. 160-6.

38. CHREE, C. (1889) The Equations of an Isotropic Elastic Solid in Polar and Cylindrical Coordinates: Their Solutions and Applications. Trans. Cambridge Phil. Soc., p. 250-369.

39. MINDLIN, R. D. and H. DERESIEWICZ (1954) Thickness-Shear and Flexural Vibrations of a Circular Disk. J. Appl. Phys., Vol. 25, p. 1329-1332.

40. DERESIEWICZ, H. and R. D. MINDLIN (1955) Axially Symmetric Flexural Vibrations of a Circular Disk. J. Appl. Mech., p. 86-88.

41. MINDLIN, R. D. (1951) Thickness-Shear and Flexural Vibrations of Crystal Plates. J. Appl. Phys., Vol. 22, p. 316-323.

42. TIERSTEN, H. F. and MINDLIN, R. D. (1962) Forced Vibrations of Piezoelectric Crystal Plates. Quart. Appl. Math., p. 107-120.

43. MINDLIN, R. D. (1960) Waves and Vibrations in Isotropic, Elastic Plates. Proc. First Sym. Naval Struct. Mech., p. 192-232.

44. CALLAHAN, W. R. (1956) On the Flexural Motions of Circular and Elliptical Plates. Quart. Appl. Math., p. 371-380.

45. KALNINS, A. and P. M. NAGHDI (1960) Axisymmetric Vibrations of Shallow Elastic Spherical Shells. J. Acous. Soc. Amer., p. 342-347.

46. KALNINS, A. (1961) On Vibrations of Shallow Spherical Shell. J. Acous. Soc. Amer., p. 1102-1107.

47. SHARMA, R. L. (1957) Dependence of the Frequency Spectrum of a Circular Disk on Poisson's Ratio. J. Appl. Mech., p. 53-54.

48. BERGMAN, S. and M. SCHIFFER (1953) Kernel Functions and Elliptic Differential Equations in Mathematical Physics. Academic Press Inc., New York, 432 p.

49. KALNINS, A. (1966) On Fundamental Solutions and Green's Functions in the Theory of Elastic Plates. J. Appl. Mech., p. 31-38.

50. REISSNER, E. (1954) On Axisymmetric Vibrations of Circular Plates of Uniform Thickness, Including the Effects of Transverse Shear and Rotary Inertia. J. Acous. Soc. Amer., p. 252-253.

51. HUANG, T. C. (1961) Application of Variational Methods to the Vibration of Plates Including Rotary Inertia and Shear. Proc. Seventh Midwestern Mechanics Conference, Plenum Press, New York, p. 61-72.

52. CONWAY, H. D. (1951) Axially Symmetric Plates with Varying Thickness. J. Appl. Mech., p. 140-142.

53. CONWAY, H. D. (1953) Closed Form Solutions for Plates of Variable Thickness, J. Appl. Mech., p. 564.

54. RAMBERG WALTER (1949) Transient Vibration in an Airplane Wing Obtained by Several Methods. National Bur. of Standards Jour. Res., Vol. 42, p. 437-447.

55. JAMES SHENG (1965) The Response of Cylindrical Shell to Transient Surface Loadings. AIAA Journal, Vol. 3, p. 701-709.

56. ISAKON, G. (1950) A Survey of Analytical Methods for Determining Transient Stresses in Elastic Structures. Office of Naval Research, M.I.T., Project NR-035-259.

57. DOHRENWEND, C. O, D. C. DRUCKER and P. MOORE (1944) Transverse Transient Impacts. Proc. Soc. for Expt. Stress Analysis, Vol. 1, p. 1-10.

58. PLASS, Jr., H. J. (1958) Timoshenko Beam Equation for Short-Pulse Type Loading. J. Appl. Mech., p. 379-385.

59. DANA YOUNG (1948) Vibration of a Beam with Concentrated Mass, Spring and Dashpot. J. Appl. Mech., p. 65-72.

60. LEE, W. F. G. and E. SEIBEL (1952) Free Vibrations of Restrained Beams. J. Appl. Mech., p. 471-477.

61. SNOWDON, J. C. (1964) Longitudinal Vibration of Internally Damped Rods. J. Acous. Soc. Amer., p. 502-510.

62. SNOWDON, J. C. (1963) Transverse Vibration of Simply Clamped Beams. J. Acous. Soc. Amer., p. 1152-1161.

63. SNOWDON, J. C. (1964) Response of Simply Clamped Beam to Vibrating Forces and Moments. J. Acous. Soc. Amer., p. 495-501.

64. SNOWDON, J. C. (1963) Transverse Vibration of Beams with Internal Damping, Rotary Inertia and Shear. J. Acous. Soc. Amer., p. 1997-2006.

65. SNOWDON, J. C. (1964) Approximate Expressions for the Mechanical Impedance and Transmissibility of Beams Vibrating in Their Transverse Modes. J. Acous. Soc. Amer., p. 366-375.

66. SNOWDON, J. C. (1966) Response of Cantilever Beams to Which Dynamic Absorbers are Attached. J. Acous. Soc. Amer., p. 878-886.

67. SNOWDON, J. C. (1968) Vibration and Shock in Damped Mechanical Systems. Wiley, New York, 486 p.

68. SNOWDON, J. C. (1965) Rubberlike Materials, Their Internal Damping and Their Role in Vibration Isolation. J. Sound Vibr., p. 175-193.

69. SNOWDON, J. C. (1963) Representation of the Mechanical Damping Possessed by Rubberlike Materials and Structures. J. Acous. Soc. Amer., p. 821-829.

70. SNOWDON, J. C. (1960) Dynamic Mechanical Properties of Rubberlike Materials with Reference to the Isolation of Mechanical Vibration. Noise Control, Vol. 6, p. 18-23.

71. SKUDRZYK, E. (1968) Simple and Complex Vibrating Systems. The Pennsylvania University Press, University Park, 514 p.

72. WATSON, G. N. (1945) A Treatise on the Theory of Bessel Functions. Macmillan, New York, 804 p.

73. McLACHLAN, N. W. (1961) Bessel Functions for Engineers. Oxford University Press, New York, 239 p.

74. LEHNHOFF, T. F. (1968) The Influence of Transverse Shear on the Small Displacement Theory of Circular Plates. Ph. D. Thesis, Department of Theoretical and Applied Mechanics, University of Illinois, Urbana., (AIAA Journal, Vol. 7, August 1969, p. 1499-1505.)

75. NOVOZHILOV, V. V. (1961) Theory of Elasticity. Pergamon Press, New York, 448 p.

76. BORESI, A. P. (1965) Elasticity in Engineering Mechanics. Prentice-Hall, New Jersey, 264 p.

77. ERIC REISSNER (1945) The Effect of Transverse Shear Deformation on the Bending of Elastic Plates. J. Appl. Mech., p. 69-77.

78. ERIC REISSNER (1944) On the Theory of Bending of Elastic Plates. J. Math. Phys., Vol. 23, p. 184-191.

79. ERIC REISSNER (1947) On Bending of Elastic Plates. Quart. Appl. Mech., Vol. 5, p. 55-68.

80. DONNEL, L. H., DRUCKER, D. C., GOODIER, J. N. (1946) Discussion of ' The Effect of Transverse Shear Deformation on the Bending of Elastic Plates', by E. Reissner. J. Appl. Mech., p. A-249-252.

81. GOLDENVEIZER, A. (1960) On Reissner's Theory of the Bending of Plates. NASA TT no. F-27.

82. LANGHAAR, H. L. (1962) Energy Methods in Applied Mechanics. Wiley, New York, 350 p.

83. LORD RAYLEIGH (1889) On the Free Vibration of an Infinite Plate of Homogeneous isotropic Elastic Matter. Proc. of London Math. Soc., Vol. 10, p. 225-234.

84. LAMB, H. (1917) On Waves in an Elastic Plate. Proc. of Royal Soc. of London, Vol. 93, p. 114-128.

85. TIMOSHENKO, S. (1922) On the Transverse Vibration of Bars of Uniform Cross-Section. Phil. Magazine, Vol. 43, p. 125-131.

86. TIMOSHENKO, S. and J. N. GOODIER (1951) Theory of Elasticity. McGraw-Hill, New York, 506 p.

87. KOLSKY, H. (1963) Stress Waves in Solids. Dover, New York, 213 p.

88. LOVE, A. E. H. (1944) A Treatise on Mathematical Theory of Elasticity. Dover, New York, 643 p.

89. TIMOSHENKO, S. and S. WOINOWSKY-KRIEGER (1959) Theory of Plates and Shells. McGraw-Hill, New York, 580 p.

90. ARMSTRONG, E. K. (1966) Natural Frequencies of Bladed Discs. Proc. of Institution of Mechanical Engineers. London, Vol. 180, p. 110-123.

91. DHALIWAL, R. S. (1962) Effect of Shear Deformation on the Bending of Rectangular Plates under Hydrostatic Pressure. J. Sci. Engg. Res., India, Vol. 6, p. 287-296.

92. EHRICH, F. F. (1956) A Matrix Solution for the Vibration Modes of Non-Uniform Disks. J. Appl. Mech, p. 109-115.

93. ESSENBURG, F. (1958) On Axially Symmetrical Plates of Variable Thickness. J. Appl. Mech., p. 625-626.

94. GLADWELL, G. M. L. and G. ZIMMERMANN (1966) On Energy and Complementary Energy Formulations of Acoustic and Structural Vibration Problems. J. Sound Vibr., p. 233-241.

95. GLADWELL, G. M. L. (1966) Variational Formulation of Damped Acousto-Structural Vibration Problems. J. Sound Vibr., p. 172-186.

96. JAROSLAV, PACHNER (1949) Pressure Distribution in the Acoustical Field Excited by a Vibrating Plate. J. Acous. Soc. Amer., p. 617-625.

97. KACZKOWSKI, Z. (1960) The Influence of the Shear Forces and the Rotary Inertia on the Vibration of an Anisotropic Plate. Arch. Mech. Stos., Vol. 12, p. 531-532.

98. KOELLER, R. C. and ESSENBURG, F. (1962) Shear Deformation in Rectangular Plates. Proc. Fourth U. S. Nat. Cong. Appl. Mech., Vol. 1, p. 555-561.

99. LANGHAAR, H. L. (1964) Paradoxes in the Theories of Plates and Shells. Dev. in TAM, Proc. 2nd Southeastern Conf. on TAM, Vol. 2, p. 1-8.

100. SALERNO, V. L. and M. A. GOLDBERG (1960) Effect of Shear Deformations on the Bending of Rectangular Plates. J. Appl. Mech., p. 54-58.

101. THOMAS G. CARLEY and H. L. LANGHAAR (1968) Transverse Shearing Stress in Rectangular Plates. J. Engg. Mech. Div., ASCE, February 1968, p. 137-151.

102. VOLTERRA, E. (1960) Discussion of 'Effect of Shear Deformations on the Bending of Rectangular Plates'. J. Appl. Mech., p. 594-596.

103. ANDERSON, R. A. (1967) Fundamentals of Vibration. Macmillan, New York, 412 p.

104. BICKLEY, W. G. and A. TALBOT (1961) An Introduction to the Theory of Vibrating Systems. Oxford University Press, Inc., New York, 238 p.

105. BISHOP, R. E. D. and D. C. JOHNSON (1960) The Mechanics of Vibration. Cambridge University Press, Cambridge, 592 p.

106. BISHOP, R. E. D., G. M. L. GLADWELL and S. MICHALSON (1965) The Matrix Analysis of Vibration. Cambridge University Press, Cambridge, 404 p.

107. BOLOTIN, V. V. (1964) The Dynamic Stability of Elastic Systems. Holden-Day Inc., San Francisco, 449 p.

108. CHEN YU (1966) Vibrations; Theoretical Methods. Addison-Wesley, Mass., 285 p.

109. CONTE, S. D. (1965) Elementary Numerical Analysis. McGraw-Hill, New York, 278 p.

110. COURANT, R. and D. HILBERT (1961) Methods of Mathematical Physics. Vol. 1, Inter-Science, New York, 561 p.

111. DIMITRY, D. L. and T. H. MOTT, Jr. (1966) Introduction to Fortran IV Programming. Holt, Rinehart and Winston, New York, 334 p.

112. DOLEZAL, VACLAV (1967) Dynamics of Linear Systems. P. Noordhoff, Groningen, 244 p.

113. DUFF, G. F. D. and NAYLOR (1966) Differential Equations of Applied Mathematics. Wiley, New York, 423 p.

114. FRIEDMAN, B. (1956) Principles and Techniques of Applied Mathematics. Wiley, New York, 315 p.

115. GREENWOOD, D. T. (1965) Principles of Dynamics. Prentice-Hall, New Jersey, 518 p.

116. GREEN, A. E. and W. ZERNA (1968) Theoretical Elasticity. Oxford University Press, London, 457 p.

117. Dr. GUNTER HELLWIG (1964) Differential Operators of Mathematical Physics. Addison-Wesley, Mass., 296 p.

118. HANS SAGAN (1961) Boundary Value Problems of Mathematical Physics. Wiley, New York, 381 p.

119. HARRY F. OLSON (1948) Elements of Acoustical Engineering. Van Nostrand Co., Inc., New York, 539 p.

120. HILDEBRAND, F. B. (1965) Methods of Applied Mathematics. 2nd Ed., Prentice-Hall, New Jersey, 362 p.

121. JACOBSON, L. S. and R. S. AYRE (1958) Engineering Vibrations. McGraw-Hill, New York, 564 p.

122. JON MATHEWS and R. L. WALKER (1964) Mathematical Methods of Physics. W. A. Benjamin, Inc., New York, 475 p.

123. JULES HAAG (1962) Oscillatory Motions. Wadsworth Publishing Co. Inc., Belmont, California, Vol. 1, 193 p., Vol. 2, 201 p.

124. Dr. E. KAMKE (1948) Differentialgleichungen-Losungsmethoden und Losungen. Band 1, Chelsea Publishing Co., New York, 666 p.

125. KAPLAN, W (1962) Operational Methods for Linear Systems. Addison-Wesley, Mass., 577 p.

126. KINSLER, L. E. and A. R. FREY (1962) Fundamentals of Acoustics. Wiley, New York, 524 p.

127. KORN and KORN (1967) Mathematical Handbook for Scientists and Engineers. McGraw-Hill, New York, 1129 p.

128. KUPRADZE, V. D. (1963) Dynamic Problems in Elasticity. Wiley, New York, 259 p.

129. KUPRADZE, V. D. (1966) Potential Methods in the Theory of Elasticity. D. Davey, New York, 339 p.

130. KYUICHIRO WASHIZU (1968) Variational Methods in Elasticity and Plasticity. Pergamon Press, New York, 349 p.

131. LOUIS, A. PIPES (1963) Matrix Methods for Engineering . Prentice-Hall, New Jersey, 427 p.

132. LUKE, Y. L. (1962) Integrals of Bessel Functions. McGraw-Hill, New York, 419 p.

133. LURE, A. I. (1964) Three-Dimensional Problems of the Theory of Elasticity. Inter-Science, New York, 493 p.

134. MACKENZIE, G. W. (1964) Acoustics. Focal Press, New York, 224 p.

135. MANSFIELD, E. H. (1964) The Bending and Stretching of Plates. Macmillan, London, 148 p.

136. McLACHLAN, N. W. (1951) Theory of Vibrations. Dover, New York, 160 p.

137. NOWACKI, W. (1962) Dynamics of Elastic Systems. Wiley, New York, 357 p.

138. PAUL, A. CRAFTON (1961) Shock and Vibrations in Linear Systems. Harper and Brothers, New York, 415 p.

139. PESTEL, E. C. and F. A. Leckie (1963) Matrix Methods in Elastomechanics. McGraw-Hill, New York, 435 p.

140. PRESCOTT, J. (1946) Applied Elasticity. Dover, New York, 726 p.

141. RAYLEIGH, J. W. S. (1945) The Theory of Sound. Vol. 1, Dover, New York, 480 p.

142. STAKGOLD, I. (1968) Boundary Value Problems of Mathematical Physics. Vol. 2, Macmillan, New York, 408 p.

143. THOMSON, W. T. (1960) Laplace Transformation. 2nd Ed., Prentice-Hall, New Jersey, 255 p.

144. TONG, K. N. (1960) Theory of Mechanical Vibration. Wiley, New York, 348 p.

145. TRELOAR, L. R. G. (1958) The Physics of Rubber Elasticity. Oxford University Press, London, 342 p.

146. VIERCK, R, K. (1967) Vibration Analysis. International Textbook Co., Scranton, Pennsylvania, 378 p.

147. VOLTERRA, E. and E. C. ZACHMANOGLOU (1965) Dynamics of Vibrations. Charles E. Merrill Books, Inc., Columbus, Ohio, 622 p.

148. WARREN, P. MASON (1964) Physical Acoustics, Principles and Methods. Vol. 1, Part B, Academic Press, New York, 376 p.

149. WEBSTER, A. G. (1955) Partial Differential Equations of Mathematical Physics. Dover, New York, 263 p.

XV. VITA

Perakatte Joseph George was born on July 1, 1931, in Kerala, India. He received a Bachelor of Science Degree in Mechanical Engineering from the University of Kerala, India, in March 1953 and a Master of Science Degree in Mechanical Engineering from the University of Missouri-Rolla, in July 1960. Since January 1968, he has been pursuing a Doctor of Philosophy Degree in the Mechanical Engineering Department at the University of Missouri-Rolla. He has held an ICA (International Cooperation Administration, USA) Fellowship during his M.S. program and a UNESCO (United Nations Educational, Scientific and Cultural Organization) Fellowship during his Ph.D. program. Since September 1953, he has been in the Faculty of Mechanical Engineering of the University of Kerala, India.